

# **Identifizierung und Charakterisierung von Quorum-Sensing-Inhibitoren mittels biophysikalischer Methoden**

## **DISSERTATION**

zur Erlangung des Grades  
des Doktors der Naturwissenschaften  
der Naturwissenschaftlich-Technischen Fakultät III  
Chemie, Pharmazie, Bio- und Werkstoffwissenschaften  
der Universität des Saarlandes

von

**Dipl. LM-Chem. Elisabeth Weidel**

Saarbrücken

2015

Tag des Kolloquiums: 13.05.2015

Dekan: Prof. Dr. Dirk Bähre

Berichterstatter: Prof. Dr. Rolf W. Hartmann

Prof. Dr. Claus-Michael Lehr

Vorsitz: Prof. Dr. Claus Jacob

Akad. Mitarbeiter: Dr. Marcel Albrecht

Die vorliegende Arbeit wurde von September 2011 bis Februar 2015 unter Anleitung von Herrn Prof. Dr. Rolf W. Hartmann in der Fachrichtung 8.2 Pharmazeutische und Medizinische Chemie der Naturwissenschaftlich-Technischen Fakultät III der Universität des Saarlandes angefertigt.

„So eine Arbeit wird eigentlich nie fertig, man muss sie für fertig erklären, wenn  
man nach der Zeit und den Umständen das Möglichste getan hat.“

Johann Wolfgang von Goethe

## SUMMARY

The multidrug-resistant bacterium *Pseudomonas aeruginosa* (PA) has recently gained a lot of attention in research as well as from the general public, highlighting the interest in finding new anti-infectives to weaken the bacterium's severe effects to the human body. The pathogenicity of PA is controlled by a cell-density dependent, intercellular communication system. As the enzyme PqsD is involved in the production of the utilized signal molecules, it can be targeted in an anti-virulence strategy to specifically combat PA.

Using various biophysical methods, the binding sites and binding modes of two PqsD inhibitor classes were elucidated. The 2-nitrophenylmethanol derivatives are binding and competing with the natural substrate in the active center of PqsD, whereas the 2-benzamidobenzoic acids act as channel blockers, keeping the substrate away from its binding site.

Furthermore, in order to identify novel scaffolds serving as PqsD inhibitors, three frequently used screening strategies were evaluated. Two of these approaches used focused libraries, which were arranged by consideration of target-associated effects. A direct screening of a fragment library, covering a large chemical space, served as comparison. Regarding efficiency and efficacy, the rationality-driven approaches outperform the unfocussed one, indicating this type of screening represents a time-effective method.

## ZUSAMMENFASSUNG

*Pseudomonas aeruginosa* (PA) ist immer weiter in den Fokus der Wissenschaft sowie des öffentlichen Interesses gerückt, da die Notwendigkeit der Entwicklung neuer Wirkstoffe aufgrund der Multidrug-Resistenz stetig angestiegen ist. Die Pathogenität von PA wird durch ein Zelldichte-abhängiges, interzelluläres Kommunikationssystem gesteuert. Das Enzym PqsD ist an der Biosynthese der benötigten Signalmoleküle beteiligt und eignet sich deshalb als Target im Rahmen einer spezifisch auf PA zugeschnittenen Anti-Virulenz Strategie.

Mittels biophysikalischer Methoden konnten die Bindestellen zweier PqsD-Inhibitorklassen identifiziert und deren Bindungsmodi aufgeklärt werden. Während die 2-Nitrophenylmethanol-Derivate im aktiven Zentrum von PqsD binden und mit dem natürlichen Substrat kompetitieren, agieren die 2-Benzamidobenzoësäuren als Kanalblocker und verhindern so den Zugang des Substrates zu seiner Bindestelle.

Des Weiteren wurden zur Identifizierung neuer PqsD Inhibitoren drei häufig verwendete Screeningstrategien evaluiert. In zwei der Ansätze wurden fokussierte Bibliotheken getestet, die unter Berücksichtigung Target-assozierter Aspekte zusammengestellt wurden. Zum Vergleich diente ein Screening einer Fragmentbibliothek, die strukturell möglichst unterschiedliche Verbindungen beinhaltete. Die Effizienz und Effektivität der rational geleiteten Ansätze übertrifft die der unfokussierten, wodurch deutlich wird, dass diese zeiteffektive Methoden darstellen.

## PUBLIKATIONEN

Die vorliegende Arbeit gliedert sich in drei Publikationen, die im Text durch Buchstaben gekennzeichnet sind.

**A      Structure Optimization of 2-Benzamidobenzoic Acids as PqsD Inhibitors for *Pseudomonas aeruginosa* Infections and Elucidation of Binding Mode by SPR, STD NMR, and Molecular Docking**

Elisabeth Weidel, Johannes C. de Jong, Christian Brengel, Michael P. Storz, Andrea Braunshausen, Matthias Negri, Alberto Plaza, Anke Steinbach, Rolf Müller, and Rolf W. Hartmann

*J. Med. Chem.*, 2013, **56** (15), 6146–6155.

**B      Biochemical and Biophysical Analysis of a Chiral PqsD Inhibitor Revealing Tight-binding Behavior and Enantiomers with Contrary Thermodynamic Signatures**

Michael P. Storz, Christian Brengel, Elisabeth Weidel, Michael Hoffmann, Klaus Hollemeyer, Anke Steinbach, Rolf Müller, Martin Empting, and Rolf W. Hartmann

*ACS Chem. Biol.*, 2013, **8** (12), 2794–2801.

**C      Composing Compound Libraries for Hit Discovery – Rationality-Driven Preselection or Random Choice by Structural Diversity?**

Elisabeth Weidel, Matthias Negri, Martin Empting, Stefan Hinsberger, and Rolf W. Hartmann

*Future Med. Chem.*, 2014, **6** (18), 2057-2072.

WEITERE PUBLIKATIONEN DER AUTORIN, DIE NICHT GEGENSTAND DIESER DISSERTATION SIND

**D Molecular Basis of HHQ Biosynthesis: Molecular Dynamics Simulations, Enzyme Kinetic and Surface Plasmon Resonance Studies**

Anke Steinbach, Christine K. Maurer, Elisabeth Weidel, Claudia Henn, Christian Brengel, Rolf W. Hartmann, and Matthias Negri

*BMC Biophysics*, 2013, 6:10.

**E Catechol-Based Substrates of Chalcone Synthase as a Scaffold for Novel Inhibitors of PqsD**

Giuseppe Allegretta, Elisabeth Weidel, Martin Empting, and Rolf W. Hartmann

*Eur. J. Med. Chem.* 2015, **90**, 351–359.

**F Exploring the chemical space of ureidothiophene-2-carboxylic acids as inhibitors of the quorum sensing enzyme PqsD from *Pseudomonas aeruginosa***

Jan Henning Sahner, Martin Empting, Ahmed Kamal, Elisabeth Weidel, Carsten Börger, and Rolf W. Hartmann

*Eur. J. Med. Chem.* 2015, **96**, 14–21.

## Abkürzungsverzeichnis

2-ABA	2-Aminobenzoylacetat
2-ABA-CoA	2-Aminobenzoylacetat- Coenzym A
ACoA	Anthraniloyl-Coenzym A
AHL	N-Acyl-L-Homoserinlacton
AI	Autoinducer
C4-HSL	<i>N</i> -(butanoyl)-L-Homoserinlacton
CMD	Carboxymethyldextran
CoA	Coenzym A
DHQ	2,4-Dihydroxychinolin
EDC	<i>N</i> -Ethyl- <i>N'</i> -(dimethylaminopropyl)carbodiimid
EDTA	Ethyldiamintetraessigsäure
HAQ	4-Hydroxy-2-alkylchinolin
HHQ	4-Hydroxy-2-heptylchinolin
HQNO	4-Hydroxy-2-heptylchinolin- <i>N</i> -oxid
HTS	Hochdurchsatz Screening (High-Throughput-Screening)
IC <sub>50</sub>	mittlere, inhibitorische Konzentration
ITC	Isotherme Titrationskalorimetrie (Isothermal Titration Calorimetry)
LE	Liganden Effizienz
Maldi	Matrix-unterstützte Laser-Desorption/Ionisation (Matrix-assisted laser desorption/ionization)
MS	Massenspektrometer (mass spectrometry)
NHS	<i>N</i> -Hydroxysuccinimid
NMR	Kernspinresonanz (Nuclear Magnetic Resonance)
PA	<i>Pseudomonas aeruginosa</i>

X |

PQS	3,4-Dihydroxy-2-heptylchinolin
3-oxo-C12-HSL	<i>N</i> -(3-oxododecanoyl)-L-Homoserinlacton
QS	Quorum Sensing
RU	Resonance unit
SAR	Struktur-Wirkungs-Beziehung (Structure activity relationship)
SPR	Surface Plasmon Resonance
STD	Sättigungstransfer-Differenz (Saturation Transfer Difference)
TOF	Flugzeit (Time of flight)

# Inhaltsverzeichnis

<b>1 Grundlagen .....</b>	<b>1</b>
1.1 <i>Surface Plasmon Resonance</i> Spektroskopie .....	1
1.1.1 Physikalisches Prinzip der SPR .....	1
1.1.2 Immobilisierung des Zielmoleküls .....	2
1.1.3 Das Sensorgramm.....	4
1.1.4 SPR in der Wirkstoffentwicklung .....	4
1.2 <i>Pseudomonas aeruginosa</i> .....	6
1.2.1 Quorum Sensing in <i>P. aeruginosa</i> .....	7
1.2.2 <i>pqs</i> -Quorum Sensing System .....	9
1.2.3 Inhibition des <i>pqs</i> -QS Systems als Anti-Virulenzstrategie .....	11
<b>2 Ziele der Arbeit.....</b>	<b>14</b>
<b>3 Ergebnisse .....</b>	<b>16</b>
3.1 Structure Optimization of 2-Benzamidobenzoic Acids as PqsD Inhibitors for <i>Pseudomonas aeruginosa</i> Infections and Elucidation of Binding Mode by SPR, STD NMR, and Molecular Docking.....	16
3.2 Biochemical and Biophysical Analysis of a Chiral PqsD Inhibitor Revealing Tight-Binding Behavior and Enantiomers with Contrary Thermodynamic Signatures.....	27
3.3 Composing Compound Libraries for Hit Discovery – Rationality-Driven Preselection or Random Choice by Structural Diversity? .....	36
<b>4 Zusammenfassung der Ergebnisse.....</b>	<b>37</b>
4.1 Aufklärung der Bindungsmodi von PqsD Inhibitoren .....	38
4.1.1 Charakterisierung des Bindungsmodus der 2-Benzamidobenzoësäuren .....	40
4.1.2 Charakterisierung des Bindungsmodus der 2-Nitrophenolmethanole .....	42
4.1.3 Finale Diskussion der Bindungsmodi.....	45
4.2 SPR Screenings.....	46
4.2.1 „ <i>me-too</i> “ Ansatz .....	47
4.2.2 Fragmentscreening .....	49
4.2.3 Virtuelles Screening .....	50
4.2.4 SPR Evaluierung .....	51

4.2.5 Finale Diskussion der Screeningansätze.....	52
4.3. Fazit.....	54
<b>5 Literaturverzeichnis.....</b>	<b>55</b>
<b>6 Supporting information .....</b>	<b>64</b>
6.1 Supporting Information der Publikation A .....	64
6.2 Supporting Information der Publikation B.....	90
6.3 Supporting Information der Publikation C.....	102
<b>7 Appendix .....</b>	<b>119</b>
7.1 Curriculum Vitae .....	119
7.2 Publikationen .....	120
7.3 Poster Präsentationen.....	121
<b>8. Danksagung.....</b>	<b>122</b>

# 1 Grundlagen

## 1.1 Surface Plasmon Resonance Spektroskopie

Die Oberflächenplasmon Resonanz Spektroskopie (*Surface Plasmon Resonance spectroscopy, SPR*) ist eine biophysikalische Methode, die auf der Totalreflexion von parallel polarisiertem Licht basiert. Sie ermöglicht die Analyse von Interaktionen in Echtzeit. Diese Studien sind insbesondere bei der Entwicklung von neuen, potentiellen Arzneimitteln gefragt, da aufgrund der hohen Sensitivität Wechselwirkungen zwischen den Wirkstoffen und den zu adressierenden Biomolekülen wie z.B. DNA, RNA oder Proteinen labelfrei und mit hohem Durchsatz detektiert werden können (1-3).

### 1.1.1 Physikalisches Prinzip der SPR

Das Prinzip der SPR beruht darauf, dass einfallendes, linear polarisiertes Licht durch ein Prisma auf einen Sensorchip scheint, welcher mit einem dünnen Metallfilm überzogen ist. Dieser Metallfilm funktioniert wie ein Spiegel und bewirkt eine Reflexion des Lichtes (Abb. 1).

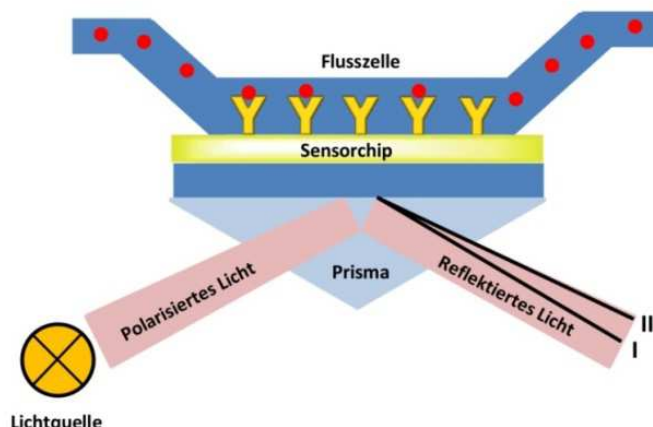


Abb. 1: Schematischer Aufbau einer SPR: Linear polarisiertes Licht wird am Sensorchip, der auf einem Prisma aufgelagert ist, reflektiert. Der reflektierte Lichtstrahl wird vom Detektor erfasst. Findet eine Interaktion zwischen Analyt (●) und Liganden (Y) statt, führt die Massenzunahme zu einer Änderung des Brechungsindexes und fernerhin zu einer Veränderung des Winkels, bei dem das Reflexionsintensitätsspektrum ein Minimum aufweist (Verschiebung von I nach II) (modifiziert nach Szabo et al. (4)).

Wird der Winkel des einfallenden Lichtes verändert, gibt es einen Winkel, bei dem ein deutlicher Intensitätsverlust der reflektierten Strahlung zu beobachten ist. Ausschlaggebend ist die durch Absorption übertragene Energie der Photonen auf die freien Elektronen der Metallschicht, wodurch diese zur Oszillation angeregt werden (= Resonanz) und ein elektromagnetisches Feld (= evaneszentes Feld) erzeugt wird. Die oszillierenden Elektronen werden auch als Oberflächenplasmone bezeichnet (5, 6).

Am sogenannten SPR-Winkel ist der Intensitätsverlust des reflektierten Lichtes am größten (6). Dieser Winkel ist abhängig von den Brechungsindizes der Medien auf beiden Seiten der Goldschicht. Bei Bindung von Proteinen oder Molekülen an die Sensorchipoberfläche ändert sich der Brechungsindex auf der Seite des Metalls, wohingegen der Brechungsindex auf Seite des Prismas konstant bleibt (6-8). Diese Änderung führt zu einer Verschiebung des SPR-Winkels, welche vom Detektor erfasst und in ein Resonanzsignal umgewandelt wird (Abb. 2) (6).

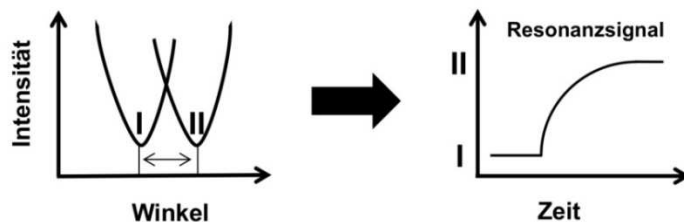


Abb. 2: Die Bindung von Molekülen an die Sensorchipoberfläche führt zu einer Winkelverschiebung (**I** → **II**), die vom Detektor erfasst und in ein Resonanzsignal umgewandelt wird (modifiziert nach Schasfoort and Tudos (6)).

Das Resonanzsignal wird gewöhnlich in der Einheit „*Resonance Unit*“ (RU) erfasst und ist proportional zur Konzentration des Analyten. Anhand experimenteller Untersuchungen zur Korrelation zwischen Massenabsorption und Resonanzsignal wurde folgende Beziehung ermittelt: (8)

$$1 \text{ RU} = 1 \text{ pg/mm}^2$$

Da die Penetrationstiefe des elektromagnetischen Feldes mit zunehmender Entfernung schwächer wird, muss das Zielmolekül relativ nah an der Sensorchipoberfläche fixiert werden (6).

### 1.1.2 Immobilisierung des Zielmoleküls

Der erste Schritt einer SPR-Messung beinhaltet die Kopplung des Targets (= Ligand) an die Sensorchipoberfläche. Dieser Prozess wird als Immobilisierung des Liganden bezeichnet, wobei der Begriff Immobilisierung häufig als eine starre Fixierung des Targets missverstanden wird. Die Beweglichkeit des Liganden wird jedoch durch Bindung an die flexiblen Carboxymethyldextran (CMD)-Ketten der Sensorchipmatrix gewährleistet, da dies unter Beibehaltung eines Großteils an Rotations- und Translationsfreiheitsgraden geschieht. Gleichzeitig wird die Zugänglichkeit des Liganden durch die von der Sensorchipoberfläche entfernte Positionierung verbessert. Darüber hinaus übt die Matrix eine Schutzfunktion auf sensible Liganden vor Denaturierung aus, die durch Austrocknen der Oberfläche verursacht werden kann (9).

Experimentelle Vergleiche von gelösten und immobilisierten Proteinen ergaben, dass in beiden Fällen ähnliche Bindungsparameter erhalten wurden (10-13). Dies zeigt, dass durch die Immobilisierung meistens keine entscheidende Veränderung in der Struktur und damit in der Funktion des Liganden

hervorgerufen wird und diese deshalb keinen Nachteil zur Bestimmung von Reaktionskinetiken darstellt.

Die Bindung des Proteins an den Sensorchip kann über verschiedene Techniken erfolgen, wie zum Beispiel der Amidkupplung, der Biotin-Streptavidin-Kupplung oder einem „Capturing“ mittels Antikörper. Die Amidkupplung stellt meist die erste Wahl dar, da diese Technik zu stabilen Bindungen und guten Ausbeuten führt (6). Der Nachteil dieser Fixierungsmethode liegt in der zufälligen Orientierung des Liganden, was teilweise zu unzugänglichen Bindestellen führen kann. Darüber hinaus können die genutzten pH-Werte zur Inaktivierung des Proteins führen (14).

Um ein Protein über die Aminogruppen der Oberflächenlysine an den Chip zu binden (Abb. 3), werden zuerst die Carboxylsäuregruppen der Matrix aktiviert, wofür häufig EDC (*N*-Ethyl-*N'*-(dimethylaminopropyl)carbodiimid) verwendet wird (14). Bei pH-Werten zwischen 4,5 und 6,5 wird ein *O*-Acylisoharnstoff-Intermediat gebildet, welches im Anschluss durch NHS (*N*-Hydroxysuccinimid) unter Ausbildung von stabileren Aktivesterintermediaten ersetzt wird (14). Im Anschluss wird das Protein in einer Lösung, deren pH-Wert eine Einheit unter dem isoelektrischen Punkt liegt, injiziert. Dies soll bewirken, dass das Protein positiv geladen vorliegt. Elektrostatische Anziehungskräfte führen zu einer Akkumulation des Proteins an den negativ geladenen CMD-Ketten. Bei Annäherung des Proteins reagiert dessen Aminogruppe mit den aktivierte Estern unter Freisetzung von NHS und Ausbildung einer kovalenten Amidbindung (14). Der letzte Schritt der Immobilisierung beinhaltet die Inaktivierung der teils ungenutzten NHS-Ester mittels Ethanolamin (15, 16), um eine unreaktive Sensorchipoberfläche zu gewährleisten.

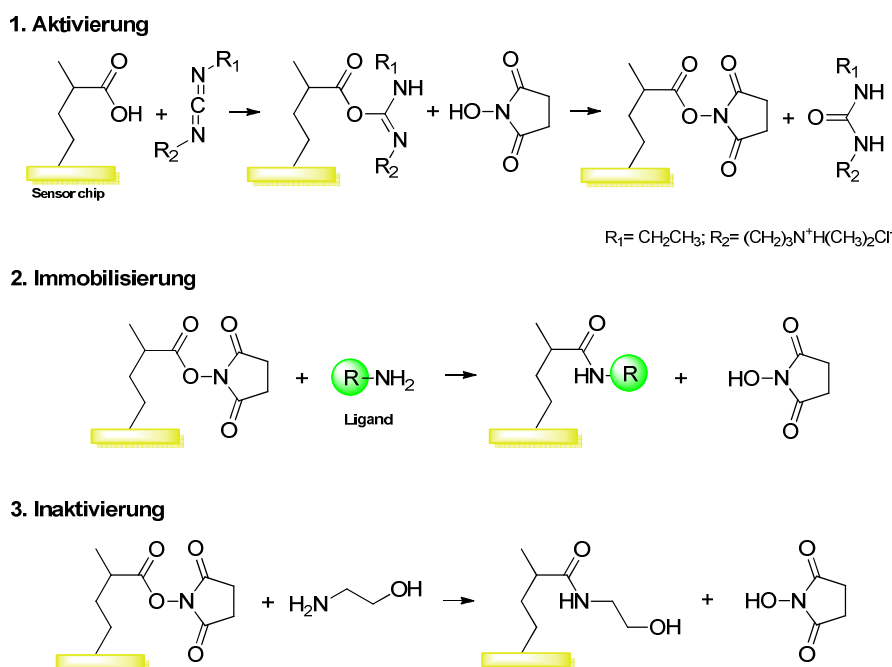


Abb. 3: Übersicht über die ablaufenden Reaktionen der Amidkupplung (modifiziert nach Fischer und Johnsson (14, 17)).

### 1.1.3 Das Sensorgramm

Wird ein Analyt in Lösung injiziert und fließt über den immobilisierten Liganden, kann es zu einer Interaktion kommen. Die hieraus resultierende Massenzunahme führt zu einer Veränderung des Brechungsexponenten, welche wiederum vom Detektor in Echtzeit aufgezeichnet und in ein sogenanntes Sensorgramm umgewandelt wird. Der Verlauf des Sensorgramms beschreibt die Interaktion zwischen Analyt und Liganden und kann in mehrere Phasen unterteilt werden (Abb. 4).

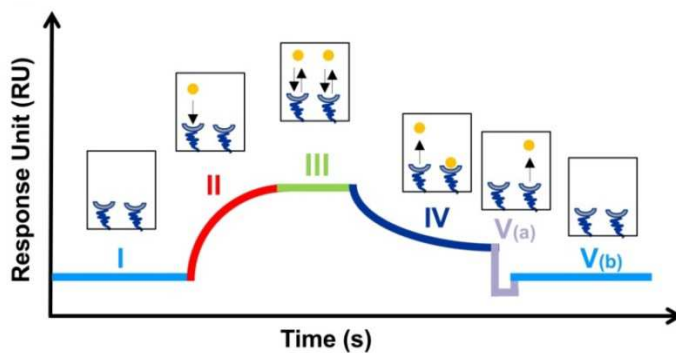


Abb. 4: Schematische Darstellung eines vom Detektor in Echtzeit aufgezeichneten Sensorgramms mit den nacheinander ablaufenden Phasen: (I) Aufzeichnung des Baselinesignals, (II) Assoziation, (III) Steady State, (IV) Dissoziation, (V<sub>a</sub>) Regeneration und (V<sub>b</sub>) abschließende Aufzeichnung des Baselinesignals (modifiziert nach Schasfoort and Tudos (6)).

Am Anfang eines jeden Sensorgramms wird die **Baseline** für einige Minuten aufgenommen, wobei lediglich Pufferlösung über den Liganden fließt. Wird der Analyt injiziert, kommt es infolge der Wechselwirkung mit dem Liganden und der daraus resultierenden Brechungsexponentenveränderung zu einem Anstieg im Resonanzsignal. Diese Phase wird als **Assoziation** bezeichnet. Im sich anschließenden **Steady State** besteht ein kontinuierliches Gleichgewicht zwischen assoziierenden und dissoziierenden Analyten. Ist die Injektion des Analyten beendet, findet keine weitere Assoziation statt und noch gebundener Analyt dissoziiert (= **Dissoziationsphase**). Diese Phase wird durch das abfallende Signal charakterisiert. Möglicherweise verläuft die Dissoziation des Analyten aufgrund starker Wechselwirkungen unvollständig. Durch den Einsatz von Säuren oder Basen, die eine pH-Wert Änderung herbeiführen, wird versucht, diese Interaktionen unter so milden Bedingungen wie möglich aufzuheben (= **Regeneration**). Im Anschluss wird im optimalen Fall das Baselinenniveau wieder erreicht und ein neuer Analyt kann injiziert werden.

### 1.1.4 SPR in der Wirkstoffentwicklung

Hochdurchsatzscreenings (*High Throughput Screening*, HTS) sind oft eine unerlässliche Komponente in *Drug Discovery* Programmen. Für deren Erfolg ist es wichtig, die Hits zu identifizieren, die am besten für die Optimierung geeignet sind (18-21). In diesem Zusammenhang finden funktionelle Screenings häufig Anwendung. Sie werden entweder *in vitro* am isolierten Enzym oder *in cellulo* bei unbekanntem Target in der Zelle durchgeführt. Diese Screening-Methoden besitzen oft den Nachteil,

dass sie sehr komplex und zeitintensiv sind, wodurch die Wahrscheinlichkeit, eine neue Leitverbindung zu detektieren, limitiert ist (22, 23). Aus diesem Grund ist die pharmazeutische Industrie bestrebt, neue Methoden zu entwickeln, die die Suche nach geeigneten Kandidaten erleichtern (24). Als eine dieser alternativen Strategien hat sich die SPR-Technologie bewährt. Diese Methode ermöglicht eine freie Wahl der zu untersuchenden Bibliothek, da aufgrund der hohen Sensitivität neben den größeren, wirkstoffartigen („*drug-like*“) Molekülen auch weniger affine Fragmente getestet werden können (25-33). SPR-basierte Screenings können die Forderungen nach einfacher Handhabung, hoher Sensitivität und großem Durchsatz bei gleichzeitig geringem Materialverbrauch erfüllen und eignen sich daher ideal als HTS-Methode (26).

Am Ende des Screenings werden Hits erhalten, die noch mittels eines funktionellen Enzymsassays validiert werden müssen, um nicht zur Optimierung geeignete Verbindungen aufzudecken, die unspezifisch oder außerhalb der katalytischen Seite binden. (34, 35). Viele als promiskuitive Verbindungen bezeichnete Substanzen entfalten ihre inhibitorische Wirkung durch unspezifische Aggregationsbildung. Mittels SPR ist es möglich solche Verbindungen zu identifizieren (36, 37). Darüber hinaus können Moleküle, die unspezifisch ans Zielmolekül binden, mittels Bindungsstudien detektiert werden. Dies kann entweder durch ein paralleles Screening gegen das Target und „*Off-Targets*“ erfolgen (27, 29, 32, 37) oder an einem an der Bindestelle blockierten Zielmolekül stattfinden (10, 29, 31). Eine weitere Möglichkeit stellt der Einsatz von Mutanten dar, bei denen gezielt Aminosäuren in der gewünschten Bindestelle ausgetauscht wurden (29, 38, 39). Hierdurch wird es ermöglicht, Verbindungen, die spezifisch an dieses Areal des Targets binden, zu identifizieren (38).

Neben der Hitidentifizierung und Validierung erfolgt auf der letzten Ebene die Charakterisierung der Hitverbindungen (Abb. 5). Anhand der gewonnenen Informationen kann dann entschieden werden, welche Verbindungen die vielversprechendsten Kandidaten zur Optimierung darstellen (40, 41).

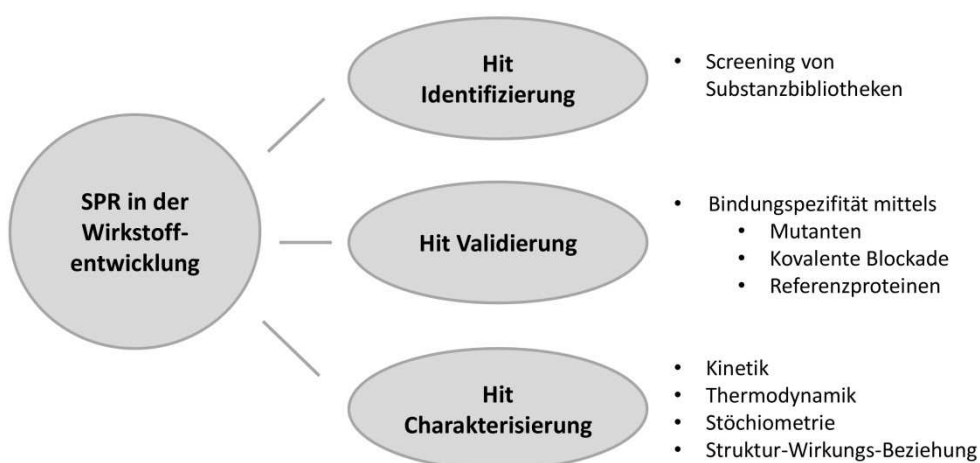


Abb. 5: Einsatz von SPR in verschiedenen Bereichen der Wirkstoffentwicklung (modifiziert nach Danielson (30)).

SPR kann in diesem Fall zur Bestimmung von kinetischen Parametern, aber auch von thermodynamischen Größen wie der Freien Enthalpie oder der Entropie, sowie zur Bestimmung der Stöchiometrie eingesetzt werden. Darüber hinaus können die erhaltenen Bindungsparameter genutzt werden, um Struktur-Wirkungs-Beziehungen (SAR) abzuleiten (42-44).

## 1.2 *Pseudomonas aeruginosa*

*Pseudomonas aeruginosa* (PA) ist ein ubiquitär vorkommendes, Gram-negatives Pathogen, welches sich den Proteobakterien zuordnen lässt und sich an viele Umweltbedingungen anpassen kann. Das opportunistische Pathogen stellt die häufigste Ursache für nosokomiale Infektionen bei immunsupprimierten Menschen dar und ist meist für die Morbidität und Mortalität von Mukoviszidose-Patienten verantwortlich (45-48). Wird die Lunge der Patienten durch PA kolonisiert, zieht dies eine Verschlechterung der Lungenfunktion mit sich (49-51). Die hohe Pathogenität von PA beruht auf der Bildung einer Vielzahl von Virulenzfaktoren, die teilweise zytotoxische Aktivitäten aufweisen (52) oder das Immunsystem des Wirtes angreifen und schädigen (zusammengefasst in (53)). Eine Behandlung mittels Antibiotikum ist aufgrund der hohen Resistenz des Bakteriums schwierig (54-56). In diesem Zusammenhang ist unter anderem die Zellmembran von zentraler Bedeutung, denn sie stellt eine schwer überwindbare Barriere für Antibiotika dar (57). Von Li *et al.* konnte gezeigt werden, dass die Wirksamkeit vieler Antibiotika durch den Einsatz von Permeationsverbesserern wie EDTA (Ethylendiamintetraessigsäure) erhöht werden kann (58). Zusätzlich spielen Effluxpumpen eine wichtige Rolle, da diese ein großes Substratspektrum aufweisen und verschiedenste Antibiotika aus der Zelle schleusen. Die Effluxpumpe MexAB-OprM von PA ist in der Lage, Tetracycline, Chloramphenicole, Trimethoprim,  $\beta$ -Lactame sowie  $\beta$ -Lactamase-Inhibitoren aus der Zelle zu pumpen, wodurch diese Medikamente zur Behandlung vieler PA Infektionen unwirksam geworden sind (59-61). Daneben stellt die Biofilmbildung der Bakterien einen weiteren, zentralen Aspekt für die Unwirksamkeit vieler Antibiotika dar. Bakterien, die in einer mikrobiellen Gemeinschaft leben, werden als Biofilm bezeichnet. Diese Gemeinschaft ist irreversibel mit einer Oberfläche assoziiert, wobei die einzelnen Zellen zusätzlich aneinander haften. Das kohärente Zellcluster ist in eine aus extrazellulären polymeren Substanzen bestehende Matrix eingebettet, die die Zellen selbst produziert (62, 63). Durch die Ausbildung eines Biofilms wird eine Diffusionsbarriere gebildet, die den Bakterien zusätzlichen Schutz vor Angriffen des Immunsystems und der Behandlung durch Antibiotika verleiht (64, 65).

PA ist in der Lage, über ein Zell-zu-Zell-Kommunikationssystem die Produktion der Virulenzfaktoren, die Expression der Effluxpumpen sowie die Ausbildung und Reifung des Biofilms zu steuern (66). Dieses System wird als Quorum Sensing (QS) System bezeichnet und beschreibt die zelldichteabhängige, interzelluläre Kommunikation von Bakterien, welche über kleine, diffusionsfähige Signalmoleküle abläuft (zusammengefasst in (67)). Dieses Kommunikationssystem

ermöglicht den Bakterien, die Zelldichte zu messen und abhängig davon das kollektive Verhalten des Zellverbandes zu steuern (66, 68-71).

### 1.2.1 Quorum Sensing in *P. aeruginosa*

Das erste QS System wurde in dem Meeresbakterium *Vibrio fischeri* entdeckt (72, 73), welches das typische Schema der bakteriellen Zell-zu-Zell-Kommunikation Gram-negativer Bakterien repräsentiert. Die Bildung und Freisetzung von Signalmolekülen, sogenannten Autoinducern (AI), ist die Basis des QS Systems (zusammengefasst in (74)). Zellverbände mit geringer Zelldichte bilden nur ein minimales Level an AI. Wenn die bakterielle Population wächst, erhöht sich ebenfalls die Konzentration an Signalmolekülen bis zum Erreichen einer Schwellenkonzentration, bei welcher das Signalmolekül an einen AI-abhängigen Rezeptor bindet (zusammengefasst in (75)). Diese Bindung löst eine physiologische Antwort in allen Mitgliedern der Population aus, was letztendlich zur kollektiven Umprogrammierung der Genexpression führt (76), die entweder als Induktion oder als Suppression spezifischer Zielgene erfolgt. Diese Kaskade ermöglicht den Bakterien in Abhängigkeit von der Zelldichte die Expression spezifischer Gene zu kontrollieren und auf Veränderungen in der Umgebung entsprechend zu reagieren (75).

PA besitzt drei verschiedene QS Systeme mittels derer die Produktion der Virulenzfaktoren und die Biofilmbildung gesteuert wird. Das *las* und das *rhl* System nutzen als Signalmoleküle Acylhomoserinlactone (AHL) und bestehen aus den Rezeptorproteinen LasR und RhlR sowie den Autoinducer-Synthasen LasI und RhlI (77-79). Durch Induktion von LasR und LasI erfolgt die Synthese des *las* eigenen AI, das *N*-(3-oxododecanoyl)-L-homoserinlacton (3-oxo-C12-HSL). Bindet dieses an den Transkriptionsregulator LasR, wird unter anderem die Produktion der Virulenzfaktoren Elastase, LasA Protease und der Exotoxine aktiviert (77, 80, 81). Das *rhl* System hingegen nutzt als AI *N*-Butanoyl-L-Homoserinlacton (C4-HSL), dessen Synthese RhlI vermittelt stattfindet. Analog zum *las* System bindet C4-HSL an RhlR, wodurch dieser aktiviert wird und die Produktion von Virulenzfaktoren wie Rhamnolipiden, Elastase, LasA Protease, Cyanwasserstoff, Pyocyanin, Siderophoren oder der cytotoxischen Lectine PA-I und PA-II reguliert (79, 82-86).

Neben diesen zwei auf AHL basierenden Systemen besitzt PA noch das *pqs* System, welches die 4-Hydroxy-2-Alkylchinoline (HAQ) als Signalmoleküle nutzt (87-90). Binden 3,4-Dihydroxy-2-heptylchinolon (*Pseudomonas* Quinolone Signal, PQS) und 4-Hydroxy-2-heptylchinolin (HHQ) an den membranassoziierten LysR-Typ Transkriptionsaktivator PqsR, wird durch dessen Aktivierung unter anderem die Produktion der Virulenzfaktoren Pyocyanin, Elastase, Phospholipase und Rhamnolipide stimuliert (91-93). Zusätzlich wird die Biofilmbildung und dessen Reifung (94) sowie die Expression von Effluxpumpen (95) und der Operone *pqsABCDE* und *phnAB* PqsR-abhängig gesteuert (89, 92, 93). Die polycistronischen Operone *pqsABCDE* und *phnAB* sind für die HAQ-

Synthese essentiell, dadurch ist PQS in der Lage, über PqsR seine eigene Synthese zu regulieren, wodurch der sprunghafte Anstieg in der Signalmolekülkonzentration ermöglicht wird (96).

Alle drei PA QS-Systeme sind stark miteinander vernetzt (s. Abb. 6) (97). Hierarchisch gesehen steht das *las* System an der Spitze dieses Netzwerkes, da es die beiden anderen Systeme reguliert. Dies erfolgt zum einen durch Transkriptionskontrolle des *rhl* Systems, indem die Expression von *rhlR* und *rhlI* durch den LasR/3-oxo-C12-HSL Komplex induziert wird. Zum anderen findet aber auch eine negative, posttranskriptionale Regulation statt, denn 3-oxo-C12-HSL weist eine Affinität zu RhlR auf und kann dadurch die RhlR/C4-HSL Interaktion blockieren (84, 96, 98). Das *pqs* System wird ebenfalls von *las* reguliert, da der LasR/3-oxo-C12-HSL-Komplex zur Aktivierung von PqsR führt und darüber hinaus das zur Umwandlung von HHQ zum potenteren PQS benötigte Enzym PqsH kontrolliert (87, 89, 92, 99). Die Suppression des *pqs* Systems findet hingegen *rhl* vermittelt statt. Die Transkription des *pqsABCDE* Operons kann durch den RhlR-C4-HSL-Komplex inhibiert werden (100). Dies dient zur Kontrolle der produzierten Menge an PQS, denn hohe Konzentrationen führen zu einer vermehrt stattfindenden Autolyse (101, 102). Die Produktion von PQS findet vor allem in der späten, logarithmischen Wachstumsphase statt und erreicht ein Plateau, bei dem gleichzeitig eine Hochregulation des *rhl* Systems erfolgt. Dies geschieht durch PQS-abhängige Induktion der Expression von *rhlI* sowie der Produktion von *rhl*-abhängigen Exoproducten (95, 97). Diese Aktivierung bewirkt einen negativen Feedbackmechanismus, wodurch das *pqs* System herunter reguliert wird (96). Demgegenüber steht der in geringem Maße mögliche, positive Einfluss des *pqs* Systems auf die Transkription von LasR (97). Anhand dieser Beziehungen wird deutlich, dass das *pqs* System die Position des Bindeglieds zwischen den beiden AHL-abhängigen Systemen einnimmt.

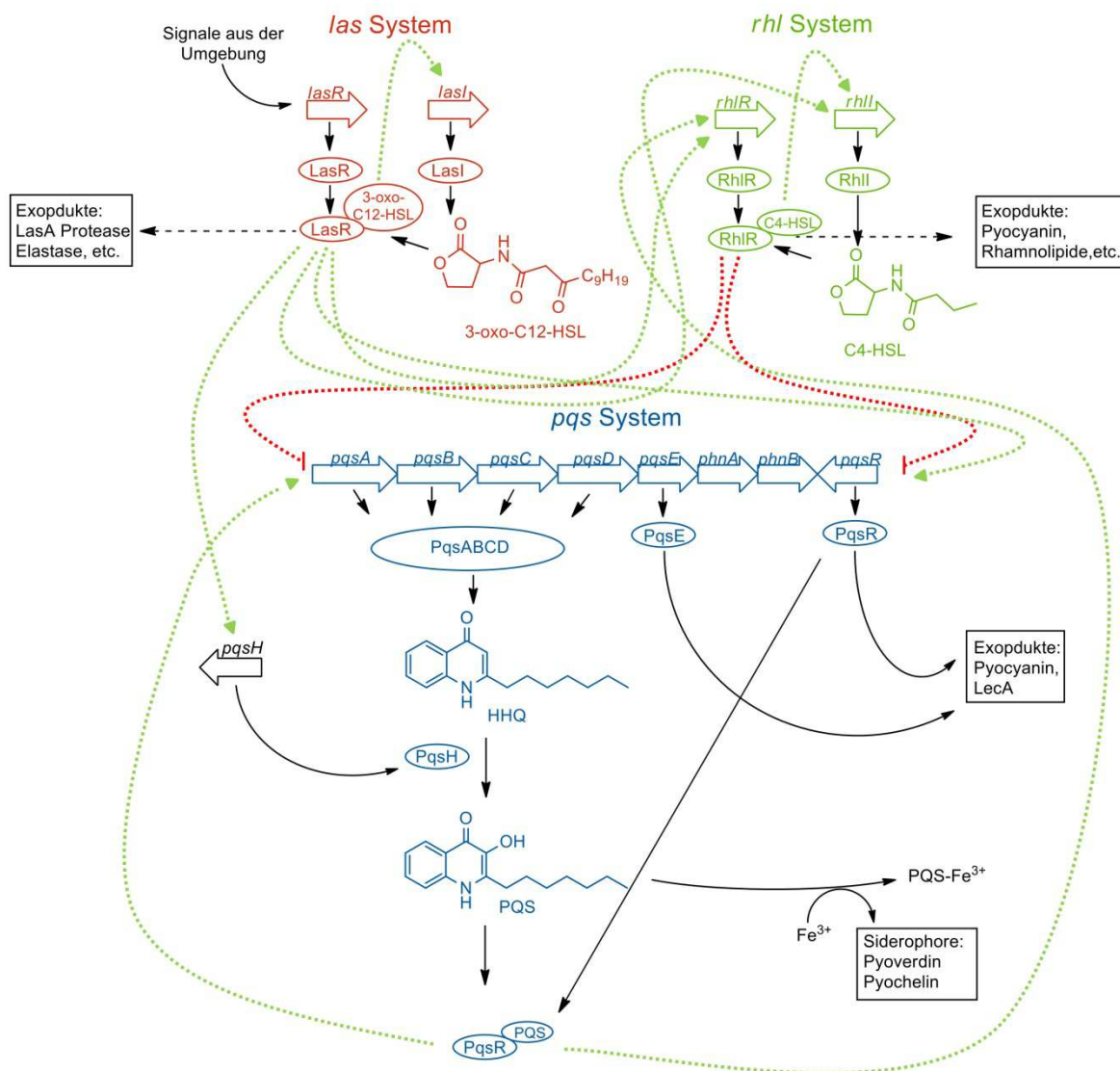


Abb. 6: Übersicht der verschiedenen Regulationswege im Quorum Sensing Netzwerk von PA sowie die gegenseitige Beeinflussung der drei QS Systeme: *las*, *rhl* und *pqs* (modifiziert nach (99)).

## 1.2.2 *pqs*-Quorum Sensing System

Das *pqs*-QS System produziert viele HAQs, die mittels einer LC-MS/MS Analyse in PA14 identifiziert wurden und sich in fünf verschiedene Klassen einteilen lassen (Abb. 7). Als Unterscheidungsmerkmale dienen unter anderem das Vorkommen einer Hydroxylgruppe in 3-Position, eine N-Oxidgruppe anstelle des Chinolinstickstoffs und die Sättigung der aliphatischen Seitenkette (88, 89).

Die wichtigsten Vertreter des *pqs*-QS Systems sind die Signalmoleküle HHQ und PQS, wobei PQS als Hauptsignalmolekül den wichtigsten Regulator in der Virulenz von PA darstellt (103), sowie das antimikrobiell wirksame HQNO (4-Hydroxy-2-heptylchinolin-N-oxid) (87-89, 95).

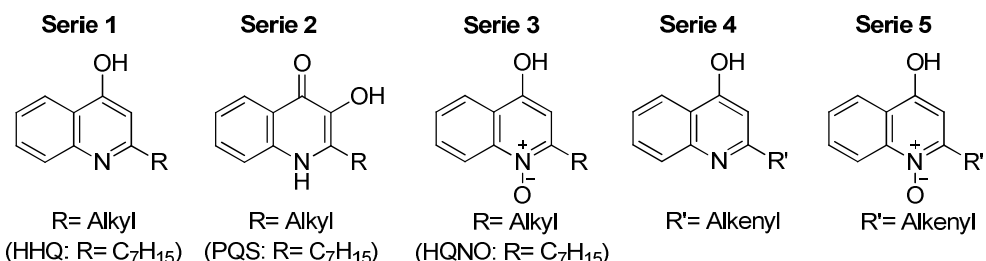


Abb. 7: Chemische Strukturen der fünf unterschiedlichen Verbindungsklassen von HAQs, die mittels LC-MS/MS identifiziert wurden (modifiziert nach Deziel *et al.* (89)).

Die ersten Informationen darüber, welche Proteine für die Biosynthese der HAQs verantwortlich sind, wurden in einem Transposon Mutagenese Screening erhalten. Dabei zeigte sich, dass die Gene des *phnAB* und *pqsABCD* Operons essentiell für die PQS Produktion sind (92). Das *phnAB* Operon vermittelt die Bildung von Anthranilsäure, welche das Vorläufermolekül aller HAQs darstellt (89, 104). PqsA, eine Coenzym A Ligase, aktiviert Anthranilsäure zu einem Anthranilsäurethioester (105), welcher mit PqsD reagiert (89, 106). Anhand einer Kristallstruktur wird deutlich, dass Anthraniloyl kovalent an Cys112 gebunden vorliegt, welches im aktiven Zentrum von PqsD lokalisiert ist (106). Der Anthraniloyl-PqsD-Komplex kann mit Malonyl-CoA das Intermediat 2-Aminobenzoylacetat (2-ABA-CoA) bilden (107), welches aufgrund seiner geringen Stabilität spontan zu 2,4-Dihydroxychinolin (DHQ) und 2-Aminoacetophenon (2-AA) zerfallen kann (Abb. 8) (108).

Lange wurde vermutet, dass die Bildung von HHQ ähnlich zu DHQ über PqsA und PqsD verläuft, da PqsD *in vitro* die Reaktion von ACoA und  $\beta$ -Ketodecansäure zu HHQ katalysieren kann (109, 110). Dulcey *et al.* haben jedoch gezeigt, dass diese Umsetzung biologisch nicht relevant ist. Die Biosynthese von HHQ verläuft bis zum Schritt der Bildung von 2-ABA-CoA analog zur DHQ Biosynthese. Durch Umsetzung von 2-ABA-CoA zu 2-ABA (2-Aminobenzoylacetat) und anschließender PqsC-katalysierter Reaktion mit Octanoyl, welches aus dem Substrat Octanoyl-CoA stammt, entsteht unter Decarboxylierung HHQ (108). Die Aufgabe von PqsB in diesem Zusammenhang ist unklar, allerdings ist PqsC in Abwesenheit von PqsB nicht in der Lage HHQ zu bilden, während der coexprimierte Komplex Aktivität zeigt. Demnach liegt die Rolle von PqsB möglicherweise darin, PqsC zu stabilisieren und dadurch die korrekte Faltung des Proteins zu gewährleisten (108). Das so gebildete HHQ wird in einer PqsH katalysierten Reaktion zu PQS umgewandelt (89). Beide Signalmoleküle sind in der Lage, an PqsR zu binden und diesen zu aktivieren, wodurch die Expression des *phnAB* und *pqsABCDE* Operons erfolgt (89, 90, 92, 93, 96, 111). Allerdings ist PQS ca. 100fach potenter als HHQ.

HQNO, das dritte, wichtige HAQ, hemmt das Wachstum von Gram-positiven Bakterien und führt dadurch zu einem Wachstumsvorteil für PA (88). Durch Labeling-Experimente konnte gezeigt werden, dass HHQ nicht das Vorläufermolekül von HQNO ist. Demzufolge müssen die N-Oxide Endprodukte eines alternativen Reaktionsweges sein, welcher PqsR unabhängig reguliert wird (89).

Neuere Studien zeigten, dass für die Biosynthese der *N*-Oxide die Monooxygenase PqsL benötigt wird, welche 2-AA zu den Endprodukten wie HQNO umsetzt (88, 89, 108).

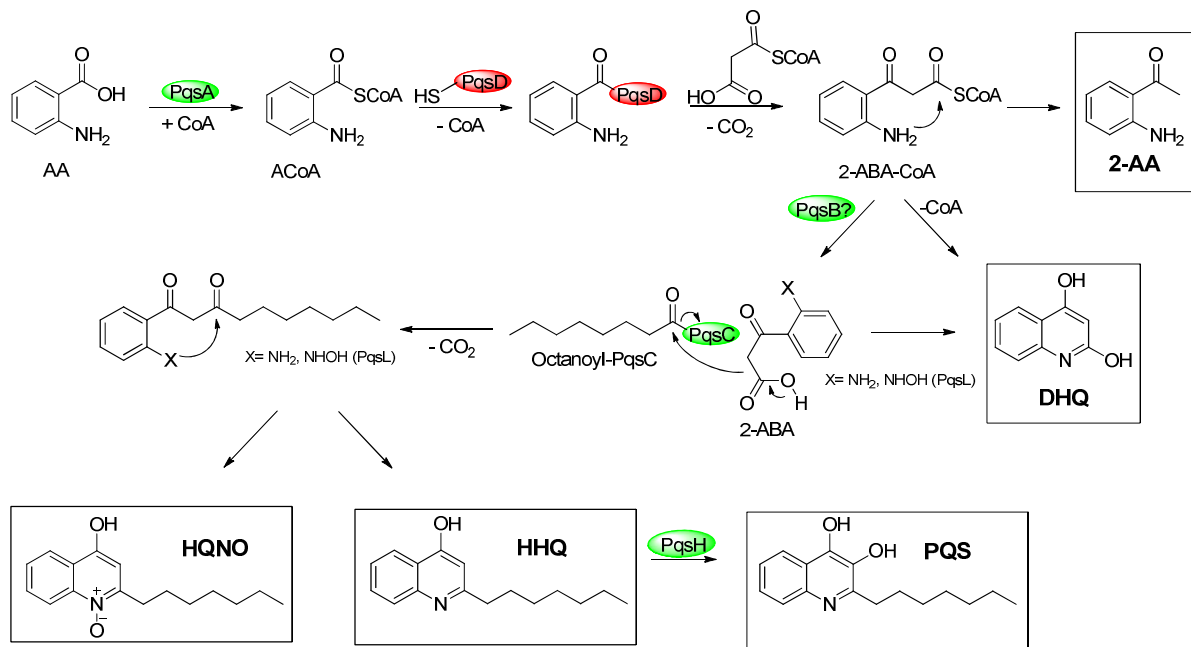


Abb. 8: Schematische Darstellung der Biosynthese der Signalmoleküle HHQ, PQS sowie von HQNO, DHQ und 2-AA (modifiziert nach Dulcey *et al.* (108)).

### 1.2.3 Inhibition des *pqs*-QS Systems als Anti-Virulenzstrategie

Die Behandlung bakterieller Infektionen erfolgte bisher mit Antibiotika, die das Bakterium töten oder dessen Wachstum inhibieren. Die Problematik hierbei ist die rasche Entwicklung von Resistzenzen, die infolge des Eingriffes in die Viabilität und des damit verbundenen Selektionsdrucks ausgebildet werden (112). Ursache für die schnelle Resistenz-Entstehung in Gegenwart eines Antibiotikums liegt darin, dass ein Bakterium, welches resistant ist, einen enormen Wachstumsvorteil gegenüber seinen Konkurrenten in einer bakteriellen Population besitzt (zusammengefasst in (113)).

Von der Entwicklung potenzieller Wirkstoffe, die mit dem QS System interferieren und dadurch die Pathogenität absenken, ohne die Viabilität zu beeinflussen, verspricht man sich einen verringerten, selektiven Druck und damit keine bzw. eine langsamere Resistenzentwicklung (114-117). Allerdings besteht beim Eingriff in die AHL-basierenden Systeme das Risiko, dass auch nicht pathogene Bakterienstämme beeinflusst werden, da AHLs auch in Gram-negativen Bakterien weit verbreitet sind. Aus diesem Grund stellt das *pqs*-QS System einen attraktiven Angriffspunkt dar, da dieses einzigartig für PA und *Burkholderia* spp ist (118). Dadurch ist es möglich durch Interferenz mit diesem System eine spezifische Inhibition zu erreichen.

Da PA einen vollständig funktionalen QS Kreislauf zur Entfaltung der vollen Virulenz benötigt (62, 119), gibt es mehrere, vielversprechende Ansatzpunkte um mit dem *pqs*-System zu interferieren. Dies

kann durch Eingriff in die Biosynthese und damit zur Reduzierung der Signalmolekül-Verfügbarkeit erreicht werden. Eine weitere Möglichkeit liegt in der Erkennung des Signalmoleküls durch die Empfängerzelle (76).

Auf Ebene der Signalmolekülerkennung kann durch Blockade des PQS-Rezeptors (PqsR) eine Absenkung der Pathogenität erreicht werden, denn wie von Rahme *et al.* gezeigt, ist diese in einer PqsR Mutante im Vergleich zum PA-Wildtyp reduziert (52). Erste PqsR Antagonisten, die strukturell von HHQ abgeleitet wurden, zeigten eine gute antagonistische Aktivität in einem PA Reportergen-Assay und waren auch in der Lage, die Produktion des Virulenzfaktors Pyocyanin zu senken (120). Darüber hinaus haben wir kürzlich gezeigt, dass durch Behandlung mit PqsR-Antagonisten die Mortalität von PA14-infizierten *Galleria mellonella* und *Caenorhabditis elegans* verringert wird (120, 121).

PqsE wird ebenfalls durch das *pqsABCDE* Operon codiert. Die Funktion des Proteins ist kaum verstanden, es scheint jedoch eine große Rolle für die Regulation der Zell-zu-Zell-Kommunikation zu spielen (91, 122). Experimentelle Untersuchungen an einer PqsE Mutante weisen darauf hin, dass PqsE an der Produktion von Virulenzfaktoren wie Pyocyanin, Lektinen und Elastase beteiligt ist (92, 95), aber keine Bedeutung für die Biosynthese von HHQ und PQS zu haben scheint, da bei einem *pqsE* Knockoutstamm vergleichbare Signalmolekulkonzentrationen zum Wildtyp vorliegen (89, 92). Durch Zugabe von PQS zu einer PqsE Mutante konnte die Produktion der Virulenzfaktoren nicht wieder hergestellt werden (95), was darauf hinweist, dass PqsE entweder für die Zellantwort auf PQS benötigt wird (92) oder aber in der Bildung eines bisher nicht identifizierten Signalmoleküls involviert ist (123). Fernerhin scheint PqsE für die Biofilmentwicklung benötigt zu werden und eine negative Regulation auf das *pqsABCDE* Operon auszuüben (124), wodurch PqsE zusätzlich noch an Bedeutung für die Pathogenität von PA gewinnt und ein höchstattraktives Target in einer Antivirulenzstrategie darstellt. Die fehlenden Kenntnisse über die Funktion des Proteins erschweren die Entwicklung von Inhibitoren erheblich, da eine Target-bezogene Evaluation derer nicht möglich ist.

Auf der Biosyntheseebene stellen PqsA, PqsB, PqsC und PqsD attraktive Targets dar. So findet in einer PqsA Mutante die Biosynthese von DHQ, HHQ und PQS nicht mehr statt und auch die Bildung der extrazellulären Matrix, welche für den Biofilm wichtig ist, erfolgt nur noch in geringen Mengen (94, 102). Mittels PqsA Inhibitoren war es möglich, die Aktivierung von Anthranilsäure zu hemmen und dadurch zu einer verringerten HHQ und damit auch PQS Produktion zu führen (104, 125). Bei Infektion von Mäusen mit einem PA14-Stamm und Behandlung mit halogenierten Anthranilsäure-Analoga ist die Überlebensrate größer als die der Kontrollgruppe. Dies zeigt, dass eine reduzierte Pathogenität durch PqsA-Inhibition und der damit verbundenen Hemmung der PQS Biosynthese erzielt werden kann (125).

Neben PqsA sollten PqsB, PqsC und PqsD als Targets geeignet sein, da sie ebenfalls an der Signalmolekülbiosynthese beteiligt sind. Dementsprechend sollte ein Ausschalten einer dieser drei Proteine zu ähnlichen Effekten führen (106). Kürzlich wurden erste Hinweise auf die Funktionen von PqsB und PqsC erhalten (108). Da aber keine strukturellen Informationen wie zum Beispiel eine Kristallstruktur vorhanden sind, erschwert dies die Entwicklung von Inhibitoren. Für PqsD ist eine Kristallstruktur vorhanden (106) und fernerhin wird in einer PqsD Mutante kein PQS mehr gebildet (92). Wir konnten kürzlich zeigen, dass es mittels erster, beschriebener PqsD Inhibitoren möglich war die Signalproduktion in PA zu verringern und gleichzeitig auch Auswirkungen auf die Biofilmmasse zu erzielen, wodurch PqsD ein höchst attraktives Antivirulenztarget darstellt (126).

## 2 Ziele der Arbeit

Der Bedarf an neuen Antiinfektiva steigt aufgrund der zunehmenden Resistenzbildung gegenüber den herkömmlichen Antibiotika kontinuierlich an (zusammengefasst in (127)). Der zusätzliche Druck durch die geringe Anzahl an neu zugelassenen Arzneistoffen sowie die teilweise sehr kurzen Zeitspannen zwischen Markteintritt und dem Auftreten einer ersten Resistenz verschärfen das Problem (127-129). Konsequenterweise lassen sich bakterielle Infektionen immer schwieriger behandeln (130-134). Die wenigen, neuen Antibiotika auf dem Markt sind oftmals Derivate von vorhandenen Arzneistoffen, die aufgrund der Ähnlichkeit zu dem bestehenden Wirkstoff anfällig für die bereits existierenden Resistenzmechanismen sind. Aus diesem Grund sind neue Strukturen nötig, die andere Wirkmechanismen aufweisen oder neue Targets adressieren (135-138). Idealerweise solche, die die Resistenzentwicklung vermeiden oder zumindest verzögern. Einer dieser Ansätze stellt die Entwicklung von QS-Inhibitoren dar. Mittels dieser Verbindungen ist es möglich, die Pathogenität des Bakteriums zu vermindern, ohne gleichzeitig seine Viabilität zu beeinflussen (114-117). Zu diesem Zweck sollten im Rahmen des Projektes Inhibitoren entwickelt werden, die über PqsD mit dem *pqs*-QS von PA interferieren und dessen Virulenz absenken, ohne dabei das Zellwachstum zu beeinflussen (126, 139).

In einem Liganden-basierten Ansatz wurde eine neue Verbindungsklasse von PqsD Inhibitoren entdeckt, die Hemmungen im einstellig mikromolaren Bereich aufweisen (126). Diese und eine zweite Klasse, die aufgrund der Homologie von PqsD zu FabH identifiziert wurde (109), sind vielversprechende Verbindungen, um über das *P. aeruginosa* Protein PqsD mit dem *pqs*-QS zu interferieren. Um die Effektivität beider Substanzklassen zu steigern, ist die Durchführung weiterer Optimierungsschritte notwendig. Zur Identifizierung geeigneter Partialstrukturen, an welchen das Molekül optimiert werden kann, sind Einblicke in die Inhibitor-Protein-Wechselwirkungen essentiell. Zu diesem Zweck war ein Ziel dieser Arbeit, die Bindemechanismen beider Substanzklassen aufzuklären. Zur Identifizierung der Bindestellen wurden unter anderem SPR Experimente durchgeführt. Diese erfolgten zum einen an PqsD, welches im aktiven Zentrum mittels des natürlichen Substrats blockiert wurde, und zum anderen an PqsD Mutanten, deren Aminosäuren in der Nähe des aktiven Zentrums gezielt ausgetauscht wurden. Anhand dieser Experimente können Aussagen darüber getroffen werden, ob die Inhibitoren im aktiven Zentrum binden oder nicht. Die detailliertere Aufklärung der Protein-Inhibitor-Wechselwirkungen erfolgte über den Einsatz von ITC (*Isothermal Titration Calorimetry*), STD-NMR (*Saturation Transfer Difference- Nuclear Magnetic Resonance*) und molekularem Docking. Die durchgeföhrten Experimente zeigen sowohl die Aminosäuren auf Proteinseite, als auch die funktionellen Gruppen auf der Molekülseite auf, die maßgeblich an der Wechselwirkung beteiligt sind. Anhand dieser Einblicke können nicht an der Interaktion beteiligte,

funktionelle Gruppen ausgetauscht, eliminiert oder vergrößert werden, um eine stärkere Wechselwirkung mit dem Protein und eine damit verbundene, gesteigerte Aktivität zu erreichen.

Im zweiten Teil der Arbeit stand die Identifizierung von neuen Leitstrukturen im Fokus. Zu diesem Zweck werden häufig SPR-basierte Screenings von großen Bibliotheken, bestehend aus einer Vielzahl an strukturell unterschiedlichen Verbindungen, durchgeführt (28, 29). Oftmals sind die Hitraten sehr gering und der Hitidentifizierungsprozess sehr zeitaufwändig. Um die Effizienz zu steigern, sind Ansätze von besonderem Interesse, mittels derer es möglich ist, die Hitrate zu erhöhen und gleichzeitig die Größe der Bibliothek zu reduzieren. Unter Berücksichtigung dieses Aspektes wurden drei häufig verwendete Screeningstrategien miteinander verglichen. Zwei dieser Ansätze beinhalteten eine auf das Target bezogene Vorselektion der mittels SPR zu untersuchenden Verbindungen, wie Inhibition eines homologen Proteins oder ein vorgeschaltetes, virtuelles Screening. Demgegenüber steht der dritte Ansatz, bei dem ein SPR Screening einer Fragment Bibliothek, die einen großen chemischen Raum abdeckt, durchgeführt wurde. Die Hits aus allen Screenings wurden anschließend im funktionellen Assay auf ihre Fähigkeit PqsD zu inhibieren getestet.

Der Vergleich zwischen den verschiedenen Ansätzen soll aufzeigen, welche Strategie im Hinblick auf Durchführbarkeit und Effizienz zur Identifizierung von neuen PqsD Inhibitoren am besten geeignet ist. Darüber hinaus bieten die Ergebnisse aus SPR und funktionellen Assay eine Grundlage, um der Frage nachzugehen, inwiefern SPR als Screeningmethode geeignet ist.

### 3 Ergebnisse

#### 3.1 Structure Optimization of 2-Benzamidobenzoic Acids as PqsD Inhibitors for *Pseudomonas aeruginosa* Infections and Elucidation of Binding Mode by SPR, STD NMR, and Molecular Docking

Elisabeth Weidel, Johannes C. de Jong, Christian Brengel, Michael P. Storz, Andrea Braunshausen, Matthias Negri, Alberto Plaza, Anke Steinbach, Rolf Müller, and Rolf W. Hartmann

Reprint with permission from *J. Med Chem.* **2013**, *56*(15), 6146-6155.

Copyright: © 2013 American Chemical Society.

#### Publikation A

#### Beitrag der Autorin zu Publikation A

Die Autorin plante und führte alle SPR Bindungsstudien durch. Zusätzlich trug sie signifikant zur SAR Diskussion bei, die auf Basis des erhaltenen Bindungsmechanismus stattfand. Des Weiteren war sie maßgeblich an der Planung des Konzeptes und am Schreiben des Manuskriptes beteiligt.

## Structure Optimization of 2-Benzamidobenzoic Acids as PqsD Inhibitors for *Pseudomonas aeruginosa* Infections and Elucidation of Binding Mode by SPR, STD NMR, and Molecular Docking

Elisabeth Weidel,<sup>‡,||,⊥</sup> Johannes C. de Jong,<sup>†,⊥</sup> Christian Brengel,<sup>†</sup> Michael P. Storz,<sup>†</sup> Andrea Braunshausen,<sup>†</sup> Matthias Negri,<sup>†</sup> Alberto Plaza,<sup>§</sup> Anke Steinbach,<sup>†</sup> Rolf Müller,<sup>§</sup> and Rolf W. Hartmann\*,<sup>†,‡,§</sup>

<sup>†</sup>Helmholtz-Institute for Pharmaceutical Research Saarland (HIPS), Department of Drug Design and Optimization, Campus C2.3, 66123 Saarbrücken, Germany

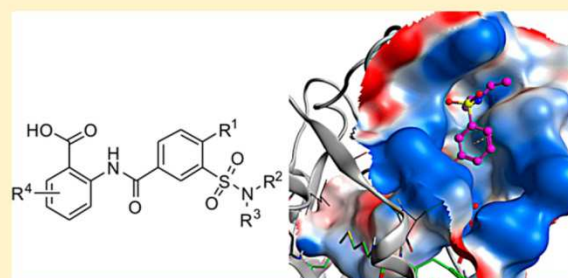
<sup>‡</sup>Pharmaceutical and Medicinal Chemistry, Saarland University, Campus C2.3, 66123 Saarbrücken, Germany

<sup>§</sup>Helmholtz-Institute for Pharmaceutical Research Saarland (HIPS), Department of Microbial Natural Products, Campus C2.3, 66123 Saarbrücken, Germany

<sup>||</sup>ElexoPharm GmbH, Im Stadtwald A1.2, 66123 Saarbrücken, Germany

### Supporting Information

**ABSTRACT:** *Pseudomonas aeruginosa* employs a characteristic *pqs* quorum sensing (QS) system that functions via the signal molecules PQS and its precursor HHQ. They control the production of a number of virulence factors and biofilm formation. Recently, we have shown that sulfonamide substituted 2-benzamidobenzoic acids, which are known FabH inhibitors, are also able to inhibit PqsD, the enzyme catalyzing the last and key step in the biosynthesis of HHQ. Here, we describe the further optimization and characterization of this class of compounds as PqsD inhibitors. Structural modifications showed that both the carboxylic acid *ortho* to the amide and 3'-sulfonamide are essential for binding. Introduction of substituents in the anthranilic part of the molecule resulted in compounds with IC<sub>50</sub> values in the low micromolar range. Binding mode investigations by SPR with wild-type and mutated PqsD revealed that this compound class does not bind into the active center of PqsD but in the ACoA channel, preventing the substrate from accessing the active site. This binding mode was further confirmed by docking studies and STD NMR.



### INTRODUCTION

The Gram-negative bacterium *Pseudomonas aeruginosa* is an opportunistic pathogen that is commonly associated with hospital-acquired life-threatening infections. Especially, patients with severe burns and immunocompromised individuals,<sup>1</sup> like those undergoing chemotherapy or having HIV/AIDS,<sup>2</sup> are highly susceptible to infections with *P. aeruginosa*. A wide variety of infection sites can be observed, such as ocular, ear, urinary tract, bloodstream, skin and soft tissue infections, and hospital-acquired pneumonia. Furthermore, it is the dominant cause of chronic lung infections in the majority of people with cystic fibrosis (CF).<sup>3–5</sup> Because of the high intrinsic resistance of *P. aeruginosa* to many antimicrobial agents, antimicrobial therapy is challenging. The resistance arises from the combination of low outer membrane permeability and resistance mechanisms such as efficient multidrug efflux pumps and β-lactamases.<sup>6</sup> Treatment is further hampered when the bacterium is growing in biofilms.<sup>7,8</sup> As a consequence, infections caused by bacterial biofilms are generally chronic and

very difficult to eradicate.<sup>9</sup> Because of the rising levels of resistance to conventional antibiotics, there is an urgent need for new therapeutic options.

The production of several virulence factors as well as biofilm formation<sup>10,11</sup> is coordinated by a cell density dependent mechanism termed quorum sensing (QS) using a number of QS signal molecules.<sup>12,13</sup> This mechanism of communication enables bacteria to coordinate the regulation of gene expression with subsequent effects on metabolism, protein synthesis, and virulence.<sup>14</sup> Three different QS systems are known for *P. aeruginosa*. The *las*<sup>15,16</sup> and *rhl*<sup>17,18</sup> systems use 3-oxo-C12-HSL (*N*-(3-oxododecanoyl) homoserine lactone) and C4-HSL (*N*-butyryl homoserine lactone), respectively, as signal molecules, whereas the *pqs* system utilizes the 2-heptyl-3-hydroxy-4(1*H*)-quinolone, called *Pseudomonas* quinolone signal (PQS) and its immediate precursor 2-heptyl-4-quinolone (HHQ).<sup>19,20</sup> Both

Received: April 29, 2013

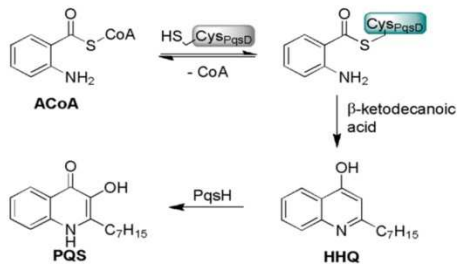
Published: July 8, 2013



PQS and HHQ bind to the transcriptional regulator PqsR, the receptor of the *pqs* system. Among other factors, this system is involved in the regulation of multiple virulence determinants<sup>21,22</sup> such as elastase, rhamnolipids, and pyocyanin and also influences biofilm formation.<sup>23,24</sup> Therefore, PqsD is considered as an attractive therapeutic target for drug development and treatment of *P. aeruginosa* infections. It is believed that disrupting the cell-to-cell communication instead of killing the bacteria will result in less selective pressure than with conventional antibacterial agents such as antibiotics<sup>25</sup> and thus will circumvent the problem of resistance.

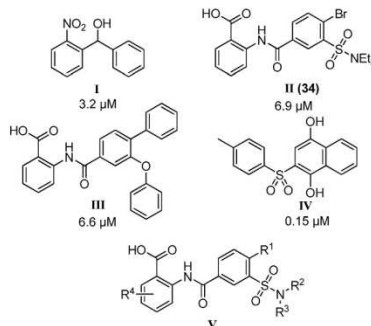
Using a ligand-based approach, we developed the first highly potent competitive PqsR antagonists, which were able to reduce the production of the virulence factor pyocyanin.<sup>26,27</sup> As HHQ and PQS activate PqsR, inhibition of their synthesis should lead to a decrease of virulence factor production without interfering with bacterial growth.<sup>28,29</sup> PqsD is an essential enzyme in the biosynthesis of HHQ and PQS as it catalyzes the last step in HHQ formation, the condensation of anthraniloyl-CoA (ACoA) with  $\beta$ -ketodecanoic acid (Scheme 1).<sup>30</sup>

**Scheme 1. Biosynthesis of Signal Molecules HHQ and PQS**



Recently, we have shown for the first time that inhibition of PqsD with a small molecule (compound I, Scheme 2) leads to a

**Scheme 2. Structures of the PqsD Inhibitor I and the FabH Inhibitors II, III, and IV As Well As the According PqsD IC<sub>50</sub> Values (V Represents the General Structure of Synthesized Compounds)**



strong reduction of extracellular HHQ and PQS levels and a significant reduction of biofilm volume.<sup>31</sup> Structurally, PqsD most closely resembles  $\beta$ -ketoacyl-ACP synthase (FabH), having the same catalytic triad consisting of Cys112, His257, and Asn287. Therefore, we postulated that inhibitors of FabH might also act as PqsD inhibitors. For three FabH inhibitors (compound II, III, and IV, Scheme 2),<sup>30,32,33</sup> two of them were

anthranilic acid derived, we could demonstrate that they indeed inhibit PqsD.

In the current work, we report about the optimization of compound II for which a series of 3-sulfonamide substituted benzamido benzoic acids (general structure V) were synthesized. The binding mode of the potent inhibitors was investigated using surface plasmon resonance spectroscopy (SPR), molecular docking studies, and saturation transfer difference nuclear magnetic resonance (STD NMR).

## ■ RESULTS AND DISCUSSION

**Chemistry.** Reaction of amines 1, 3, 7–8, and 11–12 with the appropriate acid chloride afforded the amides 2a, 4a, 9a–10a, and 13a–14a (see Supporting Information). Subsequent basic hydrolysis of the carboxylic ester groups yielded the corresponding acids 2, 4, 9–10, and 13–14. Carboxamide 6 was prepared from 2-aminobenzamide (5) and 3-(*N,N*-diethylsulfamoyl)benzoyl chloride (Scheme 3).

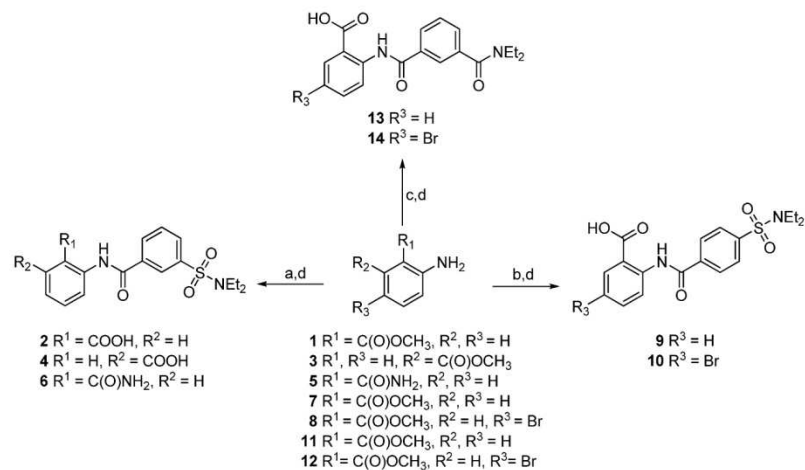
As outlined in Scheme 4, the synthesis of 3-sulfamoylbenzoic acids 22–33 started from *para*-substituted benzoic acids 15–17, which were converted into 3-(chlorosulfonyl)benzoic acids 18–20 by reaction with chlorosulfonic acid at 100 °C in 82–88% yield.

Compound 21 was commercially available. The sulfonyl chlorides 18–21 were then reacted with ammonia or a secondary amine to afford 3-sulfamoylbenzoic acids 22–33. Reaction of the carboxylic acids with thionyl chloride, either in dichloromethane at room temperature or in toluene at 80 °C, gave the corresponding acid chlorides, which were reacted under standard conditions with the methyl ester of anthranilic acids. The resulting compounds 34a–52a and 57a–64a (see Supporting Information) were hydrolyzed with a mixture of 1N NaOH (aq), MeOH, and THF, yielding the corresponding 2-(3'-(sulfamoyl)benzamido) benzoic acids 34–52 and 57–64. Phenyl substituted compounds 53–56 were obtained in 60–76% yield by means of a Suzuki reaction of methyl 5-bromo-2-(3-(*N,N*-diethylsulfamoyl) benzamido) benzoate (43a) with phenylboronic acids. Under the reaction conditions used, the intermediate methyl esters were already hydrolyzed to the desired carboxylic acids.

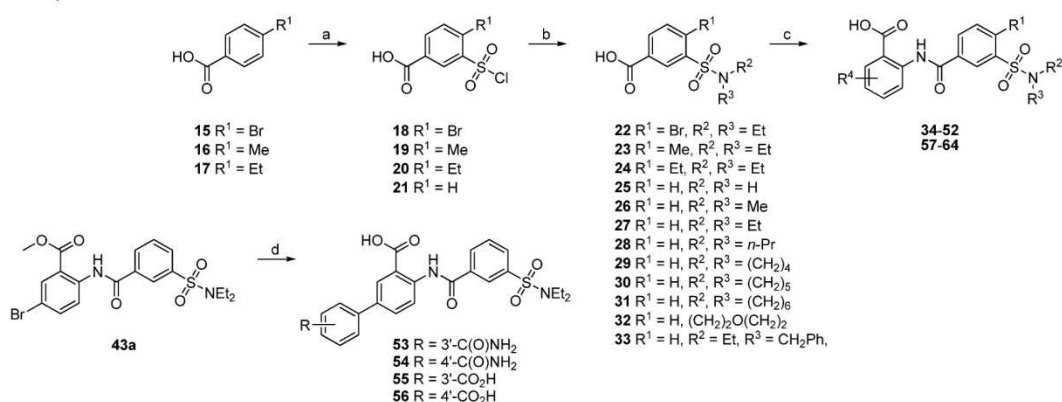
**PqsD Inhibition.** To investigate the importance of the carboxylic acid and the sulfonamide moiety of the 3'-sulfonamide substituted benzamido benzoic acids (general structure V), 2-(3'-(*N,N*-diethylsulfamoyl)benzamido) benzoic acid (2) and two regioisomers (4 and 9) were synthesized. Furthermore, the carboxylic acid and sulfonamide were replaced by a carboxamide (6 and 13, Scheme 5).

Compound 2 lacking the Br substituent showed reduced activity compared to 34 ( $IC_{50} = 19.8$  vs  $6.9 \mu\text{M}$ ). The carboxylic acid *ortho* to the NH turned out to be essential for activity. Changing the position of the carboxylic acid to the *meta* position (4) as well as replacement with a carboxamide (6) led to a dramatic loss in activity. Shifting the *N,N*-diethylsulfamoyl group from 3'-position to 4'-position<sup>34</sup> (9) also resulted in reduced activity, whereas replacement with an *N,N*-diethylcarboxamide (13) gave an inactive compound. As the structure of compound 2, having a carboxylic group next to the amide and with the sulfonamide in 3'-position, seemed to be optimal, we turned our attention to the introduction of additional substituents on both aromatic rings (Table 1).

**Binding Mode Characterization. SPR Measurements.** To gain some insight into the binding mode of the potent inhibitors SPR experiments were performed. At first,

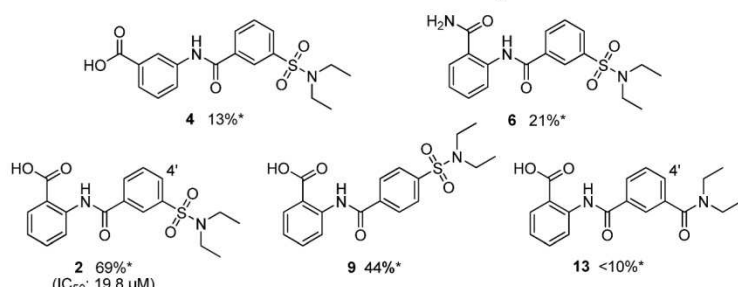
Scheme 3. Reaction of Benzoyl Chlorides with Methyl Aminobenzoates and 2-Aminobenzamide<sup>a</sup>

<sup>a</sup>Reagents and conditions: (a) 3-(N,N-diethylsulfamoyl)benzoyl chloride **1**, **3**, K<sub>2</sub>CO<sub>3</sub>, N-methylimidazole, TMEDA, CH<sub>3</sub>CN; **5**, toluene; (b) 4-(N,N-diethylsulfamoyl)benzoyl chloride, K<sub>2</sub>CO<sub>3</sub>, N-methylimidazole, TMEDA, CH<sub>3</sub>CN; (c) 3-(diethylcarbamoyl)benzoyl chloride, K<sub>2</sub>CO<sub>3</sub>, N-methylimidazole, TMEDA, CH<sub>3</sub>CN; (d) 1N NaOH (aq), MeOH, THF (not **S**).

Scheme 4. Synthesis of 3'-Sulfonamide Substituted Benzamidobenzoic Acids and Their Intermediates<sup>a</sup>

<sup>a</sup>Reagents and conditions: (a) ClSO<sub>3</sub>H, 100 °C, overnight; (b) HNR<sup>2</sup>R<sup>3</sup>, CH<sub>2</sub>Cl<sub>2</sub>; (c) (i) SOCl<sub>2</sub>, DMF (cat.), CH<sub>2</sub>Cl<sub>2</sub>, overnight or SOCl<sub>2</sub>, DMF (cat.), toluene, 80 °C, 4h; (ii) methyl anthranilate; (iii) 1N NaOH (aq), MeOH, THF, rt; (d) phenylboronic acid, cesium carbonate, DME/water 1/1, 100 °C, 3.5 h.

Scheme 5. Influence of Sulfonamide and Benzoic Acid Modifications on PqsD Inhibition



compounds **43** and **48** were tested in absence of ACoA and strong interactions with PqsD were observed (Figure 1A). In a second experiment, the PqsD loaded sensor chip was first treated with ACoA. Nucleophilic attack of Cys112 to the thioester of ACoA and subsequent elimination of CoA is

known to result in an anthranilate–PqsD complex,<sup>35</sup> in which the catalytic center is occupied by the covalent bound anthranilate. Subsequent injection of compounds **43** and **48** resulted in Figure 1B, showing comparable signals for the ACoA-treated and the -untreated PqsD. This indicates that the

**Table 1.** PqsD Inhibition by Compounds 10, 14, and 2-(3'-Sulfamoyl)benzamido Acids 2 and 34–64<sup>a</sup>

Compd	R <sup>1</sup>	R <sup>2</sup>	R <sup>3</sup>	IC <sub>50</sub> (μM)
2	H	3'-SO <sub>2</sub> NEt <sub>2</sub>		19.8 ± 4.5
34	H	4'-Br, 3'-SO <sub>2</sub> NEt <sub>2</sub>		6.9 ± 0.8
35	H	4'-Me, 3'-SO <sub>2</sub> NEt <sub>2</sub>		27.3 ± 1.9
36	H	4'-Et, 3'-SO <sub>2</sub> NEt <sub>2</sub>		39%*
37	4-Cl	3'-SO <sub>2</sub> NEt <sub>2</sub>		9.4 ± 1.3
38	4-F	3'-SO <sub>2</sub> NEt <sub>2</sub>		8.0 ± 1.2
39	4-NO <sub>2</sub>	3'-SO <sub>2</sub> NEt <sub>2</sub>		6.3 ± 1.1
40	5-Me	3'-SO <sub>2</sub> NEt <sub>2</sub>		18.4 ± 3.2
41	5-CF <sub>3</sub>	3'-SO <sub>2</sub> NEt <sub>2</sub>		12.4 ± 3.0
42	5-F	3'-SO <sub>2</sub> NEt <sub>2</sub>		11.4 ± 1.9
43	5-Br	3'-SO <sub>2</sub> NEt <sub>2</sub>		9.9 ± 2.1
44	5-CN	3'-SO <sub>2</sub> NEt <sub>2</sub>		26.2 ± 10.4
45	5-NO <sub>2</sub>	3'-SO <sub>2</sub> NEt <sub>2</sub>		8.9 ± 1.8
10	5-Br	4'-SO <sub>2</sub> NEt <sub>2</sub>		13.0 ± 1.8
14	5-Br	3'-C(O)NEt <sub>2</sub>		25.5 ± 5.5
46	5-F	4'-Br, 3'-SO <sub>2</sub> NEt <sub>2</sub>		6.6 ± 0.1
47	5-Br	4'-Br, 3'-SO <sub>2</sub> NEt <sub>2</sub>		3.8 ± 1.0
48	5-Ph	3'-SO <sub>2</sub> NEt <sub>2</sub>		3.0 ± 0.7
49	6-OMe	3'-SO <sub>2</sub> NEt <sub>2</sub>		44 %*
50	6-Cl	3'-SO <sub>2</sub> NEt <sub>2</sub>		39.0 ± 1.9
51	6-F	3'-SO <sub>2</sub> NEt <sub>2</sub>		24.9 ± 4.0
52	6-OH	3'-SO <sub>2</sub> NEt <sub>2</sub>		1.2 ± 0.1
53		3'-SO <sub>2</sub> NEt <sub>2</sub>	3"-C(O)NH <sub>2</sub>	3.8 ± 0.4
54		3'-SO <sub>2</sub> NEt <sub>2</sub>	4"-C(O)NH <sub>2</sub>	1.9 ± 0.1
55		3'-SO <sub>2</sub> NEt <sub>2</sub>	3"-CO <sub>2</sub> H	1.5 ± 0.3
56		3'-SO <sub>2</sub> NEt <sub>2</sub>	4"-CO <sub>2</sub> H	2.7 ± 0.3
57	H	3'-SO <sub>2</sub> NH <sub>2</sub>		43.6 ± 1.3
58	H	3'-SO <sub>2</sub> NMe <sub>2</sub>		35%*
59	H	3'-SO <sub>2</sub> N( <i>n</i> -Pr) <sub>2</sub>		5.4 ± 1.0
60	H			47%*
61	H			14.4 ± 2.4
62	H			14.8 ± 2.4
63	H			16%*
64	H			16.5 ± 3.8

<sup>a</sup>Data shown are mean ± SD, n = 3. \*Inhibition at 50 μM.

compounds do not occupy the catalytic site of PqsD. These results are in contrast to what was observed for the sulfone (**IV**) (Figure 1C, D). Performing the experiment in the same way, no signal for **IV** was observed when injected after preincubation with ACoA, indicating that this compound is competing with anthranilate for the same binding site.

This also means that the two inhibitor classes have different modes of action: compound **IV** is competing with the catalytic triad, whereas the anthranilic acid derivatives are “channel blockers”. Another SPR experiment was performed by inverting the compound order. PqsD was preincubated with **48**, and ACoA was injected subsequently. The finding that in contrast to the untreated surface no binding of ACoA to PqsD was observed indicates that **48** blocks the ACoA channel and prevents ACoA from reaching its binding site.

Further support for this mode of action comes from our screening assay. In the standard procedure, purified PqsD was first incubated with test compound. After 10 min, ACoA and β-ketodecanoic acid were added and the enzyme activity was

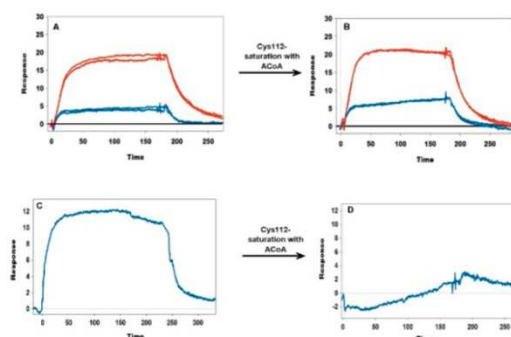


**Figure 1.** SPR binding studies of compounds **43**, **48**, and **IV**. (A) Binding of **43** (blue) and **48** (red) to PqsD. (B) Binding of **43** (blue) and **48** (red) after pretreatment of the chip with ACoA, which results in a covalent anthranilate–Cys112–PqsD complex with part of the active site being blocked. (C, D) Same experiments performed with **IV**.

monitored by measuring the amount of HHQ being formed during 40 min reaction time. In a modified assay procedure, a 30 min preincubated enzyme/ACoA mixture was first added to the test compound. After 10 min, the reaction was started by addition of β-ketodecanoic acid and the enzyme activity was monitored as mentioned before. In contrast to experiments with compound **IV**, very similar IC<sub>50</sub> values were observed in both settings, indicating that the benzamidobenzoic acids do not compete in the active site of PqsD with the covalently bound anthranilate (Table 2).

**Table 2.** Comparison of IC<sub>50</sub> Values Obtained with Standard Procedure (SP) and Modified Procedure (MP)<sup>a</sup>

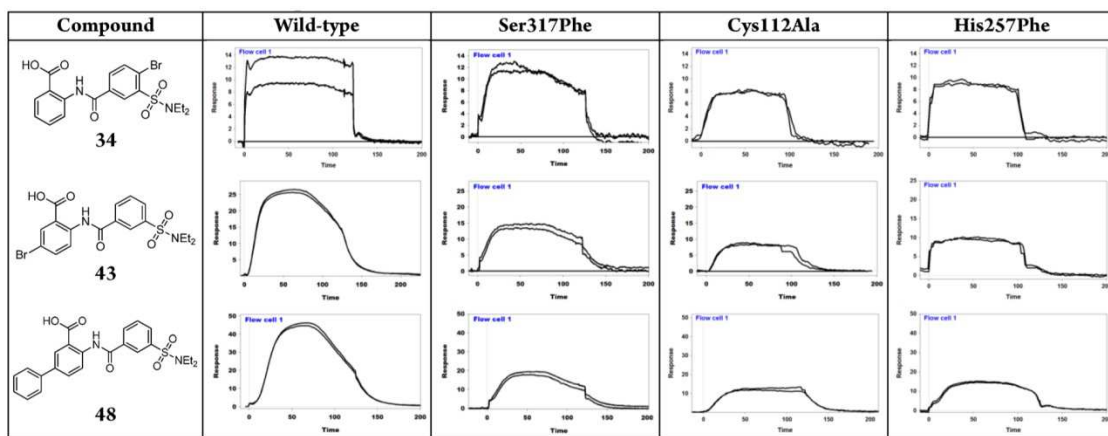
Compd	IC <sub>50</sub> [μM] SP	IC <sub>50</sub> [μM] MP
<b>IV</b>	0.15 ± 0.1	1.1 ± 0.1
<b>2</b>	19.8 ± 4.5	19.4 ± 0.8
<b>43</b>	9.9 ± 2.1	7.0 ± 0.4
<b>48</b>	3.0 ± 0.7	4.2 ± 0.3
<b>52</b>	1.2 ± 0.1	1.1 ± 0.2
<b>55</b>	1.5 ± 0.3	1.6 ± 0.1
<b>56</b>	2.7 ± 0.3	2.0 ± 0.2
<b>64</b>	16.5 ± 3.8	12.9 ± 0.1

<sup>a</sup>Data shown are mean ± SD, n = 3.

For further binding mode investigation, additional SPR experiments were performed with compounds **34**, **43**, and **48** differing in the size of the substituents in position 5 of the anthranilate. To investigate how deep they reach into the channel, the compounds were tested on wild-type and on three PqsD mutants in which active site residues were exchanged (Ser317Phe, Cys112Ala, and His257Phe). Notably, different binding behaviors were observed. For compound **34**, no differences in binding signals were seen, indicating that the binding is not influenced by the amino acid exchanges. Increasing the size of the substituent (H to Br, **43**) resulted in slightly decreased binding signals compared to wild-type PqsD. This observation is more pronounced for compound **48**, where the additional phenyl ring leads to strongly reduced binding signals (Table 3).

These results suggest that bulky substituents on the anthranilate are likely to reach the active center potentially interacting with Ser317, Cys112, and His257. The decreased

**Table 3.** SPR Based Binding Studies with Wild-Type and Mutated PqsD (Ser317Phe, Cys112Ala, and His257Phe) for Compounds 34, 43, and 48 ( $n = 2$ )



binding signals observed in the mutants might either be due to missing interactions caused by amino acid replacement or due to conformational changes in the active site. The fact that the three investigated compounds are differently influenced by the amino acid exchanges is very likely to be caused by the size of the substituents the more bulky ones reaching deeper into the catalytic center.

**Docking Studies.** To rationalize the SPR experiments and to establish a basis to explain the SAR of the PqsD inhibitors, molecular docking studies were performed with selected compounds. For compound **2**, three main binding clusters were found all localized within the ACoA channel (Figure 2 and Supporting Information). In binding mode I (Figure 2I), **2** is placed deep into the channel: it is stabilized by hydrogen bonds to Cys112 (carboxylic acid) and Arg262 (sulfonamide oxygens), CH- $\pi$  interactions to Leu193 (anthranilic ring) and Asn260 (*N,N*-diethylsulfonamidebenzene moiety), and hydrophobic interactions with further amino acids. In binding mode II (Figure 2II), the inhibitor is placed more central in the channel: hydrogen bonds are formed to Asn287 (carboxylic acid) and Arg36/Arg223 (sulfonamide oxygens),  $\pi$ -stackings to Pro259/Met225 (anthranilic ring) and Met220 and Arg262 (sulfonamidebenzene), and additional hydrophobic interactions. In mode III (Figure 2III), **2** is rotated 180°, placing the anthranilic ring at the channel entrance: the carboxylic acid binds to Arg262 and Arg36, while CH- $\pi$  interactions with Thr37, Pro259, and Ile263 stabilize the aromatic scaffold. The *N,N*-diethyl group is buried into the catalytic center, forming hydrophobic interactions.

In the most common pose of compound **48**, the phenyl ring in position 5 is sandwiched between Met225 and Pro259, as seen for the anthranilic ring of compound **2** in binding mode II. The rest of the molecule is slightly pushed outward (Figure 3 and Supporting Information Figure S1), with the anthranilate forming hydrogen bonds to Arg262, Asn154, or Asn260. In contrast to compound **2**, no hydrogen bonds are found to the sulfonamide oxygens.  $\pi$ -Stacking with Phe226 (anthranilic ring) and Phe32 (diethyl-sulfonamide-benzene) and hydrophobic interactions (Supporting Information Figure S1) further stabilize the inhibitor.

For compound **48**, a dissociation constant ( $K_D$ ) of 5.2  $\mu\text{M}$  was determined by ITC (Figure 4). An explanation for these results could be that the main interactions for this compound

are hydrophobic. The low value of enthalpy could be due to a desolvation penalty ( $\Delta G = -7.2 \text{ kcal/mol}$ ,  $\Delta H = -2.3 \text{ kcal/mol}$ ,  $-\Delta S = -5.0 \text{ kcal/mol}$ ). In two of the PqsD structures (PDB IDs 3H76 and 3H78), a water molecule is present bridging to the catalytic residues Cys112, His257, and Asn287. When this water molecule was included in the docking process as part of the protein, compound **52** was found deeper in the channel. The OH group forms an intramolecular hydrogen bond to the carboxylic acid (maintaining its planarity), which binds to Asn287, but also interacts via the structural water molecule with Cys112 and His257 (Supporting Information Figure S2). This would explain the strong increase in activity and is further supported by the fact that for the methoxy derivative less than 50% inhibition at 50  $\mu\text{M}$  is observed.

**STD NMR Studies.** To identify the orientation and mode of binding to PqsD, we recorded saturation transfer difference (STD) NMR<sup>36</sup> spectra of **2**, **48**, **52**, and **64** in the presence of PqsD (Figure 5 and Supporting Information S4–S7). STD NMR is a powerful technique that allows the precise definition of binding epitopes on small molecule ligands. Samples contained an 80-fold excess of the compounds relative to PqsD with respective concentrations of 0.8 mM and 10  $\mu\text{M}$  were recorded at 298 K. As seen in Figure 5 for compound **2**, normalization of the signal of greatest intensity (H-6) in the difference spectrum (red) to the one of the reference spectrum (black) showed signals for the anthranilate protons H-5 (95%), H-4 (86%), and H-3 (81%) to display the strongest enhancements. Signals for the benzene protons H-2' and H-4', H-5', and H-6' showed enhancements of ~70%, while significantly reduced enhancements were observed for the methylene (42%) and methyl protons (39%, Supporting Information Figure S4). These results indicate that the protons of the anthranilate ring of **2** are in closer contact to the protein.

Similar epitope binding profiles were observed for **52**, where once again the anthranilate protons showed the strongest enhancements (Supporting Information Figure S5). The STD NMR spectrum of **64** in the presence of PqsD (Supporting Information Figure S6) displayed the strongest enhancements for anthranilate protons H-6 (100%), H-4 (99%), and H-3 (90%) for benzene proton H-5' (93%) and for the N-benzylidene proton H-4'' (90%). It is worthwhile to note that enhancements of 87 and 80% were observed for methylene protons H-

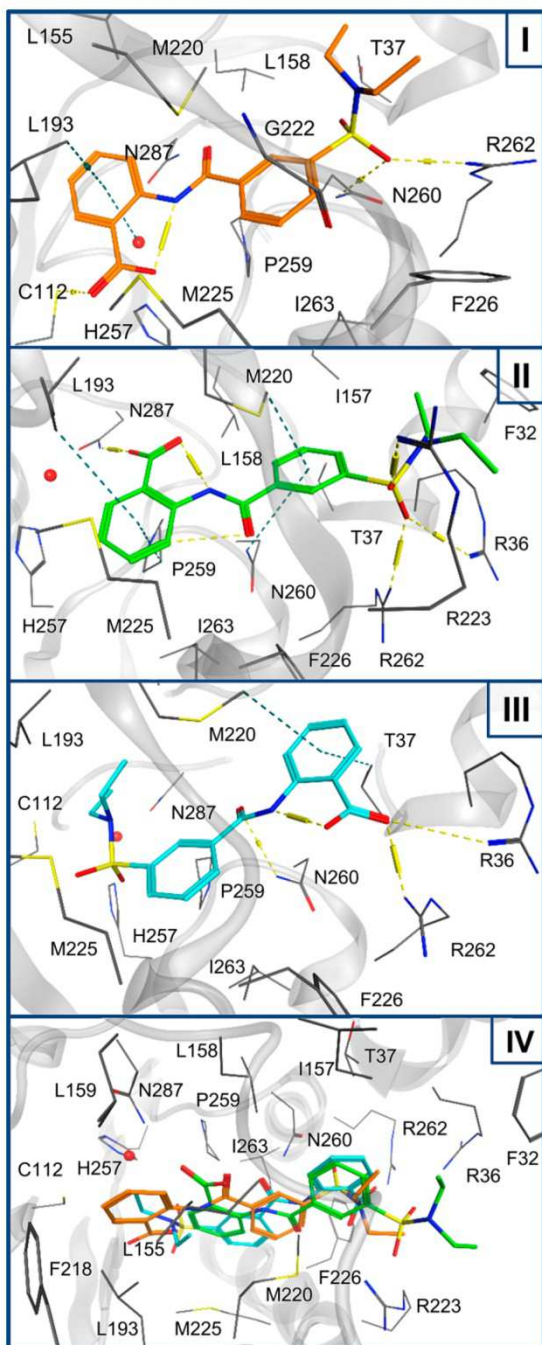


**Figure 2.** Three main binding modes I, II, and III of compound 2 in the ACoA channel of PqsD and (IV) superimposition of the three main binding modes of compound 2 shown as orange (binding mode I), green (binding mode II), and cyan (binding mode III) sticks. The main interacting amino acids are shown as lines, and key interactions are highlighted as dotted lines (polar in yellow, hydrophobic in dark cyan).

$1''$  and methyl protons H-2, respectively. The spectra of **2**, **52**, and **64** revealed a similar binding mode for all compounds, which is independent of the substitution on the anthranilic acid

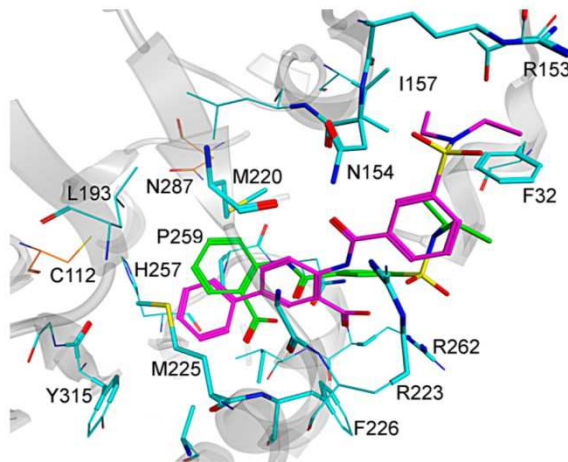


**Figure 3.** Docking pose of compound 2 (binding mode II, green) and 48 (magenta).

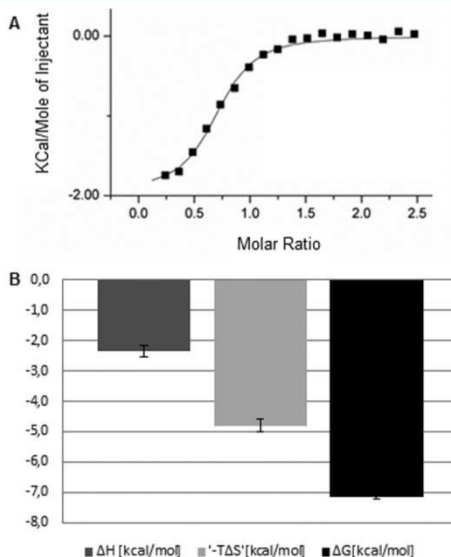


**Figure 4.** ITC experiments with compound 48 and wild-type PqsD. (A) Integrated heats (black squares) plotted against the molar ratio of the reactants. (B) Thermodynamic profile of 48. Data shown are mean  $\pm$  SD,  $n = 3$ .

ring or on the sulfonamide moiety. Low signal-to-noise ratio and spectral overlap did not allow to integrate individual peaks corresponding to the benzene protons of **48** in the STD NMR spectrum (Supporting Information Figure S7). However, it was clear that the benzene protons together with the methylene protons showed the highest intensities.

The results of SPR, STD NMR, and docking as presented are consistent with binding mode II, where the methylene protons are within van der Waals contact distances (2.5–3.5 Å) to Pro259 and Met225. In particular, the SPR experiment with ACoA injection after pretreatment with inhibitor clearly speaks in favor of a channel-blocking mechanism for these inhibitors. Further, NMR results exclude binding mode III, where the anthranilic ring is almost exposed at the entrance of the ACoA channel (no correspondence between the intense signals and

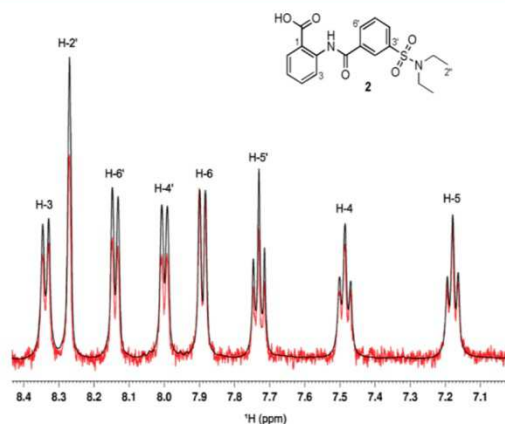


**Figure 5.** Reference (black) and STD NMR difference (red) spectra of **2** in complex with PqsD. Samples contained an 80-fold excess of the compounds relative to PqsD with respective concentrations of 0.8 mM and 10  $\mu$ M were recorded at 298 K. Overlaid spectra were normalized to the signal for H-6 ( $\delta$  7.90), which gave the strongest enhancement.

close enough residues), and disfavor binding mode I, where the methyl groups are predicted to be in closer contact to the protein.

**SAR Discussion.** From binding mode II of **2**, it becomes apparent that an important interaction partner is the carboxylic acid group in *ortho* position to the NH, which forms hydrogen bonds with Asn 287. Shifting to *meta* position (**4**) as well derivatization to carboxamide (**6**) strongly reduces activity (Scheme 5), as this interaction can no longer be sustained. Also of high importance is the 3-position of the *N,N*-diethylsulfamoyl group to perfectly fit into the channel and which must not be exchanged by *N,N*-diethylcarboxamide as only the sulfur oxygens can establish hydrogen bonds with Arg 36 and Arg 223 (compounds **9** and **13**, respectively, Scheme 5).

The finding that the sulfonamides lacking the diethyl residues (**57–64**) exhibit weak or no inhibition can be explained by the strong interactions between the methylene and methyl protons with the protons of the protein as shown in the NMR experiments. Introduction of substituents in **2** resulted in different effects which are in accordance with the proposed binding mode II. An example is the Br substitution *ortho* to the sulfonamide group, which showed improved binding (**34, 46–47**) compared to the unsubstituted parent compounds. In binding mode II, the benzene ring is oriented in a way in which the Br can build orthogonal halogen bonds with amino acids of the protein backbone, for example, with Arg36 and Thr37 (Supporting Information Figure S8). A reduced activity depending on the size of the substituents is observed when they were introduced into the 6-position of the anthranilic acid ring (**49–51**). This is possibly due to a steric interference with the carboxylic acid group, which in turn can no longer optimally interact with Asn287. **52** is an exception, where introduction of OH in 6-position leads to a high inhibitory activity. As shown above, a plausible reason for this could be the ability of the OH group to build a hydrogen bond network with the carboxylic acid group and the amino acid residues of the active site (ITC and docking results). The introduction of small substituents in 4 and 5 position of the anthranilic acid ring leads to increased PqsD inhibition (**37–47**). As shown in the SPR experiments with mutated PqsD, the docking results and NMR experiments

the anthranilic acid ring is oriented toward the active center, whereby substituents at positions 4 and 5 reach deeper into the channel and thus can form additional interactions. This effect is more pronounced for **48**, where a phenyl ring is attached in 5-position, leading to a slight shift in the binding mode compared to compound **2** (see above). Obviously, the gain in binding activity by the phenyl ring sandwiched between Met225 and Pro259 is higher than the loss of binding activity due to the missing interactions of the sulfonamide ethyl groups. The introduction of an amide or carboxylic acid group in *meta* or *para*-position (**53–56**) to address Asn 287 and His257, however, led only to slightly improved inhibition compared to the parent compound **48**.

## CONCLUSION

In summary, we synthesized a series of sulfonamide substituted 2-benzamidobenzoic acids which inhibit PqsD in the low  $\mu$ M range. The carboxylic acid was essential for activity. Systematic variation of substituents in 4- and 5-position of the 2-aminobenzoic acid part of the scaffold resulted in the most potent PqsD inhibitors. Activity was reduced significantly when substituents were introduced in 6-position. However, introduction of a hydroxyl group in this position resulted in a compound with increased potency ( $IC_{50} = 1.2 \mu$ M). SPR, ITC, modeling, and NMR experiments suggest these inhibitors to bind within the ACoA channel of PqsD, thereby acting as entropy-driven channel-blockers that prevent ACoA from reaching the catalytic site. Further biological evaluation of our compounds is under investigation.

## EXPERIMENTAL SECTION

**Chemical Synthesis. General Methods.** Chemicals were purchased from commercial sources and used without further purification.  $^1$ H NMR spectra were recorded on a Bruker DRX-500 (500 MHz) and a Bruker Fourier 300 (300 MHz) spectrometer. Chemical shifts are given in parts per million (ppm), with the solvent resonance as internal standard. Data are reported as follows: chemical shift, multiplicity (s = singlet, d = doublet, t = triplet, q = quartet, m = multiplet, bs = broad signal or as a combination of these, e.g. dd, dt, etc.), coupling constants (Hz), and integration.  $^{13}$ C NMR spectra were recorded on a Bruker DRX-500 (125 MHz) with complete proton decoupling. Chemical shifts are given in parts per million (ppm), with the solvent resonance as internal standard. Mass spectrometry (HPLC/MS) was performed on a MSQ electro spray mass spectrometer (Thermo Fisher). The system was operated by the standard software Xcalibur. A RP C18 NUCLEODUR 100–5 (125 mm  $\times$  3 mm) column (Macherey-Nagel GmbH) was used as stationary phase. The mobile phase was a mixture of CH<sub>3</sub>CN (0.1% TFA) and H<sub>2</sub>O (0.1% TFA). All solvents were HPLC grade. Flash chromatography was performed on silica gel 60, 70–230 mesh (Fluka), and the reaction progress was determined by thin-layer chromatography (TLC) analyses on silica gel 60, F<sub>254</sub> (Merck). Visualization was accomplished with UV light and staining with basic potassium permanganate (KMnO<sub>4</sub>). Melting points were determined in open capillaries using a SMP3 melting point apparatus of Bibby Sterilin Ltd. with a gradient of 2 °C/min. The reported yields are the actual isolated yields of purified material, unless stated otherwise, and are not optimized. Purities of all test compounds used in the biological assays were determined by HPLC/MS using the area percentage method on the UV trace recorded at a wavelength of 254 nm. All compounds were found to have  $\geq 95\%$  purity. Yields and characterization of all compounds are provided in the Supporting Information.

**General Procedure A for the Preparation of 3-Sulfamoylbenzoic Acids.** At 0 °C, the amine (30.0 mmol) was added to a stirred solution of 3-(chlorosulfonyl)benzoic acid (2.21 g, 10.0 mmol) in dichloromethane (25 mL). After stirring overnight at room temperature, 1N

HCl (aq, 25 mL) was added. The organic solvent was removed by evaporation under reduced pressure. The solid was isolated by suction filtration, washed thoroughly with water, and dried under reduced pressure at 50 °C.

**General Procedure B for the Preparation of 3-Sulfamoylbenzoyl Chlorides.** Thionyl chloride (2.9 mL, 40.0 mmol) was added slowly to a stirred solution of 3-sulfamoylbenzoic acid (4.00 mmol) in dichloromethane (25 mL) followed by 1–2 drops of DMF. After stirring overnight at room temperature, the solution was evaporated under reduced pressure. The crude 3-sulfamoylbenzoyl chloride was used without further purification.

**General Procedures C for the Preparation of 2-Benzamidobenzoic Acid Methyl Esters.** **Procedure C1.** 3-(*N,N*-Diethylsulfamoyl)-benzoyl chloride (1.00 mmol) was added to a stirred solution of anthranilic acid methyl ester (1.00 mmol) in pyridine (4 mL). After stirring overnight, the solvent was removed by evaporation under reduced pressure. The residue was stirred with 1N HCl (aq, 4 mL). The solid was isolated by suction filtration, washed with water, and heated briefly with a small amount of methanol. After cooling to room temperature, the product was isolated by suction filtration, washed with some methanol, and dried under reduced pressure at 50 °C.

**Procedure C2.** 3-(*N,N*-Diethylsulfamoyl)benzoyl chloride (1.50 mmol) was added to a stirred suspension of anthranilic acid methyl ester (1.00 mmol), potassium carbonate (207 mg, 1.50 mmol), *N*-methylimidazole (8 mg, 0.10 mmol), and *N,N,N',N'*-tetramethylethylenediamine (12 mg, 0.10 mmol) in acetonitrile (1 mL). After stirring for 2.5 h at room temperature, 1N HCl (aq) was added. The solid was isolated by suction filtration, washed thoroughly with water, and heated briefly with a small amount of methanol (2 mL). After cooling to room temperature, the product was isolated by suction filtration, washed with some methanol, and dried under reduced pressure at 50 °C.

**Procedure C3.** A solution of 3-(*N,N*-diethylsulfamoyl)benzoyl chloride (3.00 mmol) and anthranilic acid methyl ester (3.00 mmol) in toluene (10 mL) was heated to reflux for 1.5 h. The solvent was evaporated under reduced pressure, and the residue was heated briefly with a small amount of methanol. After cooling to room temperature, the solid was isolated by suction filtration, washed with some methanol, and dried under reduced pressure at 50 °C.

**General Procedure D for the Hydrolysis of 2-Benzamidobenzoic Acid Methyl Esters.** A mixture of 2-benzamidobenzoic acid methyl ester (1.30 mmol), THF/MeOH 2/1 (9 mL), and 1N NaOH (aq, 2.6 mL, 2.6 mmol) was stirred overnight at room temperature. 1N HCl (aq, 2.6 mL, 2.6 mmol) was added, and the solid was isolated by suction filtration, washed with water, and dried under reduced pressure.

**Procedure for the Synthesis of compound IV.** 1,4-Naphthoquinone (31.6 mmol) was dissolved in DCM (45 mL). Then TFA (2.45 mL) and *p*-toluenesulfonate (33.18 mmol) dissolved in water (30 mL) were added and the mixture was stirred for 1 h. Solid precipitates were obtained. The solution was purified over a column and stirred for additional 5 h. The solid was filtered off and washed several times with water and DCM.<sup>32,37</sup>

**Screening Assay Procedure for in Vitro PqsD Inhibition.** The assay was performed monitoring the enzyme activity by measuring the HHQ formation as described by Storz and co-workers.<sup>31</sup> Quantification of HHQ was performed analogous to Storz et al.,<sup>31</sup> but with some modifications: the flow rate amounted 750 μL/min and an Accucore RP-MS column, 150 mm × 2.1 mm, 2.6 μm (Thermo Scientific, Waltham, Massachusetts, USA), was used. All test compound reactions were performed in triplicate in three independent runs. In the modified protocol, PqsD and the first substrate were preincubated for 30 min prior to adding them to the test compounds. Then β-ketodecanoic acid was added, and the further steps were performed analogous to the standard protocol.

**Surface Plasmon Resonance.** SPR binding studies were performed using a Reichert SR7500DC instrument optical biosensor (Reichert Technologies, Depew, NY, USA) and CMD500 M sensor chips obtained from XanTec (XanTec Bioanalytics, Düsseldorf,

Germany). Scrubber software was used for processing and analyzing data.

**Preparation of PqsD Mutants.** Ser317Phe, Cys112Ala, and His257Phe PqsD mutants were generated using the QuikChange Site-Directed Mutagenesis Kit (Stratagene, La Jolla, CA) according to the manufacturer's instructions using the pET28b(+)/*pqsD* plasmid as a template. Briefly, *pqsD* gene was amplified through 16 cycles of PCR. After treatment with *Dpn*I, the PCR product was transformed into *Escherichia coli* strain XL1-Blue. Plasmid DNA was purified using the GenElute HP Plasmid Miniprep Kit (Sigma-Aldrich, St. Louis, MO) and sequenced to confirm the site-directed mutations. For the primer sequence of the mutations, see the Supporting Information.

**Expression and Purification of Recombinant PqsD Wild-Type and Mutants in E. coli.** *E. coli* BL21 (*λ*DE3) cells were transformed with plasmid harboring PqsD (PET28b(+)/*pqsD*).<sup>30</sup> Overexpression, purification, and storage of the His<sub>6</sub>-tagged PqsD was performed as described by Storz et al.<sup>31</sup> The expression and purification of recombinant PqsD used for the NMR studies is described in the Supporting Information

**Immobilization of His<sub>6</sub>-PqsD.** PqsD (38 kDa, >90% pure based on SDS-PAGE) was immobilized on a CMD500 M (carboxymethyl-dextran-coated) sensor chip at 12 °C analogous to the method described by Henn and co-workers.<sup>38</sup> The PqsD immobilization levels were 2217 RU for the binding studies with ACoA and 3085 RU in the mutagenesis studies to serve as reference. The PqsD mutants were immobilized analogous to the wild-type at densities of 6789 RU (Ser317Phe), 3903 RU (Cys112Ala), and 4272 RU (His257Phe).

**Binding Studies.** The binding studies were performed at a constant flow rate of 50 μL/min in instrument running buffer (50 mM MOPS, pH 8.0, 150 mM NaCl, 5% DMSO (v/v), 0.1% Triton-X 100 (v/v)). IV (100 μM), 43, and 48 (20 μM) were injected consecutively for 180 s association and 300 s dissociation times. Experiments were performed twice. In the second experiment, ACoA (100 μM) was injected for 40 min with a constant flow of 5 μL/min to reach saturation of the ACoA binding site. Afterward, the flow rate was increased to 50 μL/min (30 min) in order to flush all CoA away. Once the baseline signal was stable, additional ACoA (10 μM) was injected to ensure that the anthraniloyl binding site was completely saturated (no additional signal was observed). Afterward, IV (100 μM), 43, and 48 (20 μM) were consecutively injected.

In the experiment with inverted compound order, PqsD was preincubated with compound 48, therefore the compound was added to the running buffer (20 μM). The sensor chip surface was flushed for several hours at a constant flow rate of 50 μL/min until the baseline was stable. Afterward, the flow rate was decreased to 10 μL/min and ACoA was injected (100 μM) twice for 120 s association and 15 min dissociation. The binding studies with PqsD mutants were performed analogously to the wild-type experiments. The compounds were injected twice for 120 s association and 300 s dissociation time.

**Molecular Docking.** Molecular docking studies were performed by means of GOLD v5.0<sup>39,40</sup> using the CHEMPLP scoring function. One hundred runs per molecule were performed. Default GOLD parameters were used with carbons, halogens, and nonpolar sulfur atoms matching hydrophobic regions. All three 3D-structures of PqsD (PDB IDs 3H76, 3H77, 3H78) were used. For 3H77 (anthranilate-Cys112) and 3H78 (Ala112), the residue 112 of both chain A and B was mutated back into wild-type Cys112. Before docking geometry optimization of the enzymes has been performed using the LigX module of the Molecular Operating Environment (MOE).<sup>41</sup> The active site was determined including all residues within 8 Å of the cocrystallized ACoA molecule of 3H77.

**Saturation-Transfer Difference NMR.** Experiments were recorded with the carrier set at -2 ppm for on-resonance irradiation and 40 ppm for off-resonance irradiation. Control spectra were recorded under identical conditions on samples containing free compound 2 to test for artifacts. Selective protein saturation (2 s) was accomplished using a train of 50 ms Gauss-shaped pulses, each separated by a 1 ms delay, at an experimentally determined optimal power (60 dB on our probe); a T<sub>1ρ</sub> filter (25 ms) was incorporated to suppress protein resonances. Experiments were recorded using a minimum of 2048

scans and 32K points. On- and off-resonance spectra were processed independently and subtracted to provide a difference spectrum. The expression and purification of recombinant PqsD from *E. coli* for STD NMR analysis is described in the Supporting Information.

**Isothermal Titration Calorimetry.** ITC experiments were carried out using an ITC200 instrument (Microcal Inc., GE Healthcare). ITC measurements were routinely performed at 25 °C in PBS-buffer, pH 7.4, 10% glycerol (v/v), and 5% DMSO (v/v). The titrations were performed on 83–102 μM His<sub>6</sub>-PqsD in the 200 μL sample cell using 2 μL injections of 1.0 mM ligand solution every 180 s. Raw data were collected, and the area under each peak was integrated. To correct for heats of dilution and mixing, the final baseline consisting of small peaks of the same size at the end of the experiment was subtracted. The experimental data were fitted to a theoretical titration curve (one site binding model) using MicroCal Origin 7 software, with  $\Delta H$  (enthalpy change in kcal mol<sup>-1</sup>),  $K_A$  (association constant in M<sup>-1</sup>), and  $N$  (number of binding sites) as adjustable parameters. Thermodynamic parameters were calculated from equation;

$$\Delta G = \Delta H - T\Delta S = RT \ln K_A = -RT \ln K_D$$

where  $\Delta G$ ,  $\Delta H$ , and  $\Delta S$  are the changes in free energy, enthalpy, and entropy of binding, respectively,  $T$  is the absolute temperature, and  $R = 1.98 \text{ cal mol}^{-1} \text{ K}^{-1}$ . For compound **48**, four independent experiments were performed.

## ■ ASSOCIATED CONTENT

### Supporting Information

Additional figures docking study and STD NMR, ITC measurement, experimental details, biological methods, and compound characterizations. This material is available free of charge via the Internet at <http://pubs.acs.org>.

## ■ AUTHOR INFORMATION

### Corresponding Author

\*Phone: +49 681 302 70300. Fax: +49 681 302 70308. E-mail: rolf.hartmann@helmholtz-hzi.de.

### Present Address

#Syncrom, Kadijk 3, 9747 AT Groningen, The Netherlands.

### Author Contributions

<sup>†</sup>E.W. and J.C.d.J. contributed equally.

### Notes

The authors declare no competing financial interest.

## ■ ACKNOWLEDGMENTS

We thank Dr. Claudia Henn for preparing the Ser317Phe and His257Phe mutants of PqsD, Dr. Simon Lucas for the synthesis of compound **IV**, Simone Amann for her help in performing the PqsD assay, and Dr. Joseph Zapp for NMR analyses.

## ■ ABBREVIATIONS USED

ACoA, anthraniloyl-CoA; HHQ, 2-heptyl-4-quinolone; ITC, isothermal titration calorimetry; PQS, *Pseudomonas* quinolone signal; QS, quorum sensing; SPR, surface plasmon resonance; STD, saturation transfer difference

## ■ REFERENCES

- (1) Hakki, M.; Limaye, A. P.; Kim, H. W.; Kirby, K. A.; Corey, L.; Boeckh, M. Invasive *Pseudomonas aeruginosa* infections: high rate of recurrence and mortality after hematopoietic cell transplantation. *Bone Marrow Transplant.* **2007**, *39*, 687–693.
- (2) Asboe, D.; Gant, V.; Aucken, H. M.; Moore, D. A.; Umasankar, S.; Bingham, J. S.; Kaufmann, M. E.; Pitt, T. L. Persistence of *Pseudomonas aeruginosa* strains in respiratory infection in AIDS patients. *AIDS* **1998**, *12*, 1771–1775.
- (3) Govan, J. R. W.; Deretic, V. Microbial pathogenesis in cystic fibrosis: Muoid *Pseudomonas aeruginosa* and *Burkholderia cepacia*. *Microbiol. Rev.* **1996**, *60*, 539–574.
- (4) Gomez, M. I.; Prince, A. Opportunistic infections in lung disease: *Pseudomonas* infections in cystic fibrosis. *Curr. Opin. Pharmacol.* **2007**, *7*, 244–251.
- (5) Wagner, V. E.; Iglesias, B. H. *P. aeruginosa* Biofilms in CF Infection. *Clin. Rev. Allergy Immunol.* **2008**, *35*, 124–134.
- (6) Hancock, R. E. W.; Speert, D. P. Antibiotic resistance in *Pseudomonas aeruginosa*: mechanisms and impact on treatment. *Drug Resist. Updates* **2000**, *3*, 247–255.
- (7) Hoiby, N.; Bjarnsholt, T.; Givskov, M.; Molin, S.; Ciofu, O. Antibiotic resistance of bacterial biofilms. *Int. J. Antimicrob. Agents* **2010**, *35*, 322–332.
- (8) Ciofu, O.; Fussing, V.; Bagge, N.; Koch, C.; Hoiby, N. Characterization of paired mucoid/non-mucoid *Pseudomonas aeruginosa* isolates from Danish cystic fibrosis patients: antibiotic resistance, beta-lactamase activity and RiboPrinting. *J. Antimicrob. Chemother.* **2001**, *48*, 391–396.
- (9) Costerton, J. W.; Stewart, P. S.; Greenberg, E. P. Bacterial biofilms: a common cause of persistent infections. *Science* **1999**, *284*, 1318–1322.
- (10) Williams, P.; Camara, M.; Hardman, A.; Swift, S.; Milton, D.; Hope, V. J.; Winzer, K.; Middleton, B.; Pritchard, D. I.; Bycroft, B. W. Quorum sensing and the population-dependent control of virulence. *Philos. Trans. R. Soc., B* **2000**, *355*, 667–680.
- (11) Rumbaugh, K. P.; Griswold, J. A.; Hamood, A. N. The role of quorum sensing in the *in vivo* virulence of *Pseudomonas aeruginosa*. *Microb. Infect.* **2000**, *2*, 1721–1731.
- (12) Van Delden, C.; Iglesias, B. H. Cell-to-cell signaling and *Pseudomonas aeruginosa* infections. *Emerg. Infect. Dis.* **1998**, *4*, 551–560.
- (13) Swift, S.; Downie, J. A.; Whitehead, N. A.; Barnard, A. M. L.; Salmon, G. P. C.; Williams, P. Quorum sensing as a population-density-dependent determinant of bacterial physiology. *Adv. Microb. Physiol.* **2001**, *45*, 199–270.
- (14) Antunes, L. C. M.; Ferreira, R. B. R.; Buckner, M. M. C.; Finlay, B. B. Quorum sensing in bacterial virulence. *Microbiol. SGM* **2010**, *156*, 2271–2282.
- (15) Gambello, M. J.; Iglesias, B. H. Cloning and Characterization of the *Pseudomonas aeruginosa LasR Gene*, A Transcriptional Activator of Elastase Expression. *J. Bacteriol.* **1991**, *173*, 3000–3009.
- (16) Passador, L.; Cook, J. M.; Gambello, M. J.; Rust, L.; Iglesias, B. H. Expression of *Pseudomonas aeruginosa* Virulence Genes Requires Cell-to-Cell Communication. *Sci.* **1993**, *260*, 1127–1130.
- (17) Ochsner, U. A.; Koch, A.; Fiechter, A.; Reiser, J. Isolation and Characterization of a Regulatory Gene Affecting Rhamnolipid Biosurfactant Synthesis in *Pseudomonas aeruginosa*. *J. Bacteriol.* **1994**, *176*, 2044–2054.
- (18) Ochsner, U. A.; Reiser, J. Autoinducer-Mediated Regulation of Rhamnolipid Biosurfactant Synthesis in *Pseudomonas aeruginosa*. *Proc. Natl. Acad. Sci. U. S. A.* **1995**, *92*, 6424–6428.
- (19) Xiao, G. P.; Deziel, E.; He, J. X.; Lepine, F.; Lesic, B.; Castonguay, M. H.; Milot, S.; Tampakaki, A. P.; Stachel, S. E.; Rahme, L. G. MvfR, a key *Pseudomonas aeruginosa* pathogenicity LTTR-class regulatory protein, has dual ligands. *Mol. Microbiol.* **2006**, *62*, 1689–1699.
- (20) Pesci, E. C.; Milbank, J. B. J.; Pearson, J. P.; McKnight, S.; Kende, A. S.; Greenberg, E. P.; Iglesias, B. H. Quinolone signaling in the cell-to-cell communication system of *Pseudomonas aeruginosa*. *Proc. Natl. Acad. Sci. U. S. A.* **1999**, *96*, 11229–11234.
- (21) Déziel, E.; Gopalan, S.; Tampakaki, A. P.; Lépine, F.; Padfield, K. E.; Saucier, M.; Xiao, G. P.; Rahme, L. G. The contribution of MvfR to *Pseudomonas aeruginosa* pathogenesis and quorum sensing circuitry regulation: multiple quorum sensing-regulated genes are modulated without affecting lasRI, rhlRI or the production of *N*-acyl-L-homoserine lactones. *Mol. Microbiol.* **2005**, *55*, 998–1014.

- (22) Gallagher, L. A.; McKnight, S. L.; Kuznetsova, M. S.; Pesci, E. C.; Manoil, C. Functions required for extracellular quinolone signaling by *Pseudomonas aeruginosa*. *J. Bacteriol.* **2002**, *184*, 6472–6480.
- (23) Müsken, M.; Di Fiore, S.; Dötsch, A.; Fischer, R.; Häussler, S. Genetic determinants of *Pseudomonas aeruginosa* biofilm establishment. *Microbiology SGM* **2010**, *156*, 431–441.
- (24) Diggle, S. P.; Winzer, K.; Chhabra, S. R.; Chhabra, S. R.; Worrall, K. E.; Camara, M.; Williams, P. The *Pseudomonas aeruginosa* quinolone signal molecule overcomes the cell density-dependency of the quorum sensing hierarchy, regulates rhl-dependent genes at the onset of stationary phase and can be produced in the absence of LasR. *Mol. Microbiol.* **2003**, *50*, 29–43.
- (25) Hentzer, M.; Givskov, M. Pharmacological inhibition of quorum sensing for the treatment of chronic bacterial infections. *J. Clin. Invest.* **2003**, *112*, 1300–1307.
- (26) Klein, T.; Henn, C.; de Jong, J. C.; Zimmer, C.; Kirsch, B.; Maurer, C. K.; Pistorius, D.; Müller, R.; Steinbach, A.; Hartmann, R. W. Identification of Small-Molecule Antagonists of the *Pseudomonas aeruginosa* Transcriptional Regulator PqsR: Biophysically Guided Hit Discovery and Optimization. *ACS Chem. Biol.* **2012**, *7*, 1496–1501.
- (27) Lu, C. B.; Kirsch, B.; Zimmer, C.; de Jong, J. C.; Henn, C.; Maurer, C. K.; Müsken, M.; Häussler, S.; Steinbach, A.; Hartmann, R. W. Discovery of Antagonists of PqsR, a Key Player in 2-Alkyl-4-quinolone-Dependent Quorum Sensing in *Pseudomonas aeruginosa*. *Chem. Biol.* **2012**, *19*, 381–390.
- (28) Suga, H.; Smith, K. M. Molecular mechanisms of bacterial quorum sensing as a new drug target. *Curr. Opin. Chem. Biol.* **2003**, *7*, 586–591.
- (29) Rasmussen, T. B.; Givskov, M. Quorum-sensing inhibitors as anti-pathogenic drugs. *Int. J. Med. Microbiol.* **2006**, *296*, 149–161.
- (30) Pistorius, D.; Ullrich, A.; Lucas, S.; Hartmann, R. W.; Kazmaier, U.; Müller, R. Biosynthesis of 2-Alkyl-4(1*H*)-Quinolones in *Pseudomonas aeruginosa*: Potential for Therapeutic Interference with Pathogenicity. *ChemBioChem* **2011**, *12*, 850–853.
- (31) Storz, M. P.; Maurer, C. K.; Zimmer, C.; Wagner, N.; Brengel, C.; de Jong, J. C.; Lucas, S.; Müsken, M.; Häussler, S.; Steinbach, A.; Hartmann, R. W. Validation of PqsD as an Anti-biofilm Target in *Pseudomonas aeruginosa* by Development of Small-Molecule Inhibitors. *J. Am. Chem. Soc.* **2012**, *134*, 16143–16146.
- (32) Alhamadsheh, M. M.; Waters, N. C.; Sachdeva, S.; Lee, P.; Reynolds, K. A. Synthesis and biological evaluation of novel sulfonylnaphthalene-1,4-diols as FabH inhibitors. *Bioorg. Med. Chem. Lett.* **2008**, *18*, 6402–6405.
- (33) Nie, Z.; Perretta, C.; Lu, J.; Su, Y.; Margosiak, S.; Gajiwala, K. S.; Cortez, J.; Nikulin, V.; Yager, K. M.; Appelt, K.; Chu, S. S. Structure-based design, synthesis, and study of potent inhibitors of beta-ketoacylacyl carrier protein synthase III as potential antimicrobial agents. *J. Med. Chem.* **2005**, *48*, 1596–1609.
- (34) Larsen, S. D.; Hester, M. R.; Ruble, J. C.; Kamilar, G. M.; Romero, D. L.; Wakefield, B.; Melchior, E. P.; Sweeney, M. T.; Marotti, K. R. Discovery and initial development of a novel class of antibacterials: Inhibitors of *Staphylococcus aureus* transcription/translation. *Bioorg. Med. Chem. Lett.* **2006**, *16*, 6173–6177.
- (35) Bera, A. K.; Atanasova, V.; Robinson, H.; Eisenstein, E.; Coleman, J. P.; Pesci, E. C.; Parsons, J. F. Structure of PqsD, a *Pseudomonas* Quinolone Signal Biosynthetic Enzyme, in Complex with Anthranilate. *Biochemistry* **2009**, *48*, 8644–8655.
- (36) Mayer, M.; Meyer, B. Group epitope mapping by saturation transfer difference NMR to identify segments of a ligand in direct contact with a protein receptor. *J. Am. Chem. Soc.* **2001**, *123*, 6108–6117.
- (37) Bruce, J. M.; Lloydwilliams, P. Benzoquinones and Related Compounds 0.6. Addition of Benzenesulfonic Acid to Substituted 1,4-Quinones. *J. Chem. Soc., Perkin Trans. 1* **1992**, 2877–2884.
- (38) Henn, C.; Boettcher, S.; Steinbach, A.; Hartmann, R. W. Catalytic enzyme activity on a biosensor chip: combination of surface plasmon resonance and mass spectrometry. *Anal. Biochem.* **2012**, *428*, 28–30.
- (39) Jones, G.; Willett, P.; Glen, R. C.; Leach, A. R.; Taylor, R. Development and validation of a genetic algorithm for flexible docking. *J. Mol. Biol.* **1997**, *267*, 727–748.
- (40) Verdonk, M. L.; Cole, J. C.; Hartshorn, M. J.; Murray, C. W.; Taylor, R. D. Improved protein–ligand docking using GOLD. *Proteins: Struct., Funct., Genet.* **2003**, *52*, 609–623.
- (41) *Molecular Operating Environment (MOE)*, 2010.10; Chemical Computing Group Inc.: Sherbrooke St. W, S. M., Quebec H3A 2R7, Canada, 2010.

### 3.2 Biochemical and Biophysical Analysis of a Chiral PqsD Inhibitor Revealing Tight-Binding Behavior and Enantiomers with Contrary Thermodynamic Signatures

Michael P. Storz, Christian Brengel, Elisabeth Weidel, Michael Hoffmann, Klaus Hollemeyer, A. Steinbach, Rolf Müller, Martin Empting, and Rolf W. Hartmann

Reprint with permission from *ACS Chem. Biol.* **2013**, 8(12), 2794-2801.

Copyright: © 2013 American Chemical Society.

#### Publikation B

#### Beitrag der Autorin zu Publikation B

Die Autorin plante und führte die SPR Bindungsstudien durch. Des Weiteren war sie an der Interpretation der Ergebnisse sowie am Schreiben des Manuskriptes beteiligt.

# Biochemical and Biophysical Analysis of a Chiral PqsD Inhibitor Revealing Tight-binding Behavior and Enantiomers with Contrary Thermodynamic Signatures

Michael P. Storz,<sup>1,†</sup> Christian Brengel,<sup>1,†</sup> Elisabeth Weidel,<sup>1,‡</sup> Michael Hoffmann,<sup>§</sup> Klaus Hollemeyer,<sup>||</sup> Anke Steinbach,<sup>†</sup> Rolf Müller,<sup>§</sup> Martin Empting,<sup>\*,†</sup> and Rolf W. Hartmann<sup>\*,†,‡</sup>

<sup>†</sup>Helmholtz-Institute for Pharmaceutical Research Saarland (HIPS), Department Drug Design and Optimization, Campus C2.3, 66123 Saarbrücken, Germany

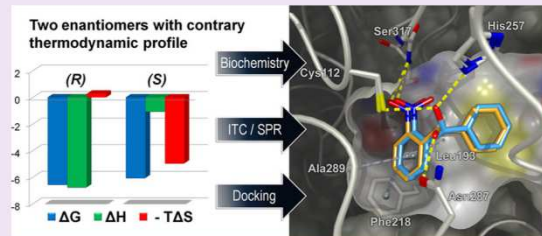
<sup>‡</sup>Pharmaceutical and Medicinal Chemistry, Saarland University, Campus C2.3, 66123 Saarbrücken, Germany

<sup>§</sup>Helmholtz-Institute for Pharmaceutical Research Saarland (HIPS), Department Microbial Natural Products, Campus C2.3, 66123 Saarbrücken, Germany

<sup>||</sup>Biochemical Engineering, Saarland University, Campus A1.5, 66123 Saarbrücken, Germany

## Supporting Information

**ABSTRACT:** Antivirulence strategies addressing bacterial pathogenicity without exhibiting growth inhibition effects represent a novel approach to overcome today's crisis in antibiotic development. In recent studies, we examined various inhibitors of PqsD, an enzyme involved in formation of *Pseudomonas aeruginosa* cell-to-cell signaling molecules, and observed desired cellular effects for 2-nitrophenyl derivatives. Herein, we investigated the binding characteristics of this interesting compound class using several biochemical and biophysical methods. The inhibitors showed time-dependent activity, tight-binding behavior, and interactions with the catalytic center. Furthermore, isothermal titration calorimetry (ITC) experiments with separated enantiomers revealed contrary thermodynamic signatures showing either enthalpy- or entropy-driven affinity. A combination of site-directed mutagenesis and thermodynamic profiling was used to identify key residues involved in inhibitor binding. This information allowed the proposal of experimentally confirmed docking poses. Although originally designed as transition state analogs, our results suggest an altered position for both enantiomers. Interestingly, the main difference between stereoisomers was found in the orientation of the hydroxyl group at the stereogenic center. The predicted binding modes are in accordance with experimental data and, thus, allow future structure-guided optimization.



Antimicrobial resistance is a worldwide emerging problem since current treatment becomes more and more inefficient.<sup>1</sup> In *P. aeruginosa*, which is considered as the major cause of mortality in cystic fibrosis patients,<sup>2</sup> several resistance mechanisms against commonly used antibiotics are known. For example, the limited permeability of the outer membrane<sup>3</sup> in combination with broad spectrum multidrug efflux systems<sup>4</sup> can result in a dramatically lowered intracellular drug concentration. Thus, it is all the more important that the compound blocks its target efficiently providing sufficient drug residence time to achieve the desired effects. In the case of competitive inhibitors interacting with the same binding site as the substrate, effectiveness can be drastically diminished by mass-action competition with the substrate. Thus, it was proposed to avoid this unfavorable situation through (pseudo-) irreversible inhibition.<sup>5</sup>

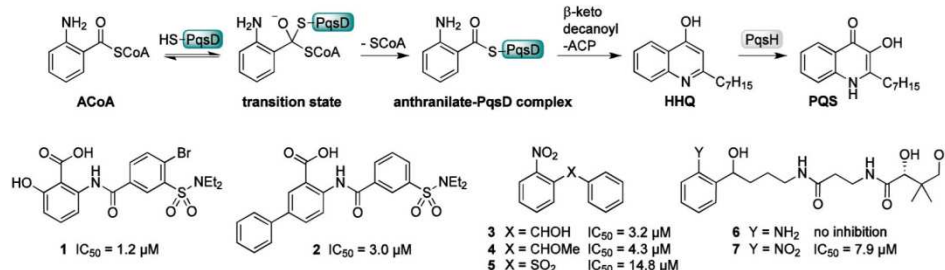
Bacteria apply cell-to-cell communication to coordinate group behavior, a phenomenon that became known as quorum sensing (QS). Thereby, small diffusible signal molecules are produced by bacterial cells and released into the environment.

The extracellular concentration reflects the cell density of the population, which can be in turn measured by single members of the colony. Once a special threshold is reached, the population collectively alters its gene expression pattern. Multiple QS systems based on various signal molecules are present in beneficial as well as pathogenic bacteria. *P. aeruginosa* utilizes the quinolone-based pqs system, which is characteristic for particular *Pseudomonas* and *Burkholderia* species.<sup>6</sup> The pqs system is reported to have crucial influence on biofilm formation and virulence factor production.<sup>7,8</sup> In this regard, inhibition of the pqs system is an attractive strategy to overcome biofilm-mediated resistance. Furthermore, QS inhibitors might ideally address pathogenicity without affecting bacterial cell viability. Hence, compared to the current treatment by bactericidal and bacteriostatic antibiotics, less

Received: July 15, 2013

Accepted: October 7, 2013

Published: October 7, 2013

Scheme 1. PqsD-Mediated Formation of HHQ and PQS and Structures of Known PqsD Inhibitors<sup>a</sup>

<sup>a</sup>  $IC_{50}$  values were taken from refs 11 and 12 and were measured using the screening procedure described in the methods section.

selection pressure to develop resistance against this novel mode of action is expected.<sup>9</sup> Another advantage of *pqs* inhibitors is the absence of quinolone signals in beneficial bacteria, and therefore, the natural microbial flora should not be affected.

PqsD is a key enzyme in the biosynthesis of the *pqs* signal molecules 2-heptyl-4-hydroxyquinoline (HHQ) and 2-heptyl-3-hydroxy-4-quinolone (*Pseudomonas* quinolone signal, PQS) (Scheme 1).<sup>10</sup> For this reason, we consider PqsD as an attractive target for the development of novel anti-infectives.<sup>11</sup> We have identified the first PqsD inhibitors by testing known inhibitors of FabH, a structurally and functionally related enzyme.<sup>10</sup> Structural optimization decreased  $IC_{50}$  values to 1.2  $\mu$ M (Scheme 1, 1 and 2).<sup>12</sup> However, these compounds were not capable of potently reducing the extracellular signal molecule levels in *P. aeruginosa* PA14 (unpublished data).

Recently, we have identified 2-nitrophenyl derivatives as potent PqsD inhibitors in a ligand-based approach (Scheme 1, 3–5, 7).<sup>11</sup> The most active compound of this series 3 was capable of reducing the HHQ and PQS levels as well as the biofilm volume in *P. aeruginosa* PA14 without affecting cell viability. In our original concept, (2-aminophenyl)methanol derivative 6 was designed as transition state analog of the reaction between PqsD and its primary substrate anthraniloyl-CoA (ACoA) (Scheme 1). Since transition states are the most tightly bound species of a catalytic reaction, transition state analogs are a reasonable strategy to achieve high potency.<sup>13</sup> However, we unexpectedly observed no activity for 6, while the corresponding nitro compound 7 effectively inhibited PqsD. Thus, it is open to question how the optimized nitro compound 3 interacts with PqsD on a molecular level.

To address this question, we conducted a surface plasmon resonance (SPR) competition experiment to validate the binding site. Various modifications of the *in vitro* assay were used to elucidate time dependency of inhibition as well as functional reversibility. Mass spectrometry was applied to investigate the nature of interaction between the protein and the inhibitors. Site-directed mutagenesis in combination with ITC analysis revealed key interaction features responsible for affinity and astonishing differences in the thermodynamic profile of the separated enantiomers. This information was used to deduce plausible binding modes, which may explain the efficacy of the compound class.

## RESULTS AND DISCUSSION

**Binding Site Analysis by SPR.** To investigate whether our compounds bind in the active site, we performed binding experiments using SPR. Compound 2, which was described as a channel blocker interacting in the upper part of the tunnel<sup>12</sup>

and 3 were separately added to PqsD immobilized on an SPR sensor chip. Figure 1A/B shows the resulting response curves, indicating affinity to the enzyme for both compounds.

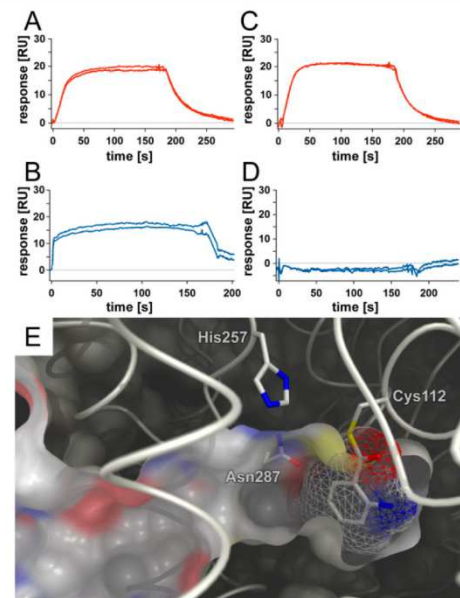


**Figure 1.** Elucidation of the binding site by SPR. Addition of inhibitor to native PqsD leads to response curves (A) and (B) for compounds 2 and 3, respectively. In contrast to compound 2 (C), no response curve for 3 (D) is observed after addition to PqsD pretreated with ACoA. (E) Binding pocket of PqsD and space-filling model of covalent anthranilate adduct (wireframe). Picture was generated using the crystal structure [Protein Data Bank (PDB) entry 3H77].<sup>14</sup>

In a second experiment, the first substrate of PqsD, ACoA, was added until saturation of all active-site Cys112 by formation of an anthranilate thioester was reached (Figure 1E). Noteworthy, the X-ray structure of this key intermediate shows no significant conformational changes compared to untreated PqsD,<sup>14</sup> which eliminates the possibility of allosteric effects. Addition of inhibitors 2 or 3 was subsequently repeated. In the case of 2, response curves were very similar to those obtained using unmodified enzyme (Figure 1C). Thus, affinity of 2 is not affected by covalently bound anthranilate, which is consistent with previous results.<sup>12</sup> In contrast, no response was observed for 3 (Figure 1D), indicating that the binding site of 3 is blocked by anthranilate. Moreover, this experiment shows

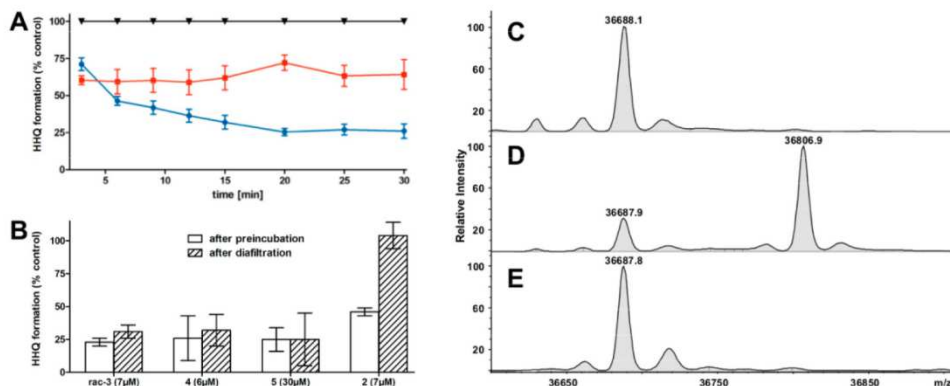


**Figure 2.** Mode of action analysis. (A) Time dependency of PqsD inhibition by 3  $\mu\text{M}$  of FabH inhibitor-derived compound **2** (■) and 6  $\mu\text{M}$  of 2-nitrophenyl derivative **3** (●) compared to untreated control (▼). Values are given in the Supporting Information. (B) Reversibility of PqsD inhibition by compounds **2–5**. Centrifugal filter devices with a molecular weight limit of 10k were used to remove at least 95% inhibitor by three diafiltration steps as controlled by HPLC analysis, while PqsD was retained. (C–E) HPLC-ESI mass spectra of untreated PqsD (C) and after preincubation with 5 mM ACoA (D) or 2.5 mM of compound **3** (E), respectively.

that the binding pocket around Cys112 is the only target site of **3**. This is supported by a 1:1 interaction stoichiometry determined in the ITC experiment.<sup>11</sup>

To gather further evidence for the proposed binding site, we preincubated PqsD with ACoA prior to continuation of the original assay procedure. In the case of the FabH inhibitor-derived compounds **1** and **2**, no significant differences in  $IC_{50}$  values determined by both procedures were observed ( $IC_{50,\text{mod}}$  values in Supporting Information (SI) Table S2). In contrast to this, the  $IC_{50}$  values of **3–5** were increased at least 3-fold when PqsD was preincubated with the substrate. This provides further evidence that nitrophenyl derivatives and the anthraniloyl moiety share a common binding site.

**Time-Dependent Inhibition and Reversibility.** To investigate the time dependency of PqsD inhibition by **3**, the protein was added to a mixture of substrates and inhibitor before HHQ formation was measured at different time points. Figure 2A (blue) shows decreasing HHQ production over time compared to the untreated control, indicating slow binding kinetics for **3**. For reference compound **2** (red), a nearly constant HHQ formation rate is observed, which is due to a rapid establishment of binding equilibrium with the enzyme.

Inhibition by **3** has not reached the equilibrium after 10 min, which is the standard preincubation time in the *in vitro* assay. Consequently,  $IC_{50}$  data and structure–activity relationships derived in this compound class are dependent on the rate of complex formation. Furthermore, the potency is underestimated compared to the FabH inhibitor-derived compound class. This becomes apparent when the preincubation period was extended from 10 min ( $IC_{50}$ ) to 30 min ( $IC_{50,\text{ext}}$  values in SI Table S2). While the inhibitory potency of **1** and **2** did not increase, the  $IC_{50,\text{ext}}$  of **3–5** showed significantly lowered values. This effect is most pronounced for the alcohol **3**, which is probably due to the slowest binding kinetics.

There are two general modes of interaction between enzyme and inhibitor resulting in time-dependent inhibition. First, the enzyme inactivation is practically irreversible, for example by covalent binding. As the reaction progresses, enzyme inhibition will be increased. In the second case, slow binding kinetics can lead to an equilibrium establishment of a reversible inhibition, which is slow compared to enzyme turnover. To address this issue, we examined the reversibility by modification of our *in*

*vitro* functional assay. Therefore, PqsD was preincubated with inhibitor and the remaining HHQ formation was quantified with and without removal of unbound inhibitor by diafiltration. After preincubation with 7  $\mu\text{M}$  of the FabH inhibitor-derived compound **2**, 46% of HHQ formation remained compared to the untreated control. After removal of unbound inhibitor, PqsD activity was fully restored, since binding of the inhibitor is nonpermanent (Figure 2B). In the case of the 2-nitrophenyl derivatives **3–5**, PqsD activity was not significantly increased. However, providing reversible inhibition, HHQ formation should be very sensitive to changes in inhibitor concentration, since the dose-inhibition curves are very steep at the concentrations used (SI Figure S1 for compound **3**). Hence, inhibition by this compound class is apparently irreversible. However, it should be mentioned that the time available for dissociation between the diafiltration steps is limited due to enzyme denaturation ( $t_{1/2} \approx 100$  min at RT). Thus, the irreversible behavior of **3–5** may be restricted to the time period that is covered by the experiment.

To distinguish between irreversible inhibition by formation of a covalent bond or tight-binding characterized by slow off-rates, mass spectrometry (MS) techniques were applied. First, PqsD was incubated with or without ACoA as well as compound **3**, and the samples were subjected to HPLC-ESI analysis (Figure 2C). In absence of any additives, the main signal was observed at  $m/z = 36688.1$ , which corresponds to the calculated average mass of PqsD (36688.1 Da). Formation of the anthranilate–PqsD complex by addition of the substrate led to the expected mass shift of +119.2 toward 36806.9 (calculated: 36807.2). In presence of a 100 fold excess of inhibitor **3**, no covalent adduct or oxidation product was observed. This was also the case when any reductive reagents were avoided (SI Figure S2). Thus, we exclude a redox-based inhibition mechanism.

To exclude a possible dissociation during HPLC, we also analyzed PqsD with or without compound **3** by MalDI-TOF after tryptic digestion. In the case of unmodified PqsD, more than 99% of the sequence was covered by the peptides observed in the mass spectra. (Results are shown and discussed in detail in the MalDI-TOF section of the Supporting Information.) Thus, apart from 6 of 340 amino acids, which are unlikely to be involved in inhibitor binding, the

modification should be captured by this technique. However, no novel signal appeared after preincubation of PqsD with compound 3 (SI Table S4). The only difference compared to untreated PqsD is the disappearance of one fragment, which is not involved in substrate or inhibitor binding, since it is located far away from the active site. This fragment is also unresolved in the X-ray structure of PqsD, which is probably due to conformational flexibility. Thus, possible allosteric effects are unlikely. Considering both experiments, we exclude covalent binding, simultaneously denoting 3 as a tight-binding inhibitor.

**Elucidation of the Binding Mode.** The data presented so far were obtained using a racemic mixture of 3, since we have already shown that both enantiomers possess very similar  $IC_{50}$  values.<sup>11</sup> The SPR experiment using the separated stereoisomers revealed that both enantiomers bind near the active site residues deep in the binding channel and in an exclusive manner with respect to one another (SI Figures S9). Furthermore, (R)-3 and (S)-3 showed the same behavior as the racemic mixture 3 in the diafiltration experiment (SI Figure S10). However, when we analyzed the thermodynamic profile of binding to PqsD by ITC, surprising differences between both enantiomers were observed, even though very similar values for  $\Delta G$  were determined (Figure 3 and Table 1).

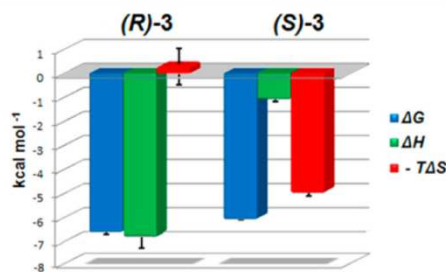


Figure 3. ITC analysis of thermodynamic profiles of enantiomers binding to PqsD wild-type.

Whereas the affinity of (R)-3 is driven enthalpically, (S)-3 shows a pronounced entropic binding profile. The combination of the values obtained for both enantiomers is in accordance with the balanced profile determined for their racemic mixture ( $\Delta H = -3.47$  kcal mol<sup>-1</sup>,  $-T\Delta S = -3.20$  kcal mol<sup>-1</sup>). The differences in the thermodynamic profiles are evident, even if uncertainties in  $\Delta H$ , and thus also in  $T\Delta S$ , of ~24% have to be

expected for the technique (value determined by an interlaboratory comparison).<sup>16</sup>

With respect to the dissimilar thermodynamic profiles, we were interested whether differences in the interaction with the amino acid residues are detectable. Because of a lack in cocrystal structure, we decided to execute a combined approach of site-directed mutagenesis and ITC as a promising method to identify specific spots of interaction.<sup>17</sup> Due to the SPR results, the binding site of both enantiomers should be located near the catalytic triad characterized by Cys112, His257 and Asn287. Furthermore, the adjacent Ser317 represents another possible interaction partner. Thus, we mutated the aforementioned amino acids. Only S317A possessed catalytic activity comparable to the wild-type. C112S retained 8% activity, whereas all other mutations led to inactivity (SI Table S1). However, the aforementioned PqsD variants allowed to investigate the contribution of the respective residue side chains to inhibitor binding.

ITC analyses using (R)-3 revealed Cys112 and His257 as mainly interacting residues, since mutation led to a loss of affinity by more than factor 2.3, as measured by deterioration in  $\Delta G$  by more than 0.5 kcal mol<sup>-1</sup> (Table 1). Binding affinity of (S)-3 does not seem to be significantly changed by any of these mutations with the exception of a small loss in affinity for both Ser317 mutants. For C112A standard deviations in  $\Delta G$  are too high for a reliable interpretation.

Based on these results, we docked both enantiomers to propose binding poses. Calculation of the protonation state revealed that the Cys112 and His257 residues exist in a neutral form at physiological pH. In all high-ranked docking poses, the scaffold of both enantiomers had the same position, whereas one phenyl ring was located directly adjacent to the bottom of the channel and the other oriented toward the tunnel entrance (Figure 4A). For (R)-3, the nitro group was observed at both phenyl rings. However, since both enantiomers retained comparable inhibitory activity even for elongated substituents instead of phenyl (data not shown), we concluded that the nitro-phenyl moiety is apparently located at the bottom of the channel. Thereby, the nitro group forms an asymmetrical bifurcated hydrogen bond (2.85 and 3.10 Å) to the backbone NH of Ser317 (Figure 4B).<sup>18</sup> The hydroxyl group is involved in a hydrogen bond network between the side chains of Cys112 (3.07 Å) and His257 (2.90 Å). The observed distances are typical for weak hydrogen bonds,<sup>19,20</sup> which explains the loss in affinity and enthalpy for the C112A and H257F mutants. The

Table 1. Effects of Mutated Amino Acids on Thermodynamic Profiles of the Enantiomers of 3<sup>a</sup>

	(R)-3 <sup>b</sup>			(S)-3 <sup>b</sup>		
	$\Delta G$ [kcal mol <sup>-1</sup> ]	$\Delta H$ [kcal mol <sup>-1</sup> ]	$-T\Delta S$ [kcal mol <sup>-1</sup> ]	$\Delta G$ [kcal mol <sup>-1</sup> ]	$\Delta H$ [kcal mol <sup>-1</sup> ]	$-T\Delta S$ [kcal mol <sup>-1</sup> ]
	$\Delta\Delta G$ [kcal mol <sup>-1</sup> ]	$\Delta\Delta H$ [kcal mol <sup>-1</sup> ]	$-T\Delta\Delta S$ [kcal mol <sup>-1</sup> ]	$\Delta\Delta G$ [kcal mol <sup>-1</sup> ]	$\Delta\Delta H$ [kcal mol <sup>-1</sup> ]	$-T\Delta\Delta S$ [kcal mol <sup>-1</sup> ]
WT	$-6.56 \pm 0.14$	$-6.99 \pm 1.02$	$0.43 \pm 1.15$	$-6.13 \pm 0.20$	$-1.11 \pm 0.34$	$-5.02 \pm 0.18$
C112A	$-0.82 \pm 0.11^c$	$-5.36 \pm 0.60^c$	$4.54 \pm 0.86^c$	$0.10 \pm 0.40$	$-0.30 \pm 0.53$	$0.40 \pm 0.22$
C112S	$-0.75 \pm 0.14^c$	$-5.87 \pm 0.78^c$	$5.12 \pm 0.86^c$	$-0.03 \pm 0.10$	$-0.39 \pm 0.36$	$0.36 \pm 0.36$
S317F	$-0.58 \pm 0.14^c$	$-6.09 \pm 0.72^c$	$5.51 \pm 0.86^c$	$-0.30 \pm 0.10^c$	$-0.78 \pm 0.22^c$	$0.40 \pm 0.20$
S317A	$0.10 \pm 0.10$	$-1.10 \pm 0.67$	$1.26 \pm 0.76$	$-0.22 \pm 0.10^c$	$0.14 \pm 0.36$	$-0.36 \pm 0.36$
N287A	$-0.18 \pm 0.10$	$-1.16 \pm 0.61$	$0.98 \pm 0.70$	$-0.02 \pm 0.10$	$-0.02 \pm 0.20$	$-0.01 \pm 0.20$
H257F	$-0.61 \pm 0.30^c$	$-5.83 \pm 0.67^c$	$5.22 \pm 0.76^c$	$0.03 \pm 0.30$	$-0.19 \pm 0.36$	$0.22 \pm 0.36$

<sup>a</sup> $\Delta\Delta G$ ,  $\Delta\Delta H$ , and  $-T\Delta\Delta S$  are  $\Delta G_{WT} - \Delta G_{mutant}$ ,  $\Delta H_{WT} - \Delta H_{mutant}$ , and  $-T(\Delta S_{WT} - \Delta S_{mutant})$ , respectively. Negative values indicate a loss; positive values, a gain compared to wild-type. Significance: effect of the mutations on thermodynamic parameters of ligand binding compared to wild-type indicates a difference in interaction. <sup>b</sup>Absolute configurations were derived from measurement of the optical rotation and comparison to literature.<sup>15</sup> <sup>c</sup> $p < 0.05$ .

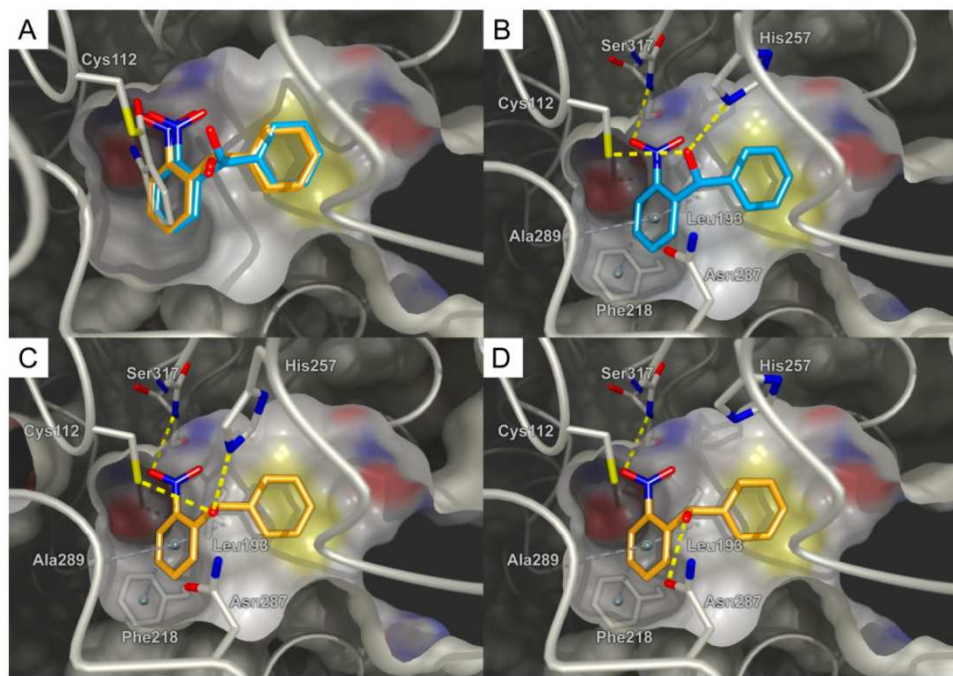


**Figure 4.** (A) Superimposition of the covalent anthranilate–PqsD complex (PDB entry 3H77) and docking poses for both enantiomers. Observed hydrogen bonds and CH- $\pi$  interactions of *R*-enantiomer (B) and the *S*-enantiomer (C/D) of compound 3 in PqsD wild-type. Nitrogen, blue; oxygen, red; sulfur, yellow; carbons of PqsD, gray; carbons of *R*-enantiomer, light blue; carbons of *S*-enantiomer, orange; hydrogen left out for clarity.

C112S mutant showed strongly reduced affinity, which is probably due to the shorter van der Waals radius of oxygen compared to sulfur,<sup>21</sup> leading to an interruption of the hydrogen bond network. No interaction was observed with the side chains of Asn287 and Ser317, which is in accordance with the collected ITC data (Table 1). However, introduction of a bulky phenyl ring in S317F probably results in sterical hindrance.

In the case of (*S*)-3, docking results were unambiguous with respect to the positioning of the nitro group, since in all high-ranked poses a short hydrogen bond between NO<sub>2</sub> and NH of Ser317 was observed (Figure 4C/D). However, the hydroxyl group was involved in different interactions, either facing toward Asn287 or His256/Cys112. We speculate that no singular mutation of the aforementioned residues significantly reduced affinity, since the hydroxyl group is able to switch to an alternative interaction mode. Noteworthy, this is not possible for the *R*-enantiomer due to the different orientation of the OH functionality.

Recently, two enantiomers with similar binding affinity for acetylcholinesterase but different thermodynamic profiles were reported.<sup>22</sup> X-ray cocrystal structures revealed multiple conformations stabilized by weak interactions for one enantiomer, leading to a gain in  $T\Delta S$  of 2.4 kcal mol<sup>-1</sup> compared to its counterpart. A similar effect might be contributing to the significant change in  $T\Delta S$  of 5.3 kcal mol<sup>-1</sup> for our compounds. Furthermore, a gain in entropy is characteristic for the classical hydrophobic effect.<sup>23</sup> Thereby, the release of ordered water from well-solvated hydrophobic pockets upon ligand binding increases the water molecules degree of freedom.<sup>24</sup> However, we were not able to identify such a displacement of water when comparing our docking results with the published X-ray structures.

Since small changes in structure without significant effect on  $\Delta G$  can lead to large changes in  $\Delta H$  and  $T\Delta S$ , the phenomenon of entropy-enthalpy compensation may also help to explain the contrary thermodynamic profiles of the enantiomers.<sup>25</sup> The physical origin of the compensation is still not fully understood, and it has been repeatedly discussed whether a structural interpretation is even possible.<sup>25,26</sup> According to this, the altered position of OH may well be the source of the shift in thermodynamic contributions.

Nevertheless, besides the interpretation of the thermodynamic profile, the proposed models should enable us to perform structure-guided optimization. Thus, the docking poses have to be in accordance with previous structure–activity relationship observations.<sup>11</sup> First, as soon as the amino group of 6 was substituted by nitro, the compounds turned active. As has been described above, (2-nitrophenyl)(phenyl)methanol 3 was originally designed as transition state analog. However, in the transition state, which has formed by attack of Cys112 on the thioester bond of ACoA, the generated oxyanion is stabilized by backbone nitrogen atoms of Cys112 and Ser317.<sup>14</sup> In our model, this position is in each case rather occupied by the nitro group (Figure 4A), which cannot be mimicked by the corresponding amine geometrically and spatially. As a consequence, this compound does not interact with PqsD as expected for a transition state analog. Furthermore, it is noteworthy that the nitrophenyl moiety aligns quite accurately with the benzoate moiety in an X-ray structure of anthranilate bound to a C112A mutant.<sup>14</sup> This indicates the preference for this kind of isoelectronic groups at this point of the channel. Second, a carbonyl linker between both phenyl rings, which conjugates the  $\pi$ -systems, leads to inactivity. This can now be explained, as the banana-shaped bottom of the channel is not able to accommodate the planar

molecule anymore. Furthermore, substitution of the methylene-H abolished inhibitory activity, either due to a steric clash with Asn287 (*R*), or because a substitution is followed by a twist of the molecule, which destabilizes the biological active conformation (*S*). Hence, the experimental results are in good accordance with our binding model.

**Conclusions.** 2-Nitrophenyl derivatives and FabH inhibitor-derived compounds show similar  $IC_{50}$  values, but only congeners of the former class are capable of significantly reducing signal molecule production and biofilm formation in *P. aeruginosa* PA14. We have shown that both inhibitor classes possess fundamentally different profiles regarding binding site, time-dependent inhibition and reversibility. Besides possible advantages in cell permeability of the (2-nitrophenyl)methanol derivatives due to their low molecular weight, the deeply buried binding site at the bottom of the substrate channel and the apparent irreversibility could be crucial factors for their intracellular efficacy.

Furthermore, the calorimetric characterization of two enantiomers revealed remarkable differences in their thermodynamic signatures. The detailed binding modes were examined by a combined approach using site-directed mutagenesis, ITC, and docking. This enabled us to propose binding poses for both enantiomers only differing in the position of the hydroxyl group. Notably, the nitro group occupies the oxyanion hole forming strong interactions with the enzyme backbone. However, this site was expected to accommodate the aforementioned hydroxyl group. Hence, the position of the scaffold is altered compared to the transition state (Figure 4A). The predicted enzyme–inhibitor complexes explain the reported structure–activity relationship and, therefore, enable the structure-guided design of PqsD inhibitors toward improved inhibitory activity.

## METHODS

**Preparation of PqsD Mutants.** PqsD mutants were generated using the QuikChange Site-Directed Mutagenesis Kit (Stratagene) according to the manufacturer's instructions using the pET28b(+)/*pqsD* plasmid as a template. Briefly, *pqsD* gene was amplified through 16 cycles of PCR. After treatment with *Dpn*I, the PCR product was transformed into *E. coli* strain XL1-Blue. Plasmid DNA was purified using the GenElute HP Plasmid Miniprep Kit (Sigma-Aldrich) and sequenced to confirm the site-directed mutations. For the primer sequence of the mutations see Supporting Information.

**Expression and Purification of Recombinant PqsD Wild-type and Mutants in *E. coli*.** *E. coli* BL21 (λDE3) cells were transformed with plasmid harboring PqsD (pET28b(+)/*pqsD*).<sup>10</sup> Overexpression, purification, and storage of the His<sub>6</sub>-tagged PqsD was performed as described recently.<sup>11</sup>

**Screening Assay Procedures for *In Vitro* PqsD Inhibition.** The standard assay for determination of  $IC_{50}$  values was performed monitoring the enzyme activity by measuring the HHQ concentration as described recently.<sup>10</sup> PqsD was preincubated with inhibitor for 10 min prior to addition of the substrates ACoA and β-ketodecanoic acid. The concentration of PqsD applied in the assay was 0.1 μM. Quantification of HHQ was performed analogously, but with some modifications: The flow rate was set to 750 μL min<sup>-1</sup> and an Accucore RP-MS column, 150 × 2.1 mm, 2.6 μm, (Thermo Scientific) was used. All test compound reactions were performed in sextuplicate. Synthesis of ACoA and β-ketodecanoic acid was performed as described in the Supporting Information. In the modified protocol used for the determination of  $IC_{50,\text{mod}}$  PqsD and the first substrate ACoA were preincubated for 30 min prior to adding them to the test compounds. Then, β-ketodecanoic acid was added and the further steps were performed identical to the standard protocol.  $IC_{50,\text{ext}}$  values were

determined analogously to the normal  $IC_{50}$  values, with the sole exception that PqsD was preincubated with inhibitor for 30 min.

**Surface Plasmon Resonance (SPR) Spectrometry.** SPR binding studies were performed using a Reichert SR7500DC instrument optical biosensor (Reichert Technologies) and CMD500 M sensor chips obtained from XanTec Bioanalytcs. PqsD was immobilized on a CMD500 M (carboxymethyldextran-coated) sensor chip at 12 °C using standard amine coupling conditions according to the manufacturers' instructions. PqsD was diluted with sodium acetate buffer (10 mM, pH 4.5) to a final concentration of 100 μg mL<sup>-1</sup>. PqsD was immobilized at densities of 2217 RU and 2918 RU.

**SPR Competition Study.** The binding studies were performed at a constant flow rate of 50 μL min<sup>-1</sup> in instrument running buffer (50 mM MOPS, pH 8.0, 150 mM NaCl, 5% DMSO (v/v), 0.1% Triton X-100 (v/v)). 10 mM stock solutions of compounds 2 and 3 in DMSO were directly diluted to a concentration of 500 μM (50 mM MOPS, pH 8.0, 150 mM NaCl, 0.1% Triton X-100 (v/v)) and then diluted to a final concentration of 100 μM (3) and 20 μM (2) in running buffer. Before the compounds were injected, six warm-up blank injections were performed. Buffer blank injections and DMSO calibration were included for double referencing. The compounds were injected for 180 s association and 300 s dissociation times. Experiments were performed twice with two independently prepared PqsD coated CMD500 M sensor chips. Scrubber software was used for processing and analyzing the data.

Compounds 2 and 3 were first tested in the absence of ACoA. In the second experiment ACoA (100 μM) was injected for 40 min with a constant flow of 5 μL min<sup>-1</sup> to reach saturation of the active-site Cys112. After this, the flow rate was increased to 50 μL min<sup>-1</sup> for 30 min in order to remove residual reagents. Once the baseline signal was stable, additional ACoA (10 μM) was injected to ensure that the anthranilate binding site is completely saturated (no additional signal was observed). Afterward, compounds 2 (20 μM) and 3 (100 μM) were consecutively injected.

**Elucidation of Time-Dependent PqsD Inhibition.** The assay was performed analogously to the screening assay procedure for *in vitro* PqsD inhibition described above, except that inhibitor and substrate were mixed and the reaction was started by addition of enzyme. The reactions were stopped after 3, 6, 9, 12, 15, 20, 25, and 30 min by addition of methanol containing 1 μM amitriptyline as internal standard. The percentage of inhibition was determined as the mean value of duplicates and HHQ concentrations measured without inhibitor at each time point were set to 100%. The uncertainty was calculated assuming uncorrelated standard deviations of the HHQ levels with or without inhibitor using a first-order Taylor series expansion. Percentages of inhibition are given in the Supporting Information.

**Examination of Reversibility by Diafiltration.** The diafiltration experiment was performed using identical conditions as for the screening assay procedure, but with doubled enzyme concentration (0.2 μM). PqsD was preincubated with inhibitor for 10 min, and the solutions were divided into two fractions. While the first one was stored under 4 °C, the second was diafiltrated (3×) at 1200 g for 6 min at 4 °C using Nanosep Centrifugal Devices equipped with a Omega membrane (MWCO = 10 K), which were obtained from Pall Corporation. Between diafiltration steps, the samples were diluted from 30 μL to 500 μL with buffer (identical chemical composition as used for preincubation). The enzyme inhibitor complex was allowed to dissociate for 1 min at RT. Afterward, the substrates ACoA and β-ketodecanoic acid were added to both fractions and the assay was continued as described in the screening assay procedure.

**HPLC-ESI Experiment.** PqsD (25 μM) was preincubated with compound 9 (2.5 mM) for 60 min at 37 °C in Tris-HCl buffer (50 mM, pH 8.0) with 0.5% DMSO (v/v). Dithiothreitol was added, and the samples were analyzed by HPLC-ESI. All ESI-MS-measurements were performed on a Dionex Ultimate 3000 RSLC system using an Aeris Widepore XB-C8, 150 × 2.1 mm, 3.6 μm dp column (Phenomenex). Separation of 2 μL samples were achieved by a linear gradient from (A) H<sub>2</sub>O + 0.05% TFA (v/v) to (B) ACN + 0.05% TFA (v/v) at a flow rate of 250 μL min<sup>-1</sup> and 45 °C. The gradient was

initiated by a 1.0 min isocratic step at 15% B, followed by an increase to 80% B within 4.5 min to end up with a 6 min step at 80% B before re-equilibration with initial conditions. UV spectra were recorded by a DAD in a range from 200 to 600 nm. The LC flow was split to 75  $\mu\text{L}$   $\text{min}^{-1}$  before entering the maXis 4G hr-ToF mass spectrometer (Bruker Daltonics) using the standard Bruker ESI source. In the source region, the temperature was set to 180 °C, the capillary voltage was 4000 V, the dry-gas flow was 6.0 l  $\text{min}^{-1}$ , and the nebulizer was set to 1.1 bar. Mass spectra were acquired in positive ionization mode ranging from 600 to 1800  $m/z$  at 2.5 Hz scan rate. Protein masses were deconvoluted using the Maximum Entropy algorithm (Copyright 1991–2004 Spectrum Square Associates, Inc.).

**Maldi-TOF Experiment.** PqsD (10  $\mu\text{M}$ ) was preincubated with compound 3 (2.5 mM) for 60 min at 37 °C using identical buffer composition as in the screening assay procedure (50 mM MOPS, pH 7.0 with 0.005% ( $v/v$ ) Triton X-100 and 0.5% DMSO ( $v/v$ )). The buffer was exchanged by an NH<sub>4</sub>HCO<sub>3</sub> buffer (50 mM, pH 8.1) in three diafiltration steps. Diafiltration was performed at 1200 g for 6 min at 4 °C in Nanosep Centrifugal Devices (MWCO = 10 K) of Pall Corporation. The protein was digested with trypsin overnight and dithiothreitol was added.  $\alpha$ -Cyano-4-hydroxycinnamic acid was used as matrix component. Analysis of the peptides were performed on a 4800 TOF/TOF Analyzer mass spectrometer (Applied Biosystems) in positive reflector mode using a pulsed 200 Hz solid state Nd:YAG laser with a wavelength of 355 nm. Laser energy was set to 2000–2300 units for standards and to 2700–3200 units for real samples. Source 1 voltage was set to 20 kV with a grid voltage of 16 kV. Reflector detector voltage was 2.19 kV. Spectra of standard peptides used for wide range calibration ranging from 0.8 to 4 kDa (des-arg1-bradykinin, angiotensin I, glu1-fibrinopeptide B, ACTH 1–17 clip, ACTH 18–39 clip and ACTH 7–38 clip) were measured with a delay time of 600 ns. One single mass spectrum was formed from 20 subspectra per spot using 25 accepted laser impulses each. From the standard peptides, exclusively monoisotopic ions were used with a minimum signal-to-noise ( $S/N$ ) ratio of 20 and a resolution >10000. Mass tolerance was set to 0.3 Da with maximum outlier of 5 ppm. Accepted calibration settings were used to measure real sample spectra in the range 1–3.5 kDa with a minimum  $S/N$  range of 10 and a resolution >8000. An internal algorithm defined the isotope cluster area subsequently named intensity (I), based on the peptides' molecular weight and their general elemental composition. MALDI-TOF MS resulted in pmfs consisting of mass-intensity spectra ( $m/z - I_{\text{abs}}$  al).

**Isothermal Titration Calorimetry (ITC).** ITC experiments were carried out using an ITC200 instrument (Microcal Inc., GE Healthcare). Final ligand concentrations were obtained by dilution 1:20 ( $v/v$ ) in the experimental buffer resulting in a final DMSO concentration of 5% ( $v/v$ ). Protein concentration was determined by measuring the absorbance at 280 nm using a theoretical molarity extinction coefficient of 17 780  $\text{M}^{-1} \text{cm}^{-1}$ . DMSO concentration in the protein solution was adjusted to 5% ( $v/v$ ). ITC measurements were routinely performed at 25 °C in PBS-buffer, pH 7.4, 10% glycerol ( $v/v$ ), 5% DMSO ( $v/v$ ). The titrations were performed on 83–102  $\mu\text{M}$  PqsD-His<sub>6</sub> and mutants-His<sub>6</sub> in the 200  $\mu\text{L}$  sample cell using 2  $\mu\text{L}$  injections of 3.5 mM ligand solution every 180 s. Raw data were collected, and the area under each peak was integrated. To correct for heats of dilution and mixing, the final baseline consisting of small peaks of the same size at the end of the experiment was subtracted. The experimental data were fitted to a theoretical titration curve (one site binding model) using MicroCal Origin 7 software, with  $\Delta H$  (enthalpy change in kcal mol<sup>-1</sup>),  $K_A$  (association constant in M<sup>-1</sup>), and  $N$  (number of binding sites) as adjustable parameters. Thermodynamic parameters were calculated from equation

$$\Delta G = \Delta H - T\Delta S = RT \ln K_A = -RT \ln K_D$$

where  $\Delta G$ ,  $\Delta H$ , and  $\Delta S$  are the changes in Gibbs free energy, enthalpy, and entropy of binding, respectively.  $T$  is the absolute temperature, and  $R = 1.98 \text{ cal mol}^{-1} \text{ K}^{-1}$ . For every mutant, three independent experiments were performed.

**In Silico Experiments.** Docking poses of PqsD inhibitors (R)-3 and (S)-3 were generated with YASARA structure (YASARA

Biosciences) using the AMBER03 force field on an Intel Core i7-2600 workstation with eight virtual cores.<sup>27,28</sup> Receptor coordinates were prepared using a crystal structure of the PqsD-anthranioloyl complex (PDB entry 3H77).<sup>14</sup>

First, the covalent and noncovalent ligands were removed without altering the dihedral angle of the Cys112 side chain and protonation states were assigned automatically at pH 7.4. Then, a grid box of 27 × 20 × 20 Å<sup>3</sup> was set up around the residues forming the active site tunnel of PqsD. Finally, the binding mode of the ligand was calculated using the flexible local docking procedure of the implemented AutoDock 4 algorithm with 999 docking runs.<sup>29</sup> In every case, at least the five highest-ranked poses were found to belong to one cluster. Predicted PqsD-inhibitor complexes were further refined by an additional energy minimization step with fixed receptor backbone atoms and then analyzed using MOE 2012 (Chemical Computing Group).<sup>30</sup>

## ■ ASSOCIATED CONTENT

### § Supporting Information

Primer sequence of mutations and catalytic activity; synthesis of the substrates used in the enzymatic inhibition assays; percentages of inhibition of the time dependency experiment; detailed analysis of the Maldi-TOF experiment; additional HPLC-ESI MS, diafiltration and SPR experiments; separation and purity of the enantiomers; representative ITC curves. This material is available free of charge via the Internet at <http://pubs.acs.org>.

## ■ AUTHOR INFORMATION

### Corresponding Authors

\*Phone: +49 681 302 70300. Fax: +49 681 302 70308. E-mail: rolf.hartmann@helmholtz-hzi.de.

\*E-mail: martin.empting@helmholtz-hzi.de.

### Author Contributions

<sup>†</sup>M.P.S. and C. B. contributed equally.

### Notes

The authors declare no competing financial interest.

## ■ ACKNOWLEDGMENTS

We thank S. Amann and C. Scheid for their help in performing all HPLC-MS/MS-based assays.

## ■ REFERENCES

- (1) Levy, S. B., and Marshall, B. (2004) Antibacterial resistance worldwide: Causes, challenges and responses. *Nat. Med.* 10, S122–S129.
- (2) Govan, J. R., and Deretic, V. (1996) Microbial pathogenesis in cystic fibrosis: Mucoioid *Pseudomonas aeruginosa* and *Burkholderia cepacia*. *Microbiol. Rev.* 60, 539–574.
- (3) Nikaido, H. (1989) Outer membrane barrier as a mechanism of antimicrobial resistance. *Antimicrob. Agents Chemother.* 33, 1831–1836.
- (4) Poole, K. (2001) Multidrug efflux pumps and antimicrobial resistance in *Pseudomonas aeruginosa* and related organisms. *J. Mol. Microbiol. Biotechnol.* 3, 255–264.
- (5) Swinney, D. C. (2004) Biochemical mechanisms of drug action: What does it take for success? *Nat. Rev. Drug Discovery* 3, 801–808.
- (6) Diggle, S. P., Lumjaiaktase, P., Dipilato, F., Kunakorn, M., Barrett, D. A., Chhabra, S. R., Camara, M., and Williams, P. (2006) Functional genetic analysis reveals a 2-alkyl-4-quinolone signaling system in the human pathogen *Burkholderia pseudomallei* and related bacteria. *Chem. Biol.* 13, 701–710.
- (7) Yang, L., Nilsson, M., Gjermansen, M., Givskov, M., and Tolker-Nielsen, T. (2009) Pyoverdine and PQS mediated subpopulation interactions involved in *Pseudomonas aeruginosa* biofilm formation. *Mol. Microbiol.* 74, 1380–1392.

- (8) Summarized in: Dubern, J.-F., and Diggle, S. P. (2008) Quorum sensing by 2-alkyl-4-quinolones in *Pseudomonas aeruginosa* and other bacterial species. *Mol. BioSyst.* 4, 882–888.
- (9) Hentzer, M., Wu, H., Andersen, J. B., Riedel, K., Rasmussen, T. B., Bagge, N., Kumar, N., Schembri, M. A., Song, Z., Kristoffersen, P., Manefield, M., Costerton, J. W., Molin, S., Eberl, L., Steinberg, P., Kjelleberg, S., Hoiby, N., and Givskov, M. (2003) Attenuation of *Pseudomonas aeruginosa* virulence by quorum sensing inhibitors. *EMBO J.* 22, 3803–3815.
- (10) Pistorius, D., Ullrich, A., Lucas, S., Hartmann, R. W., Kazmaier, U., and Müller, R. (2011) Biosynthesis of 2-alkyl-4(1*H*)-quinolones in *Pseudomonas aeruginosa*: Potential for therapeutic interference with pathogenicity. *ChemBioChem* 12, 850–853.
- (11) Storz, M. P., Maurer, C. K., Zimmer, C., Wagner, N., Brengel, C., de Jong, J. C., Lucas, S., Müsken, M., Häussler, S., Steinbach, A., and Hartmann, R. W. (2012) Validation of PqsD as an anti-biofilm target in *Pseudomonas aeruginosa* by development of small-molecule inhibitors. *J. Am. Chem. Soc.* 134, 16143–16146.
- (12) Weidel, E., de Jong, J. C., Brengel, C., Storz, M. P., Braunschäusen, A., Negri, M., Plaza, A., Steinbach, A., Müller, R., and Hartmann, R. W. (2013) Structure optimization of 2-benzamidobenzoic acids as PqsD inhibitors for *Pseudomonas aeruginosa* infections and elucidation of binding mode by SPR, STD NMR, and molecular docking. *J. Med. Chem.*.
- (13) Schloss, J. V. (1988) Significance of slow-binding enzyme inhibition and its relationship to reaction-intermediate analogues. *Acc. Chem. Res.* 21, 348–353.
- (14) Bera, A. K., Atanasova, V., Robinson, H., Eisenstein, E., Coleman, J. P., Pesci, E. C., and Parsons, J. F. (2009) Structure of PqsD, a *Pseudomonas* quinolone signal biosynthetic enzyme, in complex with anthranilate. *Biochemistry* 48, 8644–8655.
- (15) Duan, H.-F., Xie, J.-H., Shi, W.-J., Zhang, Q., and Zhou, Q.-L. (2006) Enantioselective rhodium-catalyzed addition of arylboronic acids to aldehydes using chiral spiro monophosphite ligands. *Org. Lett.* 8, 1479–1481.
- (16) Myszka, D. G., Abdiche, Y. N., Arisaka, F., Byron, O., Eisenstein, E., Hensley, P., Thomson, J. A., Lombardo, C. R., Schwarz, F., Stafford, W., and Doyle, M. L. (2003) The ABRF-MIRG'02 study: Assembly state, thermodynamic, and kinetic analysis of an enzyme/inhibitor interaction. *J. Biomol. Technol.* 14, 247–269.
- (17) Ciulli, A., Williams, G., Smith, A. G., Blundell, T. L., and Abell, C. (2006) Probing hot spots at protein–ligand binding sites: A fragment-based approach using biophysical methods. *J. Med. Chem.* 49, 4992–5000.
- (18) Allen, F. H., Baalham, C. A., Lommerse, J. P. M., Raithby, P. R., and Sparr, E. (1997) Hydrogen-bond acceptor properties of nitro-O atoms: A combined crystallographic database and *ab initio* molecular orbital study. *Acta Crystallogr. B53*, 1017–1024.
- (19) Allen, F. H., Bird, C. M., Rowland, R. X., and Raithby, P. R. (1997) Hydrogen-bond acceptor and donor properties of divalent sulfur (Y-S-Z and R-S-H). *Acta Crystallogr. B53*, 696–701.
- (20) Vianello, L., Kovačević, B., Ambrožić, G., Mavri, J., and Maksić, Z. B. (2004) Hydrogen bonding in complex of serine with histidine: Computational and spectroscopic study of model compounds. *Chem. Phys. Lett.* 400, 117–121.
- (21) Bondi, A. (1964) Van der Waals volumes and radii. *J. Phys. Chem.* 68, 441–451.
- (22) Berg, L., Niemic, M. S., Qian, W., Andersson, C. D., Wittung-Stafshede, P., Ekström, F., and Linusson, A. (2012) Similar but different: Thermodynamic and structural characterization of a pair of enantiomers binding to acetylcholinesterase. *Angew. Chem., Int. Ed.* 51, 12716–12720.
- (23) Tanford, C. (1978) The hydrophobic effect and the organization of living matter. *Science* 200, 1012–1018.
- (24) Biela, A., Sielaff, F., Terwesten, F., Heine, A., Steinmetzer, T., and Klebe, F. (2012) Ligand binding stepwise disrupts water network in thrombin: Enthalpic and entropic changes reveal classical hydrophobic effect. *J. Med. Chem.* 55, 6094–6110.
- (25) Bissantz, C., Kuhn, B., and Stahl, M. (2010) A medicinal chemist's guide to molecular interactions. *J. Med. Chem.* 53, 5061–5084.
- (26) Chodera, J. D., and Mobley, D. L. (2013) Entropy–enthalpy compensation: Role and ramifications in biomolecular ligand recognition and design. *Annu. Rev. Biophys.* 42, 121–142.
- (27) Krieger, E., Koraiann, G., and Virend, G. (2002) Increasing the precision of comparative models with YASARA NOVA—A self-parameterizing force field. *Proteins* 47, 393–402.
- (28) Duan, Y., Wu, C., Chowdhury, S., Lee, M. C., Xiong, G., Zhang, W., Yang, R., Cieplak, P., Luo, R., and Lee, R. (2003) A point-charge force field for molecular mechanics simulations of proteins based on condensed-phase quantum mechanical calculations. *J. Comput. Chem.* 24, 1999–2012.
- (29) Morris, G. M., Goodsell, D. S., Halliday, R. S., Huey, R., Hart, W. E., Belew, R. K., and Olson, A. J. (1998) Automated docking using a Lamarckian genetic algorithm and empirical binding free energy function. *J. Comput. Chem.* 19, 1639–1662.
- (30) Molecular Operating Environment (MOE), 2012.10; (2012), H3A 2R7, Chemical Computing Group Inc., Montreal, QC, Canada.

### **3.3 Composing Compound Libraries for Hit Discovery – Rationality-Driven Preselection or Random Choice by Structural Diversity?**

Elisabeth Weidel, Matthias Negri, Martin Empting, Stefan Hinsberger, and Rolf W. Hartmann

Der Artikel ist online verfügbar unter:

<http://www.future-science.com/doi/pdf/10.4155/fmc.14.142>

Die Supporting Information ist online verfügbar unter:

<http://www.future-science.com/doi/suppl/10.4155/fmc.14.142>

#### **Publikation C**

#### **Beitrag der Autorin zu Publikation C**

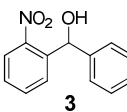
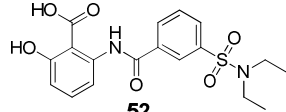
Die Autorin plante die SPR Experimente und führte diese durch. Sie war maßgeblich an der Erstellung des Konzepts und am Schreiben des Manuskriptes beteiligt

## 4 Zusammenfassung der Ergebnisse

Die ersten, beschriebenen PqsD Inhibitoren stammen aus der Klasse der 2-Benzamidobenzoesäuren. Die Identifizierung dieser Verbindungsklasse ist Ergebnis eines „*me-too*“ Ansatzes, bei dem sich die strukturelle Ähnlichkeit von PqsD und der  $\beta$ -Ketoacyl-Acyl Carrier Protein Synthase III (FabH) zu Nutze gemacht wurde. Der ursprüngliche von Nie *et al.* synthetisierte FabH Inhibitor zeigte eine moderate PqsD-Hemmung im funktionellen Assay mit einem IC<sub>50</sub>-Wert von 65  $\mu\text{M}$  (109, 140). Nach Optimierung wurde die Aktivität bis in den einstelligen, mikromolaren Bereich gesteigert und ein IC<sub>50</sub>-Wert von 1,2  $\mu\text{M}$  erhalten (Verbindung **52**) (139). Gleichzeitig wurde die Substanzklasse der 2-Nitrophenylmethanol-Derivate entwickelt, die vom Übergangszustand des natürlichen Substrates ACoA abgeleitet wurden. Im initialen Optimierungsprozess wurde hier Verbindung **3** erhalten, die einen IC<sub>50</sub>-Wert von 3,2  $\mu\text{M}$  aufweist (126).

Während im funktionalen Assay ähnlich gute Hemmwerte für beide Strukturklassen erhalten wurden, waren die Wirkungen im Bakterium sehr unterschiedlich (Tab. 1). Die 2-Nitrophenylmethanol-Derivate zeigten sowohl eine Reduktion des Biofilmvolumens, als auch eine Absenkung der Produktion der Signalmoleküle HHQ und PQS (126), wohingegen keine Effekte der 2-Benzamidobenzoesäuren zu beobachten waren.

Tab. 1: Übersicht über **3** und **52** sowie deren Ergebnisse in den biologischen Assays

	2-Nitrophenylmethane	2-Benzamidobenzoesäuren
Prominentester Vertreter	 <b>3</b>	 <b>52</b>
IC <sub>50</sub> -Wert	3,2 ± 0,7 $\mu\text{M}$	1,2 ± 0,1 $\mu\text{M}$
HHQ Hemmung	38 ± 6% @ 250 $\mu\text{M}$	keine Inhibition @ 250 $\mu\text{M}$
PQS Hemmung	37 ± 6% @ 250 $\mu\text{M}$	keine Inhibition @ 250 $\mu\text{M}$
Reduktion Biofilmmasse	38% @ 500 $\mu\text{M}$	keine Reduktion @ 125 $\mu\text{M}$

Die Ursache für die Ineffektivität der 2-Benzamidobenzoesäuren kann möglicherweise auf die hohe Lipophilie der Verbindungsklasse und damit resultierender Permeationsprobleme zurückgeführt werden. Eine andere Möglichkeit wäre, dass diese Verbindungsklasse durch Effluxpumpen ausgeschleust wurde. Durch Identifizierung der Teile des Moleküls, die an der Interaktion mit dem Protein beteiligt sind, könnten die Verbindungen dahingehend optimiert werden, dass nicht zur Aktivität beitragende Teile des Moleküls eliminiert oder ersetzt werden und dadurch die Lipophilie gesenkt wird. Gleichzeitig könnte dies zu einer Verbesserung der Permeation führen und dadurch zu einer erhöhten *in cellulo* Aktivität.

Dem gegenüber stehen die vom Übergangszustand abgeleiteten 2-Nitrophenylmethanol-Derivate, die *in cellulo* Effekte aufwiesen. Der Frage, ob diese Verbindungsklasse im aktiven Zentrum bindet, wie von Übergangszustandsanaloga zu erwarten ist, wurde mittels SPR nachgegangen. Darüber hinaus kann die Identifizierung der Bindestelle und der an der Interaktion beteiligten, funktionellen Gruppen aufzeigen, an welcher Stelle die Optimierung vorgenommen werden kann.

## 4.1 Aufklärung der Bindungsmodi von PqsD Inhibitoren

Zur Identifizierung der Bindestellen wurden SPR-basierte Kompetitionsexperimente durchgeführt. Dabei wurde das aktive Zentrum von PqsD mit dem natürlichen Substrat ACoA vorinkubiert, wodurch eine kovalente Beladung mit Anthraniloyl erreicht wurde. Im Anschluss wurde überprüft, ob die Verbindungen noch binden können. Beide Substanzklassen zeigten dabei ein unterschiedliches Verhalten (s. Publikationen A und B).

Nach der Anthraniloyl-Beladung des aktiven Zentrums blieben die SPR-Signale für die 2-Benzamidobenzoesäuren unverändert. Dies deutete darauf hin, dass diese Substanzklasse eine Bindestelle aufweist, die durch den gebundenen Anthraniloyl-Rest nicht beeinflusst wurde. Eine Verdrängung des Substrates und ein daraus resultierendes, unverändertes Signal ist unwahrscheinlich, da der Anthraniloyl-Rest kovalent an PqsD gebunden vorliegt (106). Die 2-Nitrophenylmethanol-Derivate hingegen zeigten nach der Vorinkubation keine Bindung mehr. Der Verlust der Affinität aufgrund einer durch die Anthraniloyl-Bindung ausgelösten Konformationsänderung kann durch den Vergleich der Kristallstrukturen von PqsD und PqsD in Komplex mit Anthraniloyl ausgeschlossen werden (106). Dies zeigt, dass die 2-Nitrophenylmethanol-Derivate an die Anthraniloyl-Bindestelle oder zumindest in unmittelbarer Nähe von dieser binden.

Ähnliche Ergebnisse wurden im funktionellen Assay erhalten, in welchem die Verbindungen mit unterschiedlichen Protokollen getestet wurden. Im Standardprotokoll wurde das Protein mit dem Inhibitor vorinkubiert und anschließend mit den Substraten ACoA und  $\beta$ -Ketodecansäure versetzt und die gebildete Menge an HHQ bestimmt. Im modifizierten Protokoll hingegen wurde die Reihenfolge so geändert, dass das Enzym mit ACoA vorinkubiert wurde und anschließend dann zuerst der Inhibitor und danach die  $\beta$ -Ketodecansäure zugefügt wurden. Die 2-Benzamidobenzoesäuren zeigten in beiden Assay Setups ähnliche IC<sub>50</sub>-Werte (Tab 2). Dies unterstützt die Annahme, dass diese Verbindungsklasse außerhalb des aktiven Zentrums bindet. Fernerhin deutete die unveränderte Hemmung darauf hin, dass die Inhibition der HHQ Synthese unabhängig von der ACoA Bindung ist und möglicherweise auf einer Hemmung der Kondensationsreaktion mit dem zweiten Substrat  $\beta$ -Ketodecansäure basiert.

Tab. 2: Vergleich der IC<sub>50</sub>-Werte ausgewählter 2-Nitrophenylmethanole und 2-Benzamidobenzoësäuren bei Anwendung des Standardprotokolls und des modifizierten Protokolls\*.

		IC <sub>50</sub> -Werte Standardprotokoll	IC <sub>50</sub> -Werte modifiziertes Protokoll
2-Nitrophenyl- methanole	<b>3</b>	3,2 ± 0,1 µM	24,6 ± 6,2 µM
	<b>49</b>	1,8 ± 0,9 µM	37,8 ± 1,9 µM
	<b>63</b>	1,8 ± 0,5 µM	2,8 ± 0,3 µM
2-Benzamido- benzoësäuren	<b>34</b>	19,8 ± 4,5 µM	19,4 ± 0,8 µM
	<b>43</b>	9,9 ± 2,1 µM	7,0 ± 0,4 µM
	<b>48</b>	3,0 ± 0,7 µM	4,2 ± 0,3 µM
	<b>52</b>	1,2 ± 0,1 µM	1,1 ± 0,2 µM

\*Im modifizierten Protokoll wurde die Reihenfolge der Inkubation verändert (siehe Text).

Demgegenüber stehen die starken Zunahmen der IC<sub>50</sub>-Werte vieler 2-Nitrophenylmethanol-Derivate, die wahrscheinlich darauf zurückzuführen sind, dass die Verbindungen aufgrund der Anwesenheit des Anthraniloyl-Restes während der Präinkubationsphase nicht mehr binden konnten.

Anhand der durchgeföhrten Experimente konnte gezeigt werden, dass die 2-Benzamidobenzoësäure-Derivate nicht im aktiven Zentrum von PqsD binden. Eine Bindung im Kanal, die vom dem kovalent gebundenen Anthraniloyl-Rest unbeeinflusst ist, kann jedoch nicht ausgeschlossen werden, weshalb zusätzliche SPR Experimente durchgeföhr wurden. Hierzu wurde PqsD mit Verbindung **48**, welche dem SPR-Laupuffer zugefügt wurde, um einen permanenten Überschuss der Verbindung zu gewährleisten, vorinkubiert und anschließend die Bindung von Verbindung **3** und ACoA untersucht (Abb. 9). Weder **3** noch ACoA waren in der Lage zu binden, wodurch eine Interaktion der 2-Benzamidobenzoësäuren im Kanal sehr wahrscheinlich erscheint. Bei umgekehrter Reihenfolge, wenn PqsD mit **3** vorinkubiert und **48** anschließend injiziert wurde, war eine Bindung zu beobachten, die aber im Vergleich zum unbehandelten Protein geschwächt war. Dieses Ergebnis zeigt, dass Verbindung **48** im Kanal bindet und diesen blockiert. Die Abschwächung im Bindesignal durch Anwesenheit von Verbindung **3**, die räumlich anspruchsvoller als das kovalent gebundene Anthranilat ist, spricht dafür, dass die 2-Benzamidobenzoësäuren in den unteren Teil des Kanals ragen. Um dies zu überprüfen, wurden weitere Untersuchungen zum Bindungsmodus mit verschiedenen, biophysikalischen Methoden wie SPR, NMR und ITC durchgeföhr (Publikation A).

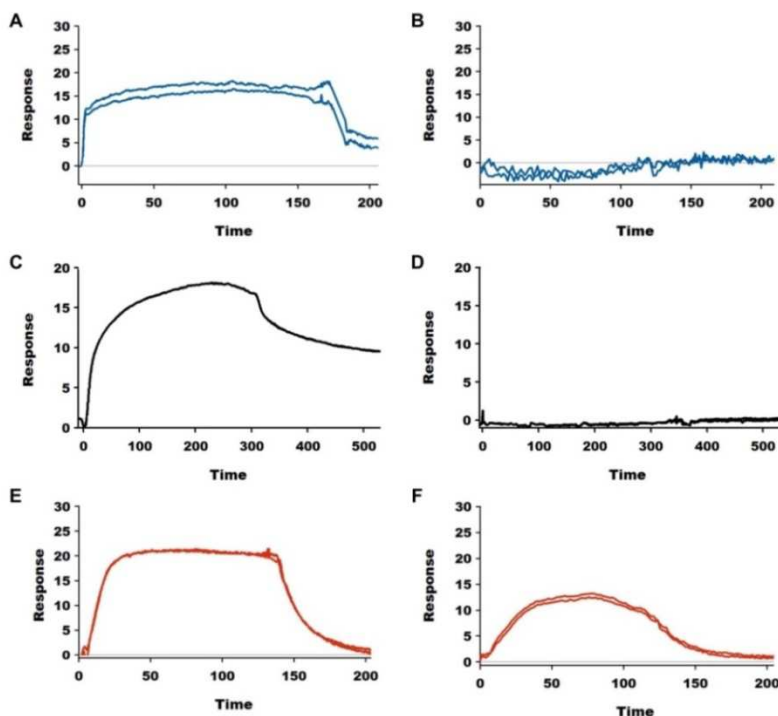


Abb. 9: SPR-basierte Bindungsstudien nach Vorinkubation von PqsD mit **48** und **3**. Die Bindungssignale von **3** sind in blau dargestellt. In A) sind die Signale an einer unbehandelten PqsD Oberfläche und in B) nach Vorinkubation von PqsD mit **48** zu sehen. Die Signale von ACoA an C) der unbehandelten PqsD Oberfläche und D) nach Vorinkubation von PqsD mit **48** sind in schwarz dargestellt. Die Bindungssignale von **48** (rot) sind in E) an einer unbehandelten PqsD Oberfläche und in F) nach Vorinkubation mit **3** gezeigt.

#### 4.1.1 Charakterisierung des Bindungsmodus der 2-Benzamidobenzoesäuren

Um der Frage nachzugehen, ob die 2-Benzamidobenzoesäuren im Kanal so positioniert sind, dass sie in den unteren Abschnitt des Kanals ragen, wurden kombinierte Experimente aus SPR und zielgerichteter Mutagenese durchgeführt. Hierfür wurden drei Verbindungen der Klasse ausgewählt, die unterschiedlich großen Raumbedarf in 5-Position am Anthranilsäurerest besitzen (Abb. 10). Diese wurden anschließend mittels SPR auf ihre Bindung an PqsD Mutanten untersucht, bei denen selektiv Aminosäuren im oder in der Nähe des aktiven Zentrums (Cys112Ala, Ser317Phe und His257Phe) ausgetauscht worden waren.

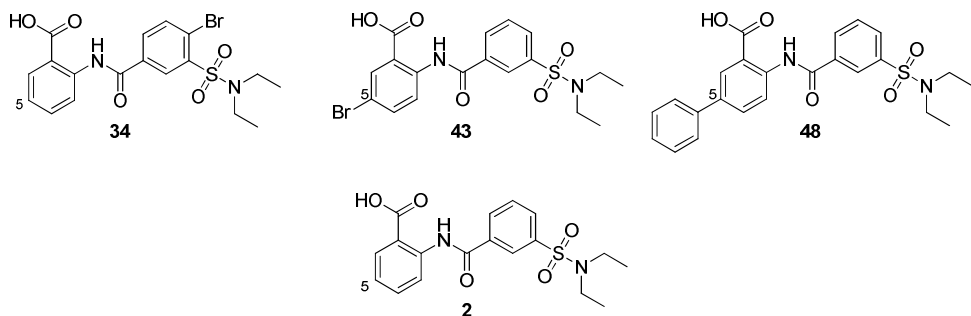


Abb. 10: Strukturen der 2-Benzamidobenzoesäuren, die in den Bindungsstudien an den PqsD Mutanten eingesetzt wurden, sowie von Verbindung **2**, die im molekularen Docking verwendet wurde.

Die Bindung der drei Benzoësäure-Derivate wurde an den verschiedenen Mutanten unterschiedlich stark beeinflusst (s. Publikation A, Tab. 3). Während die am Anthranilsäurering unsubstituierte Verbindung **34** an allen Mutanten dasselbe Bindeverhalten zeigte, war eine Abschwächung der Bindesignale von **43**, welche in 5-Position ein Bromid aufweist, zu beobachten. Die stärkste Beeinflussung der Bindung wurde im Fall von **48** erhalten, die einen zusätzlichen Phenylring besitzt. Diese Beobachtungen weisen darauf hin, dass die Größe des Substituenten in 5-Position von Bedeutung ist. Da sich die ausgetauschten Aminosäuren im aktiven Zentrum befinden, deutet dies stark darauf hin, dass die Benzoësäuren so ausgerichtet sind, dass der Anthranilsäurering in Richtung des aktiven Zentrums orientiert vorliegt, so dass die größeren Substituenten mit den dort lokalisierten Aminosäuren interagieren können.

Die schwächeren Signale von Verbindung **43** und **48** an den verschiedenen Mutanten können entweder aus dem Fehlen wichtiger Interaktionspartner, dem Austausch gegen die sterisch anspruchsvolle Aminosäure Phe oder aus einer durch den Austausch induzierten Konformationsänderung herrühren. Da sich Ser317 oberhalb des aktiven Zentrums befindet, hat die Mutation zu Phe wahrscheinlich zur Abschirmung des aktiven Zentrums geführt, wodurch möglicherweise Interaktionspartner unerreichbar geworden sind. Ähnliche Ursachen dürften für die schwächeren Signale der His257-Mutante vorliegen. Die verringerten Signale an der Cys112Ala-Mutante sind allerdings aufgrund der annäherungsweise vergleichbaren Größe der beiden Aminosäuren auf fehlende Interaktionen mit dem Cys zurückzuführen.

Um eine Vorstellung darüber zu erhalten, wie die Bindung an das Protein erfolgt und welche Aminosäuren an der Interaktion beteiligt sind, wurde ein molekulares Docking der unsubstituierten 2-Benzamidobenzoësäure (Verbindung **2**) durchgeführt. Die drei am höchsten bewerteten Bindungsmodi stimmten insofern miteinander überein, dass in allen das Benzamidobenzoësäuremolekül im Kanal gebunden vorlag. Unterschiede waren jedoch zum einen in der Orientierung des Anthranilsäurerings zu finden, aber auch darin, wie tief die Bindestelle in den Kanal hineinreicht. Während in den Bindungsmodi I und II das Molekül mit dem Anthranilsäurerest in Richtung des aktiven Zentrums orientiert ist, lag die Verbindung in Modus III um 180 Grad gedreht vor, wodurch der Anthranilsäurerest in Richtung des Tunneleingangs zeigte. Modus I unterschied sich von Modus II insofern, dass hier das Molekül tief in das aktive Zentrum ragte, während es in II mehr zentral platziert war. Anhand der SPR Beobachtungen, dass die Substituenten des Anthranilsäurerings in der Lage sind, mit den Aminosäuren des aktiven Zentrums zu interagieren, konnte Bindungsmodus III ausgeschlossen werden. Daraüber hinaus lieferten die SPR Versuche einen Hinweis darauf, dass Bindungsmodus II wahrscheinlicher ist, da im Falle von Bindungsmodus I aufgrund der Position des Moleküls tief im aktiven Zentrum die Bindung aller Verbindungen an den Mutanten hätte beeinflusst sein müssen.

Um weitere, experimentelle Hinweise auf den vorliegenden Bindungsmodus zu erhalten, wurden STD-NMR Experimente (141) dieser Verbindungsklasse an PqsD durchgeführt. In einem STD-NMR Spektrum zeigen die Protonen des Liganden die höchsten Intensitäten, die den engsten Kontakt zum Protein aufweisen. Im Fall der 2-Benzamidobenzoësäuren wurden die höchsten Intensitäten bei den Protonen des Anthranilsäurerings beobachtet. Da in Bindungsmodus III diese Protonen kaum mit den Aminosäuren des Tunneleingangs interagieren, sprechen zusätzlich zu den SPR Daten auch die NMR Ergebnisse gegen diesen Bindungsmodus. Die geringe Signalstärke der Methylgruppe des Sulfonamides widerlegt Bindungsmodus I, da durch den engen Kontakt der Protonen der Methylgruppe zum Protein stärkere Signale zu erwarten gewesen wären. Nur im Falle von Bindungsmodus II spiegeln die STD-NMR Signale die räumliche Lage des Liganden im Protein wider, wodurch dieser Bindungsmodus experimentell unterstützt wird.

Anhand der SPR, NMR und Docking Ergebnisse konnte eine klare Vorstellung darüber erhalten werden, welche funktionellen Gruppen der Inhibitoren an der Interaktion mit den Aminosäuren des Proteins beteiligt sind. Die Bindungsabstände und Bindungswinkel des mit den SPR- sowie STD-NMR-Ergebnissen übereinstimmenden Bindungsmodus legen nahe, dass die Carboxylatgruppe über eine Wasserstoffbrücke mit Asn287 interagieren kann und die Substituenten in 5-Position in der Lage sind, mit den Aminosäuren Cys112 und His257 zu wechselwirken. Darüber hinaus sind  $\pi$ - $\pi$ -Interaktionen zwischen dem Anthranilsäurering und den Aminosäuren Pro259 und Met225 zu beobachten. Auf der anderen Seite des Moleküls interagiert der Sulfonamidbenzenring mit denen in der Mitte des Kanals lokalisierten Aminosäuren Met220 und Arg262. Die in Richtung des Tunneleingangs orientierte Sulfonamidgruppe ist in der Lage, Wasserstoffbrücken mit Arg36 und Arg223 auszubilden.

Abschließend kann festgehalten werden, dass es mittels biophysikalischer Methoden möglich war den Bindungsmodus der 2-Benzamidobenzoësäuren aufzuklären. Die Ergebnisse zeigen, dass die PqsD-Hemmung drauf zurückzuführen ist, dass diese Verbindungsklasse als Kanalblocker agiert und dadurch verhindert, dass das natürliche Substrat ACoA an seine Bindestelle gelangt. Die gewonnenen Kenntnisse über die Interaktion der Verbindungsklasse mit dem Protein bieten eine gute Grundlage für zukünftige Optimierungsprozesse. Diese könnten zum Beispiel am Anthranilsäurering erfolgen, da im aktiven Zentrum noch Platz für weitere Substituenten vorhanden ist, wodurch möglicherweise zusätzliche Wechselwirkungen erzielt werden und dadurch die Aktivität verbessert wird.

#### 4.1.2 Charakterisierung des Bindungsmodus der 2-Nitrophenolmethanole

Die 2-Nitrophenylmethanol-Derivate wurden als Analoga des Übergangzustandes designt und dementsprechend ist eine Bindung im aktiven Zentrum zu erwarten. Um dies zu untersuchen wurden kombinierte Experimente aus SPR und zielgerichteter Mutagenese durchgeführt. Hierfür wurden

unterschiedliche Verbindungen der Substanzklasse (Abb. 11) an drei verschiedenen PqsD Mutanten (Cys112Ala, Ser317Phe und His257Phe) getestet.

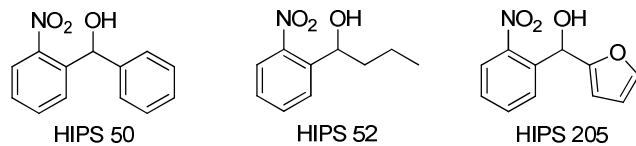


Abb. 11: Strukturen der 2-Nitrophenylmethanole, die in den Bindungsstudien an den PqsD Mutanten eingesetzt wurden.

Im Vergleich zu den 2-Benzamidobenzoësäuren wurden alle drei 2-Nitrophenylmethanol-Derivate an den jeweiligen Mutanten gleich beeinflusst (Abb. 12). Dies deutet darauf hin, dass alle Verbindungen die gleiche oder eine ähnliche Bindestelle aufweisen. Bei Austausch von Ser317 gegen Phe konnten alle Substanzen noch binden. Die Bindungen waren aber signifikant schlechter als am Wildtyp. Dies ist wahrscheinlich darauf zurückzuführen, dass der Zugang zum aktiven Zentrum durch den sterisch anspruchsvollen Phe-Rest eingeschränkt wurde, was zu einer schlechteren Bindung geführt hat. Keine Bindung war mehr zu beobachten, wenn die Aminosäuren im aktiven Zentrum (Cys112Ala und His257Phe) ausgetauscht wurden. Dies deutet darauf hin, dass His257 und Cys112 wichtige Interaktionspartner der 2-Nitrophenylmethanol-Derivate sind.

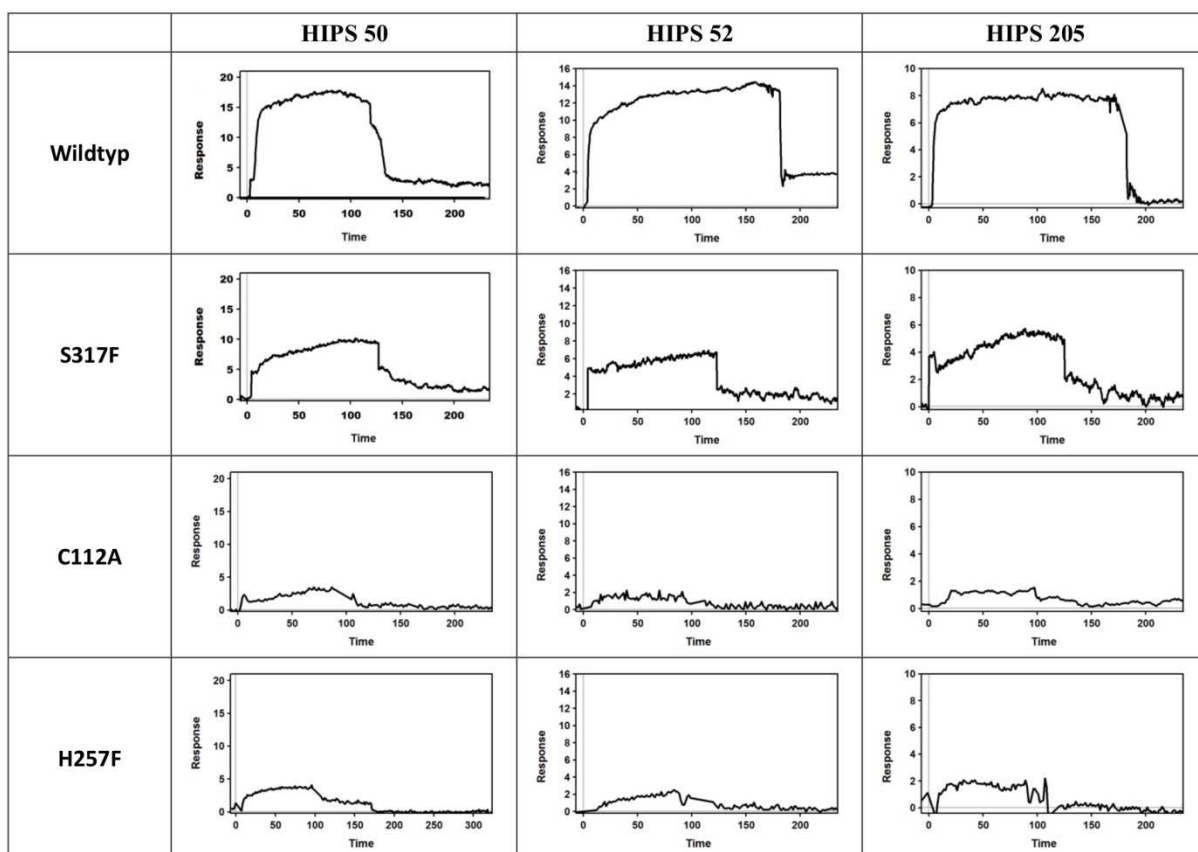


Abb. 12: Vergleich der mittels SPR erhaltenen Bindungssignale zwischen dem PqsD Wildtyp und den PqsD Mutanten (Ser317Phe, Cys112Ala und His257Phe) der Verbindungen **3**, **49** und **63**.

Da es sich bei Verbindung **3** um ein racemisches Gemisch handelt, ist es nicht auszuschließen, dass beide Enantiomere unterschiedliche Bindestellen aufweisen. Im vorangegangenen SPR Versuch, bei welchem das aktive Zentrum mit kovalent gebundenen Anthranilat beladen wurde, hat das racemische Gemisch keine Bindung mehr gezeigt. Dies spricht gegen unterschiedliche Bindestellen der Enantiomere, denn würde eines der Enantiomere außerhalb des aktiven Zentrums binden, wäre ein Signal zu beobachten gewesen. Um eine größere Gewissheit zu erlangen, wurden die SPR Experimente mit getrennten Enantiomeren wiederholt. Im initialen Test zeigten beide Enantiomere eine Bindung an PqsD. Wurde das aktive Zentrum mit dem Anthraniloylrest beladen, war keine Bindung der Enantiomere zu beobachten, wodurch bestätigt wird, dass beide im aktiven Zentrum binden. Darüber hinaus erfolgte nach Vorinkubation mit dem (*S*)-Enantiomer keine Bindung des (*R*)-Enantiomers, wodurch deutlich wird, dass beide Verbindungen dieselbe Bindestelle aufweisen. Es kann aber nicht ausgeschlossen werden, dass die Enantiomere mit verschiedenen Orientierungen mit dem Protein interagieren bzw. mit unterschiedlichen Aminosäuren wechselwirken. Zur Identifizierung wichtiger Interaktionspartner wurden ITC Experimente an verschiedenen Mutanten durchgeführt (Cy112Ala, Cys112Ser, Ser317Phe, Ser317Ala, Asn287Ala und His257Phe) (Publikation B). In diesem Fall wurden die beiden Enantiomere von Verbindung **3** an verschiedenen PqsD Mutanten untersucht, wobei nur für das (*R*)-Enantiomer signifikante Unterschiede in der Affinität zu beobachten waren. So führte der Austausch von Cys112 und His257 zu einem Affinitätsverlust von Faktor 2,3. Dieser Verlust ist ein Indiz dafür, dass es sich bei diesen zwei Aminosäuren um Hauptinteraktionspartner handelt.

Beide Enantiomere wurden gedockt und die Ergebnisse mit dem Wechselwirkungsprofil der Verbindungen verglichen. In beiden Fällen war der Nitro-substituierte Phenyrring am Kanalende platziert, während der zweite Phenyrring in Richtung Tunneleingang orientiert vorlag. Im Falle des (*R*)-Enantiomers interagierte die Nitrogruppe über Wasserstoffbrücken mit der NH-Gruppe des Ser317 und bildete über die OH-Gruppe ein Wasserstoffbrückennetzwerk mit Cys112 und His257 aus. Für das (*S*)-Enantiomer war die Bindung in Bezug auf die Position und Wechselwirkung der Nitrogruppe gleich. Der größte Unterschied zum (*R*)-Enantiomer lag in der Orientierung der OH-Gruppe, die sowohl mit Asn287, als auch mit His257 und Cys112 interagieren konnte. Dies wäre eine Erklärung dafür, dass bei den durchgeführten ITC-Experimenten keine Affinitätsverluste an den Cys112- und His257-Mutanten beobachtet wurden.

Während der Durchführung der Kompositionsexperimente mittels SPR fiel auf, dass **3** nicht vollständig dissoziiert. Wie aus dem Sensorgramm in Abb. 13 zu entnehmen ist, zeigte die Verbindung nach Beendigung der Injektion eine langsame und über den Beobachtungszeitraum unvollständige Dissoziation, welche charakteristisch für irreversible Binder ist (30, 142).

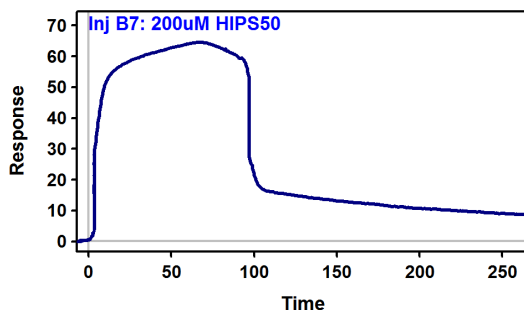


Abb. 13: Sensorgramm von **3** (200  $\mu$ M) mit unvollständiger Dissoziationsphase

Diesem Hinweis auf Irreversibilität wurde in Experimenten zur zeitabhängigen Hemmung von **3** nachgegangen. Hierbei erfolgte eine Zunahme der Inhibition mit größer werdendem Zeitintervall, welche erst nach mehreren Minuten ein Plateau erreichte. Im Vergleich zeigte die als Kontrollverbindung eingesetzte **48** eine konstante Inhibition. Das zeitabhängige Einsetzen der Hemmung kann auf zwei Mechanismen zurückgeführt werden. Zum einen könnte eine irreversible Bindung dafür verantwortlich sein. Zum anderen könnte auch eine Bindung mit sehr langsamer Bindungskinetik in Frage kommen. Um der Reversibilität der Bindung nachzugehen, wurden Diafiltrationsexperimente durchgeführt. Hierfür wurde PqsD mit dem Inhibitor vorinkubiert und die HHQ Bildung sowohl vor als auch nach dem Entfernen von ungebundenem Inhibitor durch Diafiltration gemessen. Im Gegensatz zu **48** konnte die Enzymaktivität nach Vorinkubation mit **3** nicht wieder hergestellt werden, was auf eine Irreversibilität hindeutet. Zur Überprüfung einer möglichen kovalenten Bindung wurden sowohl Maldi-TOF als auch HPLC-ESI-MS Messungen durchgeführt. In beiden Methoden konnte jedoch kein kovalentes Addukt detektiert werden, wodurch eine irreversible Bindung ausgeschlossen werden kann.

Diese Ergebnisse zeigen, dass die 2-Nitrophenylmethanol-Derivate eine langsame Reaktionskinetik besitzen, wodurch der Eindruck eines irreversiblen Bindeverhaltens entsteht. Daher handelt es sich bei dieser Verbindungsklasse um „tight binder“, die im aktiven Zentrum binden und aufgrund der gleichen Bindestelle mit dem natürlichen Substrat kompetitieren.

#### 4.1.3 Finale Diskussion der Bindungsmodi

Durch den Einsatz von biophysikalischen Methoden war es möglich, das Bindeverhalten der beiden Verbindungsklassen zu charakterisieren. Darüber hinaus konnten mittels SPR, ITC, STD-NMR und molekularem Docking die Bindestellen der Verbindungen näher beschrieben werden, während anhand von enzymatischen Assays und massenspektrometrischen Methoden die Art der Enzymhemmung klassifiziert werden konnte. Wie durch Tab. 3 deutlich wird, handelt es sich um zwei Verbindungsklassen mit stark unterschiedlichen Wirkmechanismen. Die 2-Nitrophenylmethanol-Derivate weisen eine langsame Dissoziation auf und verhindern durch Bindung an die Anthraniloylbindestelle im aktiven Zentrum die PqsD-katalysierte Umsetzung des Substrates. Dem

gegenüber stehen die 2-Benzamidobenzoësäuren, die aufgrund ihrer reversiblen Bindung im Kanal zu einer Blockade führen und dadurch die Zugänglichkeit der Substratbindestelle vermindern.

Tab. 3: Charakterisierung des Bindeverhaltens der PqsD Inhibitoren

	2-Nitrophenylmethanole	2-Benzamidobenzoësäuren
<b>Bindestelle</b>	im aktiven Zentrum	im Substrat-Zugangskanal
<b>Art der Hemmung</b>	„tight binding“	reversibel
<b>Dissoziation</b>	langsam	schnell
<b>Wirkmechanismus</b>	Kompetition mit ACoA	Blockade des Kanals und damit der Zugänglichkeit der Bindestelle

Wie anhand der präsentierten Ergebnisse deutlich wird, konnte mit Hilfe verschiedener, biophysikalischen Methoden die Aufklärung der Wirkmechanismen der beiden Verbindungsklassen erreicht und wichtige Interaktionspartner aufgezeigt werden. Die dadurch gesammelten Informationen können dazu genutzt werden, die Verbindungsklasse strukturell weiter zu optimieren und dadurch die Aktivität zu steigern. Darüber hinaus liefert das etablierte SPR-Testsystem eine einfache und schnelle Möglichkeit, um erste Informationen zur Bindestelle von neuen Inhibitoren zu erlangen (143-145). Die Identifizierung der unterschiedlichen Bindestellen der zwei PqsD Inhibitorklassen eröffnet fernerhin die Möglichkeit, diese Verbindungen als Tool-Komponenten zur Erweiterung des etablierten Testsystems zu nutzen (144).

## 4.2 SPR Screenings

Dieser Teil der Arbeit befasst sich mit der Identifizierung von PqsD Inhibitoren mit neuen Strukturen, die einen geeigneten Startpunkt zur Optimierung darstellen. Hierfür wurden drei häufig verwendete Screeningstrategien angewendet und in Hinblick auf Effektivität miteinander verglichen. Die Ansätze unterscheiden sich darin, wie die zu untersuchenden Verbindungen ausgewählt wurden. Neben dem häufig durchgeföhrten Fragmentscreening, in welchem die Bibliothek aus strukturell möglichst unterschiedlichen Verbindungen besteht und welches oftmals geringe Hitraten aufweist (31, 37), wurden zwei fokussierte Strategien evaluiert. In diesen Ansätzen erfolgt die Auswahl der Verbindungen unter Berücksichtigung von Target-assoziierten Aspekten, wodurch höhere Hitraten bei gleichzeitiger Reduktion der Anzahl an Testverbindungen erreicht werden sollten.

Zu diesen „fokussierten“ Strategien zählt unter anderem der bereits bei den 2-Benzamidobenzoësäuren angewendete „*me-too*“ Ansatz, der auf der strukturellen Ähnlichkeit der aktiven Zentren von PqsD und FabH basiert. Diese Strategie hatte bereits zu einer vielversprechenden Verbindungsklasse geführt

(139), weshalb in den nachfolgenden Untersuchungen weitere, literaturbeschriebene FabH Inhibitoren als Ausgangspunkte gewählt wurden. Darüber hinaus wurde in einem zweiten Ansatz ein virtuelles Screening an einem Pharmakophor-Modell durchgeführt. Hierbei wurden aus einem Verbindungs pool von über 900 Verbindungen die Substanzen ausgewählt, die im Rahmen des Modells die besten „*Bindingscores*“ erreichten, und zu einer Bibliothek zusammengefügt.

Die erstellten Bibliotheken der drei Ansätze wurden zuerst mittels SPR auf PqsD Bindung untersucht und anschließend in einem zellfreien, funktionellen Assay auf PqsD Inhibition überprüft. Im Gegensatz zu bisherigen Studien, die nur auf theoretischer Basis erfolgten und deren Daten darüber hinaus aus unterschiedlichen Assays an verschiedenen Targets stammen (146), wurden alle drei Ansätze am selben Target durchgeführt. Dies gewährleistet eine maximale Vergleichbarkeit und ermöglicht so eine Gegenüberstellung der unterschiedlichen Strategien in Hinblick auf Effizienz und Durchführbarkeit.

#### **4.2.1 „*me-too*“ Ansatz**

Im klassischen Sinn beschreibt der „*me-too*“ Ansatz die Nachahmung eines bereits auf dem Markt vorhandenen Arzneistoffs (zusammengefasst in (147)). Oftmals werden diese Ursprungsverbindungen in ihrer Struktur leicht modifiziert und dadurch wird eine neue, potente Verbindung erhalten. Der Nachteil einer solchen Strategie besteht darin, dass die Resistenzbildung häufig sehr schnell einsetzt. Der Grund hierfür liegt in der Ähnlichkeit der Struktur und dem daraus resultierenden, gleichen Wirkmechanismus. In unserem Ansatz wird die Bezeichnung „*me-too*“ auf die Enzymebene übertragen, indem ausgenutzt wird, dass es ein zu PqsD sehr ähnliches Enzym (FabH) gibt, für das Inhibitoren beschrieben sind. Voraussetzung ist eine strukturelle Ähnlichkeit der beiden Enzyme, die hier durch die sehr ähnliche dreidimensionale Proteinfaltung, bei einer Sequenzhomologie von ca. 40% sowie der gleichen Aminosäuren in den aktiven Zentren gegeben ist (106, 148, 149). Hieraus wurde geschlossen, dass Inhibitoren von FabH ebenfalls in der Lage sein sollten, PqsD zu inhibieren (139).

Basierend auf den Strukturen einiger, literaturbeschriebener Inhibitoren der bakteriellen Fettsäuresynthese (140, 150-154) wurde eine Substanzbibliothek aus zwölf Verbindungen zusammengestellt, die zusätzlich auch von den Strukturen abgeleitete Derivate beinhaltete (Strukturen s. Publikation C, S. 2060). Alle Verbindungen wurden sowohl mittels SPR auf ihre Bindung an PqsD überprüft, als auch im funktionellen *in vitro* Assay evaluiert. Mit Ausnahme von **A6** wurden für alle Substanzen Bindesignale erhalten. Auffallend war die hohe Signalstärke von **A11**, was auf eine starke Bindungsaffinität zu PqsD hinweist. Im funktionellen *in vitro* Assay war für neun der zwölf Verbindungen eine Hemmung der HHQ Biosynthese zu beobachten, wobei sich sechs als starke PqsD Inhibitoren herausstellten (>80% Inhibition bei 50 µM).

Der Vergleich zwischen Bindesignalen und Hemmwerten zeigt, dass eine Korrelation besteht. Ausnahme hiervon ist **A11**, die zwar das höchste Bindesignal ergab, aber im Inhibitionsassay weniger aktiv als zum Beispiel **A1** war. Innerhalb einer Verbindungsklasse ist jedoch eine deutliche Korrelation erkennbar. Am ausgeprägtesten ist dieser Trend in der Klasse der Benzamidobenzoesäuren. Hier stiegen SPR Signale und inhibitorische Aktivität in der Reihenfolge von **A9** über **A12** und **A10** zu **A11** an. Diese Tendenz war auch in den anderen Verbindungsklassen zu beobachten, in welchen immer die Verbindung mit dem höchsten Signal die stärkste Inhibition zeigte (**A2–A4** und **A5–A7**). Die geringe Korrelation zwischen Verbindungen unterschiedlicher Strukturklassen ist wahrscheinlich auf die SPR Signale zurückzuführen und mit unterschiedlichen Bindestellen zu begründen. Dies bedeutet, dass die gemessene Inhibition nicht nur von der Targetaffinität abhängt, sondern auch von der Fähigkeit, die Substrat-Enzym-Interaktion zu stören und damit die katalytische Umsetzung des Produkts. Verbindungen, die ähnliche Affinitäten besitzen, aber unterschiedliche Bindestellen besetzen und damit verschiedene Mechanismen aufweisen (z.B. vollständige oder teilweise Blockade der Bindestelle oder aber allosterische Inhibition), werden sehr wahrscheinlich unterschiedliche Aktivitäten in einem Substrat-abhängigen Enzymassay zeigen. In vorangegangen Studien wurde beobachtet, dass Verbindungen, deren Bindestelle tief im aktiven Zentrum von PqsD liegt, geringere Signalstärken aufweisen als Verbindungen, deren Bindestellen leichter zugänglich sind. So zeigte das 2-Nitrophenylmethanolderivat (Verbindung **3**, Bindung im aktiven Zentrum) im Vergleich zur 2-Benzamidobenzoesäure (Verbindung **48**, Bindung im Kanal oberhalb des aktiven Zentrums) eine höhere Aktivität im Enzymassay, aber geringere Bindesignale im SPR Experiment (**3**: 15 RU bei 100 µM. **48**: 50 RU bei 100 µM). Darüber hinaus wird eine verminderte Resistenzbildung bei Inhibitoren assoziiert, die die gleiche Bindestelle wie das natürliche Substrat aufweisen. Aus diesem Grund ist die Identifizierung der Bindestelle von größtem Interesse, da dies zusätzlich als Kriterium zur Wahl des zur Optimierung geeignetsten Inhibitors dienen kann.

Aufgrund der hohen Anzahl an Inhibitoren, die eine Reduktion der HHQ Biosynthese bewirkten, wurde im weiteren nur noch auf die Charakterisierung der vielversprechendsten Verbindungen durchgeführt, welche in diesem Fall **A1** und **A11** waren, da beide einen IC<sub>50</sub> Wert von < 5 µM aufwiesen. Für diese Verbindungen wurden mittels SPR, analog zu den Publikationen A und B, Experimente zur Identifizierung der Bindestellen durchgeführt. Diese ergaben eine Bindestelle im aktiven Zentrum von PqsD für **A1**, wohingegen **A11** vermutlich im Kanal oberhalb des aktiven Zentrums bindet. **A1** scheint die geeignete Verbindung zur Optimierung zu sein, da sie dieselbe Bindestelle wie das natürliche Substrat besitzt. Dies wird mit einem verminderten Risiko der Resistenzentwicklung assoziiert, da die Einführung von Mutationen in der Bindestelle dazu führt, dass neben dem Hemmstoff auch das natürliche Substrat nicht mehr binden kann. Es zeigte sich jedoch, dass das Hydrochinon instabil ist. Wird die Verbindung über einen längeren Zeitraum an der Luft gelagert, entsteht durch Oxidation das Chinon, welches keine Aktivität gegenüber PqsD besitzt. Aus diesem Grund wird diese Verbindung zunächst nicht weiter verfolgt.

Bei **A11** handelt es sich um ein Benzamidobenzoësäurederivat, welches sich im Vergleich zu den in Publikation A beschriebenen PqsD Inhibitoren im Substitutionsmuster am Benzamidoring unterscheidet. Die hohe strukturelle Ähnlichkeit lieferte erwartungsgemäß ein gleiches Bindungsverhalten. Wie bereits in Publikation A beobachtet, wurde auch **A11** nicht in der Bindung durch ACoA beeinflusst, zeigte aber ebenso eine Abschwächung der Bindung, wenn Aminosäuren im aktiven Zentrum ausgetauscht wurden. Dies spricht dafür, dass auch **A11** als Kanalblocker wirkt.

## 4.2.2 Fragmentscreening

Im Fragmentscreening wurden aus einer kommerziell erhältlichen Substanzbibliothek (Maybridge Library) 500 Fragmente ausgewählt, die die „*Rule of Three*“ erfüllen und die strukturell sehr unterschiedlich sind. Die Wahrscheinlichkeit in den Substrattunnel zu passen, ist aufgrund der Einfachheit der Strukturen für Fragmente höher (22). Aus diesem Grund fiel die Entscheidung darauf Fragmente zu testen. Die Bindung aller 500 Verbindungen an PqsD wurde mittels SPR überprüft. Es zeigte sich dabei, dass nahezu 60% zu einem Bindesignal führten. In Hinblick auf die literaturbeschriebenen Bindungsraten von 1-4% (31, 37) ist die hier erhaltene Rate von 62% (312 von 500 Fragmenten zeigen eine Bindung) ungewöhnlich hoch. Gründe hierfür könnten darin liegen, dass die Fragmente sehr einfache Strukturen aufweisen, die mit verschiedenen Seiten des Proteins schwache Wechselwirkungen eingehen können und die aufgrund der hohen Sensitivität des SPRs detektiert werden konnten.

Um den Assayaufwand auf einem vertretbaren Niveau zu halten, war ein Selektionskriterium essentiell. Aus diesem Grund wurden nur die 22 Verbindungen im funktionellen Assay getestet, deren Bindungssignale mindestens 40% des Signals der Positivkontrolle betragen. Drei der 22 Fragmente führten zu einer moderaten Hemmung (>50% @ 100 µM), wohingegen der Großteil der Verbindungen PqsD nicht oder nur schwach inhibierte (Strukturen sind in Publikation C auf S. 2063 abgebildet). Dies ist sehr wahrscheinlich darauf zurückzuführen, dass die Fragmente mit dem Target außerhalb des aktiven Zentrums interagieren. Die hohe Anzahl an nicht funktionalen Bindern ist ein wesentlicher Nachteil dieser Strategie. Die geringen Molekulargewichte der Fragment-ähnlichen Strukturen führen dazu, dass die Wahrscheinlichkeit Hits zu identifizieren, die eine hohe inhibitorische Aktivität besitzen, sehr gering ist (155). Dennoch konnte ein Fragment identifiziert werden, welches einen IC<sub>50</sub>-Wert im einstelligen mikromolaren Bereich zeigt.

Die geringe Hitrate von 13% (3 aus 22 aktiv) kann aus dem gewählten Auswahlkriterium (mind. 40% Bindung im Vergleich zur Positivkontrolle) resultiert haben, wodurch möglicherweise andere PqsD Inhibitoren übersehen wurden. Die zur Überprüfung im funktionellen Assay getesteten Nicht-Binder zeigten keine Hemmung, während die Inhibition der Verbindungen, die das maximal mögliche Signal ( $R_{Max}$ ) überstiegen, auf unspezifische Effekte zurückgeführt werden konnte. Dies bestätigt, dass deren

Ausschluss zulässig war. Es besteht jedoch das Risiko, dass schwächere Binder, die möglicherweise eine höhere Inhibition aufweisen, durch die willkürlich auf 40% gesetzte Grenze ausgeschlossen wurden. Da jedoch mittels dieses Ansatzes drei Fragmente identifiziert werden konnten, die zu einer Inhibition von PqsD führten, wurde dies nicht untersucht.

Zwei der drei Verbindungen stellen aufgrund ihrer hohen Liganden Effizienz (156) vielversprechende Kandidaten zur Optimierung dar (Abb. 14). SPR basierte Untersuchungen ergaben, dass sich die Bindestelle von **B91** im aktiven Zentrum von PqsD befindet, wodurch dieses Fragment einen sehr interessanten Startpunkt zur Optimierung bietet. Die Targetaktivität, die für eine Leitverbindung notwendig ist, könnte durch Anwendung von „*Fragment Linking*“ oder „*Fragment Growing*“ Strategien erzielt werden (157-159).

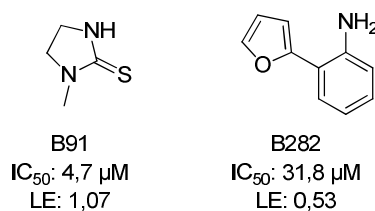


Abb. 14: Strukturen und Ligandeneffizienz der zwei potentesten Fragmente. Die Berechnung der LE erfolgte unter Verwendung folgender Gleichung:  $\text{LE} = -1,4 * \log(\text{IC}_{50}) / N$  (Anzahl der Nicht-Wasserstoffatome) (156).

#### 4.2.3 Virtuelles Screening

Im dritten Ansatz wurde ein virtuelles Screening durchgeführt. Diese Strategie wird häufig dann eingesetzt, wenn bereits Informationen über die Targetstruktur vorhanden sind. Anhand eines erstellten Pharmakophormodells können Bibliotheken von mehr als  $10^8$  Verbindungen gescreent und evaluiert werden, wodurch neben dem Vorteil der Zeitsparnis auch eine Reduktion der Verbrauchsmaterialien und von Kosten erzielt wird (zusammengefasst in (160)).

In dieser rational geleiteten Strategie wurde ein dreidimensionales Pharmakophormodell unter Verwendung der vorhandenen Kristallstrukturen von PqsD im Komplex mit dem natürlichen Substrat ACoA (PDB ID 3H77) und ohne Ligand (PDB ID 3H76) erstellt (106). Zusätzlich flossen die Docking Posen der 2-Nitrophenylmethanol-Derivate und der 2-Benzamidobenzoesäuren (139, 161) mit ein, um eine bestmögliche Vorhersagekraft des Modells zu gewährleisten. Anhand des erstellten Pharmakophormodells wurde eine Bibliothek bestehend aus ca. 900 Verbindungen virtuell durchmustert und die Verbindungen gemäß dem erhaltenen „*Bindingscore*“ eingestuft. Die besten 102 Verbindungen („*Bindingscore*“  $\geq 60$ ) wurden zu einer Bibliothek zusammengefügt und mittels SPR evaluiert. Für ca. 60% der Verbindungen wurde eine Bindung beobachtet, was als gute Vorhersagekraft des Pharmakophormodells zu werten ist. Möglicherweise besteht aber noch Spielraum für Verbesserungen durch Verfeinerung des Modells und der Bewertungskriterien.

Aufgrund der hohen Anzahl bindender Substanzen wurden nur die 18 im funktionellen Assay untersucht, deren Bindesignale mindestens 30% des Signals der Positivkontrolle entsprachen. Insgesamt zeigten 12 Verbindungen eine inhibitorische Aktivität, was einer Hitrate von 67% entspricht. Auffallend war, dass vier der sechs potentesten Inhibitoren (>50% Inhibition bei 50 µM) ein 2-Aminopyrimidin-Motiv aufwiesen. Dieses strukturelle Feature schien sich vorteilhaft auf die Inhibition von PqsD auszuwirken. Aus diesem Grund erfolgte eine Neubewertung der *in silico* Vorselektionsmethode, aber auch des SPR-Rankings, um zu überprüfen, ob eventuell Verbindungen fälschlicherweise aussortiert wurden. In der ursprünglichen Bibliothek, die für das virtuelle Screening genutzt wurde, befanden sich 115 weitere 2-Aminopyrimidine. 12 dieser Verbindungen wurden aufgrund einer fehlenden Bindung im SPR (vier Verbindungen) oder einer zu schwachen Interaktion (acht Verbindungen) ausgeschlossen. Der funktionelle Assay ergab, dass die Nicht-Binder und die schwachen Binder im Wesentlichen auch inaktiv waren. In Einzelfällen wurde eine PqsD Inhibition von 40% bei 50 µM erreicht, wodurch deutlich wird, dass deren Ausschluss vertretbar ist, da aktiver Inhibitoren identifiziert wurden.

Im virtuellen Screening wurden 103 Verbindungen aufgrund eines zu geringen „*Bindingscores*“ ausgeschlossen, von denen aber ca. 80% keine oder nur eine schwache Inhibition (<50% bei 50 µM) zeigten. Für neun der Verbindungen wurde jedoch eine PqsD-Hemmung von über 80% bei 50 µM erhalten. Dies verdeutlicht das Problem, dass die Vorhersagekraft des Pharmakophormodells stark von optimal gewählten Parametern innerhalb der „*Scoring Function*“ und dem genutzten Kraftfeld abhängt. Da jedoch durch kritische Begutachtung der initialen Hits der positive Einfluss des 2-Aminopyrimidin-Grundgerüstes erkannt wurde, konnte dieses Defizit kompensiert werden.

#### 4.2.4 SPR Evaluierung

Der im **virtuellen Screening** generierte Datensatz von Hemm- und Bindewerten kann zur Bewertung, ob ein SPR-basiertes Screening eine geeignete Strategie zur Identifizierung von neuen PqsD Inhibitoren darstellt, genutzt werden. Die erhaltenen Ergebnisse legen dar, dass zwischen dem SPR Bindungsassay und dem funktionellen Assay eine gute Korrelation existiert. So zeigten nahezu 80% der Verbindungen entweder eine Bindung und Inhibition (55%) oder keine Bindung und keine Inhibition (25%). Nur in wenigen Fällen (ca. 10%) konnte eine Bindung beobachtet werden, die nicht zu einer Hemmung von PqsD führte. Gründe hierfür liegen möglicherweise in einer zu schwachen Interaktion, die nicht ausreicht um mit dem natürlichen Substrat zu konkurrieren. Eine andere Ursache könnte eine Bindung an Proteinareale sein, die nicht an der katalytischen Reaktion beteiligt sind (zum Beispiel die Proteinoberfläche). Die verbleibenden 10% waren in der Lage, die HHQ Bildung zu reduzieren, zeigten aber keine Bindung an PqsD. Möglicherweise waren die genutzten SPR-Parameter nicht optimal gewählt (162). Vorstellbar wäre auch, dass die Verbindungen an das Substrat ACoA binden und dadurch verhindern, dass dieses zu HHQ umgesetzt wird. Da keine dieser Verbindungen

eine große Aktivität aufwies (12-27% bei 50 µM), zeigt dies, dass es vertretbar war, Verbindungen, die kein SPR-Signal zeigten, zu vernachlässigen.

Eine ähnliche Tendenz erhält man auch beim „*me-too*“ Ansatz, in welchem die Korrelation zwischen SPR und funktionellem Assay bei 83% liegt. 75% der Verbindungen zeigten sowohl Bindung als auch Inhibition, während 8% keine Bindung und keine Hemmung aufwiesen. Der Anteil an Verbindungen, für die eine Bindung detektiert, aber keine Hemmung beobachtet werden konnte ist vergleichbar zum virtuellen Screening (17%).

Eine andere Korrelation liegt jedoch beim **Fragmentscreenings** vor. Hier wurden ca. 290 aus 500 Verbindungen als Binder identifiziert, denen nur eine Zahl von 3 Inhibitoren gegenübersteht. Dieses Verhältnis muss jedoch insofern korrigiert werden, dass nicht alle 290 Fragmente auf ihre Inhibition getestet wurden, sondern nur die 22 mit den stärksten Signalen, wodurch eine Korrelation von 13% zustande kam.

Diese Ergebnisse zeigen, dass insbesondere für die fokussierten Ansätze die SPR-Technologie ein probates Mittel darstellt, um die Anzahl der potentiellen Inhibitoren auf eine praktikable Menge zu reduzieren, die dann im Anschluss mittels funktionellen Assay evaluiert werden. In Bezug auf das Fragmentscreening zeigte der Einsatz von SPR Schwächen auf, aber auch hier war durch das verwendete Auswahlkriterium die Identifizierung von drei Inhibitoren möglich. Dies zeigt, dass die SPR-Technologie unabhängig von der Strategie der Bibliothekszusammenstellung besonders im Hinblick auf Zeit- und Materialersparnisse eine adäquate Screeningmethode darstellt.

#### **4.2.5 Finale Diskussion der Screeningansätze**

Der „*me-too*“ Ansatz, der sich die strukturelle Ähnlichkeit des Targets PqsD und des homologen Proteins FabH zu Nutze gemacht hat, stellte sich als sehr erfolgreiche Strategie heraus. Durch die hohe Ähnlichkeit der Enzyme konnten neun PqsD Inhibitoren aus zwölf Testverbindungen identifiziert werden. Dies zeigt die Effektivität einer vor dem eigentlichen Screeningschritt vorangestellten, Struktur-geleiteten Verbindungsauswahl. Dieser Ansatz kann jedoch nur dann verfolgt werden, wenn ein oder mehrere homologe Proteine vorhanden und Inhibitoren dieser beschrieben sind. Dies kann gleichzeitig zum Auftreten von Selektivitätsproblemen führen, welche durch nachfolgende Optimierungsprozesse überwunden werden müssen. Da eine FabH Inhibition nur einen geringen Einfluss auf die Viabilität von *P. aeruginosa* ausübt (163, 164), dürften in diesem Fall keine ungewollten „*off-Target*“ Effekte zu beobachten sein. Die der Strategie zugrundeliegende Annahme, dass FabH Inhibitoren ebenso in der Lage sind, PqsD zu hemmen, wird dadurch bestätigt, dass in jeder der getesteten, literaturbeschriebenen Strukturklasse Verbindungen identifiziert werden konnten, die ebenso PqsD hemmen. Letztendlich muss jedoch hervorgehoben werden, dass trotz einer Hitrate von 82% am Ende nur ein zur Optimierung geeigneter Kandidat erhalten wurde. Die anderen acht

Verbindungen wurden entweder aufgrund einer geringeren Aktivität oder chemischer Instabilität nicht weiter verfolgt. Die Hitverbindung **A11** weist eine strukturelle Ähnlichkeit zu einer bereits publizierten Verbindungsklasse (139) auf, welche *in cellulo* inaktiv ist. Möglicherweise könnte durch weitere Optimierung die gewünschte Aktivität erreicht werden. Da in den anderen Strategien Kandidaten erhalten wurden, die leichter zu optimieren sind, stellt **A11** nicht die erste Wahl dar.

Beim durchgeführten **Fragmentscreening** ist die Ausbeute von nur einer potenten Verbindung gemessen an der Größe der getesteten Bibliothek sowie der Anzahl an erhaltenen primären Hits gering. Dennoch stellt die Verbindung **B91** aufgrund der vielversprechenden Inhibition und einer Bindung im aktiven Zentrum prinzipiell einen geeigneten Ausgangspunkt zur Optimierung dar. Da die Aktivität dieses Fragments im Vergleich zu den besten Inhibitoren aus Ansatz C geringer ist, wurde diese Verbindung vorerst nicht berücksichtigt. Die erhaltene Hitrate von 13% ist bezeichnend für die geringere Effizienz dieser Strategie. Eine Möglichkeit in Zukunft die Anzahl der nicht funktionellen PqsD-Binder zu reduzieren, könnte die zusätzliche Messung aller Kandidaten gegen PqsD sein, welches am aktiven Zentrum blockiert ist. Die Beladung des aktiven Zentrums kann einerseits mittels des natürlichen Substrates ACoA (139), aber auch durch einen Inhibitor, der kovalent oder pseudo-irreversibel an das Protein bindet (144), erfolgen. Dieses Vorgehen würde die direkte Identifizierung von Fragmenten ermöglichen, die im aktiven Zentrum binden, wodurch die Wahrscheinlichkeit erhöht wird, dass die dort stattfindende Enzymreaktion gehemmt wird.

Im **virtuellen Screening** konnte eine Hitrate von 67% erzielt werden, welche den Erfolg dieses Ansatzes widerspiegelt. Insgesamt wurden 30 Verbindungen identifiziert, die starke PqsD-Inhibitoren darstellen. Die Mehrheit dieser Verbindungen weist eine 2-Aminopyrimidinstruktur auf. SPR-basierte Bindestudien ergaben, dass diese Strukturklasse nicht von einer Blockade des aktiven Zentrums beeinflusst wird. Da aber auch hier durch zielgerichtete Mutagenese der Aminosäuren im aktiven Zentrum eine Reduktion der Signalstärke erfolgte, ist es wahrscheinlich, dass sich deren Bindestelle im Kanal oberhalb des aktiven Zentrums befindet. Die gemeinsame 2-Aminopyrimidinstruktur ermöglicht es eine SAR abzuleiten, wodurch diese Verbindungsklasse aufgrund der Menge an Informationen als vielversprechendster Startpunkt zur Optimierung erscheint.

Beim Vergleich der unterschiedlichen Ansätze miteinander wird deutlich, dass die fokussierten den „*random*“ Screeningmethoden deutlich überlegen sind. Diese Schlussfolgerung wurde bereits in einem von Valler und Green auf theoretischer Basis durchgeführten Vergleich erhalten, dessen Grundlage verschiedene Studien an unterschiedlichen Targets bilden (146). Der intrinsische Nachteil in Bezug auf die Vergleichbarkeit dieser Studien wird in der hier vorgestellten Arbeit behoben, da alle Experimente am selben Zielprotein durchgeführt wurden. Dennoch sind Schlussfolgerungen, die auf dieses bestimmte Protein zutreffen, möglicherweise nicht auf andere Zielmoleküle übertragbar. Trotzdem muss berücksichtigt werden, dass die fokussierten Screeningmethoden nur deshalb durchführbar waren, weil Vorarbeiten zur Aufklärung der Targetstruktur und Wechselwirkungen mit

dem Substrat bzw. Inhibitoren existierten. Auf dieser Grundlage war es möglich, die Homologie der aktiven Zentren von PqsD und FabH festzustellen (106, 165) und eine „*me-too*“ Strategie zu verfolgen. Zur Erstellung des Pharmakophormodells waren diese strukturellen Kenntnisse ebenfalls essentiell (106, 139, 161, 165). Oftmals sind diese aber nicht vorhanden, so zum Beispiel zu Beginn einer Screening Kampagne gegen ein bis dato unbekanntes Target. In diesen Fällen können die fokussierten Ansätze nicht verfolgt werden und das Fragmentscreening rückt in den Vordergrund. Diese Methode bedingt keine Kenntnisse über Targetstruktur oder das Vorhandensein von bereits entwickelten Inhibitoren benötigt. Die Ergebnisse dieser Arbeit zeigen deutlich, dass die Wahl der geeigneten Screeningmethode stark von der vorliegenden Ausgangssituation abhängt.

### 4.3 Fazit

In der vorliegenden Arbeit konnten vielfältige Einsatzmöglichkeiten der SPR erfolgreich zur Identifizierung und Charakterisierung von *pqs*-QS-Inhibitoren genutzt werden.

Zum einen war es möglich mittels SPR und weiteren biophysikalischen Methoden (NMR, ITC sowie molekularem Docking) die Bindungsmodi von PqsD Inhibitoren aufzuklären. Hierbei haben insbesondere die SPR-basierten Experimente zur Identifizierung der Bindestellen einen erheblichen Beitrag geleistet. Die dabei entwickelten Testsysteme stellen aufgrund der einfachen Handhabung gute Hilfsmittel dar, um in weiterführenden Arbeiten neue PqsD Inhibitoren hinsichtlich ihrer Bindungsmodi zu charakterisieren. Wie bereits von Sahner *et al.* gezeigt, konnten durch Einsatz eines modifizierten Testsystems wichtige Informationen zu Ureidothiophen-Derivaten und ihrer Bindungsorientierung im PqsD-Substrattunnel gewonnen werden. Auf dieser Grundlage konnte die Substanzklasse erfolgreich hinsichtlich Affinität optimiert werden (144).

Zum anderen wurden mittels SPR drei verschiedenen Screeningstrategien zur Identifizierung potentieller PqsD-Inhibitoren durchgeführt, die sich den Target-basierten Ansätzen zuordnen lassen. Diese Strategien beinhalten im Gegensatz zum Phänotyp-Screening oftmals das Problem, dass die erhaltenen Hitverbindungen unzureichende, zelluläre Effekte aufweisen. Dennoch wurden in allen Ansätzen Verbindungen identifiziert, die eine Aktivität im biologischen System besitzen. Insbesondere die 2-Aminopyrimidin-Klasse, die im virtuellen Screening Ansatz erhalten wurde, stellt einen vielversprechenden Startpunkt dar und wird derzeit weiter hinsichtlich ihrer zellulären Aktivität optimiert.

Anhand der durchgeführten Experimente wird deutlich, dass der Einsatz von SPR in verschiedenen Bereichen der Wirkstoffentwicklung ein wertvolles Toll darstellt, um „*Drug Discovery*“ Kampagnen zu erleichtern bzw. auch zu beschleunigen.

## 5 Literaturverzeichnis

- (1). de Mol, N. J., Fischer, M. J. E., Castrop, J., et al. (2006) Determination by surface plasmon resonance of the binding characteristics of a kinase and its substrates, *Biomol. Interactions* 18, 19-22.
- (2). Cooper, M. A. (2003) Label-free screening of bio-molecular interactions, *Anal. Bioanal. Chem.* 377, 834-842.
- (3). McGhee, J. D., and Hoppel, P. H. V. (1974) Theoretical Aspects of DNA-Protein Interactions - Cooperative and Non-Cooperative Binding of Large Ligands to a One-Dimensional Homogeneous Lattice, *J. Mol. Biol.* 86, 469-489.
- (4). Szabo, A., Stoltz, L., and Granzow, R. (1995) Surface plasmon resonance and its use in biomolecular interaction analysis (BIA), *Curr. Opin. Struct. Biol.* 5, 699-705.
- (5). Burstein, E., Chen, W. P., Chen, Y. J., et al. (1974) Surface Polaritons - Propagating Electromagnetic Modes at Interfaces, *J. Vac. Sci. Technol.* 11, 1004-1019.
- (6). Schasfoort, R. B. M., and Tudos, A. J. (2008) *Handbook of Surface Plasmon Resonance*, R. Soc. Chem.
- (7). Gianetti, A. M. (2011) From Experimental Design to Validated Hits: A Comprehensive Walk-Through of Fragment Lead Identification Using Surface Plasmon Resonance in *Meth. Enzymol.*, pp 169-216, Elsevier Inc., South San Francisco, California, USA.
- (8). Stenberg, E., Persson, B., Roos, H., et al. (1991) Quantitative-Determination of Surface Concentration of Protein with Surface-Plasmon Resonance Using Radiolabeled Proteins, *J. Colloid Interface Sci.* 143, 513-526.
- (9). Gedig, E. T. (2008) Surface Chemistry in SPR Technology, in *Handbook of Surface Plasmon Resonance* (Tudos, R. B. M. S. a. A. J., Ed.), pp 173-220, R. Soc. Chem.
- (10). Day, Y. S., Baird, C. L., Rich, R. L., et al. (2002) Direct comparison of binding equilibrium, thermodynamic, and rate constants determined by surface- and solution-based biophysical methods, *Protein Sci.* 11, 1017-1025.
- (11). Navratilova, I., Papalia, G. A., Rich, R. L., et al. (2007) Thermodynamic benchmark study using Biacore technology, *Anal. Biochem.* 364, 67-77.
- (12). Papalia, G. A., Leavitt, S., Bynum, M. A., et al. (2006) Comparative analysis of 10 small molecules binding to carbonic anhydrase II by different investigators using Biacore technology, *Anal. Biochem.* 359, 94-105.
- (13). Rich, R. L., Papalia, G. A., Flynn, P. J., et al. (2009) A global benchmark study using affinity-based biosensors, *Anal. Biochem.* 386, 194-216.
- (14). Johnsson, B., Lofas, S., and Lindquist, G. (1991) Immobilization of proteins to a carboxymethylextran-modified gold surface for biospecific interaction analysis in surface plasmon resonance sensors, *Anal. Biochem.* 198, 268-277.
- (15). Lofas, S., and Johnsson, B. (1990) A Novel Hydrogel Matrix on Gold Surfaces in Surface-Plasmon Resonance Sensors for Fast and Efficient Covalent Immobilization of Ligands, *J. Chem. Soc. Chem. Commun.*, 1526-1528.
- (16). Cuatrecasas, P., and Parikh, I. (1972) Adsorbents for Affinity Chromatography - Use of N-Hydroxysuccinimide Esters of Agarose, *Biochem.* 11, 2291-&.
- (17). Fischer, M. J. E. (2010) Amine coupling through EDC/NHS: a practical approach, *Methods Mol. Biol.* 627, 55-73.
- (18). Muegge, I., Heald, S. L., and Brittelli, D. (2001) Simple selection criteria for drug-like chemical matter, *J. Med. Chem.* 44, 1841-1846.
- (19). Lipinski, C. A., Lombardo, F., Dominy, B. W., et al. (1997) Experimental and computational approaches to estimate solubility and permeability in drug discovery and development settings, *Adv. Drug Deliv. Rev.* 23, 3-25.

- (20). Walters, W. P., Murcko, A., and Murcko, M. A. (1999) Recognizing molecules with drug-like properties, *Curr. Opin. Chem. Biol.* 3, 384-387.
- (21). Bohacek, R. S., McMardin, C., and Guida, W. C. (1996) The art and practice of structure-based drug design: a molecular modeling perspective, *Med. Res. Rev.* 16, 3-50.
- (22). Hann, M. M., Leach, A. R., and Harper, G. (2001) Molecular complexity and its impact on the probability of finding leads for drug discovery, *J. Chem. Inf. Comput. Sci.* 41, 856-864.
- (23). Fox, S., Wang, H., Sopchak, L., et al. (2001) High throughput screening: early successes indicate a promising future, *J. Biomol. Screen.* 6, 137-140.
- (24). Johnston, K. A. (2001) Chemical attraction: affinity techniques aid in new drug discovery, *Pharma Genomics* 28, 30-39.
- (25). Geschwindner, S., Olsson, L. L., Albert, J. S., et al. (2007) Discovery of a novel warhead against beta-secretase through fragment-based lead generation, *J. Med. Chem.* 50, 5903-5911.
- (26). Neumann, T., Junker, H. D., Schmidt, K., et al. (2007) SPR-based fragment screening: Advantages and applications, *Curr. Top. Med. Chem.* 7, 1630-1642.
- (27). Kuglstatter, A., Stahl, M., Peters, J. U., et al. (2008) Tyramine fragment binding to BACE-1, *Bioorg. Med. Chem. Lett.* 18, 1304-1307.
- (28). Nordstrom, H., Gossas, T., Hamalainen, M., et al. (2008) Identification of MMP-12 inhibitors by using biosensor-based screening of a fragment library, *J. Med. Chem.* 51, 3449-3459.
- (29). Hamalainen, M. D., Zhukov, A., Ivarsson, M., et al. (2008) Label-free primary screening and affinity ranking of fragment libraries using parallel analysis of protein panels, *J. Biomol. Screen.* 13, 202-209.
- (30). Danielson, U. H. (2009) Fragment library screening and lead characterization using SPR biosensors, *Curr. Top. Med. Chem.* 9, 1725-1735.
- (31). Perspicace, S., Banner, D., Benz, J., et al. (2009) Fragment-based screening using surface plasmon resonance technology, *J. Biomol. Screen.* 14, 337-349.
- (32). Elinder, M., Geitmann, M., Gossas, T., et al. (2011) Experimental validation of a fragment library for lead discovery using SPR biosensor technology, *J. Biomol. Screen.* 16, 15-25.
- (33). Albert, J. S., Blomberg, N., Breeze, A. L., et al. (2007) An integrated approach to fragment-based lead generation: Philosophy, strategy and case studies from AstraZeneca's drug discovery programmes, *Curr. Top. Med. Chem.* 7, 1600-1629.
- (34). Boehm, H. J., Boehringer, M., Bur, D., et al. (2000) Novel inhibitors of DNA gyrase: 3D structure based biased needle screening, hit validation by biophysical methods, and 3D guided optimization. A promising alternative to random screening, *J. Med. Chem.* 43, 2664-2674.
- (35). Sun, L., Tran, N., Tang, F., et al. (1998) Synthesis and biological evaluation of novel 3-(substituted pyrrol-2-yl)indolin-2-ones as potent and selective inhibitors of the FLK-1/KDR receptor tyrosine kinase., *Abstr. Pap. Am. Chem. Soc.* 215, U909-U909.
- (36). Giannetti, A. M., Koch, B. D., and Browner, M. F. (2008) Surface plasmon resonance based assay for the detection and characterization of promiscuous inhibitors, *J. Med. Chem.* 51, 574-580.
- (37). Navratilova, I., and Hopkins, A. L. (2010) Fragment Screening by Surface Plasmon Resonance, *ACS Med. Chem. Lett.* 1, 44-48.
- (38). Huber, W. (2005) A new strategy for improved secondary screening and lead optimization using high-resolution SPR characterization of compound-target interactions, *J. Mol. Recognit.* 18, 273-281.

- (39). Huber, W., and Mueller, F. (2006) Biomolecular interaction analysis in drug discovery using surface plasmon resonance technology, *Curr. Pharm. Des.* 12, 3999-4021.
- (40). Wong, C. H., Hendrix, M., Manning, D. D., et al. (1998) A library approach to the discovery of small molecules that recognize RNA: Use of a 1,3-hydroxyamine motif as core, *J. Am. Chem. Soc.* 120, 8319-8327.
- (41). Markgren, P. O., Hamalainen, M., and Danielson, U. H. (1998) Screening of compounds interacting with HIV-1 proteinase using optical biosensor technology, *Anal. Biochem.* 265, 340-350.
- (42). Nilsson, M., Hamalainen, M., Ivarsson, M., et al. (2009) Compounds binding to the S2-S3 pockets of thrombin, *J. Med. Chem.* 52, 2708-2715.
- (43). Sweeney, Z. K., Acharya, S., Briggs, A., et al. (2008) Discovery of triazolinone non-nucleoside inhibitors of HIV reverse transcriptase, *Bioorg. Med. Chem. Lett.* 18, 4348-4351.
- (44). Sweeney, Z. K., Dunn, J. P., Li, Y., et al. (2008) Discovery and optimization of pyridazinone non-nucleoside inhibitors of HIV-1 reverse transcriptase, *Bioorg. Med. Chem. Lett.* 18, 4352-4354.
- (45). Driscoll, J. A., Brody, S. L., and Kollef, M. H. (2007) The epidemiology, pathogenesis and treatment of *Pseudomonas aeruginosa* infections, *Drugs* 67, 351-368.
- (46). Kerr, K. G., and Snelling, A. M. (2009) *Pseudomonas aeruginosa*: a formidable and ever-present adversary, *J. Hosp. Infect.* 73, 338-344.
- (47). Lyczak, J. B., Cannon, C. L., and Pier, G. B. (2000) Establishment of *Pseudomonas aeruginosa* infection: lessons from a versatile opportunist, *Microbes Infect.* 2, 1051-1060.
- (48). Govan, J. R., and Deretic, V. (1996) Microbial pathogenesis in cystic fibrosis: mucoid *Pseudomonas aeruginosa* and *Burkholderia cepacia*, *Microbiol. Rev.* 60, 539-574.
- (49). Hoiby, N. (1975) Prevalence of Mucoid Strains of *Pseudomonas-Aeruginosa* in Bacteriological Specimens from Patients with Cystic-Fibrosis and Patients with Other Diseases, *APMIS* 83, 549-552.
- (50). Kulczycki, L. L., Murphy, T. M., and Bellanti, J. A. (1978) *Pseudomonas* Colonization in Cystic-Fibrosis - Study of 160 Patients, *J. Am. Med. Assoc.* 240, 30-34.
- (51). Pier, G. B. (1985) Pulmonary-Disease Associated with *Pseudomonas-Aeruginosa* in Cystic-Fibrosis - Current Status of the Host-Bacterium Interaction, *J. Infect. Dis.* 151, 575-580.
- (52). Rahme, L. G., Tan, M. W., Le, L., et al. (1997) Use of model plant hosts to identify *Pseudomonas aeruginosa* virulence factors, *Proc. Natl. Acad. Sci. U.S.A.* 94, 13245-13250.
- (53). Rumbaugh, K. P., Griswold, J. A., and Hamood, A. N. (2000) The role of quorum sensing in the in vivo virulence of *Pseudomonas aeruginosa*, *Microbes Infect.* 2, 1721-1731.
- (54). Kerem, E., Corey, M., Gold, R., et al. (1990) Pulmonary-Function and Clinical Course in Patients with Cystic-Fibrosis after Pulmonary Colonization with *Pseudomonas-Aeruginosa*, *J. Ped.* 116, 714-719.
- (55). Szaff, M., Hoiby, N., and Flensburg, E. W. (1983) Frequent Antibiotic-Therapy Improves Survival of Cystic-Fibrosis Patients with Chronic *Pseudomonas-Aeruginosa* Infection, *Acta Paediatr. Scand.* 72, 651-657.
- (56). Steinkamp, G., Tummler, B., Malottke, R., et al. (1989) Treatment of pseudomonas aeruginosa colonisation in cystic fibrosis, *Arch. Dis. Child.* 64, 1022-1028.
- (57). Nikaido, H. (1989) Outer-Membrane Barrier as a Mechanism of Antimicrobial Resistance, *Antimicrob. Agents Chemother.* 33, 1831-1836.

- (58). Li, X. Z., Zhang, L., and Poole, K. (2000) Interplay between the MexA-MexB-OprM multidrug efflux system and the outer membrane barrier in the multiple antibiotic resistance of *Pseudomonas aeruginosa*, *J. Antimicrob. Chemother.* 45, 433-436.
- (59). Li, X. Z., Livermore, D. M., and Nikaido, H. (1994) Role of Efflux Pump(S) in Intrinsic Resistance of *Pseudomonas-Aeruginosa* - Resistance to Tetracycline, Chloramphenicol, and Norfloxacin, *Antimicrob. Agents Chemother.* 38, 1732-1741.
- (60). Li, X. Z., Ma, D., Livermore, D. M., et al. (1994) Role of Efflux Pump(S) in Intrinsic Resistance of *Pseudomonas-Aeruginosa* - Active Efflux as a Contributing Factor to Beta-Lactam Resistance, *Antimicrob. Agents Chemother.* 38, 1742-1752.
- (61). Li, X. Z., Zhang, L., Srikumar, R., et al. (1998) beta-lactamase inhibitors are substrates for the multidrug efflux pumps of *Pseudomonas aeruginosa*, *Antimicrob. Agents Chemother.* 42, 399-403.
- (62). Bjarnsholt, T., Tolker-Nielsen, T., Hoiby, N., et al. (2010) Interference of *Pseudomonas aeruginosa* signalling and biofilm formation for infection control, *Expert Rev. Mol. Med.* 12, e11.
- (63). Donlan, R. M., and Costerton, J. W. (2002) Biofilms: Survival mechanisms of clinically relevant microorganisms, *Clin. Microbiol. Rev.* 15, 167-+.
- (64). Costerton, J. W., Lewandowski, Z., Caldwell, D. E., et al. (1995) Microbial Biofilms, *Annu. Rev. Microbiol.* 49, 711-745.
- (65). Costerton, J. W., Stewart, P. S., and Greenberg, E. P. (1999) Bacterial biofilms: A common cause of persistent infections, *Science* 284, 1318-1322.
- (66). Davies, D. G., Parsek, M. R., Pearson, J. P., et al. (1998) The involvement of cell-to-cell signals in the development of a bacterial biofilm, *Science* 280, 295-298.
- (67). Jimenez, P. N., Koch, G., Thompson, J. A., et al. (2012) The multiple signaling systems regulating virulence in *Pseudomonas aeruginosa*, *Microbiol. Mol. Biol. Rev.* 76, 46-65.
- (68). Fuqua, W. C., Winans, S. C., and Greenberg, E. P. (1994) Quorum sensing in bacteria: the LuxR-LuxI family of cell density-responsive transcriptional regulators, *J. Bacteriol.* 176, 269-275.
- (69). Engebrecht, J., Nealson, K., and Silverman, M. (1983) Bacterial bioluminescence: isolation and genetic analysis of functions from *Vibrio fischeri*, *Cell* 32, 773-781.
- (70). Engebrecht, J., and Silverman, M. (1984) Identification of genes and gene products necessary for bacterial bioluminescence, *Proc. Natl. Acad. Sci. U.S.A.* 81, 4154-4158.
- (71). Engebrecht, J., and Silverman, M. (1987) Nucleotide sequence of the regulatory locus controlling expression of bacterial genes for bioluminescence, *Nucleic Acids Res.* 15, 10455-10467.
- (72). Eberhard, A. (1972) Inhibition and activation of bacterial luciferase synthesis, *J. Bacteriol.* 109, 1101-1105.
- (73). Nealson, K. H. (1977) Autoinduction of bacterial luciferase. Occurrence, mechanism and significance, *Arch. Microbiol.* 112, 73-79.
- (74). Miller, M. B., and Bassler, B. L. (2001) Quorum sensing in bacteria, *Annu. Rev. Microbiol.* 55, 165-199.
- (75). Pesci, E. C., and Iglewski, B. H. (1999), Am. Soc. Microbiol. Washington, DC.
- (76). Rampioni, G., Leoni, L., and Williams, P. (2014) The art of antibacterial warfare: Deception through interference with quorum sensing-mediated communication, *Bioorg. Chem.* 55, 60-68.
- (77). Gambello, M. J., and Iglewski, B. H. (1991) Cloning and Characterization of the *Pseudomonas-Aeruginosa* Lasr Gene, a Transcriptional Activator of Elastase Expression, *J. Bacteriol.* 173, 3000-3009.

- (78). Passador, L., Cook, J. M., Gambello, M. J., et al. (1993) Expression of Pseudomonas-Aeruginosa Virulence Genes Requires Cell-to-Cell Communication, *Science* 260, 1127-1130.
- (79). Latifi, A., Winson, M. K., Foglino, M., et al. (1995) Multiple Homologs of Luxr and LuxI Control Expression of Virulence Determinants and Secondary Metabolites through Quorum Sensing in Pseudomonas-Aeruginosa Pao1, *Mol. Microbiol.* 17, 333-343.
- (80). Gambello, M. J., Kaye, S., and Iglewski, B. H. (1993) LasR of Pseudomonas aeruginosa is a transcriptional activator of the alkaline protease gene (apr) and an enhancer of exotoxin A expression, *Infect Immun.* 61, 1180-1184.
- (81). Toder, D. S., Gambello, M. J., and Iglewski, B. H. (1991) Pseudomonas-Aeruginosa Lasa - a 2nd Elastase under the Transcriptional Control of IasR, *Mol. Microbiol.* 5, 2003-2010.
- (82). Brint, J. M., and Ohman, D. E. (1995) Synthesis of Multiple Exoproducts in Pseudomonas-Aeruginosa Is under the Control of Rhlr-Rhli, Another Set of Regulators in Strain Pao1 with Homology to the Autoinducer-Responsive Luxr-Luxi Family, *J. Bacteriol.* 177, 7155-7163.
- (83). Diggle, S. P., Winzer, K., Lazdunski, A., et al. (2002) Advancing the quorum in Pseudomonas aeruginosa: MvaT and the regulation of N-acylhomoserine lactone production and virulence gene expression, *J. Bacteriol.* 184, 2576-2586.
- (84). Latifi, A., Foglino, M., Tanaka, K., et al. (1996) A hierarchical quorum-sensing cascade in Pseudomonas aeruginosa links the transcriptional activators LasR and RhIR (VsmR) to expression of the stationary-phase sigma factor RpoS, *Mol. Microbiol.* 21, 1137-1146.
- (85). Winson, M. K., Camara, M., Latifi, A., et al. (1995) Multiple N-Acyl-L-Homoserine Lactone Signal Molecules Regulate Production of Virulence Determinants and Secondary Metabolites in Pseudomonas-Aeruginosa, *Proc. Natl. Acad. Sci. U.S.A* 92, 9427-9431.
- (86). Winzer, K., Falconer, C., Garber, N. C., et al. (2000) The Pseudomonas aeruginosa lectins PA-IL and PA-IIL are controlled by quorum sensing and by RpoS, *J. Bacteriol.* 182, 6401-6411.
- (87). Pesci, E. C., Milbank, J. B. J., Pearson, J. P., et al. (1999) Quinolone signaling in the cell-to-cell communication system of Pseudomonas aeruginosa, *Proc. Natl. Acad. Sci. U.S.A* 96, 11229-11234.
- (88). Lepine, F., Milot, S., Deziel, E., et al. (2004) electrospray/mass spectrometric identification and analysis of 4-hydroxy-2-alkylquinolines (HAQs) produced by Pseudomonas aeruginosa, *J. Am. Soc. Mass Spectrom.* 15, 862-869.
- (89). Deziel, E., Lepine, F., Milot, S., et al. (2004) Analysis of Pseudomonas aeruginosa 4-hydroxy-2-alkylquinolines (HAQs) reveals a role for 4-hydroxy-2-heptylquinoline in cell-to-cell communication, *Proc. Natl. Acad. Sci. U.S.A.* 101, 1339-1344.
- (90). Xiao, G., Deziel, E., He, J., et al. (2006) MvfR, a key Pseudomonas aeruginosa pathogenicity LTTR-class regulatory protein, has dual ligands, *Mol. Microbiol.* 62, 1689-1699.
- (91). Deziel, E., Gopalan, S., Tampakaki, A. P., et al. (2005) The contribution of MvfR to Pseudomonas aeruginosa pathogenesis and quorum sensing circuitry regulation: multiple quorum sensing-regulated genes are modulated without affecting lasRI, rhlRI or the production of N-acyl-L-homoserine lactones, *Mol. Microbiol.* 55, 998-1014.
- (92). Gallagher, L. A., McKnight, S. L., Kuznetsova, M. S., et al. (2002) Functions required for extracellular quinolone signaling by Pseudomonas aeruginosa, *J. Bacteriol.* 184, 6472-6480.

- (93). Cao, H., Krishnan, G., Goumnerov, B., et al. (2001) A quorum sensing-associated virulence gene of *Pseudomonas aeruginosa* encodes a LysR-like transcription regulator with a unique self-regulatory mechanism, *Proc. Natl. Acad. Sci. U.S.A.* 98, 14613-14618.
- (94). Allesen-Holm, M., Barken, K. B., Yang, L., et al. (2006) A characterization of DNA release in *Pseudomonas aeruginosa* cultures and biofilms, *Mol. Microbiol.* 59, 1114-1128.
- (95). Diggle, S. P., Winzer, K., Chhabra, S. R., et al. (2003) The *Pseudomonas aeruginosa* quinolone signal molecule overcomes the cell density-dependency of the quorum sensing hierarchy, regulates rhl-dependent genes at the onset of stationary phase and can be produced in the absence of LasR, *Mol. Microbiol.* 50, 29-43.
- (96). Wade, D. S., Calfee, M. W., Rocha, E. R., et al. (2005) Regulation of *Pseudomonas* quinolone signal synthesis in *Pseudomonas aeruginosa*, *J. Bacteriol.* 187, 4372-4380.
- (97). McKnight, S. L., Iglewski, B. H., and Pesci, E. C. (2000) The *Pseudomonas* quinolone signal regulates rhl quorum sensing in *Pseudomonas aeruginosa*, *J. Bacteriol.* 182, 2702-2708.
- (98). Pesci, E. C., Pearson, J. P., Seed, P. C., et al. (1997) Regulation of las and rhl quorum sensing in *Pseudomonas aeruginosa*, *J. Bacteriol.* 179, 3127-3132.
- (99). Dubern, J. F., and Diggle, S. P. (2008) Quorum sensing by 2-alkyl-4-quinolones in *Pseudomonas aeruginosa* and other bacterial species, *Mol. Biosyst.* 4, 882-888.
- (100). McGrath, S., Wade, D. S., and Pesci, E. C. (2004) Dueling quorum sensing systems in *Pseudomonas aeruginosa* control the production of the *Pseudomonas* quinolone signal (PQS), *FEMS Microbiol. Lett.* 230, 27-34.
- (101). D'Argenio, D. A., Calfee, M. W., Rainey, P. B., et al. (2002) Autolysis and autoaggregation in *Pseudomonas aeruginosa* colony morphology mutants, *J. Bacteriol.* 184, 6481-6489.
- (102). Haussler, S., and Becker, T. (2008) The pseudomonas quinolone signal (PQS) balances life and death in *Pseudomonas aeruginosa* populations, *PLoS Pathog.* 4, e1000166.
- (103). Wagner, V. E., Li, L. L., Isabella, V. M., et al. (2007) Analysis of the hierarchy of quorum-sensing regulation in *Pseudomonas aeruginosa*, *Anal. Bioanal. Chem.* 387, 469-479.
- (104). Calfee, M. W., Coleman, J. P., and Pesci, E. C. (2001) Interference with *Pseudomonas* quinolone signal synthesis inhibits virulence factor expression by *Pseudomonas aeruginosa*, *Proc. Natl. Acad. Sci. U.S.A.* 98, 11633-11637.
- (105). Coleman, J. P., Hudson, L. L., McKnight, S. L., et al. (2008) *Pseudomonas aeruginosa* PqsA is an anthranilate-coenzyme a ligase, *J. Bacteriol.* 190, 1247-1255.
- (106). Bera, A. K., Atanasova, V., Robinson, H., et al. (2009) Structure of PqsD, a *Pseudomonas* Quinolone Signal Biosynthetic Enzyme, in Complex with Anthranilate, *Biochem.* 48, 8644-8655.
- (107). Zhang, Y. M., Frank, M. W., Zhu, K., et al. (2008) PqsD Is Responsible for the Synthesis of 2,4-Dihydroxyquinoline, an Extracellular Metabolite Produced by *Pseudomonas aeruginosa*, *J. Biol. Chem.* 283, 28788-28794.
- (108). Dulcey, C. E., Dekimpe, V., Fauville, D. A., et al. (2013) The End of an Old Hypothesis: The *Pseudomonas* Signaling Molecules 4-Hydroxy-2-Alkylquinolines Derive from Fatty Acids, Not 3-Ketofatty Acids, *Chem. Biol.* 20, 1481-1491.
- (109). Pistorius, D., Ullrich, A., Lucas, S., et al. (2011) Biosynthesis of 2-Alkyl-4(1H)-quinolones in *Pseudomonas aeruginosa*: potential for therapeutic interference with pathogenicity, *Chembiochem : a European journal of chemical biology* 12, 850-853.
- (110). Bredenbruch, F., Nimtz, M., Wray, V., et al. (2005) Biosynthetic pathway of *Pseudomonas aeruginosa* 4-hydroxy-2-alkylquinofines, *J. Bacteriol.* 187, 3630-3635.

- (111). Diggle, S. P., Matthijs, S., Wright, V. J., et al. (2007) The *Pseudomonas aeruginosa* 4-quinolone signal molecules HHQ and PQS play multifunctional roles in quorum sensing and iron entrapment, *Chem. Biol.* 14, 87-96.
- (112). Lipsitch, M., and Samore, M. H. (2002) Antimicrobial use and antimicrobial resistance: A population perspective, *Emerg. Infect. Dis.* 8, 347-354.
- (113). Heras, B., Scanlon, M. J., and Martin, J. L. (2014) Targeting Virulence not Viability in the Search for Future Antibacterials, *Br. J. Clin. Pharmacol.*
- (114). Gonzalez, J. E., and Keshavan, N. D. (2006) Messing with bacterial quorum sensing, *Microbiol. Mol. Biol. Rev.* 70, 859-+.
- (115). Williams, P. (2002) Quorum sensing: an emerging target for antibacterial chemotherapy?, *Expert Opin. Ther. Targets* 6, 257-274.
- (116). Smith, K. M., Bu, Y., and Suga, H. (2003) Induction and inhibition of *Pseudomonas aeruginosa* quorum sensing by synthetic autoinducer analogs, *Chem. Biol.* 10, 81-89.
- (117). Rasmussen, T. B., and Givskov, M. (2006) Quorum-sensing inhibitors as anti-pathogenic drugs, *Int. J. Med. Microbiol.* 296, 149-161.
- (118). Lepine, F., Deziel, E., Milot, S., et al. (2003) A stable isotope dilution assay for the quantification of the *Pseudomonas* quinolone signal in *Pseudomonas aeruginosa* cultures, *Biochim. Biophys. Acta* 1622, 36-41.
- (119). Galloway, W. R., Hodgkinson, J. T., Bowden, S., et al. (2012) Applications of small molecule activators and inhibitors of quorum sensing in Gram-negative bacteria, *Trends Microbiol.* 20, 449-458.
- (120). Lu, C., Kirsch, B., Zimmer, C., et al. (2012) Discovery of antagonists of PqsR, a key player in 2-alkyl-4-quinolone-dependent quorum sensing in *Pseudomonas aeruginosa*, *Chem. Biol.* 19, 381-390.
- (121). Lu, C., Maurer, C. K., Kirsch, B., et al. (2014) Overcoming the unexpected functional inversion of a PqsR antagonist in *Pseudomonas aeruginosa*: an in vivo potent antivirulence agent targeting pqs quorum sensing, *Angew. Chem. Int. Ed. Engl.* 53, 1109-1112.
- (122). Farrow, J. M., 3rd, Sund, Z. M., Ellison, M. L., et al. (2008) PqsE functions independently of PqsR-Pseudomonas quinolone signal and enhances the rhl quorum-sensing system, *J. Bacteriol.* 190, 7043-7051.
- (123). Diggle, S. P., Cornelis, P., Williams, P., et al. (2006) 4-Quinolone signalling in *Pseudomonas aeruginosa*: Old molecules, new perspectives, *Int. J. Med. Microbiol.* 296, 83-91.
- (124). Rampioni, G., Pustelnik, C., Fletcher, M. P., et al. (2010) Transcriptomic analysis reveals a global alkyl-quinolone-independent regulatory role for PqsE in facilitating the environmental adaptation of *Pseudomonas aeruginosa* to plant and animal hosts, *Environ. Microbiol.* 12, 1659-1673.
- (125). Lesic, B., Lepine, F., Deziel, E., et al. (2007) Inhibitors of pathogen intercellular signals as selective anti-infective compounds, *PLoS Pathog.* 3, 1229-1239.
- (126). Storz, M. P., Maurer, C. K., Zimmer, C., et al. (2012) Validation of PqsD as an anti-biofilm target in *Pseudomonas aeruginosa* by development of small-molecule inhibitors, *J. Am. Chem. Soc.* 134, 16143-16146.
- (127). Levy, S. B., and Marshall, B. (2004) Antibacterial resistance worldwide: causes, challenges and responses, *Nat. Med.* 10, S122-S129.
- (128). Cooper, M. A., and Shlaes, D. (2011) Fix the antibiotics pipeline, *Nature* 472, 32-32.
- (129). Clatworthy, A. E., Pierson, E., and Hung, D. T. (2007) Targeting virulence: a new paradigm for antimicrobial therapy, *Nat. Chem. Biol.* 3, 541-548.
- (130). Kaitin, K. I., and DiMasi, J. A. (2011) Pharmaceutical Innovation in the 21st Century: New Drug Approvals in the First Decade, 2000-2009, *Clin. Pharmacol. Therap.* 89, 183-188.

- (131). Lambert, P. A. (2002) Mechanisms of antibiotic resistance in *Pseudomonas aeruginosa*, *J. R. Soc. Med.* 95 Suppl 41, 22-26.
- (132). Livermore, D. M. (2009) Has the era of untreatable infections arrived?, *J. Antimicrob. Chemother.* 64, 29-36.
- (133). Nikaido, H. (1994) Prevention of drug access to bacterial targets: permeability barriers and active efflux, *Science* 264, 382-388.
- (134). Talbot, G. H. (2008) What is in the pipeline for Gram-negative pathogens?, *Expert Rev. Anti-Infect. Ther.* 6, 39-49.
- (135). Barrett, C. T., and Barrett, J. F. (2003) Antibacterials: are the new entries enough to deal with the emerging resistance problems?, *Curr. Opin. Biotechnol.* 14, 621-626.
- (136). Fischbach, M. A., and Walsh, C. T. (2009) Antibiotics for Emerging Pathogens, *Science* 325, 1089-1093.
- (137). Gallant, P., Finn, J., Keith, D., et al. (2000) The identification of quality antibacterial drug discovery targets: a case study with aminoacyl-tRNA synthetases, *Expert Opin. Ther. Targets* 4, 1-9.
- (138). Rivers, E. C., and Mancera, R. L. (2008) New anti-tuberculosis drugs in clinical trials with novel mechanisms of action, *Drug Discov. Today* 13, 1090-1098.
- (139). Weidel, E., de Jong, J. C., Brengel, C., et al. (2013) Structure Optimization of 2-Benzamidobenzoic Acids as PqsD Inhibitors for *Pseudomonas aeruginosa* Infections and Elucidation of Binding Mode by SPR, STD NMR, and Molecular Docking, *J. Med. Chem.* 56, 6146-6155.
- (140). Nie, Z., Perretta, C., Lu, J., et al. (2005) Structure-based design, synthesis, and study of potent inhibitors of beta-ketoacyl-acyl carrier protein synthase III as potential antimicrobial agents, *J. Med. Chem.* 48, 1596-1609.
- (141). Mayer, M., and Meyer, B. (2001) Group epitope mapping by saturation transfer difference NMR to identify segments of a ligand in direct contact with a protein receptor, *J. Am. Chem. Soc.* 123, 6108-6117.
- (142). Tegler, L. T., Nonglaton, G., Buttner, F., et al. (2011) Powerful Protein Binders from Designed Polypeptides and Small Organic Molecules-A General Concept for Protein Recognition, *Angew. Chem. Int. Ed. Engl.* 50, 1823-1827.
- (143). Allegretta, G., Weidel, E., Empting, M., et al. (2014) Catechol-based substrates of Chalcone Synthase as a scaffold for novel inhibitors of PqsD, *Eur. J. Med. Chem.* 90, 351-359.
- (144). Sahner, J. H., Brengel, C., Storz, M. P., et al. (2013) Combining in Silico and Biophysical Methods for the Development of *Pseudomonas aeruginosa* Quorum Sensing Inhibitors: An Alternative Approach for Structure-Based Drug Design, *J. Med. Chem.* 56, 8656-8664.
- (145). Sahner, J. H., Empting, M., Kamal, A., et al. (2014) Exploring the chemical space of ureidothiophene-2-carboxylic acids as inhibitors of the quorum sensing enzyme PqsD from *Pseudomonas aeruginosa*, *Eur. J. Med. Chem. submitted*.
- (146). Valler, M. J., and Green, D. (2000) Diversity screening versus focussed screening in drug discovery, *Drug Discov. Today* 5, 286-293.
- (147). Wermuth, C. G. (2006) Similarity in drugs: reflections on analogue design, *Drug Discov. Today* 11, 348-354.
- (148). Davies, C., Heath, R. J., White, S. W., et al. (2000) The 1.8 angstrom crystal structure and active-site architecture of beta-ketoacyl-acyl carrier protein synthase III (FabH) from *Escherichia coli*, *Structure* 8, 185-195.
- (149). Steinbach, A., Maurer, C. K., Weidel, E., et al. (2013) Molecular basis of HHQ biosynthesis: molecular dynamics simulations, enzyme kinetic and surface plasmon resonance studies, *BMC Biophys.* 6.

- (150). Alhamadsheh, M. M., Waters, N. C., Sachdeva, S., et al. (2008) Synthesis and biological evaluation of novel sulfonyl-naphthalene-1,4-diols as FabH inhibitors, *Bioorg. Med. Chem. Lett.* 18, 6402-6405.
- (151). Daines, R. A., Pendrak, I., Sham, K., et al. (2003) First X-ray cocrystal structure of a bacterial FabH condensing enzyme and a small molecule inhibitor achieved using rational design and homology modeling, *J. Med. Chem.* 46, 5-8.
- (152). Al-Balas, Q., Anthony, N. G., Al-Jaidi, B., et al. (2009) Identification of 2-Aminothiazole-4-Carboxylate Derivatives Active against Mycobacterium tuberculosis H37Rv and the beta-Ketoacyl-ACP Synthase mtFabH, *Plos One* 4.
- (153). Senior, S. J., Illarionova, P. A., Gurcha, S. S., et al. (2003) Biphenyl-based analogues of thiolactomycin, active against Mycobacterium tuberculosis mtFabH fatty acid condensing enzyme, *Bioorg. Med. Chem. Lett.* 13, 3685-3688.
- (154). Kim, P., Zhang, Y. M., Shenoy, G., et al. (2006) Structure-activity relationships at the 5-position of thiolactomycin: An intact (5R)-isoprene unit is required for activity against the condensing enzymes from Mycobacterium tuberculosis and Escherichia coli, *J. Med. Chem.* 49, 159-171.
- (155). Rees, D. C., Congreve, M., Murray, C. W., et al. (2004) Fragment-based lead discovery, *Nature reviews. Drug discovery* 3, 660-672.
- (156). Hopkins, A. L., Groom, C. R., and Alex, A. (2004) Ligand efficiency: a useful metric for lead selection, *Drug Discov. Today* 9, 430-431.
- (157). Howard, S., Berdini, V., Boulstridge, J. A., et al. (2009) Fragment-based discovery of the pyrazol-4-yl urea (AT9283), a multitargeted kinase inhibitor with potent aurora kinase activity, *Journal of medicinal chemistry* 52, 379-388.
- (158). Villemagne, B., Flipo, M., Blondiaux, N., et al. (2014) Ligand Efficiency Driven Design of New Inhibitors of Mycobacterium tuberculosis Transcriptional Repressor EthR Using Fragment Growing, Merging, and Linking Approaches, *J. Med. Chem.* 57, 4876-4888.
- (159). Johnson, C. N., Berdini, V., Beke, L., et al. (2014) Fragment-Based Discovery of Type I Inhibitors of Maternal Embryonic Leucine Zipper Kinase, *ACS Med. Chem. Lett.* DOI: 10.1021/ml5001245.
- (160). Walters, W. P., Stahl, M. T., and Murcko, M. A. (1998) Virtual screening - an overview, *Drug Discov. Today* 3, 160-178.
- (161). Storz, M. P., Brengel, C., Weidel, E., et al. (2013) Biochemical and biophysical analysis of a chiral PqsD inhibitor revealing tight-binding behavior and enantiomers with contrary thermodynamic signatures, *ACS Chem. Biol.* 8, 2794-2801.
- (162). Wielens, J., Headley, S. J., Rhodes, D. I., et al. (2013) Parallel Screening of Low Molecular Weight Fragment Libraries: Do Differences in Methodology Affect Hit Identification?, *J. Biomol. Screen.* 18, 147-159.
- (163). Yuan, Y. Q., Sachdeva, M., Leeds, J. A., et al. (2012) Fatty Acid Biosynthesis in *Pseudomonas aeruginosa* Is Initiated by the FabY Class of beta-Ketoacyl Acyl Carrier Protein Synthases, *J. Bacteriol.* 194, 5171-5184.
- (164). Yuan, Y. Q., Leeds, J. A., and Meredith, T. C. (2012) *Pseudomonas aeruginosa* Directly Shunts beta-Oxidation Degradation Intermediates into De Novo Fatty Acid Biosynthesis, *J. Bacteriol.* 194, 5185-5196.
- (165). Zhang, Y. M., and Rock, C. O. (2012) Will the Initiator of Fatty Acid Synthesis in *Pseudomonas aeruginosa* Please Stand Up?, *J. Bacteriol.* 194, 5159-5161.
- (166). Hinsberger, S., Husecken, K., Groh, M., et al. (2013) Discovery of novel bacterial RNA polymerase inhibitors: pharmacophore-based virtual screening and hit optimization, *J. Med. Chem.* 56, 8332-8338.

## 6 Supporting information

### 6.1 Supporting Information der Publikation A

Die vollständige Supporting Information ist online verfügbar unter:

<http://pubs.acs.org/doi/suppl/10.1021/jm4006302>

#### Additional figures docking studies

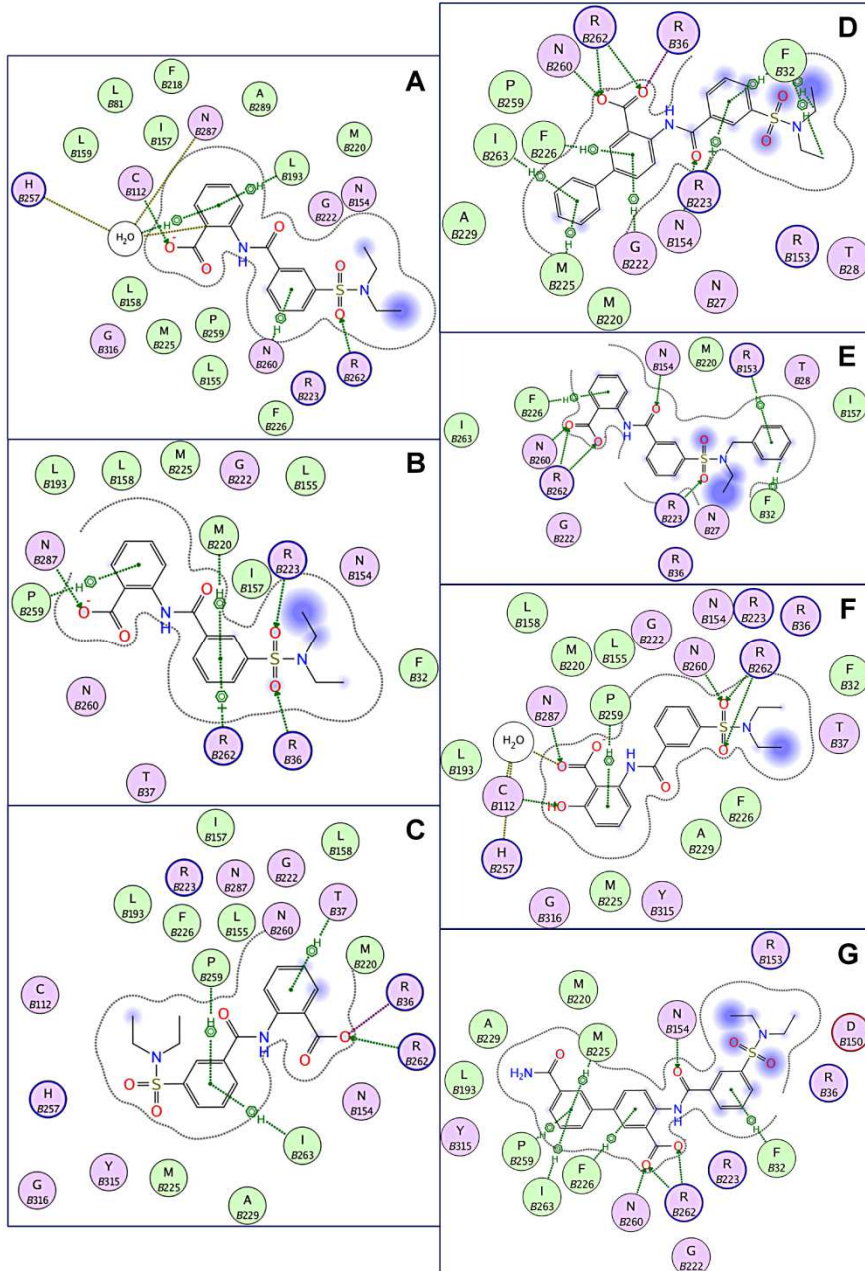


**Figure S1** Two dimensional representation of the interaction between compounds **2** (A-C), **48** (D), **64** (E), **52** (F) and **53** (G) and PqsD. Amino acids within 5.5 Å are shown and the key interactions are highlighted. Polar amino acids are colored in purple and hydrophobic amino acids in green circles (MOE).

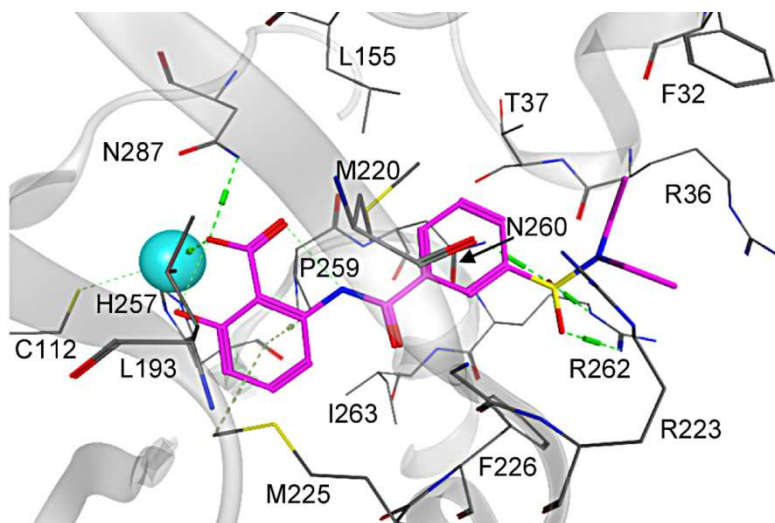


**Figure S2** Docking pose of compound **52**. In presence of a structural water molecule (cyan ball) a hydrogen bond network is formed between the hydroxyl group and the carboxylic moiety of **52** and the catalytic residues Cys112, His257, and Asn287 bridged by the water molecule.

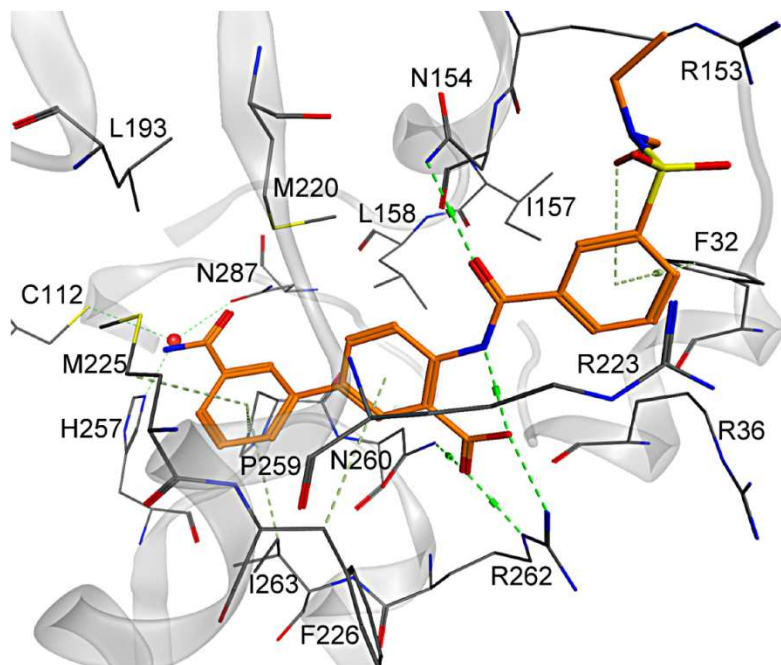


**Figure S3** Docking pose of compound **53** (orange sticks).

## Additional figures STD NMR study

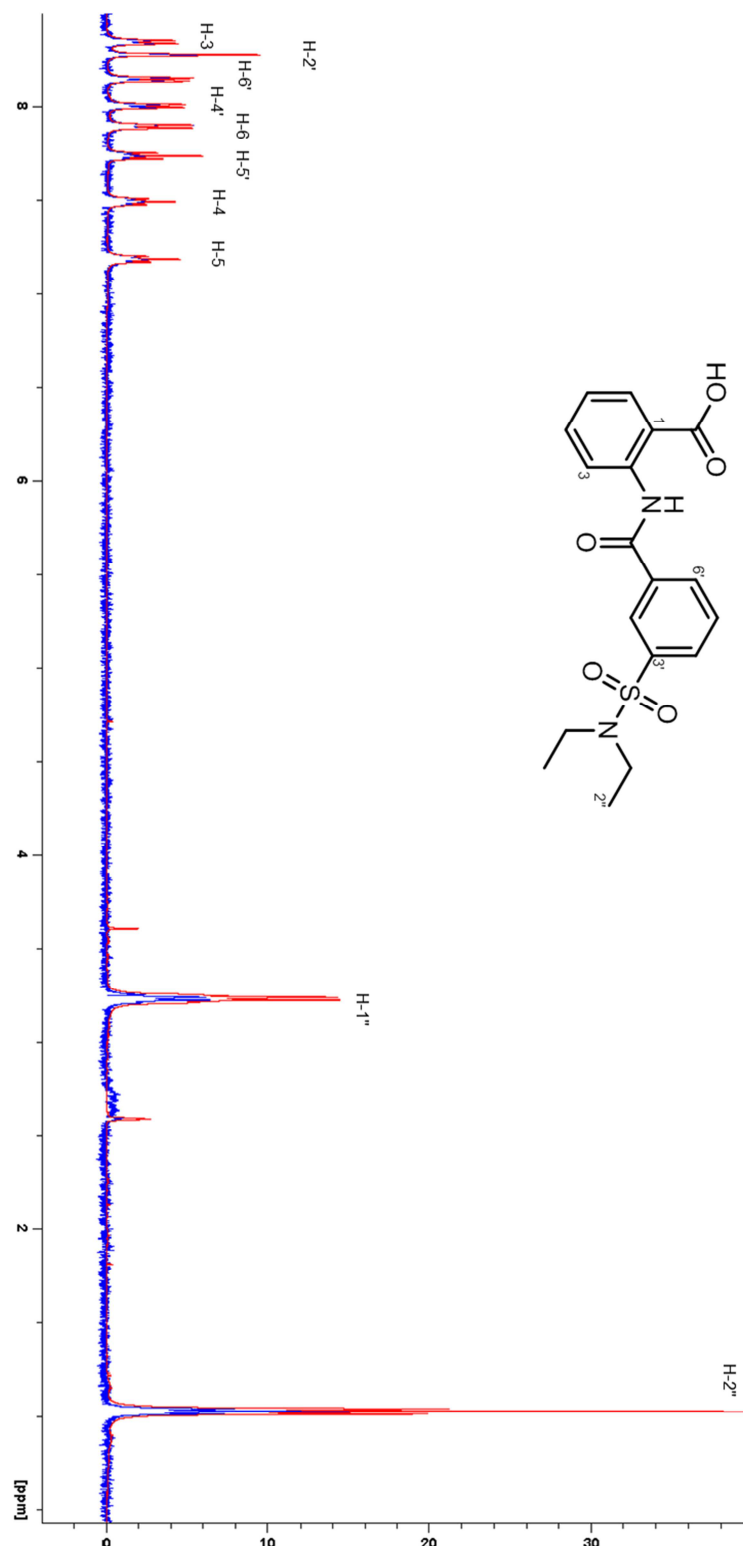


**Figure S4** Reference (red) and STD NMR difference (blue) spectra of **2** in complex with PqsD. Samples containing 80:1 **2**/PqsD were prepared in 20 mM sodium phosphate, 50 mM NaCl, 5 mM MgCl<sub>2</sub>, pH = 7.0, and spectra were recorded at 298 K. Overlaid spectra were normalized to the signal for H-6 ( $\delta$  7.90), which gave the strongest enhancement.

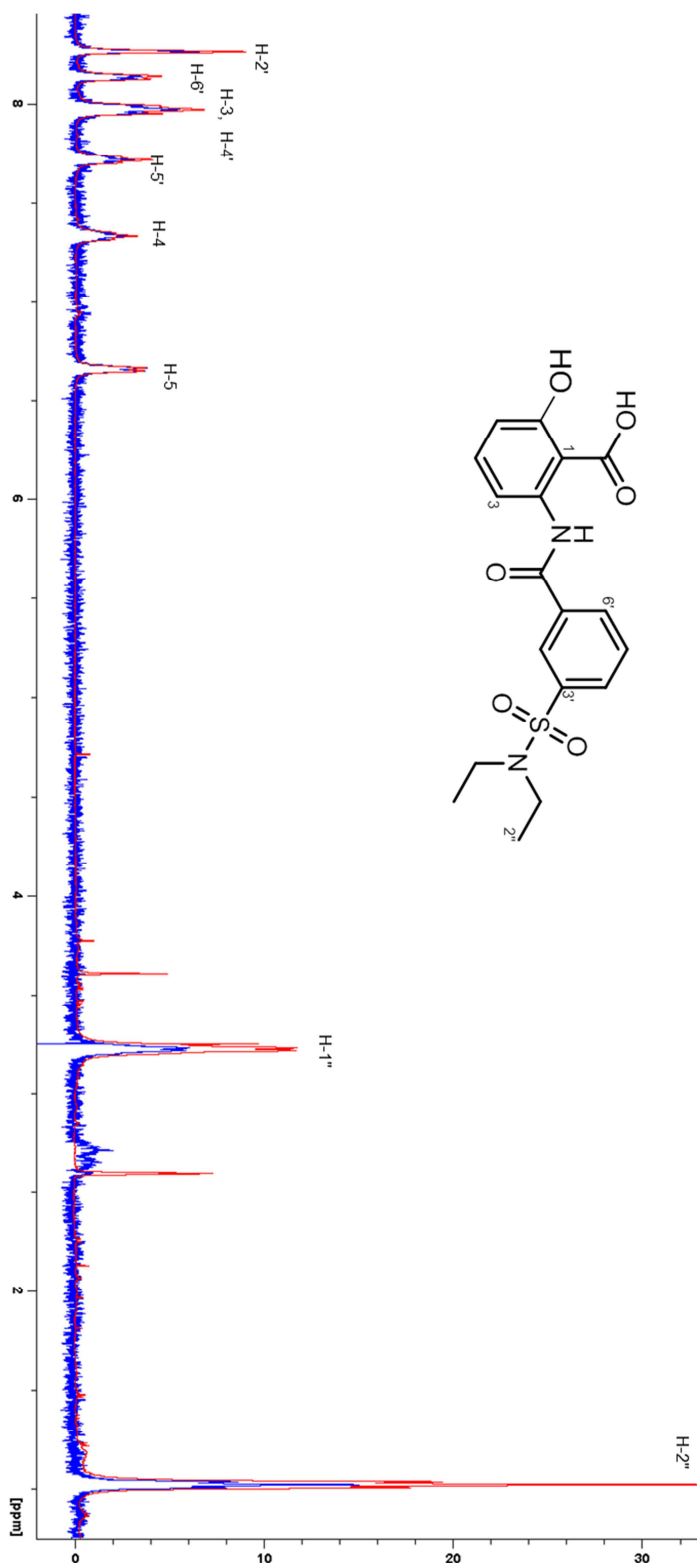


**Figure S5.** Reference (red) and STD NMR difference (blue) spectra of **52** in complex with PqsD. Samples containing 80:1 **52**/PqsD were prepared in 20 mM sodium phosphate, 50 mM NaCl, 5 mM MgCl<sub>2</sub>, pH = 7.0, and spectra were recorded at 298 K. Overlaid spectra were normalized to the signal for H-5 ( $\delta$  6.65), which gave the strongest enhancement.

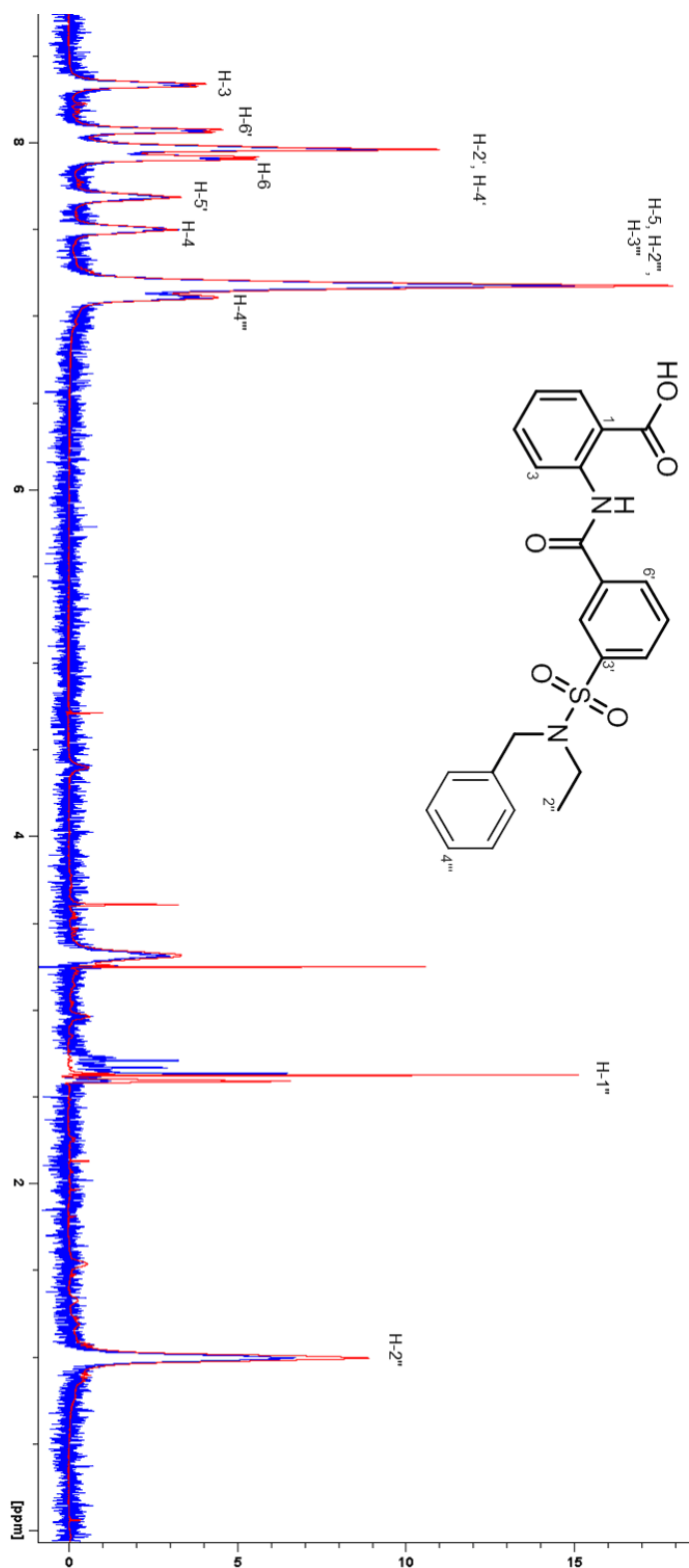


**Figure S6.** Reference (red) and STD NMR difference (blue) spectra of **64** in complex with PqsD. Samples containing 80:1 **64**/PqsD were prepared in 20 mM sodium phosphate, 50 mM NaCl, 5 mM MgCl<sub>2</sub>, pH = 7.0, and spectra were recorded at 298 K. Overlaid spectra were normalized to the signal for H-6 ( $\delta$  7.90), which gave the strongest enhancement.

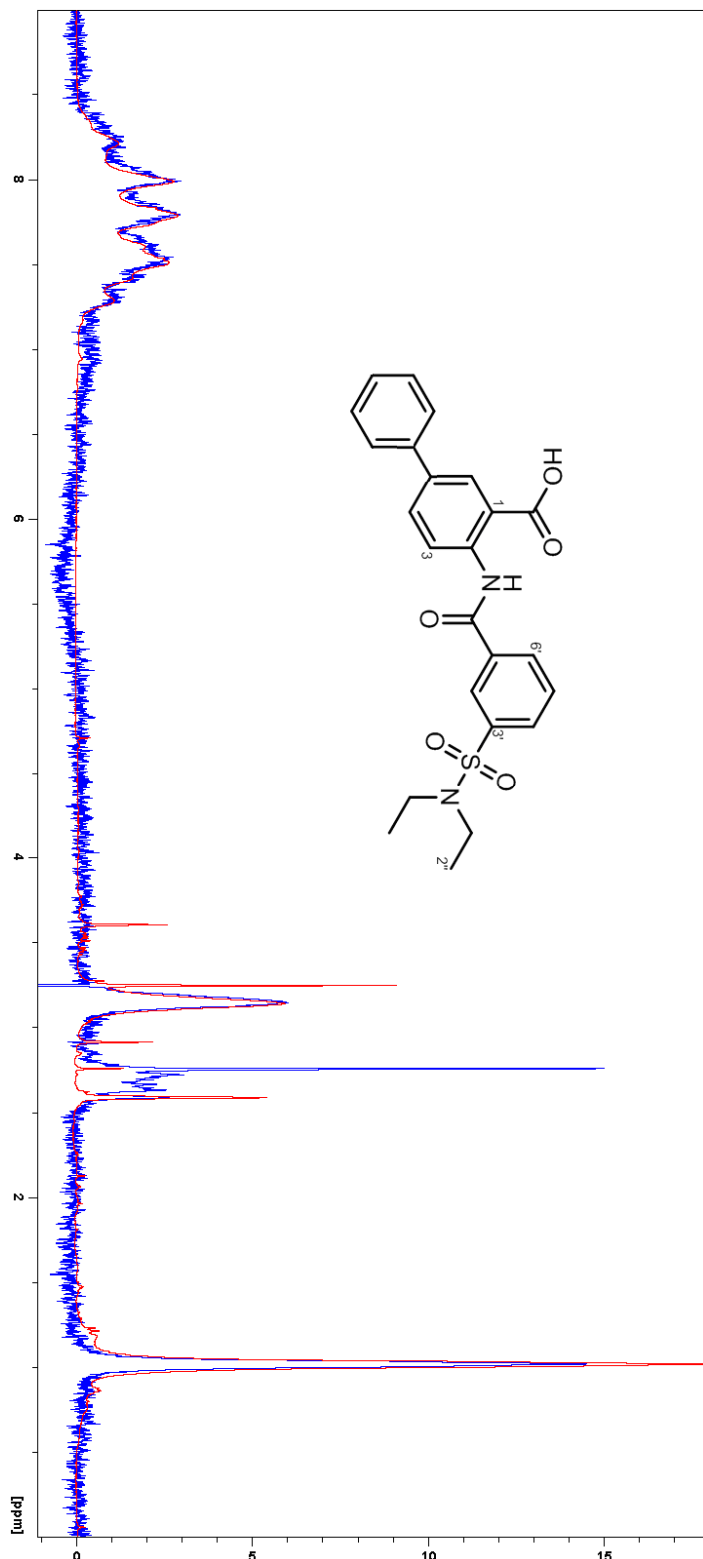


**Figure S7.** Reference (red) and STD NMR difference (blue) spectra of **48** in complex with PqsD. Samples containing 80:1 **48**/PqsD were prepared in 20 mM sodium phosphate, 50 mM NaCl, 5 mM MgCl<sub>2</sub>, pH = 7.0, and spectra were recorded at 298 K.

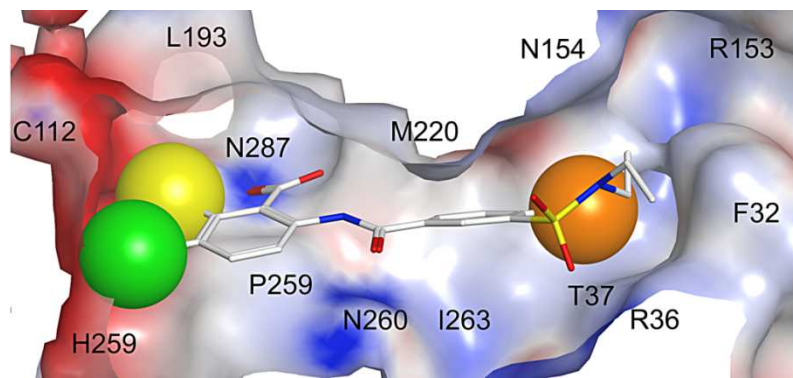


**Figure S8.** Docking pose of the 2-Benzamidobenzoic acid core structure (white sticks). Balls represent possible substituents that form specific interactions with amino acids of the active site.

## Chemistry

### Syntheses of 3-(chlorosulfonyl)benzoic acids 18-20

**4-Bromo-3-(chlorosulfonyl)benzoic acid (18)<sup>S1</sup>** A solution of 4-bromobenzoic acid (**15**, 5.03 g, 25.0 mmol) in chlorosulfonic acid (28 mL) was heated overnight at 100 °C. After cooling to room temperature the reaction mixture was added very slowly onto ice. The white solid was isolated by suction filtration, washed with water and dried under reduced pressure; 6.12 g, 82% yield. The material was used without further purification.

**3-(Chlorosulfonyl)-4-methylbenzoic acid (19)<sup>S2</sup>** A solution of 4-methylbenzoic acid (**16**, 3.00 g, 22.0 mmol) in chlorosulfonic acid (25 mL) was heated overnight at 100 °C. After cooling to room temperature the reaction mixture was added very slowly onto ice. The white solid was isolated by suction filtration, washed with water and dried under reduced pressure; 6.12 g, 82% yield. The material was used without further purification.

**3-(Chlorosulfonyl)-4-ethylbenzoic acid (20)<sup>S1,S3</sup>** A solution of 4-ethylbenzoic acid (**17**, 3.00 g, 20.0 mmol) in chlorosulfonic acid (25 mL) was heated overnight at 100 °C. After cooling to room temperature the reaction mixture was added very slowly onto ice. The white solid was isolated by suction filtration, washed with water and dried under reduced pressure; 4.57 g, 88% yield. The material was used without further purification.

### Syntheses of 3-sulfamoylbenzoic acids 22-33

**4-Bromo-3-(*N,N*-diethylsulfamoyl)benzoic acid (22)<sup>S4</sup>** The title compound was synthesized from 4-bromo-3-(chlorosulfonyl)benzoic acid (**18**) and diethylamine according to General Procedure A: 1.22 g, 91% yield. <sup>1</sup>H NMR (500 MHz, DMSO-*d*<sub>6</sub>): δ 1.06 (t, *J* = 7.1 Hz, 6H), 3.33 (q, *J* = 7.1 Hz, 4H), 7.97 (dd, *J* = 8.2 Hz, 1H), 8.00 (dd, *J* = 8.2, 1.9 Hz, 1H), 8.48 (d, *J* = 1.9 Hz, 1H).

**3-(*N,N*-Diethylsulfamoyl)-4-methylbenzoic acid (23)** The title compound was synthesized from 3-(chlorosulfonyl)-4-methylbenzoic acid (**19**) and diethylamine according to General Procedure A: 2.05 g, 76% yield. <sup>1</sup>H NMR (500 MHz, DMSO-*d*<sub>6</sub>): δ 1.04 (t, *J* = 7.1 Hz, 6H), 2.58 (s, 3H), 3.26 (q, *J* = 7.1 Hz, 4H), 7.57 (d, *J* = 7.9 Hz, 1H), 8.05 (dd, *J* = 7.9, 1.9 Hz, 1H), 8.33 (d, *J* = 1.9 Hz, 1H), 13.34 (bs, 1H); <sup>13</sup>C NMR (125 MHz, DMSO-*d*<sub>6</sub>): δ 13.59, 19.82, 40.65, 128.97, 129.36, 133.03, 133.31, 138.78, 141.95, 166.07; LC/MS: *m/z* = 271.83 [M + H]<sup>+</sup>, 312.87 [M + H + CH<sub>3</sub>CN]<sup>+</sup>, 542.54 [2M + H]<sup>+</sup>, *t*<sub>R</sub> = 9.35 min, 98.9% pure (UV).

**3-(*N,N*-Diethylsulfamoyl)-4-ethylbenzoic acid (24)** The title compound was synthesized from 3-(chlorosulfonyl)-4-ethylbenzoic acid (**20**) and diethylamine according to General Procedure A and purified by flash column chromatography (silica gel, ethyl acetate/*n*-hexane): 1.11 g, 39% yield. <sup>1</sup>H NMR (500 MHz,

DMSO-*d*<sub>6</sub>):  $\delta$  1.20 (t, *J* = 7.1 Hz, 6H), 1.33 (t, *J* = 7.6 Hz, 3H), 3.12 (q, *J* = 7.5 Hz, 2H), 3.39 (q, *J* = 7.1 Hz, 4H), 7.50 (d, *J* = 7.9 Hz, 1H), 8.18 (dd, *J* = 7.9, 1.6 Hz, 1H), 8.50 (d, *J* = 1.6 Hz, 1H); <sup>13</sup>C NMR (125 MHz, DMSO-*d*<sub>6</sub>):  $\delta$  14.00, 14.89, 26.07, 41.49, 127.03, 130.11, 131.30, 133.57, 139.46, 150.09, 170.61; LC/MS: *m/z* = 285.90 [M + H]<sup>+</sup>, 326.81 [M + H + CH<sub>3</sub>CN]<sup>+</sup>, 570.56 [2M + H]<sup>+</sup>, *t*<sub>R</sub> = 10.11 min, 96.9% pure (UV).

**3-Sulfamoylbenzoic acid (25)** The title compound was synthesized from 3-(chlorosulfonyl)benzoic acid and ammonium hydroxide (28-30%) according to a published procedure<sup>55</sup> and purified by crystallization from methanol/water: 1.25 g, 62% yield. <sup>1</sup>H NMR (300 MHz, DMSO-*d*<sub>6</sub>):  $\delta$  7.48 (s, 2H), 7.68 (t, *J* = 7.3 Hz, 1H), 8.07 (d, *J* = 7.8 Hz, 1H), 8.14 (d, *J* = 7.6 Hz, 1H), 8.43 (s, 1H), 13.28 (bs, 1H).

**3-(*N,N*-Dimethylsulfamoyl)benzoic acid (26)<sup>56</sup>** A solution of dimethylamine (40% in water, 45.3 mmol) was added to a stirred suspension of 3-(chlorosulfonyl)benzoic acid (**21**, 1.00 g, 4.53 mmol) in water (15 mL). After stirring overnight the solution was acidified with 1N HCl (aq.). The solid was isolated by suction filtration, washed thoroughly with water and dried under reduced pressure to yield the title compound: 637 mg, 61% yield. <sup>1</sup>H NMR (500 MHz, DMSO-*d*<sub>6</sub>):  $\delta$  2.76 (s, 6H), 7.70 (dt, *J* = 7.9, 0.6 Hz, 1H), 8.04 (ddd, *J* = 7.9, 1.9, 1.3 Hz, 1H), 8.35 (dt, *J* = 7.9, 1.4 Hz, 1H), 8.51 (t, *J* = 1.6 Hz, 1H).

**3-(*N,N*-Diethylsulfamoyl)benzoic acid (27)<sup>57</sup>** The title compound was synthesized from 3-(chlorosulfonyl)benzoic acid (**21**) and diethylamine according to General Procedure A: 2.19 g, 94% yield. <sup>1</sup>H NMR (300 MHz, CDCl<sub>3</sub>):  $\delta$  1.15 (t, *J* = 7.1 Hz, 6H), 3.29 (q, *J* = 7.1 Hz, 4H), 7.64 (t, *J* = 7.7 Hz, 1H), 8.07 (d, *J* = 7.5 Hz, 1H), 8.29 (d, *J* = 7.5 Hz, 1H), 8.53 (s, 1H), 10.44 (bs, 1H).

**3-(*N,N*-Di-*n*-propylsulfamoyl)benzoic acid (28)** The title compound was synthesized from 3-(chlorosulfonyl)benzoic acid (**21**) and di-*n*-propylamine according to General Procedure A: 2.78 g, 97% yield. <sup>1</sup>H NMR (300 MHz, DMSO-*d*<sub>6</sub>):  $\delta$  0.79 (t, *J* = 6.6 Hz, 1H), 1.46 (sextet, *J* = 7.0 Hz, 4H), 3.04 (t, *J* = 6.6 Hz, 4H), 7.74 (t, *J* = 7.7 Hz, 1H), 8.04 (d, *J* = 7.6 Hz, 1H), 8.19 (d, *J* = 7.6 Hz, 1H), 8.24 (s, 1H), 13.51 (bs, 1H).

**3-(Pyrrolidin-1-ylsulfonyl)benzoic acid (29)** A solution of 3-(chlorosulfonyl)benzoic acid (**21**, 1.16 g, 5.26 mmol) in dichloromethane (15 mL) was added to a stirred solution of pyrrolidine (3.74 g, 52.6 mmol) in dichloromethane (10 mL) over a period of 30 minutes. After stirring overnight at room temperature 1N HCl (aq.) was added and the aqueous phase was extracted twice with dichloromethane. The combined organic layers were dried over sodium sulfate, filtered and evaporated under reduced pressure to yield the title compound: 1.10 g, 82% yield. <sup>1</sup>H NMR (500 MHz, DMSO-*d*<sub>6</sub>):  $\delta$  1.65 (m, 4H), 3.15 (m, 4H), 7.78 (dt, *J* = 7.7, 0.6 Hz, 1H), 8.05 (ddd, *J* = 7.7, 1.9, 1.3 Hz, 1H), 8.22-8.25 (m, 2H), 13.55 (bs, 1H); <sup>13</sup>C NMR (125 MHz, DMSO-*d*<sub>6</sub>):  $\delta$  24.68, 47.84, 127.60, 130.15, 131.17, 131.88, 133.40, 136.75, 166.06; LC/MS: *m/z* = 296.92 [M + H + CH<sub>3</sub>CN]<sup>+</sup>, *t*<sub>R</sub> = 7.98 min, >95% pure (UV).

**3-(Piperidin-1-ylsulfonyl)benzoic acid (30)<sup>58</sup>** The title compound was synthesized from 3-(chlorosulfonyl)benzoic acid (**21**) and piperidine according to General Procedure A: 2.28 g, 85% yield. <sup>1</sup>H NMR (500 MHz, DMSO-*d*<sub>6</sub>):  $\delta$  1.35 (m, 2H), 1.53 (m, 4H), 2.90 (m, 4H), 7.79 (t, *J* = 1.6 Hz, 1H), 7.97 (ddd, *J* = 7.6, 2.8, 1.6 Hz, 1H), 8.18 (t, *J* = 1.6 Hz, 1H), 8.23 (ddd, *J* = 7.6, 1.6, 0.9 Hz, 1H), 13.54 (bs, 1H); <sup>13</sup>C NMR (125 MHz, DMSO-*d*<sub>6</sub>):  $\delta$  22.69, 24.63, 46.50, 127.68, 130.08, 131.39, 131.89, 133.46, 136.16; LC/MS: *m/z* = 270.09 [M + H]<sup>+</sup>, 310.57 [M + H + CH<sub>3</sub>CN]<sup>+</sup>, 538.43 [2M + H]<sup>+</sup>, *t*<sub>R</sub> = 9.10 min, 97.3% pure (UV).

**3-(Azepan-1-ylsulfonyl)benzoic acid (31)** The title compound was synthesized from 3-(chlorosulfonyl)benzoic acid (**21**) and hexamethyleneimine according to General Procedure A: 2.55 g, 90% yield. <sup>1</sup>H NMR (300 MHz, DMSO-*d*<sub>6</sub>):  $\delta$  1.48 (m, 4H), 1.61 (m, 4H), 3.21 (m, 4H), 7.74 (t, *J* = 7.6 Hz, 1H), 8.02 (d, *J* = 8.0 Hz, 1H), 8.19 (d, *J* = 7.7 Hz, 1H), 8.22 (s, 1H), 13.54 (bs, 1H).

**3-(Morpholinosulfonyl)benzoic acid (32)<sup>56</sup>** The title compound was synthesized from 3-(chlorosulfonyl)benzoic acid (**7**) and morpholine according to General Procedure A: 2.15 g, 79% yield. <sup>1</sup>H NMR (300 MHz, DMSO-*d*<sub>6</sub>):  $\delta$  2.89 (m, 4H), 3.63 (m, 4H), 7.82 (dt, *J* = 7.9, 0.6 Hz, 1H), 7.98 (ddd, *J* = 7.9, 1.9, 0.9 Hz, 1H), 8.18 (dt, *J* = 1.6, 0.6 Hz, 1H), 8.27 (ddd, *J* = 7.9, 1.6, 0.9 Hz, 1H), 13.57 (bs, 1H); LC/MS: *m/z* = 312.91 [M + H + CH<sub>3</sub>CN]<sup>+</sup>, 542.44 [2M + H]<sup>+</sup>, *t*<sub>R</sub> = 7.22 min, >99.9% pure (UV).

**3-(*N*-Benzyl-*N*-ethylsulfamoyl)benzoic acid (33)** The title compound was synthesized from 3-(chlorosulfonyl)benzoic acid (**21**) and *N*-ethylbenzylamine according to General Procedure A, followed by crystallization from toluene: 1.38 g, 43% yield.  $^1\text{H}$  NMR (500 MHz, DMSO- $d_6$ ):  $\delta$  0.84 (t,  $J$  = 7.1 Hz, 3H), 3.15 (q,  $J$  = 7.1 Hz, 2H), 4.36 (s, 2H), 7.26–7.36 (m, 5H), 7.77 (t,  $J$  = 7.7 Hz, 1H), 8.11 (ddd,  $J$  = 7.9, 1.9, 1.3 Hz, 1H), 8.23 (dt,  $J$  = 7.9, 1.3 Hz, 1H), 8.30 (t,  $J$  = 1.7 Hz, 1H), 13.54 (bs, 1H);  $^{13}\text{C}$  NMR (125 MHz, DMSO- $d_6$ ):  $\delta$  13.35, 42.57, 50.52, 127.15, 127.53, 127.94, 128.43, 130.23, 130.81, 131.97, 133.25, 136.80, 140.26; LC/MS:  $m/z$  = 319.71 [M + H] $^+$ , 360.69 [M + H + CH<sub>3</sub>CN] $^+$ , 638.46 [2M + H] $^+$ ,  $t_R$  = 10.68 min, 96.7% pure (UV).

### Syntheses of 3-sulfamoylbenzoyl chlorides 22a-33a

**4-Bromo-3-(*N,N*-diethylsulfamoyl)benzoyl chloride (22a)** The title compound was synthesized from 4-bromo-3-(*N,N*-diethylsulfamoyl)benzoic acid (**22**, 1.20 g, 3.57 mmol) according to General Procedure B. The product was analyzed as the corresponding methyl ester; LC/MS:  $m/z$  = 349.50 and 351.54 [M + H] $^+$ ,  $t_R$  = 11.68 min.

**3-(*N,N*-Diethylsulfamoyl)-4-methylbenzoyl chloride (23a)** The title compound was synthesized from 3-(*N,N*-diethylsulfamoyl)-4-methylbenzoic acid (**23**, 2.04 g, 7.52 mmol) according to General Procedure B. The product was analyzed as the corresponding methyl ester; LC/MS:  $m/z$  = 285.85 [M + H] $^+$ , 326.84 [M + H + CH<sub>3</sub>CN] $^+$ , 570.49 [2M + H] $^+$ ,  $t_R$  = 11.28 min.

**3-(*N,N*-Diethylsulfamoyl)-4-ethylbenzoyl chloride (24a)** The title compound was synthesized from 3-(*N,N*-diethylsulfamoyl)-4-ethylbenzoic acid (**24**, 1.11 g, 3.92 mmol) according to General Procedure B. The product was analyzed as the corresponding methyl ester; LC/MS:  $m/z$  = 300.02 [M + H] $^+$ , 341.05 [M + H + CH<sub>3</sub>CN] $^+$ ,  $t_R$  = 12.61 min.

**3-Sulfamoylbenzoyl chloride (25a)<sup>S9</sup>** 3-Sulfamoylbenzoic acid (**25**, 1.25 g, 6.21 mmol) was dissolved in thionyl chloride (10 mL), followed by the addition of 2 drops of DMF. The solution was heated to reflux overnight. After cooling to room temperature *n*-hexane was added and the white solid was isolated by suction filtration, washed with *n*-hexane and dried under reduced pressure at 50 °C.  $^1\text{H}$  NMR and LC-MS showed the title compound together with a small amount of 3-((dimethylamino)methylene)sulfamoylbenzoyl chloride. The product was used without further purification.  $^1\text{H}$  NMR (300 MHz, DMSO- $d_6$ ):  $\delta$  7.65 (t,  $J$  = 8.0 Hz, 1H), 7.95 (d,  $J$  = 7.6 Hz, 1H), 8.07 (d,  $J$  = 7.6 Hz, 1H), 8.24 (s, 1H), 10.02 (bs, 1H). The product was analyzed as the corresponding methyl ester; LC/MS:  $m/z$  = 256.91 [M + H + CH<sub>3</sub>CN] $^+$ , 430.75 [2M + H] $^+$ ,  $t_R$  = 6.59 min.

**3-(*N,N*-Dimethylsulfamoyl)benzoyl chloride (26a)** Thionyl chloride (915 mg, 7.69 mmol) was added slowly to a stirred suspension of 3-(*N,N*-dimethylsulfamoyl)benzoic acid (**26**, 630 mg, 2.75 mmol) in toluene (6 mL), followed by 1 drop of DMF. The reaction mixture was heated at 80 °C for 4 h. After stirring overnight at room temperature the solution was evaporated under reduced pressure. The residue was redissolved in dichloromethane (6 mL). Thionyl chloride (3.27 g, 27.5 mmol) and 1 drop of DMF were added. After stirring overnight at room temperature the solution was evaporated under reduced pressure to yield the title compound. The product was analyzed as the corresponding methyl ester; LC/MS:  $m/z$  = 243.94 [M + H] $^+$ , 284.98 [M + H + CH<sub>3</sub>CN] $^+$ ,  $t_R$  = 9.46 min.

**3-(*N,N*-Diethylsulfamoyl)benzoyl chloride (27a)** The title compound was synthesized from 3-(*N,N*-diethylsulfamoyl)benzoic acid (**27**, 2.19 g, 8.51 mmol) according to General Procedure B. The product was analyzed as the corresponding methyl ester; LC/MS:  $m/z$  = 272.04 [M + H] $^+$ , 313.04 [M + H + CH<sub>3</sub>CN] $^+$ , 542.98 [2M + H] $^+$ ,  $t_R$  = 11.48 min.

**3-(*N,N*-Di-*n*-propylsulfamoyl)benzoyl chloride (28a)** The title compound was synthesized from 3-(*N,N*-di-*n*-propylsulfamoyl)benzoic acid (**28**, 1.14 g, 4.00 mmol) according to General Procedure B. The product was analyzed as the corresponding methyl ester; LC/MS:  $m/z$  = 300.11 [M + H] $^+$ , 340.78 [M + H + CH<sub>3</sub>CN] $^+$ , 598.79 [2M + H] $^+$ ,  $t_R$  = 12.97 min.

**3-(Pyrrolidin-1-ylsulfonyl)benzoyl chloride (29a)** Thionyl chloride (1.43 g, 12.1 mmol) was added slowly to a stirred suspension of 3-(pyrrolidin-1-ylsulfonyl)benzoic acid (**29**, 1.10 g, 4.31 mmol) in toluene (9 mL), followed

by 1 drop of DMF. The reaction mixture was heated at 80 °C for 4 h. After stirring overnight at room temperature the solution was evaporated under reduced pressure to yield the title compound. The product was analyzed as the corresponding methyl ester; LC/MS:  $m/z = 269.95 [M + H]^+$ , 311.00 [ $M + H + CH_3CN$ ] $^+$ , 538.79 [ $2M + H$ ] $^+$ ,  $t_R = 10.25$  min.

**3-(Piperidin-1-ylsulfonyl)benzoyl chloride (30a)** Thionyl chloride (2.81 g, 23.6 mmol) was added slowly to a stirred suspension of 3-(piperidin-1-ylsulfonyl)benzoic acid (**30**, 2.15 g, 8.42 mmol) in toluene (17 mL), followed by 1 drop of DMF. The reaction mixture was heated at 80 °C for 4 h. After stirring overnight at room temperature the solution was evaporated under reduced pressure. The residue was redissolved in dichloromethane (20 mL). Thionyl chloride (10.0 g, 84.2 mmol) and 1 drop of DMF were added. After stirring overnight at room temperature the solution was evaporated under reduced pressure to yield the title compound. The product was analyzed as the corresponding methyl ester; LC/MS:  $m/z = 283.81 [M + H]^+$ , 324.88 [ $M + H + CH_3CN$ ] $^+$ , 566.47 [ $2M + H$ ] $^+$ ,  $t_R = 11.01$  min.

**3-(Azepan-1-ylsulfonyl)benzoyl chloride (31a)** The title compound was synthesized from 3-(azepan-1-ylsulfonyl)benzoic acid (**31**, 1.13 g, 4.00 mmol) according to General Procedure B. The product was analyzed as the corresponding methyl ester; LC/MS:  $m/z = 297.86 [M + H]^+$ , 338.84 [ $M + H + CH_3CN$ ] $^+$ ,  $t_R = 12.28$  min.

**3-(Morpholinosulfonyl)benzoyl chloride (32a)<sup>S10</sup>** Thionyl chloride (2.80 g, 23.5 mmol) was added slowly to a stirred suspension of 3-(morpholinosulfonyl)benzoic acid (**32**, 2.28 g, 8.40 mmol) in toluene (17 mL), followed by 1 drop of DMF. The reaction mixture was heated at 80 °C for 4 h. After stirring overnight at room temperature the solution was evaporated under reduced pressure. The residue was redissolved in dichloromethane (20 mL). Thionyl chloride (9.99 g, 84.0 mmol) and 1 drop of DMF were added. After stirring overnight at room temperature the solution was evaporated under reduced pressure to yield the title compound. The product was analyzed as the corresponding methyl ester; LC/MS:  $m/z = 285.80 [M + H]^+$ , 326.79 [ $M + H + CH_3CN$ ] $^+$ , 570.31 [ $2M + H$ ] $^+$ ,  $t_R = 8.84$  min.

**3-(N-Benzyl-N-ethylsulfamoyl)benzoyl chloride (33a)** The title compound was synthesized from 3-(*N*-benzyl-*N*-ethylsulfamoyl)benzoic acid (**33**, 1.35 g, 4.23 mmol) according to General Procedure B. The product was analyzed as the corresponding methyl ester; LC/MS:  $m/z = 334.01 [M + H]^+$ ,  $t_R = 12.85$  min.

### Syntheses of methyl esters **2a**, **4a**, **9a-10a**, **13a-14a**, **35a-52a**, **57a-64a**

**Methyl 2-(3-(*N,N*-diethylsulfamoyl)benzamido)benzoate (2a)** The title compound was synthesized from methyl anthranilate (236 mg, 1.56 mmol) and 3-(*N,N*-diethylsulfamoyl)benzoyl chloride (**27a**, 430 mg, 1.56 mmol) in pyridine (5 mL) according to General Procedure C1: 526 mg, 86% yield.  $^1H$  NMR (500 MHz,  $CDCl_3$ ):  $\delta$  1.17 (t,  $J = 7.1$  Hz, 6H), 3.32 (q,  $J = 7.1$  Hz, 4H), 3.96 (s, 3H), 7.15 (ddd,  $J = 7.9, 7.3, 1.3$  Hz, 1H), 7.62 (ddd,  $J = 8.5, 7.3, 1.6$  Hz, 1H), 7.67 (t,  $J = 8.0$  Hz, 1H), 8.02 (ddd,  $J = 7.9, 1.9, 1.3$  Hz, 1H), 8.10 (dd,  $J = 7.9, 1.6$  Hz, 1H), 8.21 (ddd,  $J = 7.9, 1.9, 1.3$  Hz, 1H), 8.47 (t,  $J = 1.9$  Hz, 1H), 8.89 (dd,  $J = 8.5, 0.9$  Hz, 1H), 12.20 (bs, 1H);  $^{13}C$  NMR (125 MHz,  $CDCl_3$ ):  $\delta$  14.23, 42.28, 52.51, 115.25, 120.36, 123.07, 125.91, 129.65, 130.08, 130.76, 131.01, 134.93, 136.08, 141.42, 141.49, 163.95, 169.10; LC/MS:  $m/z = 390.79 [M + H]^+$ , 431.79 [ $M + H + CH_3CN$ ] $^+$ , 780.76 [ $2M + H$ ] $^+$ ,  $t_R = 14.16$  min.

**Methyl 3-(3-(*N,N*-diethylsulfamoyl)benzamido)benzoate (4a)** The title compound was synthesized from methyl 3-aminobenzoate (151 mg, 1.00 mmol) and 3-(*N,N*-diethylsulfamoyl)benzoyl chloride (**27a**, 414 mg, 1.50 mmol) in acetonitrile (1 mL) according to General Procedure C2. After workup the product was filtered over a short pad of silica gel (ethyl acetate/*n*-hexane 1/1). The solvent was evaporated under reduced pressure and the residue was crystallized from MeOH: 113 mg, 29% yield.  $^1H$  NMR (500 MHz,  $CDCl_3$ ):  $\delta$  1.09 (t,  $J = 7.1$  Hz, 6H), 3.23 (q,  $J = 7.1$  Hz, 4H), 3.88 (s, 3H), 7.44 (t,  $J = 8.0$  Hz, 1H), 7.60 (t,  $J = 7.9$  Hz, 1H), 7.82 (d,  $J = 7.6$  Hz, 1H), 7.92 (d,  $J = 7.9$  Hz, 1H), 8.00 (d,  $J = 7.6$  Hz, 1H), 8.09 (d,  $J = 7.9$  Hz, 1H), 8.22 (s, 1H), 8.26 (s, 1H), 8.36 (bs, 1H);  $^{13}C$  NMR (125 MHz,  $CDCl_3$ ):  $\delta$  14.13, 42.18, 52.27, 121.45, 124.94, 125.27, 125.96, 129.24, 129.79, 129.94, 131.02, 131.35, 137.83, 141.18, 164.41, 166.60; LC/MS:  $m/z = 358.86 [M - OMe]^+$ , 390.81 [ $M + H + CH_3CN$ ] $^+$ , 780.97 [ $2M + H$ ] $^+$ ,  $t_R = 11.99$  min.

**Methyl 2-(4-(*N,N*-diethylsulfamoyl)benzamido)benzoate (9a)** The title compound was synthesized from methyl anthranilate (151 mg, 1.00 mmol) and 4-(*N,N*-diethylsulfamoyl)benzoyl chloride (414 mg, 1.50 mmol) in acetonitrile (4 mL) according to General Procedure C2. After stirring overnight and workup the product was heated with MeOH (2mL). After cooling to room temperature, the solids were isolated by filtration, washed with cold MeOH and dried under reduced pressure: 284 mg, 73% yield.  $^1\text{H}$  NMR (500 MHz,  $\text{CDCl}_3$ ):  $\delta$  1.13 (t,  $J = 7.1$  Hz, 6H), 3.26 (q,  $J = 7.1$  Hz, 4H), 3.96 (s, 3H), 7.15 (ddd,  $J = 8.2, 7.6, 1.3$  Hz, 1H), 7.61 (ddd,  $J = 8.8, 7.6, 1.6$  Hz, 1H), 7.94 (AB-system,  $J = 8.5$  Hz, 2H), 8.09 (dd,  $J = 8.2, 1.9$  Hz, 1H), 8.14 (AB-system,  $J = 8.5$  Hz, 2H), 8.88 (dd,  $J = 8.5, 0.9$  Hz, 1H), 12.16 (bs, 1H);  $^{13}\text{C}$  NMR (125 MHz,  $\text{CDCl}_3$ ):  $\delta$  14.43, 42.38, 52.87, 115.53, 120.71, 123.40, 127.68, 128.36, 131.29, 135.23, 138.51, 141.67, 143.78, 164.33, 169.45; LC/MS:  $m/z = 390.97$  [M + H] $^+$ ,  $t_{\text{R}} = 13.72$  min.

**Methyl 5-bromo-2-(4-(*N,N*-diethylsulfamoyl)benzamido)benzoate (10a)<sup>S11</sup>** The title compound was synthesized from methyl 2-amino-5-bromobenzoate (230 mg, 1.00 mmol) and 4-(*N,N*-diethylsulfamoyl)benzoyl chloride (414 mg, 1.50 mmol) in acetonitrile (3 mL) according to General Procedure C2. After stirring overnight and workup the product was heated with MeOH (2mL). After cooling to room temperature, the solids were isolated by filtration, washed with cold MeOH and dried under reduced pressure: 359 mg, 76% yield.  $^1\text{H}$  NMR (500 MHz,  $\text{CDCl}_3$ ):  $\delta$  1.13 (t,  $J = 7.1$  Hz, 6H), 3.26 (q,  $J = 7.1$  Hz, 4H), 3.97 (s, 3H), 7.70 (dd,  $J = 8.8, 2.5$  Hz, 1H), 7.94 (AB-system,  $J = 8.8$  Hz, 2H), 8.12 (AB-system,  $J = 8.5$  Hz, 2H), 8.21 (d,  $J = 2.5$  Hz, 1H), 8.82 (d,  $J = 8.8$  Hz, 1H), 12.07 (bs, 1H);  $^{13}\text{C}$  NMR (125 MHz,  $\text{CDCl}_3$ ):  $\delta$  14.16, 42.12, 52.93, 115.60, 116.80, 122.11, 127.48, 128.10, 133.60, 137.68, 137.84, 140.43, 143.77, 164.04, 168.06; LC/MS:  $m/z = 470.88$  and 471.86 [M + H] $^+$ ,  $t_{\text{R}} = 15.11$  min.

**Methyl 2-(3-(diethylcarbamoyl)benzamido)benzoate (13a)** The title compound was synthesized from methyl anthranilate (151 mg, 1.00 mmol) and 3-(diethylcarbamoyl)benzoyl chloride (360 mg, 1.50 mmol) in acetonitrile (3 mL) according to General Procedure C2. After stirring for 2 days and workup the product was crystallized from MeOH. After cooling to room temperature, the solids were isolated by filtration, washed with cold MeOH and dried under reduced pressure: 185 mg, 52% yield.  $^1\text{H}$  NMR (500 MHz,  $\text{CDCl}_3$ ):  $\delta$  1.14 (bs, 3H), 1.25 (bs, 3H), 3.27 (bs, 2H), 3.56 (bs, 2H), 3.94 (s, 3H), 7.12 (ddd,  $J = 7.9, 7.3, 1.3$  Hz, 1H), 7.54-7.61 (m, 3H), 8.03-8.08 (m, 3H), 8.89 (dd,  $J = 8.5, 0.9$  Hz, 1H), 12.07 (bs, 1H);  $^{13}\text{C}$  NMR (125 MHz,  $\text{CDCl}_3$ ):  $\delta$  12.85, 14.17, 39.33, 43.37, 52.49, 115.25, 120.49, 122.81, 125.63, 127.61, 129.13, 130.04, 130.95, 134.83, 135.02, 137.96, 141.64, 164.90, 169.01, 170.26; LC/MS:  $m/z = 355.40$  [M + H] $^+$ , 709.07 [2M + H] $^+$ ,  $t_{\text{R}} = 12.34$  min.

**Methyl 5-bromo-2-(3-(diethylcarbamoyl)benzamido)benzoate (14a)** The title compound was synthesized from methyl 2-amino-5-bromobenzoate (230 mg, 1.00 mmol) and 3-(diethylcarbamoyl)benzoyl chloride (360 mg, 1.50 mmol) in acetonitrile (3 mL) according to General Procedure C2. After stirring overnight and workup the product was heated with MeOH (2mL). After cooling to room temperature, the solids were isolated by filtration, washed with cold MeOH and dried under reduced pressure: 360 mg, 83% yield.  $^1\text{H}$  NMR (500 MHz,  $\text{CDCl}_3$ ):  $\delta$  1.13 (bs, 3H), 1.25 (bs, 3H), 3.27 (bs, 2H), 3.56 (bs, 2H), 3.95 (s, 3H), 7.55 (dt,  $J = 7.6, 0.6$  Hz, 1H), 7.58 (dt,  $J = 7.6, 1.6$  Hz, 1H), 7.68 (dd,  $J = 9.1, 2.5$  Hz, 1H), 8.00-8.03 (m, 2H), 8.19 (d,  $J = 2.5$  Hz, 1H), 8.82 (d,  $J = 9.1$  Hz, 1H), 11.99 (bs, 1H);  $^{13}\text{C}$  NMR (125 MHz,  $\text{CDCl}_3$ ):  $\delta$  13.14, 14.44, 39.61, 43.68, 53.07, 115.48, 117.03, 122.41, 125.89, 127.85, 129.43, 130.48, 133.76, 134.93, 137.80, 138.29, 140.93, 165.12, 168.13, 170.41; LC/MS:  $m/z = 432.90$  and 434.39 [M + H] $^+$ ,  $t_{\text{R}} = 14.05$  min.

**Methyl 2-(3-(*N,N*-diethylsulfamoyl)-4-methylbenzamido)benzoate (35a)** The title compound was synthesized from methyl anthranilate (151 mg, 1.00 mmol) and 3-(*N,N*-diethylsulfamoyl)-4-methylbenzoyl chloride (**23a**, 290 mg, 1.00 mmol) in pyridine (4 mL) according to General Procedure C1: 220 mg, 54% yield.  $^1\text{H}$  NMR (500 MHz,  $\text{CDCl}_3$ ):  $\delta$  1.21 (t,  $J = 7.1$  Hz, 6H), 2.71 (s, 3H), 3.43 (q,  $J = 7.1$  Hz, 4H), 3.97 (s, 3H), 7.14 (ddd,  $J = 7.9, 7.3, 0.9$  Hz, 1H), 7.47 (d,  $J = 8.2$  Hz, 1H), 7.61 (m, 1H), 8.08 (dd,  $J = 7.9, 2.2$  Hz, 1H), 8.09 (dd,  $J = 7.9, 1.3$  Hz, 1H), 8.46 (d,  $J = 1.9$  Hz, 1H), 8.89 (dd,  $J = 8.5, 0.9$  Hz, 1H), 12.13 (bs, 1H);  $^{13}\text{C}$  NMR (125 MHz,  $\text{CDCl}_3$ ):  $\delta$  14.19, 20.51, 41.69, 52.52, 115.21, 120.40, 122.91, 127.36, 130.56, 130.99, 132.85, 133.34, 134.88, 139.87, 141.53, 141.82, 164.08, 169.07; LC/MS:  $m/z = 404.57$  [M + H] $^+$ , 445.72 [M + H +  $\text{CH}_3\text{CN}$ ] $^+$ , 808.44 [2M + H] $^+$ ,  $t_{\text{R}} = 13.75$  min.

**Methyl 2-(3-(*N,N*-diethylsulfamoyl)-4-ethylbenzamido)benzoate (36a)** The title compound was synthesized from methyl anthranilate (151 mg, 1.00 mmol) and 3-(*N,N*-diethylsulfamoyl)-4-ethylbenzoyl chloride (**24a**, 304

mg, 1.00 mmol) in pyridine (4 mL) according to General Procedure C1: 117 mg, 28% yield. <sup>1</sup>H NMR (500 MHz, CDCl<sub>3</sub>): δ 1.21 (t, J = 7.1 Hz, 6 Hz), 1.32 (t, J = 7.4 Hz, 3H), 3.12 (q, J = 7.4 Hz, 2H), 3.43 (q, J = 7.1 Hz, 4H), 3.95 (s, 3H), 7.13 (ddd, J = 7.9, 7.3, 1.3 Hz, 1H), 7.53 (d, J = 7.9 Hz, 1H), 7.60 (ddd, J = 8.5, 7.3, 1.6 Hz, 1H), 8.08 (dd, J = 8.5, 1.7 Hz, 1H), 8.11 (dd, J = 7.9, 1.9 Hz, 1H), 8.39 (d, J = 1.9 Hz, 1H), 8.88 (dd, J = 8.5, 0.9 Hz, 1H), 12.11 (bs, 1H); <sup>13</sup>C NMR (125 MHz, CDCl<sub>3</sub>): δ 14.41, 15.01, 25.98, 42.03, 52.52, 115.21, 120.42, 122.92, 127.02, 130.58, 131.01, 131.59, 132.55, 134.90, 139.68, 141.56, 147.90, 164.13, 169.11; LC/MS: m/z = 418.70 [M + H]<sup>+</sup>, 459.72 [M + H + CH<sub>3</sub>CN]<sup>+</sup>, 836.60 [2M + H]<sup>+</sup>, t<sub>R</sub> = 14.40 min.

**Methyl 4-chloro-2-(3-(N,N-diethylsulfamoyl)benzamido)benzoate (37a)** The title compound was synthesized from methyl 2-amino-4-chlorobenzoate (289 mg, 1.56 mmol) and 3-(N,N-diethylsulfamoyl)benzoyl chloride (**27a**, 430 mg, 1.56 mmol) in pyridine (5 mL) according to General Procedure C1: 340 mg, 51% yield. The material was used as such for the next step (hydrolysis of methyl ester).

**Methyl 2-(3-(N,N-diethylsulfamoyl)benzamido)-4-fluorobenzoate (38a)** The title compound was synthesized from methyl 2-amino-4-fluorobenzoate (169 mg, 1.00 mmol) and 3-(N,N-diethylsulfamoyl)benzoyl chloride (**27a**, 303 mg, 1.10 mmol) in pyridine (4 mL) according to General Procedure C1. Purification by flash column chromatography (silica gel, EtOAc/n-hexane 20/80 followed by 30/70): 526 mg, 86% yield. <sup>1</sup>H NMR (500 MHz, CDCl<sub>3</sub>): δ 1.15 (t, J = 7.1 Hz, 6H), 3.30 (q, J = 7.1 Hz, 4H), 3.94 (s, 3H), 6.82 (ddd, J = 10.1, 7.3, 2.5 Hz, 1H), 7.66 (t, J = 8.0 Hz, 1H), 8.01 (ddd, J = 7.9, 1.9, 1.3 Hz, 1H), 8.10 (dd, J = 8.8, 6.3 Hz, 1H), 8.18 (ddd, J = 7.9, 1.9, 1.3 Hz, 1H), 8.44 (dt, J = 1.9, 0.6 Hz, 1H), 8.69 (dd, J = 12.0, 2.8 Hz, 1H), 12.32 (bs, 1H); <sup>13</sup>C NMR (125 MHz, CDCl<sub>3</sub>): δ 14.24, 42.29, 52.60, 107.63 (d, J<sub>CF</sub> = 28 Hz), 110.42 (d, J<sub>CF</sub> = 22 Hz), 111.43 (d, J<sub>CF</sub> = 3 Hz), 129.75, 130.33, 130.75, 133.34 (d, J<sub>CF</sub> = 11 Hz), 135.62, 141.60, 143.63 (d, J<sub>CF</sub> = 13 Hz), 164.10, 166.40 (d, J<sub>CF</sub> = 255 Hz), 168.47; LC/MS: m/z = 408.78 [M + H]<sup>+</sup>, 449.77 [M + H + CH<sub>3</sub>CN]<sup>+</sup>, 816.64 [2M + H]<sup>+</sup>, t<sub>R</sub> = 14.42 min.

**Methyl 2-(3-(N,N-diethylsulfamoyl)benzamido)-4-nitrobenzoate (39a)** The title compound was synthesized from methyl 2-amino-4-nitrobenzoate (110 mg, 0.56 mmol) and 3-(N,N-diethylsulfamoyl)benzoyl chloride (**27a**, 232 mg, 0.84 mmol) in acetonitrile (2 mL) according to General Procedure C2. After stirring overnight at room temperature, workup was performed as described. The isolated product was heated with MeOH (6 mL), cooled to room temperature, filtered and the solids were dried under reduced pressure: 157 mg, 64% yield. <sup>1</sup>H NMR (500 MHz, CDCl<sub>3</sub>): δ 1.15 (t, J = 7.1 Hz, 6H), 3.30 (q, J = 7.1 Hz, 4H), 4.02 (s, 3H), 7.68 (t, J = 7.9 Hz, 1H), 7.93 (dd, J = 8.8, 2.2 Hz, 1H), 8.03 (ddd, J = 7.9, 1.9, 1.3 Hz, 1H), 8.25 (d, J = 8.5 Hz, 1H), 8.44 (t, J = 1.6 Hz, 1H), 9.76 (d, J = 2.5 Hz, 1H), 12.22 (bs, 1H); <sup>13</sup>C NMR (125 MHz, CDCl<sub>3</sub>): δ 14.22, 42.27, 53.34, 115.32, 117.12, 119.48, 125.92, 129.88, 130.61, 130.78, 132.19, 135.08, 141.76, 142.31, 151.38, 164.11, 167.73; LC/MS: m/z = 435.85 [M + H]<sup>+</sup>, 476.76 [M + H + CH<sub>3</sub>CN]<sup>+</sup>, 870.51 [2M + H]<sup>+</sup>, t<sub>R</sub> = 13.80 min.

**Methyl 2-(3-(N,N-diethylsulfamoyl)benzamido)-5-methylbenzoate (40a)** The title compound was synthesized from methyl 2-amino-5-methylbenzoate (165 mg, 1.00 mmol) and 3-(N,N-diethylsulfamoyl)benzoyl chloride (**27a**, 414 mg, 1.50 mmol) in acetonitrile (1 mL) according to General Procedure C2. After stirring overnight at room temperature, workup was performed as described. The isolated product was heated with MeOH (3 mL), cooled to room temperature, filtered and the solids were dried under reduced pressure: 360 mg, 89% yield. <sup>1</sup>H NMR (500 MHz, CDCl<sub>3</sub>): δ 1.15 (t, J = 7.1 Hz, 6H), 2.35 (s, 3H), 3.30 (q, J = 7.1 Hz, 4H), 3.94 (s, 3H), 7.41 (dd, J = 8.5, 2.2 Hz, 1H), 7.64 (t, J = 8.0 Hz, 1H), 7.88 (m, 1H), 7.99 (ddd, J = 7.9, 1.9, 1.3 Hz, 1H), 8.18 (ddd, J = 7.9, 1.9, 1.3 Hz, 1H), 8.44 (dt, J = 1.9, 0.6 Hz, 1H), 8.76 (d, J = 8.5 Hz, 1H), 12.07 (bs, 1H); <sup>13</sup>C NMR (125 MHz, CDCl<sub>3</sub>): δ 14.25, 20.74, 42.29, 52.45, 115.12, 120.33, 125.87, 129.62, 129.99, 130.72, 131.13, 132.71, 135.64, 136.20, 139.04, 141.43, 163.76, 169.15; LC/MS: m/z = 372.86 [M - OMe]<sup>+</sup>, 445.82 [M + H + CH<sub>3</sub>CN]<sup>+</sup>, 808.69 [2M + H]<sup>+</sup>, t<sub>R</sub> = 14.60 min.

**Methyl 2-(3-(N,N-diethylsulfamoyl)benzamido)-5-(trifluoromethyl)benzoate (41a)** The title compound was synthesized from methyl 2-amino-5-trifluoromethylbenzoate<sup>S12</sup> (219 mg, 1.00 mmol) and 3-(N,N-diethylsulfamoyl)benzoyl chloride (**27a**, 414 mg, 1.50 mmol) in acetonitrile (1 mL) according to General Procedure C2. After stirring for 2.5 h at room temperature, workup was performed as described. The isolated product was heated with MeOH (2 mL), cooled to room temperature, filtered and the solids were dried under reduced pressure: 296 mg, 65% yield. <sup>1</sup>H NMR (500 MHz, CDCl<sub>3</sub>): δ 1.17 (q, J = 7.1 Hz, 6H), 3.32 (q, J = 7.1 Hz, 4H), 4.02 (s, 3H), 7.79 (t, J = 7.9 Hz, 1H), 7.85 (dd, J = 8.8, 2.2 Hz, 1H), 8.04 (ddd, J = 7.9, 1.9, 1.3 Hz,

1H), 8.21 (ddd,  $J = 7.9, 1.9, 0.9$  Hz, 1H), 8.37 (dd,  $J = 1.6, 0.6$  Hz, 1H), 8.58 (t,  $J = 1.9$  Hz, 1H), 9.06 (d,  $J = 8.8$  Hz, 1H), 12.33 (bs, 1H);  $^{13}\text{C}$  NMR (125 MHz,  $\text{CDCl}_3$ ):  $\delta$  14.22, 42.27, 52.98, 115.10, 120.60, 123.54 (q,  $J_{\text{CF}} = 272$  Hz), 125.00 (q,  $J_{\text{CF}} = 33.9$  Hz), 125.99, 128.35 (q,  $J_{\text{CF}} = 3.4$  Hz), 129.81, 130.48, 130.81, 131.49 (d,  $J_{\text{CF}} = 3.7$  Hz), 135.43, 141.70, 144.13, 164.20, 168.17; LC/MS:  $m/z = 458.75$  [ $\text{M} + \text{H}]^+$ , 499.70 [ $\text{M} + \text{H} + \text{CH}_3\text{CN}]^+$ , 916.64 [ $2\text{M} + \text{H}]^+$ ,  $t_{\text{R}} = 14.93$  min.

**Methyl 2-(3-(*N,N*-diethylsulfamoyl)benzamido)-5-fluorobenzoate (42a)** The title compound was synthesized from methyl 2-amino-5-fluorobenzoate (264 mg, 1.56 mmol) and 3-(*N,N*-diethylsulfamoyl)benzoyl chloride (**27a**, 430 mg, 1.56 mmol) in pyridine (5 mL) according to General Procedure C1. The material was used as such for the next step (hydrolysis of methyl ester).

**Methyl 5-bromo-2-(3-(*N,N*-diethylsulfamoyl)benzamido)benzoate (43a)** The title compound was synthesized from methyl 2-amino-5-bromobenzoate (362 mg, 1.57 mmol) and 3-(*N,N*-diethylsulfamoyl)benzoyl chloride (**27a**, 414 mg, 1.50 mmol) in toluene (10 mL) according to General Procedure C3. After reflux for 2 h the solvent was evaporated under reduced pressure. The isolated product was heated with MeOH (3 mL), cooled to room temperature, filtered and the solids were dried under reduced pressure: 545 mg, 77% yield.  $^1\text{H}$  NMR (500 MHz,  $\text{CDCl}_3$ ):  $\delta$  1.15 (t,  $J = 7.1$  Hz, 6H), 3.30 (q,  $J = 7.1$  Hz, 4H), 3.96 (s, 3H), 7.65 (t,  $J = 8.2$  Hz, 1H), 7.69 (dd,  $J = 8.8, 2.5$  Hz, 1H), 8.00 (ddd,  $J = 7.9, 1.9, 0.9$  Hz, 1H), 8.15 (ddd,  $J = 7.9, 1.9, 0.9$  Hz, 1H), 8.20 (d,  $J = 2.5$  Hz, 1H), 8.43 (t,  $J = 1.9$  Hz, 1H), 8.80 (d,  $J = 8.8$  Hz, 1H), 12.09 (bs, 1H);  $^{13}\text{C}$  NMR (125 MHz,  $\text{CDCl}_3$ ):  $\delta$  14.23, 42.27, 52.86, 115.54, 116.77, 122.02, 125.90, 129.73, 130.27, 130.74, 133.58, 135.70, 137.65, 140.44, 141.59, 163.92, 167.98; LC/MS:  $m/z = 509.79$  and 511.77 [ $\text{M} + \text{H} + \text{CH}_3\text{CN}]^+$ , 936.65, 938.73 and 940.72 [ $2\text{M} + \text{H}]^+$ ,  $t_{\text{R}} = 15.26$  min.

**Methyl 5-cyano-2-(3-(*N,N*-diethylsulfamoyl)benzamido)benzoate (44a)** The title compound was synthesized from methyl 2-amino-5-cyanobenzoate<sup>813</sup> (176 mg, 1.00 mmol) and 3-(*N,N*-diethylsulfamoyl)benzoyl chloride (**27a**, 414 mg, 1.50 mmol) in acetonitrile (1 mL) according to General Procedure C2. After stirring for 3 h at room temperature, workup was performed as described. The isolated product was heated with MeOH (3 mL), cooled to room temperature, filtered and the solids were dried under reduced pressure: 294 mg, 71% yield.  $^1\text{H}$  NMR (500 MHz,  $\text{CDCl}_3$ ):  $\delta$  1.15 (t,  $J = 7.1$  Hz, 6H), 3.30 (q,  $J = 7.1$  Hz, 4H), 4.00 (s, 3H), 7.68 (t,  $J = 7.9$  Hz, 1H), 7.84 (dd,  $J = 8.8, 2.2$  Hz, 1H), 8.03 (ddd,  $J = 7.9, 1.9, 1.3$  Hz, 1H), 8.18 (ddd,  $J = 7.9, 1.6, 0.9$  Hz, 1H), 8.40 (d,  $J = 2.2$  Hz, 1H), 8.45 (t,  $J = 1.6$  Hz, 1H), 9.05 (d,  $J = 8.8$  Hz, 1H), 12.36 (bs, 1H);  $^{13}\text{C}$  NMR (125 MHz,  $\text{CDCl}_3$ ):  $\delta$  14.23, 42.26, 53.21, 106.54, 115.55, 117.83, 120.90, 126.02, 129.89, 130.67, 130.84, 135.13, 135.45, 137.78, 141.82, 144.82, 164.26, 167.63; LC/MS:  $m/z = 416.06$  [ $\text{M} + \text{H}]^+$ , 456.85 [ $\text{M} + \text{H} + \text{CH}_3\text{CN}]^+$ , 830.80 [ $2\text{M} + \text{H}]^+$ ,  $t_{\text{R}} = 14.93$  min.

**Methyl 2-(3-(*N,N*-diethylsulfamoyl)benzamido)-5-nitrobenzoate (45a)** The title compound was synthesized from methyl 2-amino-5-nitrobenzoate (196 mg, 1.00 mmol) and 3-(*N,N*-diethylsulfamoyl)benzoyl chloride (**27a**, 276 mg, 1.00 mmol) in toluene (5 mL) according to General Procedure C3. After reflux for 1 h the solvent was evaporated under reduced pressure. The isolated product was stirred with MeOH (3 mL), filtered and the solids were dried under reduced pressure: 304 mg, 70% yield. The material was used as such for the next step (hydrolysis of methyl ester).

**Methyl 2-(4-bromo-3-(*N,N*-diethylsulfamoyl)benzamido)-5-fluorobenzoate (46a)** The title compound was synthesized from methyl 5-fluoro-2-aminobenzoate (169 mg, 1.00 mmol) and 4-bromo-3-(*N,N*-diethylsulfamoyl)benzoyl chloride (**22a**, 400 mg, 1.13 mmol) in pyridine (5 mL) according to General Procedure C1: 130 mg, 27% yield.  $^1\text{H}$  NMR (500 MHz,  $\text{DMSO}-d_6$ ):  $\delta$  1.08 (q,  $J = 7.1$  Hz, 6H), 3.38 (q,  $J = 7.1$  Hz, 4H), 7.58 (ddd,  $J = 9.1, 8.2, 3.2$  Hz, 1H), 7.70 (dd,  $J = 9.1, 3.2$  Hz, 1H), 8.03 (dd,  $J = 8.2, 2.2$  Hz, 1H), 8.11 (d,  $J = 8.2$  Hz, 1H), 8.25 (dd,  $J = 9.1, 5.4$  Hz, 1H), 8.50 (d,  $J = 2.2$  Hz, 1H), 11.28 (bs, 1H);  $^{13}\text{C}$  NMR (125 MHz,  $\text{DMSO}-d_6$ ):  $\delta$  13.78, 41.25, 52.77, 116.66 (d,  $J_{\text{CF}} = 24.7$  Hz), 120.75 (d,  $J_{\text{CF}} = 21.2$  Hz), 121.74 (d,  $J_{\text{CF}} = 7.3$  Hz), 123.56, 124.79 (d,  $J_{\text{CF}} = 8.2$  Hz), 129.84, 132.00, 133.80, 135.14 (d,  $J_{\text{CF}} = 2.7$  Hz), 136.46, 139.98, 157.83, 162.95, 166.39; LC/MS:  $m/z = 527.41$  and 529.40 [ $\text{M} + \text{H} + \text{CH}_3\text{CN}]^+$ , 974.22 [ $2\text{M} + \text{H}]^+$ ,  $t_{\text{R}} = 14.10$  min.

**Methyl 5-bromo-2-(4-bromo-3-(*N,N*-diethylsulfamoyl)benzamido)benzoate (47a)** The title compound was synthesized from methyl 5-bromo-2-aminobenzoate (230 mg, 1.00 mmol) and 4-bromo-3-(*N,N*-diethylsulfamoyl)benzoyl chloride (**22a**, 400 mg, 1.13 mmol) in pyridine (5 mL) according to General Procedure

C1: 165 mg, 30% yield.  $^1\text{H}$  NMR (500 MHz, DMSO-*d*<sub>6</sub>):  $\delta$  1.08 (q, *J* = 7.1 Hz, 6H), 3.38 (q, *J* = 7.1 Hz, 4H), 3.85 (s, 3H), 7.88 (dd, *J* = 9.1, 2.5 Hz, 1H), 8.02 (dd, *J* = 8.2, 2.2 Hz, 1H), 8.06 (d, *J* = 2.5 Hz, 1H), 8.12 (d, *J* = 8.2 Hz, 1H), 8.29 (d, *J* = 8.8 Hz, 1H), 8.50 (d, *J* = 2.2 Hz, 1H), 11.42 (bs, 1H);  $^{13}\text{C}$  NMR (125 MHz, DMSO-*d*<sub>6</sub>):  $\delta$  13.80, 41.28, 52.85, 115.74, 121.14, 123.73, 124.00, 129.79, 131.97, 132.73, 133.68, 136.51, 136.53, 138.18, 140.03, 162.94, 166.39.

**Methyl 4-(3-(*N,N*-diethylsulfamoyl)benzamido)-[1,1'-biphenyl]-3-carboxylate (48a)** The title compound was synthesized from methyl 4-amino-[1,1'-biphenyl]-3-carboxylate<sup>S14</sup> (227 mg, 1.00 mmol) and 3-(*N,N*-diethylsulfamoyl)benzoyl chloride (**27a**, 276 mg, 1.00 mmol) in pyridine (4 mL) according to General Procedure C1. Purification by flash column chromatography (silica gel, EtOAc/n-hexane 90/10 followed by MeOH/DCM). The isolated product was stirred with MeOH (3 mL), filtered and the solids were dried under reduced pressure: 84 mg, 18% yield.  $^1\text{H}$  NMR (500 MHz, CDCl<sub>3</sub>):  $\delta$  1.16 (t, *J* = 7.1 Hz, 6H), 3.32 (q, *J* = 7.1 Hz, 4H), 3.99 (s, 3H), 7.36 (m, 1H), 7.45 (m, 2H), 7.60 (dd, *J* = 8.5, 1.3 Hz, 2H), 7.67 (t, *J* = 7.7 Hz, 1H), 7.85 (dd, *J* = 8.8, 2.5 Hz, 1H), 8.02 (ddd, *J* = 7.9, 1.9, 0.9 Hz, 1H), 8.21 (ddd, *J* = 7.9, 1.9, 1.3 Hz, 1H), 8.33 (d, *J* = 2.2 Hz, 1H), 8.48 (t, *J* = 1.6 Hz, 1H), 12.20 (bs, 1H);  $^{13}\text{C}$  NMR (125 MHz, CDCl<sub>3</sub>):  $\delta$  14.26, 42.30, 52.65, 115.62, 120.84, 125.93, 126.78, 127.61, 128.94, 129.37, 129.70, 130.15, 130.78, 133.35, 136.02, 136.03, 139.44, 140.52, 141.51, 163.94, 169.10; LC/MS: *m/z* = 507.54 [M + H + CH<sub>3</sub>CN]<sup>+</sup>, 932.67 [2M + H]<sup>+</sup>, *t*<sub>R</sub> = 15.18 min.

**Methyl 2-(3-(*N,N*-diethylsulfamoyl)benzamido)-6-methoxybenzoate (49a)** The title compound was synthesized from methyl 2-amino-6-methoxybenzoate hydrochloride (218 mg, 1.00 mmol) and 3-(*N,N*-diethylsulfamoyl)benzoyl chloride (**27a**, 303 mg, 1.10 mmol) in pyridine (8 mL) according to General Procedure C1. Purification by flash column chromatography (silica gel, EtOAc/n-hexane 30/70 followed by 40/60) yielded an oil. The crude material was used as such for the next step (hydrolysis of methyl ester).  $^1\text{H}$  NMR (500 MHz, CDCl<sub>3</sub>):  $\delta$  1.14 (t, *J* = 7.1 Hz, 6H), 3.29 (q, *J* = 7.1 Hz, 1H), 3.86 (s, 3H), 3.94 (s, 3H), 6.75 (d, *J* = 8.5, 1H), 7.46 (t, *J* = 8.5 Hz, 1H), 7.63 (t, *J* = 7.9 Hz, 1H), 7.98 (ddd, *J* = 7.9, 1.9, 1.3 Hz, 1H), 8.10 (ddd, *J* = 7.9, 1.9, 1.3 Hz, 1H), 8.23 (d, *J* = 8.5 Hz, 1H), 8.36 (t, *J* = 1.7 Hz, 1H), 10.96 (bs, 1H);  $^{13}\text{C}$  NMR (125 MHz, CDCl<sub>3</sub>):  $\delta$  14.22, 42.26, 52.63, 56.35, 107.70, 113.60, 120.04, 125.76, 129.67, 130.07, 130.70, 133.66, 135.96, 139.94, 141.46, 159.64, 163.70, 169.14; LC/MS: *m/z* = 429.50 [M – OCH<sub>3</sub> + CH<sub>3</sub>CN]<sup>+</sup>, 461.71 [M + H + CH<sub>3</sub>CN]<sup>+</sup>, 840.55 [2M + H]<sup>+</sup>, *t*<sub>R</sub> = 11.38 min. Purity: 91% by UV (254 nm).

**Methyl 2-chloro-6-(3-(*N,N*-diethylsulfamoyl)benzamido)benzoate (50a)** The title compound was synthesized from methyl 2-amino-6-chlorobenzoate (186 mg, 1.00 mmol) and 3-(*N,N*-diethylsulfamoyl)benzoyl chloride (**27a**, 414 mg, 1.50 mmol) in acetonitrile (2 mL) according to General Procedure C2. After stirring for 3 h at 0 °C, workup was performed as described, yielding an oil. Attempts to crystallize the product from MeOH failed to give a solid. Therefore the crude material was used as such for the next step (hydrolysis of methyl ester). LC/MS: *m/z* = 424.66 [M + H]<sup>+</sup>, 465.71 [M + H + CH<sub>3</sub>CN]<sup>+</sup>, 848.52 [2M + H]<sup>+</sup>, *t*<sub>R</sub> = 12.31 min. Purity: 85% by UV (254 nm).

**Methyl 2-(3-(*N,N*-diethylsulfamoyl)benzamido)-6-fluorobenzoate (51a)** The title compound was synthesized from methyl 2-amino-6-fluorobenzoate (169 mg, 1.00 mmol) and 3-(*N,N*-diethylsulfamoyl)benzoyl chloride (**27a**, 414 mg, 1.50 mmol) in acetonitrile (1 mL) according to General Procedure C2. After stirring overnight at room temperature, workup was performed as described. The isolated product was heated with MeOH (3 mL), cooled to room temperature, filtered and the solids were dried under reduced pressure: 340 mg, 83% yield.  $^1\text{H}$  NMR (500 MHz, CDCl<sub>3</sub>):  $\delta$  1.15 (t, *J* = 7.1 Hz, 6H), 3.30 (q, *J* = 7.1 Hz, 4H), 3.98 (s, 3H), 6.89 (ddd, *J* = 11.0, 8.2, 0.9 Hz, 1H), 7.53 (dt, *J* = 8.5, 6.0 Hz, 1H), 7.65 (t, *J* = 7.9 Hz, 1H), 8.00 (ddd, *J* = 7.9, 1.9, 0.9 Hz, 1H), 8.15 (ddd, *J* = 7.9, 1.9, 1.3 Hz, 1H), 8.41 (t, *J* = 1.7 Hz, 1H), 8.62 (d, *J* = 8.5 Hz, 1H), 11.80 (bs, 1H);  $^{13}\text{C}$  NMR (125 MHz, CDCl<sub>3</sub>):  $\delta$  14.06, 41.87, 112.37 (d, *J*<sub>CF</sub> = 23 Hz), 113.52 (d, *J*<sub>CF</sub> = 16 Hz), 119.22 (d, *J*<sub>CF</sub> = 4 Hz), 125.29, 129.82, 130.05, 131.32, 132.86 (d, *J*<sub>CF</sub> = 11 Hz), 135.05, 138.75 (d, *J*<sub>CF</sub> = 5 Hz), 160.46 (d, *J*<sub>CF</sub> = 252 Hz), 163.70, 165.88; LC/MS: *m/z* = 376.84 [M – OMe]<sup>+</sup>, 449.83 [M + H + CH<sub>3</sub>CN]<sup>+</sup>, 816.77 [2M + H]<sup>+</sup>, *t*<sub>R</sub> = 14.93 min.

**Methyl 2-(3-(*N,N*-diethylsulfamoyl)benzamido)-6-hydroxybenzoate (52a)** The title compound was synthesized from methyl 2-amino-6-hydroxybenzoate (94 mg, 0.56 mmol) and 3-(*N,N*-diethylsulfamoyl)benzoyl chloride (**27a**, 171 mg, 0.62 mmol) in toluene (5 mL) according to General Procedure C3. After reflux for 1 h the solvent was evaporated under reduced pressure. The isolated product was stirred with MeOH (1 mL). The solids

were filtered, washed with MeOH (1 mL) and dried under reduced pressure: 150 mg, 66% yield.  $^1\text{H}$  NMR (500 MHz,  $\text{CDCl}_3$ ):  $\delta$  1.13 (t,  $J = 7.1$  Hz, 6H), 3.27 (q,  $J = 7.1$  Hz, 4H), 4.15 (s, 3H), 6.76 (m, 1H), 7.45 (dt,  $J = 8.2, 3.2$ , 1H), 7.65 (dt,  $J = 7.9, 1.6$  Hz, 1H), 7.96 (m, 1H), 8.17 (m, 1H), 8.29 (m, 1H), 8.35 (m, 1H), 10.43 (bs, 1H), 11.13 (bs, 1H);  $^{13}\text{C}$  NMR (125 MHz,  $\text{CDCl}_3$ ):  $\delta$  14.16, 42.17, 53.47, 101.71, 111.84, 113.52, 124.81, 129.94, 131.47, 136.15, 140.28, 141.35, 162.08, 163.59, 169.57; LC/MS:  $m/z = 447.77 [\text{M} + \text{H} + \text{CH}_3\text{CN}]^+$ , 813.01 [2M + H] $^+$ ,  $t_{\text{R}} = 12.21$  min.

**Methyl 2-(3-sulfamoylbenzamido)benzoate (57a)** The title compound was synthesized from methyl anthranilate (302 mg, 2.00 mmol) and 3-sulfamoylbenzoyl chloride (**25a**, 659 mg, 3.00 mmol) in acetonitrile (2 mL) according to General Procedure C2. After stirring for 2 h at 0 °C, workup was performed as described. The isolated product was heated with MeOH (15 mL), cooled to room temperature, filtered and the solids were dried under reduced pressure: 350 mg, 52% yield. As the purity was below 95% the compound was heated for a second time with MeOH (5 mL): 220 mg, 33% yield.  $^1\text{H}$  NMR (500 MHz,  $\text{DMSO}-d_6$ ):  $\delta$  3.88 (s, 3H), 7.28 (m, 1H), 7.55 (bs, 2H), 7.70 (m, 1H), 7.83 (t,  $J = 7.7$  Hz, 1H), 8.00 (dd,  $J = 8.2, 1.6$  Hz, 1H), 8.08 (ddd,  $J = 7.9, 1.9, 1.3$  Hz, 1H), 8.16 (ddd,  $J = 7.9, 1.9, 0.9$  Hz, 1H), 8.42-8.44 (m, 2H), 11.55 (bs, 1H);  $^{13}\text{C}$  NMR (125 MHz,  $\text{DMSO}-d_6$ ):  $\delta$  52.54, 118.27, 121.47, 123.84, 124.78, 128.94, 129.70, 129.77, 130.60, 134.05, 134.97, 139.40, 144.88, 163.62, 167.72; LC/MS:  $m/z = 389.71 [\text{M} + \text{H}]^+$ , 430.65 [M + H +  $\text{CH}_3\text{CN}]^+$ , 778.24 [2M + H] $^+$ ,  $t_{\text{R}} = 9.81$  min.

**Methyl 2-(3-(N,N-dimethylsulfamoyl)benzamido)benzoate (58a)** The title compound was synthesized from methyl anthranilate (151 mg, 1.00 mmol) and 3-(N,N-dimethylsulfamoyl)benzoyl chloride (**26a**, 303 mg, 1.00 mmol) in pyridine (4 mL) according to General Procedure C1: 100 mg, 28% yield.  $^1\text{H}$  NMR (500 MHz,  $\text{CDCl}_3$ ):  $\delta$  2.77 (s, 6H), 3.95 (s, 3H), 7.15 (ddd,  $J = 7.9, 7.3, 1.3$  Hz, 1H), 7.61 (ddd,  $J = 8.8, 7.6, 1.9$  Hz, 1H), 7.70 (dt,  $J = 7.9, 0.6$  Hz, 1H), 7.96 (ddd,  $J = 7.9, 1.9, 1.3$  Hz, 1H), 8.09 (dd,  $J = 6.3, 1.6$  Hz, 1H), 8.24 (ddd,  $J = 7.9, 1.9, 1.3$  Hz, 1H), 8.43 (dt,  $J = 1.9, 0.6$  Hz, 1H), 8.88 (dd,  $J = 8.5, 0.9$  Hz, 1H), 12.21 (bs, 1H);  $^{13}\text{C}$  NMR (125 MHz,  $\text{CDCl}_3$ ):  $\delta$  38.20, 52.81, 120.63, 123.40, 126.86, 129.96, 131.00, 131.30, 131.47, 135.23, 136.46, 137.06, 141.65, 164.16, 169.39; LC/MS:  $m/z = 403.65 [\text{M} + \text{H} + \text{CH}_3\text{CN}]^+$ , 724.38 [2M + H] $^+$ ,  $t_{\text{R}} = 12.07$  min.

**Methyl 2-(3-(N,N-dipropylsulfamoyl)benzamido)benzoate (59a)** The title compound was synthesized from methyl anthranilate (151 mg, 1.00 mmol) and 3-(N,N-di-n-propylsulfamoyl)benzoyl chloride (**28a**, 303 mg, 1.00 mmol) in pyridine (4 mL) according to General Procedure C1. The product was crystallized from MeOH: 232 mg, 55% yield.  $^1\text{H}$  NMR (500 MHz,  $\text{CDCl}_3$ ):  $\delta$  0.87 (t,  $J = 7.4$  Hz, 6H), 1.57 (sextet,  $J = 7.5$  Hz, 4H), 3.14 (m, 4H), 3.94 (s, 3H), 7.14 (m, 1H), 7.60 (ddd,  $J = 8.8, 7.6, 1.6$  Hz, 1H), 7.65 (t,  $J = 8.0$  Hz, 1H), 7.99 (ddd,  $J = 7.9, 1.9, 0.9$  Hz, 1H), 8.08 (dd,  $J = 8.2, 1.6$  Hz, 1H), 8.20 (ddd,  $J = 7.9, 1.9, 0.9$  Hz, 1H), 8.45 (t,  $J = 1.6$  Hz, 1H), 8.88 (dd,  $J = 8.5, 1.3$  Hz, 1H), 12.18 (bs, 1H);  $^{13}\text{C}$  NMR (125 MHz,  $\text{CDCl}_3$ ):  $\delta$  11.17, 22.14, 50.22, 52.55, 115.26, 120.38, 123.07, 125.84, 129.62, 130.18, 130.82, 131.03, 134.93, 136.01, 141.27, 141.43, 163.97, 169.09; LC/MS:  $m/z = 418.76 [\text{M} + \text{H}]^+$ , 459.78 [M + H +  $\text{CH}_3\text{CN}]^+$ , 836.75 [2M + H] $^+$ ,  $t_{\text{R}} = 15.18$  min.

**Methyl 2-(3-(pyrrolidin-1-ylsulfonyl)benzamido)benzoate (60a)** The title compound was synthesized from methyl anthranilate (217 mg, 1.44 mmol) and 3-(pyrrolidin-1-ylsulfonyl)benzoyl chloride (**29a**, 393 mg, 1.44 mmol) in pyridine (5 mL) according to General Procedure C1. The product was crystallized from MeOH: 108 mg, 27% yield.  $^1\text{H}$  NMR (500 MHz,  $\text{CDCl}_3$ ):  $\delta$  1.77 (m, 4H), 3.31 (m, 4H), 3.93 (s, 3H), 7.13 (m, 1H), 7.60 (ddd,  $J = 8.8, 7.3, 1.6$  Hz, 1H), 7.68 (dt,  $J = 7.9, 0.6$  Hz, 1H), 8.00 (ddd,  $J = 7.6, 1.6, 0.9$  Hz, 1H), 8.07 (dd,  $J = 7.9, 1.6$  Hz, 1H), 8.21 (ddd,  $J = 7.9, 1.9, 1.3$  Hz, 1H), 8.46 (t,  $J = 1.9$  Hz, 1H), 8.86 (dd,  $J = 8.5, 0.9$  Hz, 1H), 12.18 (bs, 1H);  $^{13}\text{C}$  NMR (125 MHz,  $\text{CDCl}_3$ ):  $\delta$  25.28, 48.01, 52.52, 115.22, 120.31, 123.07, 126.29, 129.62, 130.51, 131.00, 134.91, 136.16, 138.20, 141.36, 163.96, 169.08; LC/MS:  $m/z = 588.59 [\text{M} + \text{H}]^+$ , 429.71 [M + H +  $\text{CH}_3\text{CN}]^+$ , 776.38 [2M + H] $^+$ ,  $t_{\text{R}} = 12.61$  min.

**Methyl 2-(3-(piperidin-1-ylsulfonyl)benzamido)benzoate (61a)** The title compound was synthesized from methyl anthranilate (151 mg, 1.00 mmol) and 3-(piperidin-1-ylsulfonyl)benzoyl chloride (**30a**, 287 mg, 1.00 mmol) in pyridine (4 mL) according to General Procedure C1. The product was crystallized from MeOH: 100 mg, 26% yield.  $^1\text{H}$  NMR (500 MHz,  $\text{CDCl}_3$ ):  $\delta$  1.42 (m, 2H), 1.65 (quintet,  $J = 5.8$  Hz, 4H), 3.06 (t,  $J = 5.5$  Hz, 4H), 3.94 (s, 3H), 7.15 (m, 1H), 7.61 (ddd,  $J = 8.5, 7.3, 1.6$  Hz, 1H), 7.68 (t,  $J = 8.0$  Hz, 1H), 7.94 (ddd,  $J = 7.6, 1.6, 0.9$  Hz, 1H), 8.09 (dd,  $J = 8.0, 1.7$  Hz, 1H), 8.22 (dd,  $J = 7.9, 1.9, 1.3$  Hz, 1H), 8.39 (dt,  $J = 1.9, 0.6$  Hz, 1H), 8.88 (dd,  $J = 8.5, 0.9$  Hz, 1H), 12.20 (bs, 1H);  $^{13}\text{C}$  NMR (125 MHz,  $\text{CDCl}_3$ ):  $\delta$  23.47, 25.18, 47.04, 52.54,

115.25, 120.36, 123.12, 126.53, 129.62, 130.69, 131.04, 131.12, 134.97, 136.11, 137.48, 141.42, 163.99, 169.12; LC/MS:  $m/z$  = 443.59 [M + H + CH<sub>3</sub>CN]<sup>+</sup>, 804.43 [2M + H]<sup>+</sup>,  $t_R$  = 13.56 min.

**Methyl 2-(3-(azepan-1-ylsulfonyl)benzamido)benzoate (62a)** The title compound was synthesized from methyl anthranilate (151 mg, 1.00 mmol) and 3-(azepan-1-ylsulfonyl)benzoyl chloride (**31a**, 302 mg, 1.00 mmol) in pyridine (4 mL) according to General Procedure C1. The product was crystallized from MeOH: 247 mg, 59% yield. <sup>1</sup>H NMR (500 MHz, CDCl<sub>3</sub>):  $\delta$  1.59 (m, 4H), 1.73 (m, 4H), 3.34 (t,  $J$  = 6.0 Hz, 4H), 3.94 (s, 3H), 7.14 (m, 1H), 7.60 (ddd,  $J$  = 8.8, 7.6, 1.6 Hz, 1H), 7.65 (t,  $J$  = 7.7 Hz, 1H), 7.98 (ddd,  $J$  = 7.9, 1.9, 1.3 Hz, 1H), 8.08 (dd,  $J$  = 8.2, 1.6, 1H), 8.19 (ddd,  $J$  = 7.6, 1.6, 0.9 Hz, 1H), 8.43 (t,  $J$  = 1.7 Hz, 1H), 8.87 (dd,  $J$  = 8.5, 0.9 Hz, 1H), 12.18 (bs, 1H); <sup>13</sup>C NMR (125 MHz, CDCl<sub>3</sub>):  $\delta$  26.88, 29.19, 48.41, 52.53, 115.22, 120.34, 123.07, 125.71, 129.64, 130.06, 130.75, 131.02, 134.94, 136.06, 140.62, 141.42, 164.00, 169.10; LC/MS:  $m/z$  = 416.73 [M + H]<sup>+</sup>, 457.75 [M + H + CH<sub>3</sub>CN]<sup>+</sup>, 832.80 [2M + H]<sup>+</sup>,  $t_R$  = 14.70 min.

**Methyl 2-(3-(morpholinosulfonyl)benzamido)benzoate (63a)** The title compound was synthesized from methyl anthranilate (151 mg, 1.00 mmol) and 3-(morpholinosulfonyl)benzoyl chloride (**32a**, 290 mg, 1.00 mmol) in pyridine (4 mL) according to General Procedure C1. The product was crystallized from MeOH: 146 mg, 36% yield. <sup>1</sup>H NMR (500 MHz, CDCl<sub>3</sub>):  $\delta$  3.09 (m, 4H), 3.77 (m, 4H), 3.96 (s, 3H), 7.17 (m, 1H), 7.63 (m, 1H), 7.73 (t,  $J$  = 7.9 Hz, 1H), 7.96 (ddd,  $J$  = 7.6, 1.6, 0.9 Hz, 1H), 8.10 (dd,  $J$  = 7.9, 1.6 Hz, 1H), 8.28 (ddd,  $J$  = 7.9, 1.9, 1.3 Hz, 1H), 8.42 (t,  $J$  = 1.6 Hz, 1H), 8.89 (dd,  $J$  = 8.5, 0.9 Hz, 1H), 12.23 (bs, 1H); <sup>13</sup>C NMR (125 MHz, CDCl<sub>3</sub>):  $\delta$  46.08, 52.54, 66.08, 115.22, 120.33, 123.18, 126.77, 129.83, 130.76, 131.05, 131.55, 134.99, 136.32, 141.35, 163.73, 169.17; LC/MS:  $m/z$  = 445.67 [M + H + CH<sub>3</sub>CN]<sup>+</sup>, 808.37 [2M + H]<sup>+</sup>,  $t_R$  = 11.94 min.

**Methyl 2-(3-(N-benzyl-N-ethylsulfamoyl)benzamido)benzoate (64a)** The title compound was synthesized from methyl anthranilate (151 mg, 1.00 mmol) and 3-(N-benzyl-N-ethylsulfamoyl)benzoyl chloride (**33a**, 290 mg, 1.00 mmol) in pyridine (4 mL) according to General Procedure C1. The product was crystallized from MeOH: 118 mg, 26% yield. <sup>1</sup>H NMR (500 MHz, CDCl<sub>3</sub>):  $\delta$  0.94 (t,  $J$  = 7.3 Hz, 3H), 3.27 (q,  $J$  = 7.1 Hz, 2H), 3.91 (s, 3H), 4.44 (s, 2H), 7.15 (ddd,  $J$  = 7.9, 7.3, 0.9 Hz, 1H), 7.25-7.33 (m, 5H), 7.62 (ddd,  $J$  = 8.5, 7.3, 1.3 Hz, 1H), 7.68 (t,  $J$  = 7.7 Hz, 1H), 8.03 (ddd,  $J$  = 7.9, 1.9, 0.9 Hz, 1H), 8.09 (dd,  $J$  = 8.2, 1.6 Hz, 1H), 8.23 (ddd,  $J$  = 7.9, 1.9, 1.3 Hz, 1H), 8.50 (t,  $J$  = 1.6 Hz, 1H), 8.89 (dd,  $J$  = 8.5, 0.9 Hz, 1H), 12.22 (bs, 1H); <sup>13</sup>C NMR (125 MHz, CDCl<sub>3</sub>):  $\delta$  13.42, 42.60, 51.31, 52.56, 115.25, 120.38, 123.12, 125.91, 127.81, 128.24, 128.59, 129.78, 130.17, 131.05, 134.99, 136.21, 136.28, 141.44, 163.92, 169.16; LC/MS:  $m/z$  = 452.67 [M + H]<sup>+</sup>, 493.62 [M + H + CH<sub>3</sub>CN]<sup>+</sup>, 904.55 [2M + H]<sup>+</sup>,  $t_R$  = 14.35 min.

#### Syntheses of test compounds 2, 4, 6, 9-10, 13-14, 34-64

**2-(3-(N,N-Diethylsulfamoyl)benzamido)benzoic acid (2)** The title compound was synthesized from methyl 2-(3-(N,N-diethylsulfamoyl)benzamido)benzoate (**2a**, 506 mg, 1.30 mmol) according to General Procedure D, using THF/MeOH 2/1 (9 mL) and 1N NaOH (aq., 2.6 mL). The solution was acidified with 1N HCl (aq., 2.6 mL). The organic solvent was evaporated under reduced pressure. The solid was isolated by suction filtration, washed with water, redissolved in MeOH and evaporated to dryness under reduced pressure: 394 mg, 81% yield; mp: 218.1-219.7 °C; <sup>1</sup>H NMR (500 MHz, DMSO-*d*<sub>6</sub>):  $\delta$  1.06 (t,  $J$  = 7.1 Hz, 6H), 3.22 (q,  $J$  = 7.1 Hz, 4H), 7.24 (t,  $J$  = 7.6 Hz, 1H), 7.68 (dt,  $J$  = 7.9, 1.6 Hz, 1H), 7.83 (t,  $J$  = 7.8 Hz, 1H), 8.06 (m, 2H), 8.22 (d,  $J$  = 7.9 Hz, 1H), 8.33 (s, 1H), 8.66 (d,  $J$  = 8.3 Hz, 1H), 12.3 (bs, 1H), 13.9 (bs, 1H); <sup>13</sup>C NMR (125 MHz, DMSO-*d*<sub>6</sub>):  $\delta$  14.10, 41.95, 117.11, 120.13, 123.37, 124.93, 129.96, 130.42, 131.06, 131.24, 134.26, 135.46, 140.63, 140.68, 163.17, 170.04; LC/MS:  $m/z$  = 417.88 [M + H + CH<sub>3</sub>CN]<sup>+</sup>, 752.73 [2M + H]<sup>+</sup>,  $t_R$  = 12.53 min, 99.8% pure (UV).

**3-(3-(N,N-Diethylsulfamoyl)benzamido)benzoic acid (4)** The title compound was synthesized from methyl 3-(3-(N,N-diethylsulfamoyl)benzamido)benzoate (**4a**, 486 mg, 1.24 mmol) according to General Procedure D, using THF/MeOH 2/1 (6 mL) and 1N NaOH (aq., 2 mL). The solution was acidified with 1N HCl (aq., 4 mL). Water was added and the solid was isolated by suction filtration, washed with water and dried under reduced pressure: 379 mg, 81% yield; mp: 231.5-233.6 °C; <sup>1</sup>H NMR (500 MHz, DMSO-*d*<sub>6</sub>):  $\delta$  1.06 (t,  $J$  = 7.1 Hz, 6H), 3.23 (q,  $J$  = 7.1 Hz, 4H), 7.85 (t,  $J$  = 7.7 Hz, 1H), 8.08 (d,  $J$  = 8.5 Hz, 1H), 8.11 (dd,  $J$  = 8.8, 2.2 Hz, 1H), 8.22 (d,  $J$  = 7.9 Hz, 1H), 8.33 (s, 1H), 8.41 (d,  $J$  = 1.9 Hz, 1H), 8.82 (d,  $J$  = 8.8 Hz, 1H), 12.53 (s, 1H); <sup>13</sup>C NMR (125

MHz, DMSO-*d*<sub>6</sub>):  $\delta$  14.11, 41.96, 105.46, 117.86, 120.52, 125.07, 130.39, 130.57, 131.26, 134.87, 135.36, 137.52, 140.75, 144.17, 163.69, 168.60; LC/MS: m/z = 376.75 [M + H]<sup>+</sup>, 417.76 [M + H + CH<sub>3</sub>CN]<sup>+</sup>, 752.70 [2M + H]<sup>+</sup>, t<sub>R</sub> = 10.16 min, 95.7% pure (UV).

**N-(2-Carbamoylphenyl)-3-(*N,N*-diethylsulfamoyl)benzamide (**6**)** A solution of 2-aminobenzamide (**5**, 136 mg, 1.00 mmol) and 3-(*N,N*-diethylsulfamoyl)benzoyl chloride (**27a**, 276 mg, 1.00 mmol) in toluene (5 mL) was heated at 88 °C for 30 minutes. After cooling to room temperature the solid was isolated by suction filtration. Purification by flash chromatography (ethyl acetate/n-hexane 60/40) yielded the title compound (78 mg, 21% yield); mp: 148.9–152.2 °C; <sup>1</sup>H NMR (500 MHz, DMSO-*d*<sub>6</sub>):  $\delta$  1.13 (t, *J* = 7.1 Hz, 6H), 3.27 (q, *J* = 7.1 Hz, 4H), 6.88 (bs, 1H), 7.17 (ddd, *J* = 7.9, 7.3, 1.3 Hz, 1H), 7.53 (bs, 1H), 7.57 (ddd, *J* = 7.6, 7.3, 1.6 Hz, 1H), 7.64 (t, *J* = 7.7 Hz, 1H), 7.67 (dd, *J* = 8.2, 1.6 Hz, 1H), 7.97 (ddd, *J* = 7.9, 1.9, 1.3 Hz, 1H), 8.27 (ddd, *J* = 7.9, 1.9, 1.3 Hz, 1H), 8.43 (t, *J* = 1.6 Hz, 1H), 8.89 (dd, *J* = 8.5, 1.1 Hz, 1H), 12.90 (bs, 1H); <sup>13</sup>C NMR (125 MHz, DMSO-*d*<sub>6</sub>):  $\delta$  14.18, 42.25, 118.14, 121.15, 123.27, 125.06, 127.65, 129.74, 129.88, 131.92, 133.69, 136.15, 140.67, 140.96, 163.58, 172.38; LC/MS: m/z = 375.92 [M + H]<sup>+</sup>, 750.92 [2M + H]<sup>+</sup> t<sub>R</sub> = 10.87 min, 98.2% pure (UV).

**2-(4-(*N,N*-Diethylsulfamoyl)benzamido)benzoic acid (**9**)** The title compound was synthesized from methyl 2-(4-(*N,N*-diethylsulfamoyl)benzamido)benzoate (**9a**, 274 mg, 0.70 mmol) according to General Procedure D, using THF/MeOH 2/1 (4 mL) and 1N NaOH (aq., 2 mL). The solution was acidified with 1N HCl (aq., 4 mL). Water was added and the solid was isolated by suction filtration, washed with water and dried under reduced pressure: 248 mg, 94% yield; mp: 219.4–220.8 °C; <sup>1</sup>H NMR (500 MHz, DMSO-*d*<sub>6</sub>):  $\delta$  1.06 (t, *J* = 7.1 Hz, 6H), 3.22 (q, *J* = 7.1 Hz, 4H), 7.25 (ddd, *J* = 7.9, 7.6, 1.3 Hz, 1H), 7.68 (ddd, *J* = 7.9, 7.6, 1.6 Hz, 1H), 8.01 (d, *J* = 8.8 Hz, 2H), 8.06 (dd, *J* = 8.2, 1.6 Hz, 1H), 8.13 (d, *J* = 8.8 Hz, 1H), 8.64 (dd, *J* = 8.5, 0.9 Hz, 1H), 12.21 (bs, 1H), 13.81 (bs, 1H); <sup>13</sup>C NMR (125 MHz, DMSO-*d*<sub>6</sub>):  $\delta$  4.13, 41.93, 117.17, 120.24, 123.43, 127.34, 128.11, 131.23, 134.26, 137.97, 140.55, 142.79, 163.46, 169.88; LC/MS: m/z = 376.59 [M + H]<sup>+</sup>, t<sub>R</sub> = 11.80 min, 99.3% pure (UV).

**5-Bromo-2-(4-(*N,N*-diethylsulfamoyl)benzamido)benzoic acid (**10**)<sup>S11</sup>** The title compound was synthesized from methyl 5-bromo-2-(4-(*N,N*-diethylsulfamoyl)benzamido)benzoate (**10a**, 350 mg, 0.75 mmol) according to General Procedure D, using THF/MeOH 2/1 (4 mL) and 1N NaOH (aq., 1.5 mL). The solution was acidified with 1N HCl (aq., 3 mL). Water was added and the solid was isolated by suction filtration, washed with water and dried under reduced pressure: 318 mg, 94% yield; mp: 232.8–235.6 °C; <sup>1</sup>H NMR (500 MHz, DMSO-*d*<sub>6</sub>):  $\delta$  1.06 (t, *J* = 7.1 Hz, 6H), 3.21 (q, *J* = 7.1 Hz, 4H), 7.87 (dd, *J* = 9.1, 2.5 Hz, 1H), 8.01 (d, *J* = 8.8 Hz, 2H), 8.12 (d, *J* = 8.5 Hz, 2H), 8.12 (d, *J* = 2.5 Hz, 1H), 8.57 (d, *J* = 8.8 Hz, 1H), 12.11 (bs, 1H), 14.2 (bs, 1H); <sup>13</sup>C NMR (125 MHz, DMSO-*d*<sub>6</sub>):  $\delta$  14.12, 41.93, 114.92, 119.62, 122.47, 127.36, 128.17, 133.25, 136.67, 137.67, 139.65, 142.92, 163.55, 168.49; LC/MS: m/z = 454.76 and 457.38 [M + H]<sup>+</sup>, t<sub>R</sub> = 13.20 min, 98.6% pure (UV).

**2-(3-(Diethylcarbamoyl)benzamido)benzoic acid (**13**)** The title compound was synthesized from methyl 2-(3-(diethylcarbamoyl)benzamido)benzoate (**13a**, 175 mg, 0.49 mmol) according to General Procedure D, using THF/MeOH 2/1 (3 mL) and 1N NaOH (aq., 1 mL). The solution was acidified with 1N HCl (aq., 2 mL). Water was added and the solid was isolated by suction filtration, washed with water and dried under reduced pressure: 155 mg, 92% yield; mp: 162.6–164.0 °C; <sup>1</sup>H NMR (500 MHz, DMSO-*d*<sub>6</sub>):  $\delta$  1.07 (bs, 3H), 1.17 (bs, 3H), 3.20 (bs, 2H), 3.46 (bs, 2H), 7.23 (dt, *J* = 7.7, 1.3 Hz, 1H), 7.62 (dt, *J* = 7.6, 1.4 Hz, 1H), 7.66 (d, *J* = 7.6 Hz, 1H), 7.68 (m, 1H), 7.89 (t, *J* = 1.4 Hz, 1H), 8.02 (dt, *J* = 7.9, 1.4 Hz, 1H), 8.06 (dd, *J* = 7.9, 1.6 Hz, 1H), 8.68 (dd, *J* = 8.5, 1.0 Hz, 1H), 12.20 (s, 1H), 13.82 (bs, 1H); <sup>13</sup>C NMR (125 MHz, DMSO-*d*<sub>6</sub>):  $\delta$  12.78 (bs), 14.00 (bs), 42.89 (bs), 116.81, 120.05, 123.14, 124.61, 127.60, 129.26, 129.69, 131.24, 134.58, 137.90, 140.86, 163.98, 169.02, 170.03; LC/MS: m/z = 340.98 [M + H]<sup>+</sup>, 382.00 [M + H + CH<sub>3</sub>CN]<sup>+</sup>, t<sub>R</sub> = 10.49 min, 99.0% pure (UV). Mp: 162.6–164.0 °C.

**5-Bromo-2-(3-(diethylcarbamoyl)benzamido)benzoic acid (**14**)** The title compound was synthesized from methyl 5-bromo-2-(3-(diethylcarbamoyl)benzamido)benzoate (**14a**, 350 mg, 0.81 mmol) according to General Procedure D, using THF/MeOH 2/1 (4.5 mL) and 1N NaOH (aq., 1.6 mL). The solution was acidified with 1N HCl (aq., 3.2 mL). Water was added and the solid was isolated by suction filtration, washed with water and dried under reduced pressure: 298 mg, 88% yield; mp: 169.6–170.3 °C; <sup>1</sup>H NMR (500 MHz, DMSO-*d*<sub>6</sub>):  $\delta$  1.07 (bs, 3H), 1.17 (bs, 3H), 3.20 (bs, 2H), 3.46 (bs, 2H), 7.62 (dt, *J* = 7.6, 1.6 Hz, 1H), 7.66 (dt, *J* = 7.6, 0.6 Hz, 1H), 7.86 (dd, *J* = 8.8, 2.5 Hz, 1H), 7.88 (t, *J* = 1.6 Hz, 1H), 8.00 (dt, *J* = 7.9, 1.6 Hz, 1H), 8.11 (d, *J* = 2.5 Hz, 1H), 8.62

(d,  $J = 8.8$  Hz, 1H), 12.09 (s, 1H), 14.19 (bs, 1H);  $^{13}\text{C}$  NMR (125 MHz, DMSO- $d_6$ ):  $\delta$  12.79 (bs), 14.01 (bs), 42.91 (bs), 114.58, 119.24, 122.29, 124.68, 127.63, 129.29, 129.83, 133.23, 134.31, 136.68, 137.91, 139.95, 164.05, 168.63, 168.98; LC/MS:  $m/z$  = 418.84 and 420.85 [M + H] $^+$ , 459.92 and 461.88 [M + H + CH<sub>3</sub>CN] $^+$ ,  $t_R$  = 12.04 min, 99.2% pure (UV).

**2-(4-Bromo-3-(*N,N*-diethylsulfamoyl)benzamido)benzoic acid (34)** The title compound was synthesized as described by Nie *et al.*; mp: 190.9–192.4 °C;  $^1\text{H}$  NMR (500 MHz, DMSO- $d_6$ ):  $\delta$  1.08 (t,  $J = 7.1$  Hz, 6H), 3.38 (q,  $J = 7.1$  Hz, 4H), 7.25 (ddd,  $J = 7.9, 7.6, 1.3$  Hz, 1H), 7.68 (ddd,  $J = 8.2, 7.6, 1.9$  Hz, 1H), 8.04 (dd,  $J = 8.2, 2.2$  Hz, 1H), 8.06 (dd,  $J = 7.9, 1.6$  Hz, 1H), 8.11 (d,  $J = 8.2$  Hz, 1H), 8.64 (d,  $J = 2.1$  Hz, 1H), 8.76 (dd,  $J = 8.5, 1.0$  Hz, 1H);  $^{13}\text{C}$  NMR (125 MHz, DMSO- $d_6$ ):  $\delta$  13.78, 41.25, 117.20, 120.24, 123.50, 123.58, 129.48, 131.22, 131.96, 134.10, 134.28, 136.58, 140.09, 140.47, 162.60, 170.00; LC/MS:  $m/z$  = 453.17 and 455.18 [M + H] $^+$ ,  $t_R$  = 12.48 min, >99% pure (UV).

**2-(3-(*N,N*-Diethylsulfamoyl)-4-methylbenzamido)benzoic acid (35)** The title compound was synthesized from methyl 2-(3-(*N,N*-diethylsulfamoyl)-4-methylbenzamido)benzoate (**35a**, 220 mg, 0.54 mmol) according to General Procedure D, using THF/MeOH 2/1 (3 mL) and 1N NaOH (aq., 1 mL). The solution was acidified with 1N HCl (aq., 2 mL). The organic solvent was evaporated under reduced pressure. The solid was isolated by suction filtration, washed with water and dried under reduced pressure: 197 mg, 93% yield; mp: 170.4–171.0 °C;  $^1\text{H}$  NMR (500 MHz, DMSO- $d_6$ ):  $\delta$  1.07 (t,  $J = 7.1$  Hz, 6H), 2.61 (s, 3H), 3.31 (q,  $J = 7.1$  Hz, 4H), 7.23 (m, 1H), 7.67 (m, 2H), 8.06 (dd,  $J = 8.0, 1.7$  Hz, 1H), 8.08 (dd,  $J = 7.9, 2.2$  Hz, 1H), 8.37 (d,  $J = 2.2$  Hz, 1H), 8.68 (dd,  $J = 8.5, 1.0$  Hz, 1H), 12.28 (bs, 1H), 13.87 (bs, 1H);  $^{13}\text{C}$  NMR (125 MHz, DMSO- $d_6$ ):  $\delta$  13.79, 19.80, 40.90, 116.78, 120.01, 123.22, 127.10, 130.77, 131.25, 132.48, 133.60, 134.32, 139.17, 140.80, 141.18, 163.16, 170.08; LC/MS:  $m/z$  = 431.72 [M + H + CH<sub>3</sub>CN] $^+$ , 781.12 [2M + H] $^+$ ,  $t_R$  = 11.98 min, 98.0% pure (UV).

**2-(3-(*N,N*-Diethylsulfamoyl)-4-ethylbenzamido)benzoic acid (36)** The title compound was synthesized from methyl 2-(3-(*N,N*-diethylsulfamoyl)-4-ethylbenzamido)benzoate (**36a**, 103 mg, 0.25 mmol) according to General Procedure D, using THF/MeOH 2/1 (1 mL) and 1N NaOH (aq., 0.3 mL). The solution was acidified with 1N HCl (aq., 2 mL). The organic solvent was evaporated under reduced pressure. The solid was isolated by suction filtration, washed with water and dried under reduced pressure: 79 mg, 80% yield; mp: 135.5–138.5 °C;  $^1\text{H}$  NMR (500 MHz, DMSO- $d_6$ ):  $\delta$  1.08 (t,  $J = 7.1$  Hz, 6H), 1.24 (t,  $J = 7.4$  Hz, 3H), 3.00 (q,  $J = 7.4$  Hz, 2H), 3.34 (q,  $J = 7.1$  Hz, 4H), 7.15 (dt,  $J = 7.6, 1.3$  Hz, 1H), 7.54 (dt,  $J = 7.9, 1.7$  Hz, 1H), 7.67 (d,  $J = 7.9$  Hz, 1H), 8.09 (dd,  $J = 7.9, 1.6$  Hz, 1H), 8.16 (dd,  $J = 7.9, 2.0$  Hz, 1H), 8.31 (d,  $J = 1.9$  Hz, 1H), 8.69 (dd,  $J = 8.4, 0.8$  Hz, 1H), 13.85 (bs, 1H);  $^{13}\text{C}$  NMR (125 MHz, DMSO- $d_6$ ):  $\delta$  14.24, 15.13, 25.26, 41.56, 119.21, 122.57, 126.40, 130.74, 131.27, 131.97, 132.48, 132.70, 138.98, 140.84, 146.76, 162.84, 170.26; LC/MS:  $m/z$  = 445.70 [M + H + CH<sub>3</sub>CN] $^+$ , 808.42 [2M + H] $^+$ ,  $t_R$  = 12.86 min, 96.5% pure (UV).

**2-(3-(*N,N*-Diethylsulfamoyl)benzamido)-4-fluorobenzoic acid (37)** The title compound was synthesized from methyl 2-(3-(*N,N*-diethylsulfamoyl)benzamido)-4-fluorobenzoate (**37a**, 141 mg, 0.35 mmol) according to General Procedure D, using THF/MeOH 2/1 (3 mL) and 1N NaOH (aq., 1 mL). The solution was acidified with 1N HCl (aq., 2 mL). Water was added and the solid was isolated by suction filtration, washed with water and dried under reduced pressure. As the hydrolysis was incomplete the procedure as described above was repeated: 108 mg, 79% yield; mp: 241.2–243.7 °C;  $^1\text{H}$  NMR (500 MHz, DMSO- $d_6$ ):  $\delta$  1.06 (t,  $J = 7.1$  Hz, 6H), 3.22 (q,  $J = 7.1$  Hz, 4H), 7.08 (ddd,  $J = 16.7, 8.8, 2.8$  Hz, 1H), 7.84 (t,  $J = 7.9$  Hz, 1H), 8.07 (m, 1H), 8.14 (dd,  $J = 8.8, 6.6$  Hz, 1H), 8.21 (m, 1H), 8.32 (t,  $J = 1.6$  Hz, 1H), 8.52 (dd,  $J = 12.0, 2.8$  Hz, 1H), 12.54 (bs, 1H), 14.04 (bs, 1H);  $^{13}\text{C}$  NMR (125 MHz, DMSO- $d_6$ ):  $\delta$  14.10, 41.96, 106.54 (d,  $J_{\text{CF}} = 28$  Hz), 110.31 (d,  $J_{\text{CF}} = 22$  Hz), 113.19 (d,  $J_{\text{CF}} = 3$  Hz), 124.91, 130.24, 130.54, 131, 11, 134.01 (d,  $J_{\text{CF}} = 11$  Hz), 140.72, 142.88, (d,  $J_{\text{CF}} = 13$  Hz), 164.99 (d,  $J_{\text{CF}} = 250$  Hz), 169.44; LC/MS:  $m/z$  = 435.67 [M + H + CH<sub>3</sub>CN] $^+$ , 788.65 [2M + H] $^+$ ,  $t_R$  = 12.62 min, 97.1% pure (UV).

**4-Chloro-2-(3-(*N,N*-diethylsulfamoyl)benzamido)benzoic acid (38)** The title compound was synthesized from methyl 4-chloro-2-(3-(*N,N*-diethylsulfamoyl)benzamido)benzoate (**38a**, 340 mg, 0.80 mmol) according to General Procedure D, using THF/MeOH 2/1 (9 mL) and 1N NaOH (aq., 3 mL). The solution was acidified with 1N HCl. The organic solvent was evaporated under reduced pressure. The solid was isolated by suction filtration, washed with water, dried under reduced pressure and crystallized from MeOH: 102 mg, 31% yield; mp: 222.0–223.5 °C;  $^1\text{H}$  NMR (500 MHz, DMSO- $d_6$ ):  $\delta$  1.07 (t,  $J = 7.2$  Hz, 6H), 3.22 (q,  $J = 7.1$  Hz, 4H), 7.29 (dd,  $J = 8.5,$

2.2 Hz, 1H), 7.84 (t,  $J$  = 7.7 Hz, 1H), 8.06 (m, 2H), 8.20 (d,  $J$  = 7.9 Hz, 1H), 8.31 (s, 1H), 8.76 (d,  $J$  = 2.2 Hz, 1H), 12.38 (s, 1H), 14.1 (bs, 1H);  $^{13}\text{C}$  NMR (125 MHz, DMSO- $d_6$ ):  $\delta$  14.09, 41.95, 115.66, 119.40, 123.22, 124.93, 130.21, 130.50, 131.12, 132.90, 135.00, 138.64, 140.72, 141.71, 163.44, 169.38; LC/MS: m/z = 451.79 [M + H + CH<sub>3</sub>CN]<sup>+</sup>, 820.69 and 822.76 [2M + H]<sup>+</sup>,  $t_{\text{R}}$  = 12.72 min, >99.9% pure (UV).

**2-(3-(*N,N*-Diethylsulfamoyl)benzamido)-4-nitrobenzoic acid (**39**)** The title compound was synthesized from methyl 2-(3-(*N,N*-diethylsulfamoyl)benzamido)-4-nitrobenzoate (**39a**, 157 mg, 0.36 mmol) according to General Procedure D, using THF/MeOH 2/1 (3 mL) and 1N NaOH (aq., 1 mL). The solution was acidified with 1N HCl (aq., 2 mL). Water was added and the solid was isolated by suction filtration, washed with water and dried under reduced pressure: 119 mg, 78% yield; mp: 229–231.5 °C;  $^1\text{H}$  NMR (500 MHz, DMSO- $d_6$ ):  $\delta$  1.07 (t,  $J$  = 7.1 Hz, 6H), 3.23 (q,  $J$  = 7.1 Hz, 4H), 7.86 (t,  $J$  = 7.7 Hz, 1H), 8.03 (dd,  $J$  = 8.8, 2.5 Hz, 1H), 8.08 (m, 1H), 8.22 (m, 1H), 8.26 (d,  $J$  = 8.8 Hz, 1H), 8.34 (t,  $J$  = 1.6 Hz, 1H), 9.43 (d,  $J$  = 2.5 Hz, 1H), 12.33 (bs, 1H);  $^{13}\text{C}$  NMR (125 MHz, DMSO- $d_6$ ):  $\delta$  14.12, 41.98, 114.66, 117.64, 122.88, 125.03, 130.34, 130.54, 131.23, 132.65, 134.79, 140.72, 140.98, 150.11, 163.70, 168.56; LC/MS: m/z = 462.78 [M + H + CH<sub>3</sub>CN]<sup>+</sup>, 842.38 [2M + H]<sup>+</sup>,  $t_{\text{R}}$  = 12.27 min, 99.0% pure (UV).

**2-(3-(*N,N*-Diethylsulfamoyl)benzamido)-5-methylbenzoic acid (**40**)** The title compound was synthesized from methyl 2-(3-(*N,N*-diethylsulfamoyl)benzamido)-5-methylbenzoate (**40a**, 360 mg, 0.89 mmol) according to General Procedure D, using THF/MeOH 2/1 (6 mL) and 1N NaOH (aq., 2 mL). The solution was acidified with 1N HCl (aq., 4 mL). Water (10 mL) was added and the solid was isolated by suction filtration, washed with water and dried under reduced pressure: 330 mg, 95% yield; mp: 226.8–228.6 °C;  $^1\text{H}$  NMR (500 MHz, DMSO- $d_6$ ):  $\delta$  1.06 (t,  $J$  = 7.1 Hz, 6H), 2.33 (s, 3H), 3.22 (q,  $J$  = 7.1 Hz, 4H), 7.49 (d,  $J$  = 8.2 Hz, 1H), 7.82 (t,  $J$  = 7.9 Hz, 1H), 7.87 (s, 1H), 8.04 (d,  $J$  = 7.6 Hz, 1H), 8.20 (d,  $J$  = 7.9 Hz, 1H), 8.31 (s, 1H), 8.54 (d,  $J$  = 8.5 Hz, 1H), 12.17 (s, 1H), 13.79 (bs, 1H);  $^{13}\text{C}$  NMR (125 MHz, DMSO- $d_6$ ):  $\delta$  14.10, 20.24, 41.94, 120.24, 124.87, 129.88, 130.40, 131.00, 131.27, 132.59, 134.78, 135.52, 138.22, 140.63, 162.95, 170.03; LC/MS: m/z = 390.75 [M + H]<sup>+</sup>, 431.90 [M + H + CH<sub>3</sub>CN]<sup>+</sup>, 780.63 [2M + H]<sup>+</sup>,  $t_{\text{R}}$  = 12.64 min, 99.4% pure (UV).

**2-(3-(*N,N*-Diethylsulfamoyl)benzamido)-5-(trifluoromethyl)benzoic acid (**41**)** The title compound was synthesized from methyl 2-(3-(*N,N*-diethylsulfamoyl)benzamido)-5-(trifluoromethyl)benzoate (**41a**, 157 mg, 0.36 mmol) according to General Procedure D, using THF/MeOH 2/1 (6 mL) and 1N NaOH (aq., 2 mL). The solution was acidified with 1N HCl (aq., 4 mL). The solid was isolated by suction filtration, washed with water and dried under reduced pressure: 232 mg, 81% yield; mp: 192.5–193.8 °C;  $^1\text{H}$  NMR (500 MHz, DMSO- $d_6$ ):  $\delta$  1.06 (t,  $J$  = 7.1 Hz, 6H), 3.22 (q,  $J$  = 7.1 Hz, 4H), 7.84 (t,  $J$  = 7.7 Hz, 1H), 8.01 (dd,  $J$  = 8.8, 1.9 Hz, 1H), 8.07 (d,  $J$  = 7.9 Hz, 1H), 8.23 (m, 1H), 8.29 (d,  $J$  = 1.9 Hz, 1H), 8.34 (m, 1H), 8.86 (d,  $J$  = 8.8 Hz, 1H), 12.79 (br.s, 1H);  $^{13}\text{C}$  NMR (125 MHz, DMSO- $d_6$ ):  $\delta$  14.03, 41.91, 18.08, 120.42, 123.04 (q,  $J_{\text{CF}} = 32$  Hz), 123.73 (q,  $J_{\text{CF}} = 272$  Hz), 125.02, 127.81 (q,  $J_{\text{CF}} = 4$  Hz), 130.18, 130.43, 131.09, 134.99, 140.66, 143.73, 163.51, 168.77; LC/MS: m/z = 444.59 [M + H]<sup>+</sup>, 485.65 [M + H + CH<sub>3</sub>CN]<sup>+</sup>, 888.77 [2M + H]<sup>+</sup>,  $t_{\text{R}}$  = 13.28 min, 96.1% pure (UV).

**2-(3-(*N,N*-Diethylsulfamoyl)benzamido)-5-fluorobenzoic acid (**42**)** The title compound was synthesized from methyl 2-(3-(*N,N*-diethylsulfamoyl)benzamido)-5-fluorobenzoate (**42a**, 337 mg, 0.83 mmol) according to General Procedure D, using THF/MeOH 2/1 (9 mL) and 1N NaOH (aq., 3 mL). The solution was acidified with 1N HCl. The organic solvent was evaporated under reduced pressure. The solid was isolated by suction filtration, washed with water, dried under reduced pressure and crystallized from MeOH: 86 mg, 26% yield; mp: 212.5–213.9 °C;  $^1\text{H}$  NMR (500 MHz, DMSO- $d_6$ ):  $\delta$  1.06 (t,  $J$  = 7.1 Hz, 6H), 3.22 (q,  $J$  = 7.1 Hz, 4H), 7.56 (dt,  $J$  = 8.5, 3.2 Hz, 1H), 7.76 (dd,  $J$  = 9.1, 3.2 Hz, 1H), 7.82 (t,  $J$  = 7.9 Hz, 1H), 8.05 (d,  $J$  = 8.2 Hz, 1H), 8.20 (d,  $J$  = 8.2 Hz, 1H), 8.32 (s, 1H), 8.61 (dd,  $J$  = 9.1, 5.0 Hz, 1H), 12.03 (bs, 1H);  $^{13}\text{C}$  NMR (125 MHz, DMSO- $d_6$ ):  $\delta$  14.1, 41.9, 117.0 (d,  $J_{\text{CF}} = 23.8$  Hz), 119.7 (d,  $J_{\text{CF}} = 6.4$  Hz), 121.0 (d,  $J_{\text{CF}} = 2.2$  Hz), 122.7 (d,  $J_{\text{CF}} = 8.2$  Hz), 125.0, 130.0, 130.4, 131.1, 135.3, 136.9, 140.7, 157.2 (d,  $J_{\text{CF}} = 242$  Hz), 163.1, 168.7; LC/MS: m/z = 435.83 [M + H + CH<sub>3</sub>CN]<sup>+</sup>, 788.64 [2M + H]<sup>+</sup>,  $t_{\text{R}}$  = 11.68 min, 100% pure (UV).

**5-Bromo-2-(3-(*N,N*-diethylsulfamoyl)benzamido)benzoic acid (**43**)** The title compound was synthesized from methyl 5-bromo-2-(3-(*N,N*-diethylsulfamoyl)benzamido)benzoate (**43a**, 368 mg, 0.78 mmol) according to General Procedure D, using THF/MeOH 2/1 (9 mL) and 1N NaOH (aq., 3 mL). The organic solvent was evaporated under reduced pressure. 1N HCl (aq., 4 mL) was added and the solid was isolated by suction filtration, washed with water, dried under reduced pressure and crystallized from MeOH: 70 mg, 20% yield; mp:

206.5-209.0 °C; <sup>1</sup>H NMR (500 MHz, DMSO-*d*<sub>6</sub>): δ 1.06 (t, *J* = 7.1 Hz, 6H), 3.22 (q, *J* = 7.1 Hz, 4H), 7.81 (m, 2H), 7.82 (m, 1H), 8.13 (d, *J* = 2.5 Hz, 1H), 8.21 (m, 1H), 8.32 (t, *J* = 1.7 Hz, 1H), 8.60 (d, *J* = 8.8 Hz, 1H), 12.8 (bs, 1H); <sup>13</sup>C NMR (125 MHz, DMSO-*d*<sub>6</sub>): δ 14.11, 41.96, 114.70, 120.78, 122.09, 125.03, 130.00, 130.41, 131.04, 133.31, 135.36, 136.04, 139.76, 140.66, 163.18, 168.53; LC/MS: m/z = 495.76 and 497.48 [M + H + CH<sub>3</sub>CN]<sup>+</sup>, 910.86 [2M + H]<sup>+</sup>, t<sub>R</sub> = 12.69 min, 100% pure (UV).

**5-Cyano-2-(3-(*N,N*-diethylsulfamoyl)benzamido)benzoic acid (**44**)** The title compound was synthesized from methyl 5-cyano-2-(3-(*N,N*-diethylsulfamoyl)benzamido)benzoate (**44a**, 237 mg, 0.59 mmol) according to General Procedure D, using THF/MeOH 2/1 (4 mL) and 1N NaOH (aq., 1 mL). The solution was acidified with 1N HCl (aq., 2 mL). Water (10 mL) was added and the solid was isolated by suction filtration, washed with water, dried under reduced pressure and crystallized from MeOH: 137 mg, 60% yield; mp: 195.3-196.6 °C; <sup>1</sup>H NMR (500 MHz, DMSO-*d*<sub>6</sub>): δ 1.06 (t, *J* = 7.1 Hz, 6H), 3.22 (q, *J* = 7.1 Hz, 4H), 7.85 (t, *J* = 7.7 Hz, 1H), 8.08 (ddd, *J* = 7.9, 1.9, 1.3 Hz, 1H), 8.12 (dd, *J* = 8.8, 2.2 Hz, 1H), 8.22 (ddd, *J* = 7.9, 1.9, 1.3 Hz, 1H), 8.33 (t, *J* = 1.6 Hz, 1H), 8.41 (d, *J* = 2.5 Hz, 1H), 8.82 (d, *J* = 9.1 Hz, 1H), 12.54 (bs, 1H); <sup>13</sup>C NMR (125 MHz, DMSO-*d*<sub>6</sub>): δ 14.11, 41.96, 105.46, 117.90, 118.07, 120.54, 125.08, 130.40, 130.58, 131.28, 134.89, 135.37, 137.52, 140.75, 144.17, 163.71, 168.61. LC/MS: m/z = 401.63 [M + H]<sup>+</sup>, 442.73 [M + H + CH<sub>3</sub>CN]<sup>+</sup>, 802.54 [2M + H]<sup>+</sup>, t<sub>R</sub> = 11.77 min, 96.2% pure (UV).

**2-(3-(*N,N*-Diethylsulfamoyl)benzamido)-5-nitrobenzoic acid (**45**)** The title compound was synthesized from methyl 2-(3-(*N,N*-diethylsulfamoyl)benzamido)-5-nitrobenzoate (**45a**, 304 mg, 0.70 mmol) according to General Procedure D, using THF/MeOH 2/1 (3 mL) and 1N NaOH (aq., 0.7 mL). The solution was acidified with 1N HCl (aq., 4 mL). Water was added and the solid was isolated by suction filtration, washed with water, dried under reduced pressure and crystallized from MeOH: 115 mg, 39% yield; mp: 216.6-218.8 °C; <sup>1</sup>H NMR (500 MHz, DMSO-*d*<sub>6</sub>): δ 1.07 (t, *J* = 7.1 Hz, 6H), 3.23 (q, *J* = 7.1 Hz, 4H), 7.86 (t, *J* = 7.8 Hz, 1H), 8.09 (dt, *J* = 8.3, 1.5 Hz, 1H), 8.24 (dt, *J* = 7.9, 1.6 Hz, 1H), 8.34 (t, *J* = 1.6 Hz, 1H), 8.53 (dd, *J* = 9.3, 2.9 Hz, 1H), 8.78 (d, *J* = 2.8 Hz, 1H), 8.90 (d, *J* = 9.3 Hz, 1H), 12.67 (s, 1H); <sup>13</sup>C NMR (125 MHz, DMSO-*d*<sub>6</sub>): δ 14.12, 41.98, 48.56, 117.44, 120.34, 125.11, 126.52, 129.12, 130.50, 130.61, 131.32, 134.76, 140.77, 141.70, 145.87, 163.77, 168.55; LC/MS: m/z = 421.89 [M + H]<sup>+</sup>, 462.94 [M + H + CH<sub>3</sub>CN]<sup>+</sup>, 842.83 [2M + H]<sup>+</sup>, t<sub>R</sub> = 12.31 min, 99.5% pure (UV).

**2-(4-Bromo-3-(*N,N*-diethylsulfamoyl)benzamido)-5-fluorobenzoic acid (**46**)** The title compound was synthesized from methyl 2-(4-bromo-3-(*N,N*-diethylsulfamoyl)benzamido)-5-fluorobenzoate (**46a**, 110 mg, 0.23 mmol) according to General Procedure D, using THF/MeOH 2/1 (3 mL) and 1N NaOH (aq., 1 mL). The solution was acidified with 1N HCl (aq., 2 mL). The organic solvent was evaporated under reduced pressure. The solid was isolated by suction filtration, washed with water and dried under reduced pressure: 88 mg, 82% yield; mp 226.7-228.7 °C; <sup>1</sup>H NMR (500 MHz, DMSO-*d*<sub>6</sub>): δ 1.07 (t, *J* = 7.1 Hz, 6H), 3.37 (q, *J* = 7.1 Hz, 4H), 7.56 (ddd, *J* = 9.1, 8.2, 3.2 Hz, 1H), 7.75 (dd, *J* = 9.5, 3.2 Hz, 1H), 8.03 (dd, *J* = 8.2, 2.2 Hz, 1H), 8.10 (d, *J* = 8.2 Hz, 1H), 8.52 (d, *J* = 2.2 Hz, 1H), 8.56 (dd, *J* = 9.1, 5.0 Hz, 1H), 12.02 (bs, 1H), 14.14 (bs, 1H); <sup>13</sup>C NMR (125 MHz, DMSO-*d*<sub>6</sub>): δ 13.77, 41.24, 117.04 (d, *J*<sub>CF</sub> = 23.8 Hz), 119.89 (d, *J*<sub>CF</sub> = 6.4 Hz), 120.95 (d, *J*<sub>CF</sub> = 22.0 Hz), 122.85 (d, *J*<sub>CF</sub> = 7.3 Hz), 123.58, 129.54, 131.99, 133.96, 136.54, 136.69, 140.06, 157.30 (d, *J*<sub>CF</sub> = 241.91 Hz), 162.59, 168.65; LC/MS: m/z = 472.45 and 474.47 [M + H]<sup>+</sup>, 513.44 and 515.35 [M + H + CH<sub>3</sub>CN]<sup>+</sup>, 946.30 and 948.34 [2M + H]<sup>+</sup>, t<sub>R</sub> = 12.40 min, 99.7% pure (UV).

**5-Bromo-2-(4-bromo-3-(*N,N*-diethylsulfamoyl)benzamido)benzoic acid (**47**)** The title compound was synthesized from methyl 5-bromo-2-(4-bromo-3-(*N,N*-diethylsulfamoyl)benzamido)benzoate (**47a**, 145 mg, 0.26 mmol) according to General Procedure D, using THF/MeOH 2/1 (3 mL) and 1N NaOH (aq., 1 mL). The solution was acidified with 1N HCl (aq., 2 mL). The organic solvent was evaporated under reduced pressure. The solid was isolated by suction filtration, washed with water and dried under reduced pressure: 110 mg, 78% yield; mp: 218.6-220.0 °C; <sup>1</sup>H NMR (500 MHz, DMSO-*d*<sub>6</sub>): δ 1.07 (t, *J* = 7.1 Hz, 6H), 3.37 (q, *J* = 7.1 Hz, 4H), 7.85 (dd, *J* = 9.1, 2.5 Hz, 1H), 8.02 (dd, *J* = 8.2, 2.5 Hz, 1H), 8.11 (d, *J* = 8.2 Hz, 1H), 8.11 (d, *J* = 2.5 Hz), 8.51 (d, *J* = 2.2 Hz, 1H), 8.55 (d, *J* = 8.8 Hz, 1H), 12.18 (bs, 1H); <sup>13</sup>C NMR (125 MHz, DMSO-*d*<sub>6</sub>): δ 13.78, 41.25, 114.99, 119.59, 122.44, 123.75, 129.52, 131.99, 133.23, 133.82, 136.60, 136.68, 139.57, 140.10, 162.67, 168.62; LC/MS: m/z = 532.38 and 534.07 [M + H]<sup>+</sup>, 575.22 and 577.26 [M + H + CH<sub>3</sub>CN]<sup>+</sup>, t<sub>R</sub> = 13.36 min, 98.7% pure (UV).

**4-(3-(*N,N*-Diethylsulfamoyl)benzamido)-[1,1'-biphenyl]-3-carboxylic acid (**48**)** The title compound was synthesized from methyl 4-(3-(*N,N*-diethylsulfamoyl)benzamido)-[1,1'-biphenyl]-3-carboxylate (**48a**, 84 mg, 0.18 mmol) according to General Procedure D, using THF/MeOH 2/1 (1.5 mL) and 1N NaOH (aq., 0.42 mL). The solution was acidified with 1N HCl (aq., 1 mL). The organic solvent was evaporated under reduced pressure. The solid was isolated by suction filtration, washed with water and dried under reduced pressure: 60 mg, 74% yield; mp: 217.6–219.2 °C; <sup>1</sup>H NMR (500 MHz, DMSO-*d*<sub>6</sub>): δ 1.07 (t, *J* = 7.1 Hz, 6H), 3.23 (q, *J* = 7.1 Hz, 4H), 7.39 (t, *J* = 7.4 Hz, 1H), 7.49 (t, *J* = 7.6 Hz, 2H), 7.70 (d, *J* = 7.3 Hz, 2H), 7.84 (t, *J* = 7.9 Hz, 1H), 8.01 (dd, *J* = 8.7, 2.5 Hz, 1H), 8.06 (m, 1H), 8.23 (m, 1H), 8.30 (d, *J* = 2.5 Hz, 1H), 8.35 (m, 1H), 8.76 (d, *J* = 8.8 Hz, 1H), 12.32 (s, 1H); <sup>13</sup>C NMR (125 MHz, DMSO-*d*<sub>6</sub>): δ 14.12, 41.97, 117.64, 120.77, 124.95, 126.36, 127.63, 128.91, 129.07, 130.02, 130.47, 131.08, 132.28, 134.96, 135.39, 138.60, 139.86, 140.67, 163.16, 169.95; LC/MS: m/z = 493.75 [M + H + CH<sub>3</sub>CN]<sup>+</sup>, 904.57 [2M + H]<sup>+</sup>, t<sub>R</sub> = 13.49 min, 99.8% pure (UV).

**2-(3-(*N,N*-Diethylsulfamoyl)benzamido)-6-methoxybenzoic acid (**49**)** The title compound was synthesized from methyl 2-(3-(*N,N*-diethylsulfamoyl)benzamido)-6-methoxybenzoate (**49a**) according to General Procedure D, using THF/MeOH 2/1 (3 mL) and 1N NaOH (aq., 1 mL). 1N HCl (aq., 2 mL) was added and the organic solvent was evaporated under reduced pressure. The precipitate was isolated by suction filtration and crystallized from MeOH (2 mL) containing a small amount of water (0.5 mL). The white solid was isolated by suction filtration, washed with cold MeOH/water 1/1 and dried under reduced pressure: 110 mg, 27% yield over 2 steps; mp: 133.8–136.4 °C; <sup>1</sup>H NMR (500 MHz, DMSO-*d*<sub>6</sub>): δ 1.06 (t, *J* = 7.1 Hz, 6H), 3.21 (q, *J* = 7.1 Hz, 4H), 3.83 (s, 3H), 7.01 (d, *J* = 8.2 Hz, 1H), 7.29 (d, *J* = 7.9 Hz, 1H), 7.46 (t, *J* = 8.2 Hz, 1H), 7.77 (t, *J* = 7.7 Hz, 1H), 8.01 (d, *J* = 7.9 Hz, 1H), 8.17 (d, *J* = 7.9 Hz, 1H), 8.29 (s, 1H), 10.58 (s, 1H), 12.99 (bs, 1H); <sup>13</sup>C NMR (125 MHz, DMSO-*d*<sub>6</sub>): δ 14.16, 41.95, 56.04, 109.14, 117.60, 118.58, 125.50, 129.63, 129.90, 130.95, 131.42, 135.29, 136.40, 140.30, 157.24, 163.92, 167.25; LC/MS: m/z = 406.64 [M + H]<sup>+</sup>, 429.69 [M - OH + CH<sub>3</sub>CN]<sup>+</sup>, 812.53 [2M + H]<sup>+</sup>, t<sub>R</sub> = 11.05 min, 96.1% pure (UV).

**2-Chloro-6-(3-(*N,N*-diethylsulfamoyl)benzamido)benzoic acid (**50**)** The title compound was synthesized from methyl 2-chloro-6-(3-(*N,N*-diethylsulfamoyl)benzamido)benzoate (**50a**) according to General Procedure D, using THF/MeOH 2/1 (6 mL) and 1N NaOH (aq., 2 mL). The organic solvent was evaporated under reduced pressure. 1N HCl (aq., 4 mL) was added. A thick gum was formed. The water was decanted and MeOH (2 mL) was added to the residue. The mixture was stirred at room temperate yielding a white solid, which was crystallized from EtOH: 31 mg, 8% yield over 2 steps; mp: 184.3–186.3 °C; <sup>1</sup>H NMR (500 MHz, DMSO-*d*<sub>6</sub>): δ 1.06 (t, *J* = 7.1 Hz, 6H), 3.21 (q, *J* = 7.1 Hz, 4H), 7.22 (dd, *J* = 8.0, 1.1 Hz, 1H), 7.33 (t, *J* = 8.2 Hz, 1H), 7.78 (t, *J* = 7.7 Hz, 1H), 8.01 (m, 1H), 8.06 (br.d, 1H), 8.18 (m, 1H), 8.30 (t, *J* = 1.6 Hz, 1H), 12.17 (bs, 1H); <sup>13</sup>C NMR (125 MHz, DMSO-*d*<sub>6</sub>): δ 14.13, 41.96, 120.62, 125.53, 125.75, 129.17, 129.68, 130.07, 130.87, 131.21, 135.42, 137.51, 140.52, 163.10, 166.80; LC/MS: m/z = 410.61 and 412.66 [M + H]<sup>+</sup>, 822.55 [2M + H]<sup>+</sup>, t<sub>R</sub> = 10.90 min, 96.1% pure (UV).

**2-(3-(*N,N*-Diethylsulfamoyl)benzamido)-6-fluorobenzoic acid (**51**)** The title compound was synthesized from methyl 2-(3-(*N,N*-diethylsulfamoyl)benzamido)-6-fluorobenzoate (**51a**, 170 mg, 0.42 mmol) according to General Procedure D, using THF/MeOH 2/1 (3 mL) and 1N NaOH (aq., 1 mL). The solution was acidified with 1N HCl (aq., 2 mL). Water was added and the solid was isolated by suction filtration, washed with water and dried under reduced pressure: 152 mg, 93% yield; mp: 213.1–215.5 °C; <sup>1</sup>H NMR (500 MHz, DMSO-*d*<sub>6</sub>): δ 1.07 (t, *J* = 7.1 Hz, 6H), 3.22 (q, *J* = 7.1 Hz, 4H), 7.15 (dd, *J* = 9.8, 8.8 Hz, 1H), 7.60 (dd, *J* = 8.2, 6.3 Hz, 1H), 7.80 (t, *J* = 7.9 Hz, 1H), 7.83 (d, *J* = 8.5 Hz, 1H), 8.04 (d, *J* = 7.9 Hz, 1H), 8.20 (d, *J* = 7.9 Hz, 1H), 8.31 (s, 1H), 11.23 (s, 1H), 13.70 (bs, 1H); <sup>13</sup>C NMR (125 MHz, DMSO-*d*<sub>6</sub>): δ 14.06, 41.87, 112.37 (*d*, *J*<sub>CF</sub> = 23 Hz), 113.52 (*d*, *J*<sub>CF</sub> = 16 Hz), 119.22 (*d*, *J*<sub>CF</sub> = 4 Hz), 125.29, 130.05, 131.32, 132.86 (*J*<sub>CF</sub> = 11 Hz), 135.05, 138.75 (*d*, *J*<sub>CF</sub> = 5 Hz), 160.46 (*d*, *J*<sub>CF</sub> = 252 Hz), 163.70, 165.88; LC/MS: m/z = 394.71 [M + H]<sup>+</sup>, 788.78 [2M + H]<sup>+</sup>, t<sub>R</sub> = 11.79 min, 99.6% pure (UV).

**2-(3-(*N,N*-Diethylsulfamoyl)benzamido)-6-hydroxybenzoic acid (**52**)** The title compound was synthesized from methyl 2-(3-(*N,N*-diethylsulfamoyl)benzamido)-6-hydroxybenzoate (**52a**, 120 mg, 0.42 mmol) according to General Procedure D, using THF/MeOH 2/1 (3 mL) and 1N NaOH (aq., 1 mL). The solution was acidified with 1N HCl (aq., 3 mL) and extracted with dichloromethane (three times). The combined organic extracts were dried over sodium sulfate, filtered and evaporated under reduced pressure, yielding a slightly yellow oil that solidified upon standing. The product was crystallized from MeOH: 75 mg, 65% yield; mp: 175.8–176.7 °C; <sup>1</sup>H NMR (500

MHz, DMSO-*d*<sub>6</sub>): δ 1.06 (t, *J* = 7.1 Hz, 6H), 3.22 (q, *J* = 7.1 Hz, 4H), 6.71 (dd, *J* = 8.2, 0.9 Hz, 1H), 7.39 (t, *J* = 8.2 Hz, 1H), 7.79 (t, *J* = 7.9 Hz, 1H), 7.82 (dd, *J* = 8.2, 1.3 Hz, 1H), 8.02 (ddd, *J* = 7.9, 1.9, 0.9 Hz, 1H), 8.19 (ddd, *J* = 7.9, 1.9, 1.3 Hz, 1H), 8.30, (t, *J* = 1.7 Hz, 1H), 10.87 (bs, 2H), 12.14 (s, 1H); <sup>13</sup>C NMR (125 MHz, DMSO-*d*<sub>6</sub>): δ 14.12, 41.93, 106.98, 112.13, 112.80, 125.20, 129.69, 130.16, 130.99, 133.38, 135.84, 139.84, 140.53, 160.93, 163.20, 171.45; LC/MS: m/z = 392.88 [M + H]<sup>+</sup>, 433.92 [M + H + CH<sub>3</sub>CN]<sup>+</sup>, 784.83 [2M + H]<sup>+</sup>, t<sub>R</sub> = 10.51 min, 97.5% pure (UV).

**3'-Carbamoyl-4-(3-(*N,N*-diethylsulfamoyl)benzamido)-[1,1'-biphenyl]-3-carboxylic acid (53)** A solution of methyl 5-bromo-2-(3-(*N,N*-diethylsulfamoyl)benzamido)benzoate (**45a**, 219 mg, 0.48 mmol), (3-carbamoylphenyl)boronic acid (119 mg, 0.72 mmol) and cesium carbonate (470 mg, 1.44 mmol) in a mixture of DME/water 1/1 (20 mL) was degassed. A catalytic amount of tetrakis(triphenylphosphine)palladium was added. The reaction flask was put into a pre-heated oil bath (120 °C) and heated for 3.5 h under a nitrogen atmosphere. After cooling to room temperature water was added and the solution was acidified with 1N HCl (aq.). The white solid was isolated by suction filtration, washed with water and briefly heated to reflux with a few mL's of methanol. The solids were isolated by suction filtration, washed with a small amount of methanol and dried under reduced pressure to yield the title compound (182 mg, 76% yield); mp: 259.3–259.8 °C (dec.); <sup>1</sup>H NMR (500 MHz, DMSO-*d*<sub>6</sub>): δ 1.07 (t, *J* = 7.1 Hz, 6H), 3.23 (q, *J* = 7.1 Hz, 4H), 7.46 (bs, 1H), 7.57 (t, *J* = 7.7 Hz, 1H), 7.83–7.90 (m, 3H), 8.06–8.09 (m, 2H), 8.17 (bs, 1H), 8.21 (t, *J* = 1.6 Hz, 1H), 8.24 (dt, *J* = 7.6, 1.3 Hz, 1H), 8.35 (t, *J* = 1.7 Hz, 1H), 8.38 (d, *J* = 2.2 Hz, 1H), 8.78 (d, *J* = 8.8 Hz, 1H), 12.37 (bs, 1H), 14.06 (bs, 1H); <sup>13</sup>C NMR (125 MHz, DMSO-*d*<sub>6</sub>): δ 14.12, 41.97, 117.80, 120.80, 124.97, 125.31, 126.75, 129.07, 129.10, 130.04, 130.46, 131.09, 132.40, 134.35, 135.03, 135.38, 138.58, 140.07, 140.67, 163.19, 167.67, 169.95; LC/MS: m/z = 495.99 [M + H]<sup>+</sup>, 436.84 [M + H + CH<sub>3</sub>CN]<sup>+</sup>, 990.95 [2M + H]<sup>+</sup>, t<sub>R</sub> = 11.23 min, 95.7% pure (UV).

**4'-Carbamoyl-4-(3-(*N,N*-diethylsulfamoyl)benzamido)-[1,1'-biphenyl]-3-carboxylic acid (54)** A solution of methyl 5-bromo-2-(3-(*N,N*-diethylsulfamoyl)benzamido)benzoate (**43a**, 341 mg, 0.75 mmol), (4-carbamoylphenyl)boronic acid (186 mg, 1.13 mmol) and cesium carbonate (733 mg, 2.25 mmol) in a mixture of DME/water 1/1 (15 mL) was degassed. A catalytic amount of tetrakis(triphenylphosphine)palladium was added. The reaction flask was put into a pre-heated oil bath (100 °C) and heated for 3.5 h under a nitrogen atmosphere. After cooling to room temperature water (15 mL) was added and the solution was filtered over a thin layer of Celite. The filtrate was acidified with 1N HCl (aq.). The white solid was isolated by suction filtration, washed twice with water and heated to reflux with methanol (30 mL). After cooling to room temperature the solids were isolated by centrifugation and dried under reduced pressure to yield the title compound (224 mg, 60% yield); mp: 282–285 °C; <sup>1</sup>H NMR (500 MHz, DMSO-*d*<sub>6</sub>): δ 1.07 (t, *J* = 7.1 Hz, 6H), 3.24 (q, *J* = 7.1 Hz, 4H), 7.40 (bs, 1H), 7.81 (d, *J* = 8.5 Hz, 2H), 7.85 (t, *J* = 7.9 Hz, 1H), 7.99 (d, *J* = 8.5 Hz, 2H), 8.04 (bs, 1H), 8.08 (m, 2H), 8.24 (ddd, *J* = 7.6, 1.9, 1.0 Hz, 1H), 8.35 (t, *J* = 1.6 Hz, 1H), 8.37 (d, *J* = 2.5 Hz, 1H), 8.78 (d, *J* = 8.8 Hz, 1H), 12.41 (bs, 1H); <sup>13</sup>C NMR (125 MHz, DMSO-*d*<sub>6</sub>): δ 14.61, 42.46, 118.24, 121.28, 125.46, 126.60, 128.79, 129.61, 130.56, 130.97, 131.59, 132.94, 133.70, 134.43, 135.84, 140.79, 141.18, 141.61, 163.70, 167.92, 170.38; LC/MS: m/z = 495.97 [M + H]<sup>+</sup>, 536.89 [M + H + CH<sub>3</sub>CN]<sup>+</sup>, 991.01 [2M + H]<sup>+</sup>, t<sub>R</sub> = 11.12 min, 97.8% pure (UV).

**4-(3-(*N,N*-diethylsulfamoyl)benzamido)-[1,1'-biphenyl]-3,3'-dicarboxylic acid (55)** A solution of methyl 5-bromo-2-(3-(*N,N*-diethylsulfamoyl)benzamido)benzoate (**43a**, 341 mg, 0.75 mmol), (3-carboxyphenyl)boronic acid (187 mg, 1.13 mmol) and cesium carbonate (733 mg, 2.25 mmol) in a mixture of DME/water 1/1 (15 mL) was degassed. A catalytic amount of tetrakis(triphenylphosphine)palladium was added. The reaction flask was put into a pre-heated oil bath (100 °C) and heated for 3.5 h under a nitrogen atmosphere. After cooling to room temperature water (15 mL) was added and the solution was filtered over a thin layer of Celite. The filtrate was acidified with 1N HCl (aq.). The white solid was isolated by suction filtration, washed twice with water and heated to reflux with methanol (30 mL). After cooling to room temperature the solids were isolated by centrifugation and dried under reduced pressure to yield the title compound (235 mg, 63% yield); mp: 265.8–267.3 °C; <sup>1</sup>H NMR (500 MHz, DMSO-*d*<sub>6</sub>): δ = 1.07 (t, *J* = 7.1 Hz, 6H), 3.23 (q, *J* = 7.1 Hz, 4H), 7.62 (t, *J* = 7.7 Hz, 1H), 7.84 (t, *J* = 7.7 Hz, 1H), 7.94–7.98 (m, 2H), 8.04–8.07 (m, 2H), 8.21 (t, *J* = 1.7 Hz, 1H), 8.23 (m, 1H), 8.32 (d, *J* = 2.2 Hz, 1H), 8.35 (t, *J* = 1.6 Hz, 1H), 8.78 (d, *J* = 8.8 Hz, 1H), 12.33 (s, 1H), 13.15 (bs, 1H), 14.04 (bs, 1H); <sup>13</sup>C NMR (125 MHz, DMSO-*d*<sub>6</sub>): δ = 14.12, 41.97, 117.69, 120.87, 124.96, 126.87, 128.40, 128.99, 129.48, 130.04, 130.46, 130.76, 131.09, 131.59, 132.39, 133.93, 135.35, 138.91, 140.23, 140.67, 163.19, 167.13,

169.85; LC/MS: m/z = 496.90 [M + H]<sup>+</sup>, 537.77 [M + H + CH<sub>3</sub>CN]<sup>+</sup>, 992.79 [2M + H]<sup>+</sup>, t<sub>R</sub> = 12.02 min, 95.1% pure (UV).

**4-(3-(*N,N*-diethylsulfamoyl)benzamido)-[1,1'-biphenyl]-3,4'-dicarboxylic acid (56)** The title compound was synthesized from methyl 5-bromo-2-(3-(*N,N*-diethylsulfamoyl)benzamido)benzoate (**43a**, 341 mg, 0.75 mmol) and (4-carboxyphenyl)boronic acid (187 mg, 1.13 mmol) using the same procedure as described for compound **55**. The product was purified by heating with methanol, filtered and isolated as a white solid: 251 mg, 67%; mp: 282.4–283.3 °C; <sup>1</sup>H NMR (500 MHz, DMSO-*d*<sub>6</sub>): δ = 1.07 (t, J = 7.1 Hz, 6H), 3.23 (q, J = 7.1 Hz, 4H), 7.83–7.87 (m, 3H), 8.03–8.09 (m, 4H), 8.23 (d, J = 7.9 Hz, 1H), 8.34 (d, J = 1.7 Hz, 1H), 8.39 (d, J = 2.2 Hz, 1H), 8.79 (d, J = 8.5 Hz, 1H), 12.37 (s, 1H), 13.02 (bs, 1H); <sup>13</sup>C NMR (125 MHz, DMSO-*d*<sub>6</sub>): δ 14.12, 41.97, 117.64, 120.76, 124.95, 126.42, 129.23, 129.70, 130.07, 130.46, 131.09, 132.52, 133.62, 135.30, 140.53, 140.67, 142.61, 163.20, 167.03, 169.85; LC/MS: m/z = 537.70 [M + H<sup>+</sup> CH<sub>3</sub>CN], 992.84 [2M+ H<sup>+</sup>], t<sub>R</sub> = 11.07 min, 96.6% pure (UV).

**2-(Sulfamoylbenzamido)benzoic acid (57)** The title compound was synthesized from methyl 2-(3-sulfamoylbenzamido)benzoate (**57a**, 220 mg, 0.66 mmol) according to General Procedure D, using THF/MeOH 2/1 (3 mL) and 1N NaOH (aq., 1 mL). After stirring for 2 days at room temperature 1N HCl (aq., 4 mL) was added and stirring continued overnight. The solid was isolated by suction filtration, washed with water and dried under reduced pressure: 176 mg, 84% yield; mp: 224–234 °C; <sup>1</sup>H NMR (500 MHz, DMSO-*d*<sub>6</sub>): δ 7.24 (m, 1H), 7.36 (s, 2H), 7.69 (m, 1H), 7.82 (t, J = 7.9 Hz, 1H), 8.07 (m, 2H), 8.16 (m, 1H), 8.44 (t, J = 1.7 Hz, 1H), 8.67 (dd, J = 8.5, 1.0 Hz, 1H), 12.28 (s, 1H); <sup>13</sup>C NMR (125 MHz, DMSO-*d*<sub>6</sub>): δ 117.01, 120.19, 123.37, 124.51, 129.06, 129.90, 129.93, 131.24, 134.31, 135.11, 140.65, 144.95, 163.44, 170.02; LC/MS: m/z = 361.78 [M + H + CH<sub>3</sub>CN]<sup>+</sup>, 640.62 [2M + H]<sup>+</sup>, t<sub>R</sub> = 8.75 min, 95.3% pure (UV).

**2-(3-(*N,N*-Dimethylsulfamoyl)benzamido)benzoic acid (58)** The title compound was synthesized from methyl 2-(3-(*N,N*-dimethylsulfamoyl)benzamido)benzoate (**58a**, 100 mg, 0.28 mmol) according to General Procedure D, using THF/MeOH 2/1 (1.5 mL) and 1N NaOH (aq., 0.5 mL). The solution was acidified with 1N HCl (aq., 1 mL). Water was added and the solution was extracted with ethyl acetate (three times). The combined organic extracts were washed with 1N HCl (aq.), dried over sodium sulfate, filtered and evaporated under reduced pressure. The residue was stirred with a small amount of water. The solid was isolated by suction filtration, washed with water and dried under reduced pressure: 44 mg, 46% yield; mp: 226.6–229.5 °C; <sup>1</sup>H NMR (500 MHz, DMSO-*d*<sub>6</sub>): δ 2.68 (s, 6H), 7.25 (dt, J = 7.6, 1.3 Hz, 1H), 7.69 (dt, J = 7.9, 1.6 Hz, 1H), 7.89 (t, J = 8.0 Hz, 1H), 8.01 (dd, 7.9, 1.4 Hz, 1H), 8.06 (dd, J = 7.9, 1.6 Hz, 1H), 8.26 (m, 2H), 8.67 (dd, J = 8.5, 0.9 Hz, 1H), 12.31 (bs, 1H), 13.89 (bs, 1H); <sup>13</sup>C NMR (125 MHz, DMSO-*d*<sub>6</sub>): δ 37.55, 117.08, 120.13, 123.41, 125.64, 130.42, 130.77, 131.27, 131.58, 134.31, 135.51, 135.65, 140.62, 163.18, 170.06; LC/MS: m/z = 389.69 [M + H + CH<sub>3</sub>CN]<sup>+</sup>, 696.57 [2M + H]<sup>+</sup>, t<sub>R</sub> = 10.35 min, 98.4% pure (UV).

**2-(3-(*N,N*-Dipropylsulfamoyl)benzamido)benzoic acid (59)** The title compound was synthesized from methyl 2-(3-(*N,N*-dipropylsulfamoyl)benzamido)benzoate (**59a**, 217 mg, 0.52 mmol) according to General Procedure D, using THF/MeOH 2/1 (3 mL) and 1N NaOH (aq., 1 mL). The solution was acidified with 1N HCl (aq., 2 mL). Water was added and the solid was isolated by suction filtration, washed with water and dried under reduced pressure: 195 mg, 93% yield; mp: 213.0–213.8 °C; <sup>1</sup>H NMR (500 MHz, DMSO-*d*<sub>6</sub>): δ 0.81 (t, J = 7.4 Hz, 6H), 1.49 (sextet, J = 7.4 Hz, 4H), 3.08 (t, J = 7.6 Hz, 4H), 7.24 (t, J = 7.6 Hz, 1H), 7.68 (dt, J = 7.7, 1.4 Hz, 1H), 7.84 (t, J = 7.9 Hz, 1H), 8.06 (2H), 8.22 (d, J = 7.9 Hz, 1H), 8.33 (s, 1H), 8.67 (d, J = 8.2 Hz, 1H), 12.30 (bs, 1H), 13.86 (bs, 1H); <sup>13</sup>C NMR (125 MHz, DMSO-*d*<sub>6</sub>): δ 10.94, 21.57, 49.61, 117.06, 120.15, 123.38, 125.02, 130.04, 130.40, 131.00, 131.24, 134.29, 135.40, 140.42, 140.63, 163.18, 170.03. LC/MS: m/z = 445.78 [M + H + CH<sub>3</sub>CN]<sup>+</sup>, 808.72 [2M + H]<sup>+</sup>, t<sub>R</sub> = 13.20 min, 98.8% pure (UV).

**2-(3-(Pyrrolidin-1-ylsulfonyl)benzamido)benzoic acid (60)<sup>S15</sup>** The title compound was synthesized from methyl 2-(3-(pyrrolidin-1-ylsulfonyl)benzamido)benzoate (**60a**, 82 mg, 0.21 mmol) according to General Procedure D, using THF/MeOH 2/1 (1.5 mL) and 1N NaOH (aq., 0.42 mL). The solution was acidified with 1N HCl (aq., 1 mL). The solid was isolated by suction filtration, washed with water and dried under reduced pressure: 33 mg, 42% yield; mp: 226.6–227.8 °C; <sup>1</sup>H NMR (500 MHz, DMSO-*d*<sub>6</sub>): δ 1.67 (m, 4H), 3.20 (m, 4H), 7.25 (m, 1H), 7.69 (m, 1H), 7.87 (t, J = 7.9 Hz, 1H), 8.06 (m, 1H), 8.08 (m, 1H), 8.26 (m, 1H), 8.33 (m, 1H), 8.67 (dd, J = 8.5, 0.9 Hz, 1H), 12.3 (bs, 1H); <sup>13</sup>C NMR (125 MHz, DMSO-*d*<sub>6</sub>): δ 29.96, 53.14, 122.40, 125.36,

128.64, 130.67, 135.67, 135.76, 136.50, 136.70, 139.52, 140.69, 142.35 145.87, 168.46, 175.29; LC/MS: m/z = 415.67 [M + H + CH<sub>3</sub>CN]<sup>+</sup>, 748.42 [2M + H]<sup>+</sup>, t<sub>R</sub> = 10.85 min, >99% pure (UV).

**2-(3-(Piperidin-1-ylsulfonyl)benzamido)benzoic acid (61)**<sup>S15</sup> The title compound was synthesized from methyl 2-(3-(piperidin-1-ylsulfonyl)benzamido)benzoate (**61a**, 146 mg, 0.36 mmol) according to General Procedure D, using THF/MeOH 2/1 (1.5 mL) and 1N NaOH (aq., 0.40 mL). The solution was acidified with 1N HCl (aq., 1 mL). The solid was isolated by suction filtration, washed with water and dried under reduced pressure: 50 mg, 48% yield; mp: 224.4-227.0 °C; <sup>1</sup>H NMR (500 MHz, DMSO-d<sub>6</sub>): δ 1.34 (m, 2H), 1.55 (m, 4H), 2.95 (m, 4H), 7.25 (dt, J = 7.6, 1.3 Hz, 1H), 7.69 (dt, J = 7.9, 1.6 Hz, 1H), 7.88 (t, J = 8.0 Hz, 1H), 7.99 (dd, 7.9, 1.4 Hz, 1H), 8.07 (dd, J = 7.9, 1.6 Hz, 1H), 8.26 (m, 2H), 8.67 (dd, J = 8.5, 0.9 Hz, 1H), 12.32 (bs, 1H), 13.88 (bs, 1H); <sup>13</sup>C NMR (125 MHz, DMSO-d<sub>6</sub>): δ 22.72, 24.65, 46.58, 117.10, 120.12, 123.41, 125.61, 130.39, 130.66, 131.27, 131.47, 134.31, 135.45, 136.45, 140.61, 163.16, 170.04; LC/MS: m/z = 429.72 [M + H + CH<sub>3</sub>CN]<sup>+</sup>, 776.56 [2M + H]<sup>+</sup>, t<sub>R</sub> = 11.72 min, 99.3% pure (UV).

**2-(3-(Azepan-1-ylsulfonyl)benzamido)benzoic acid (62)** The title compound was synthesized from methyl 2-(3-(azepan-1-ylsulfonyl)benzamido)benzoate (**62a**, 230 mg, 0.55 mmol) according to General Procedure D, using THF/MeOH 2/1 (3 mL) and 1N NaOH (aq., 1 mL). The solution was acidified with 1N HCl (aq., 2 mL). Water was added and the solid was isolated by suction filtration, washed with water and dried under reduced pressure: 209 mg, 94% yield; mp: 210.7-211.8 °C; <sup>1</sup>H NMR (500 MHz, DMSO-d<sub>6</sub>): δ 1.50 (m, 4H), 1.64 (m, 4H), 3.26 (t, J = 5.8 Hz, 4H), 7.24 (dt, J = 7.6, 1.3 Hz, 1H), 7.68 (m, 1H), 7.84 (t, J = 7.7 Hz, 1H), 8.04 (m, 1H), 8.07 (dd, J = 7.9 Hz, 1H), 1.6 Hz, 1H), 8.22 (m, 1H), 8.31 (t, J = 1.7 Hz, 1H), 8.66 (dd, J = 8.5, 0.9 Hz, 1H), 12.30 (bs, 1H), 13.87 (bs, 1H); <sup>13</sup>C NMR (125 MHz, DMSO-d<sub>6</sub>): δ 26.28, 28.52, 47.79, 117.09, 120.14, 123.38, 124.83, 129.91, 130.42, 131.07, 131.25, 134.28, 135.44, 139.85, 140.63, 163.19, 170.04; LCMS: m/z = 443.79 [M + H + CH<sub>3</sub>CN]<sup>+</sup>, 804.62 [2M + H]<sup>+</sup>, t<sub>R</sub> = 12.66 min, 97.8% pure (UV).

**2-(3-(Morpholinosulfonyl)benzamido)benzoic acid (63)**<sup>S15</sup> The title compound was synthesized from methyl 2-(3-(morpholinosulfonyl)benzamido)benzoate (**63a**, 146 mg, 0.36 mmol) according to General Procedure D, using THF/MeOH 2/1 (3 mL) and 1N NaOH (aq., 1 mL). The solution was acidified with 1N HCl (aq., 1 mL). Water was added and the solution was extracted with ethyl acetate (three times). The combined organic extracts were washed with 1N HCl (aq.), dried over sodium sulfate, filtered and evaporated under reduced pressure. The residue was stirred with a small amount of water. The solid was isolated by suction filtration, washed with water and dried under reduced pressure: 85 mg, 60% yield; mp: 245-248 °C; <sup>1</sup>H NMR (500 MHz, DMSO-d<sub>6</sub>): δ 2.94 (m, 4H), 3.65 (m, 4H), 7.25 (dt, J = 7.6, 1.3 Hz, 1H), 7.69 (dt, J = 7.9, 1.6 Hz, 1H), 7.90 (t, J = 7.7 Hz, 1H), 8.00 (dd, 7.9, 1.4 Hz, 1H), 8.07 (dd, J = 7.9, 1.6 Hz, 1H), 8.27 (m, 2H), 8.66 (dd, J = 8.5, 0.9 Hz, 1H), 12.34 (bs, 1H), 13.89 (bs, 1H); <sup>13</sup>C NMR (125 MHz, DMSO-d<sub>6</sub>): δ 45.88, 65.23, 117.24, 120.13, 123.42, 125.92, 130.51, 130.84, 131.26, 131.81, 134.25, 135.35, 135.68, 140.59, 163.15, 170.00; LC/MS: m/z = 431.70 [M + H + CH<sub>3</sub>CN]<sup>+</sup>, 780.44 [2M + H]<sup>+</sup>, t<sub>R</sub> = 10.23 min, >99.9% pure (UV).

**2-(3-(N-Benzyl-N-ethylsulfamoyl)benzamido)benzoic acid (64)** The title compound was synthesized from methyl 2-(3-(N-benzyl-N-ethylsulfamoyl)benzamido)benzoate (**64a**, 118 mg, 0.26 mmol) according to General Procedure D, using THF/MeOH 2/1 (3 mL) and 1N NaOH (aq., 1 mL). The solution was acidified with 1N HCl (aq., 1 mL). Water was added and the solution was extracted with ethyl acetate (three times). The combined organic extracts were washed with 1N HCl (aq.), dried over sodium sulfate, filtered and evaporated under reduced pressure. The residue was stirred with a small amount of water. The solid was isolated by suction filtration, washed with water and dried under reduced pressure: 70 mg, 61% yield; mp: 182.0-183.9 °C; <sup>1</sup>H NMR (500 MHz, DMSO-d<sub>6</sub>): δ 0.86 (t, J = 7.1 Hz, 3H), 3.19 (q, J = 7.1 Hz, 2H), 4.40 (s, 2H), 7.25 (dt, J = 7.6, 1.3 Hz, 1H), 7.29 (m, 1H), 7.34 (m, 4H), 7.69 (dt, J = 7.9, 1.6 Hz, 1H), 7.86 (t, J = 8.0 Hz, 1H), 8.06 (dd, J = 7.9, 1.6 Hz, 1H), 8.13 (m, 1H), 8.25 (m, 1H), 8.38 (t, J = 1.7 Hz, 1H), 8.67 (dd, J = 8.5, 0.9 Hz, 1H), 12.31 (bs, 1H), 13.87 (bs, 1H); <sup>13</sup>C NMR (125 MHz, DMSO-d<sub>6</sub>): δ 13.49, , 42.74, 50.68, 117.17, 120.19, 123.42, 124.99, 127.54, 128.00, 128.43, 130.12, 130.52, 131.26, 131.31, 134.29, 135.54, 136.89, 140.52, 140.61, 163.16, 170.03. LC/MS: m/z = 438.73 [M + H]<sup>+</sup>, 479.66 [M + H + CH<sub>3</sub>CN]<sup>+</sup>, 876.53 [2M + H]<sup>+</sup>, t<sub>R</sub> = 12.71 min, 99.7% pure (UV).

## Biological Methods

**Expression and purification of recombinant PqsD from *E. coli* for STD NMR analysis.** Following the expression procedure described above, the cell pellet was resuspended in 80 mL binding buffer (20 mM sodium phosphate, pH 7.0, 50 mM NaCl, 5 mM MgCl<sub>2</sub>, 20 mM imidazole) and lysed by sonication for a total process time of 4.0 min. Cell debris were removed by centrifugation (18500 rpm, 40 min, 4 °C) and the supernatant was filtered through a syringe filter (0.20 µm). The clarified supernatant was immediately applied to a Ni-NTA column, washed with binding buffer and eluted with 20 mM sodium phosphate, pH 7.0, 50 mM NaCl and 250 mM imidazole. The protein containing fractions were buffer-exchanged into storage buffer (20 mM sodium phosphate, pH 7.0, 50 mM NaCl, 5 mM MgCl<sub>2</sub>) using a PD10 column. Subsequently the His-tag was removed by thrombin cleavage using 1 unit thrombin per mg protein in presence of 2.5 mM CaCl<sub>2</sub> for 16 h at 16 °C. The protein was separated from any uncleaved or His-containing protein by running the mixture through another Ni-NTA column under the same conditions as the first time. The cleaved protein was buffer-exchanged into storage buffer using a PD10 column and further purified by a HiLoad 16/600 Superdex 200 column and storage buffer as eluent. The protein containing fractions were pooled, concentrated using a Vivaspin 20, 10K MWCO to a final concentration of 377 µM and stored in aliquots at -80 °C.

**Synthesis of ethyl 3-oxodecanoate<sup>S17</sup>** At 0 °C octanoyl chloride (24 mL, 141 mmol) was added slowly by means of a syringe to a stirred solution of Meldrum's acid (20.0 g, 139 mmol), 4-dimethylaminopyridine (4.0 g, 32.7 mmol) in a mixture of pyridine (150 mL) and dichloromethane (350 mL). The cooling bath was removed and the reaction was stirred for 5½ h at room temperature. Dichloromethane (50 mL) was added and the solution was extracted with 2N aqueous HCl (4 x 250 mL). The organic layer was dried over sodium sulfate and evaporated under reduced pressure. The residue was dissolved in ethanol (150 mL) and refluxed overnight. The solvent was evaporated under reduced pressure. The product was purified by column chromatography (SiO<sub>2</sub>, petroleum ether/ethyl acetate 20/1) to give the title compound as a yellow oil: 25 g, 83% yield. <sup>1</sup>H NMR (500 MHz, CDCl<sub>3</sub>): δ 0.84 (t, *J* = 7.0 Hz, 3H), 1.23-1.28 (m, 11H), 1.54 (quintet, *J* = 7.0 Hz, 2H), 2.49 (t, *J* = 7.0 Hz, 2H), 3.39 (s, 2H), 4.16 (m, 2H).

## Primer sequence of mutations

Mutant	Primer	
	forward 5' → 3'	reverse 3' → 5'
<b>S317F</b>	GCTGGTCCTGACCTACGG <u>TTTGGCGCGACCTGGGGCG</u>	CGCCCCAGGT <u>CGCGCCAAACCGTAGGTCAGGACCAGC</u>
<b>C112A</b>	GCTGGATATCCGGGCAC <u>AGGCGAGCGGGTTGCTGTACG</u>	CGTACAGCAACCCG <u>CTGCCGTGCCGGATATCCAGC</u>
<b>H257F</b>	CGACCATGTGATCTG <u>TTCAACCGAACCTGC</u>	GCAGGTT <u>CGGTTGAAAGCAGATCACATGGTCG</u>

## References

- (S1) Dolle, R. E.; Worm, K.; Zhou, Q. J. Sulfamoyl benzamide derivatives and methods of their use. U.S. Patent Application 2006/0079557 A1, Adolor Corporation, 2006.
- (S2) Kendall, J. D.; Giddens, A. C.; Yee Tsang, K.; Frédéric, R.; Marshall, E. S.; Singh, R.; Lill, C. L.; Lee, W.-J.; Kolekar, S.; Chao, M.; Malik, A.; Yu, S.; Chaussade, C.; Buchanan, C.; Newcastle, G. W.; Baguley, B. C.; Flanagan, J. U.; Jamieson, S. M. F.; Denny, W. A.; Shepherd, P. R. Novel pyrazolo[1,5-a]pyridines as p110 $\alpha$ -selective PI3 kinase inhibitors: Exploring the benzenesulfonohydrazide SAR. *Bioorg. Med. Chem.* **2012**, *20*, 58–68.
- (S3) Ichinose, M.; Suematsu, H.; Yasutomi, Y.; Nishioka, Y.; Uchida, T.; Katsuki, T. Enantioselective intramolecular benzylic C-H bond amination: Efficient synthesis of optically active benzosultams. *Angew. Chem. Int. Ed.* **2011**, *50*, 9884–9887.

- (S4) Nie, Z.; Perretta, C.; Lu, J.; Su, Y.; Margosiak, S.; Gajiwala, K. S.; Cortez, J.; Nikulin, V.; Yager, K. M.; Appelt, K.; Chu, S. Structure-based design, synthesis, and study of potent inhibitors of  $\beta$ -ketoacyl-acyl carrier protein synthase III as potential antimicrobial agents. *J. Med. Chem.* **2005**, *48*, 1596–1609.
- (S5) Gaillard, P.; Quattropani, A.; Pomel, V; Rueckle, T.; Klicic, J.; Church, D. Pyrazine derivatives and use as PI3K inhibitors. WO Patent Application 2007/023186 A1, Applied Research Systems ARS Holding N.V., 2007.
- (S6) Bernotas, R. C.; Singhaus, R.; Nagpal, S.; Thompson, C. Novel quinoline esters useful for treating skin disorders. WO Patent Application 2012/004748 A1, Wyeth LLC, 2012.
- (S7) Ji, J.; Lee, C.-H.; Sippy, K. B.; Li, T.; Gopalakrishnan, M. Novel 1,2,4 oxadiazole compounds and methods of use thereof. WO Patent Application 2009/148452, Abbott Laboratories, 2009.
- (S8) Armer, R. E.; Maillol, C. E. A.; Dorgan, C. R.; Wynne, G. M.; Vile, J. Compounds having CRTH2 antagonist activity. WO Patent Application 2009/093029, Oxagen Limited, 2009.
- (S9) Lang, H.-J.; Muschaweck, R. Thiazolidinderivate und Verfahren zu ihrer Herstellung. Ger. Offen. DE 2436263, February 12, 1976.
- (S10) Stiff, C. M.; Zhong, M.; Sarver, R. W.; Gao, H.; Andrea M. Ho, A. M.; Sweeney, M. T.; Zurenkod, G. E.; Romeroa, D. L. Correlation of carboxylic acid pK<sub>a</sub> to protein binding and antibacterial activity of a novel class of bacterial translation inhibitors. *Bioorg. Med. Chem. Lett.* **2007**, *17*, 5479–5482.
- (S11) Thorarensen, A.; Ruble, C. J.; Romero, D.L. Antibacterial agents. WO Patent Application 2004/018414 A2, Pharmacia & Upjohn Company, 2004.
- (S12) Castro Palomino Laria, J. L.; Terricabras Belart, E.; Erra Sola, M.; Navarro Romero, E.; Fonquerma Pou, S.; Cardus Figueras, A.; Lozoya Toribio, M. E. Azabiphenylaminobenzoic acid derivatives as DHODH inhibitors. WO Patent Application 2009/021696 A1, Laboratorios Almirall, S.A., 2009.
- (S13) Wall, M. J.; Player, M. R.; Patch, R. J.; Meegalla, S.; Liu, J.; Illig, C.R.; Chueng, W.; Chen, J.; Asgari, D. Quinolinone derivatives as inhibitors of C-FMS kinase. WO Patent Application 2005/009967 A2, Janssen Pharmaceutica, N.V., 2005.
- (S14) Andersen, H. S.; Olsen, O. H.; Iversen, L. F.; Sørensen, A. L. P.; Mortensen, S. B.; Christensen, M.S.; Branner, S.; Hansen, T.K.; Lau, J.F.; Jeppesen, L.; Moran, E.J.; Su, J.; Bakir, F.; Judge, L.; Shahbaz, M.; Collins, T.; Vo, T.; Newman, M. J.; Ripka, W. C.; Møller, N. P. H. Discovery and SAR of a Novel Selective and Orally Bioavailable Nonpeptide Classical Competitive Inhibitor Class of Protein-Tyrosine Phosphatase 1B. *J. Med. Chem.* **2002**, *45*, 4443–4459.
- (S15) Ulven, T.; Frimurer, T.; Rist, Ø.; Kostenis, E.; Höglberg, T. CRTH2 receptor ligands for therapeutic use. WO Patent Application 2005/115374 A1, 7TM Pharma A/S, 2005.
- (S16) Simon, E. J.; Shemin, D. The preparation of S-succinyl coenzyme. *A. J. Am. Chem. Soc.* **1953**, *75*, 2520.
- (S17) Kocieński, P. J.; Pelotier, B.; Pons, J.-M.; Prideaux, H. Asymmetric syntheses of panclicins A–E via [2+2] cycloaddition of alkyl(trimethylsilyl)ketenes to a  $\beta$ -silyloxyaldehyde. *J. Chem. Soc., Perkin Trans. 1* **1998**, 1373–1382.
- (S18) Cook, L.; Ternai, B.; Ghosh, P. Inhibition of human sputum elastase by substituted 2-pyrone. *J. Med. Chem.* **1987**, *30*, 1017–1023.

## 6.2 Supporting Information der Publikation B

Die vollständige Supporting Information ist online verfügbar unter:

[http://pubs.acs.org/doi/suppl/10.1021/cb400530d/suppl\\_file/cb400530d\\_si\\_001.pdf](http://pubs.acs.org/doi/suppl/10.1021/cb400530d/suppl_file/cb400530d_si_001.pdf)

### 6.2.1 Primer Sequence of Mutations

Mutant	Primer	
	forward 5' → 3'	reverse 3' → 5'
S317F	GCTGGTCCTGACCTACGGTTTGGCGCGAC CTGGGGCG	CGCCCCAGGT CGGCCAAACCGTAGGTCA GGACCAGC
C112A	GCTGGATATCCGGGCACAG <u>GGCGAGCGGGT</u> TGCTGTACG	CGTACAGCAACCCGCT <u>CGCCTGTGCCCGGAT</u> ATCCAGC
H257F	CGACCATGTGATCTGCT <u>TTCAACCGAACCT</u> GC	GCAGGGTTCGGTTGA <u>AAGCAGATCACATGGT</u> CG
C112S	GCTGGATATCCGGGCACAG <u>AGCAGCGGGT</u> TGCTGTACG'	CGTACAGCAACCCGCT <u>GCTCTGTGCCCGGAT</u> ATCCAGC
S317A	GCTGGTCCTGACCTACGGT <u>GC</u> GGCGCGA CCTGGGGCG	CGCCCCAGGT CGGCC <u>CGCACCGTAGGTCA</u> GGACCAGC
N287A	CGTCTGG <u>GC</u> CGATGGCTTCGGCC	GGCCGAAGCCAT <u>CGC</u> CCCAGACG

6.2.2 Table S1: Catalytic Activity of PqsD Wild-type and Mutants<sup>a</sup>

	wild-type	S317F	C112A	H257F	C112S	S317A	N287A
Formed HHQ [nM]	2154	15	1	18	171	2182	7

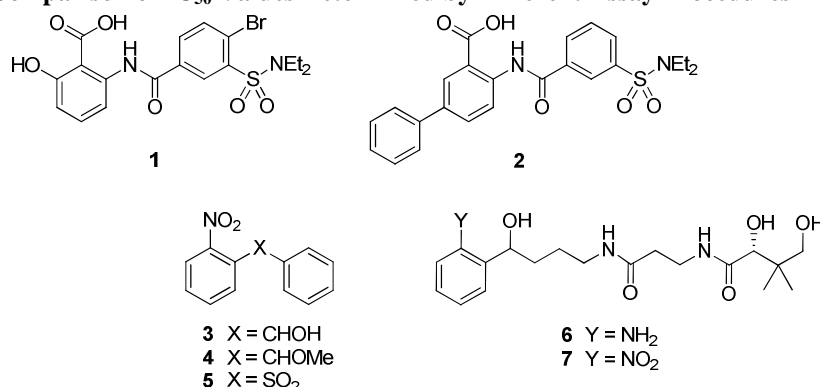
<sup>a</sup>Reactions were performed according to the screening assay procedure described in the Methods Section using 1.0 μM of *P. aeruginosa* PqsD.

### 6.2.3 Synthesis of Substrates Used in the Enzymatic Inhibition Assays

**Synthesis of anthraniloyl-S-CoA thioester.**<sup>S1</sup> Anthraniloyl-CoA (ACoA) was synthesized from isatoic anhydride and coenzyme A (CoA) using a previously described method. ACoA was purified by HPLC (Agilent 1200 series consisting of a quaternary pump, a fraction collector and an MWD; Agilent Technologies) after freeze drying of the aqueous reaction mixture (25 ml) and resuspending of the dried residue in 3 ml of a mixture of 50% methanol and water (v/v). A 10 μm RP C18 150-30 column (30 x 100 mm, Agilent) was used along with a mobile phase consisting of water containing 1% TFA (A) and acetonitrile containing 1% TFA (B) with a flow rate of 5 ml min<sup>-1</sup>. The following gradient was used: 0–35 min, linear gradient 10% – 100% B (v/v); 35–42 min, 100% B; 42–43 min, 10% B (v/v) (initial conditions). ACoA containing fractions were pooled and freeze dried.

**Synthesis of β-ketodecanoic acid.**<sup>S2</sup> Ethyl 3-oxodecanoate (300 mg, 1.4 mmol) was stirred with NaOH (56 mg, 1.4 mmol) in 2 ml of water overnight. Any remaining ester was removed by washing with Et<sub>2</sub>O (10 ml). The aqueous layer was cooled and acidified with 32% HCl (w/v) to pH = 6. After filtration the 3-oxodecanoic acid was dried *in vacuo* and obtained as white solid (100 mg, 38%). <sup>1</sup>H-NMR (500 MHz, CDCl<sub>3</sub>) δ 0.86 (t, *J* = 7.0, 3H), 1.25–1.29 (m, 8H), 1.58 (m, 2H), 2.54 (t, *J* = 7.5, 2H), 3.49 (s, 2H). LC/MS (ESI) *m/z* 242.0, 99% (UV).

**Synthesis of ethyl 3-oxodecanoate.**<sup>S3</sup> To a THF solution of 2 M LDA (20 ml, 40 mmol) was added ethyl acetoacetate (2.16 g, 16.6 mmol) at 0°C. The deep yellow clear solution was stirred at 0°C for 1 h. To this solution the 1-iodohexane was added (4.20 g, 19.81 mmol) at -78°C. The temperature was allowed to reach an ambient temperature over 14 h and the solution was stirred at room temperature for 2 h. To the solution was added 200 ml of 10% HCl (v/v) and the mixture was extracted with Et<sub>2</sub>O (4 × 250 ml). The combined organic layers were dried over Na<sub>2</sub>SO<sub>4</sub>, filtered, and the filtrate was concentrated *in vacuo*. The residue was purified by column chromatography (*n*-hexane/ethyl acetate, 30/1) to give ethyl 3-oxodecanoate as a yellow oil (1.98 g, 55%). <sup>1</sup>H-NMR (500 MHz, CDCl<sub>3</sub>) δ 0.84 (t, *J* = 7.0, 3H), 1.23–1.28 (m, 11H), 1.54 (m, 2H), 2.49 (t, *J* = 7.0, 2H), 3.39 (s, 2H), 4.16 (m, 2H). LC/MS (ESI) *m/z* 458.0, 87% (UV).

**6.2.4 Table S2: Comparison of IC<sub>50</sub> Values Determined by Different Assay Procedures**

Cmpd.	IC <sub>50</sub> [μM] <sup>ab</sup>	IC <sub>50,mod</sub> [μM] <sup>ac</sup>	IC <sub>50,ext</sub> [μM] <sup>ad</sup>
1	1.2 ± 0.1	1.1 ± 0.2	1.8 ± 0.4
2	3.0 ± 0.7	4.2 ± 0.3	7.6 ± 1.5
3	3.2 ± 0.1	24.6 ± 6.2	1.0 ± 0.4
4	4.3 ± 1.0	19.7 ± 8.9	2.6 ± 0.5
5	14.8 ± 2.9	>50	9.7 ± 1.4
6	n.i.	n.d.	n.d.
7	7.9 ± 0.7	n.d.	n.d.

a n.i. no inhibition (<10% at 50 μM); n.d. not determined. b PqsD and inhibitor were preincubated for 10 min prior to addition of the substrates. c Modified procedure including additional 30 min preincubation of enzyme and ACoA. d Preincubation time of PqsD/inhibitors was extended to 30 min.

### 6.2.5 Percentages of Inhibition and Uncertainty of the Time Dependency Experiment

**Table S3. HHQ formation in presence of compounds **2** and **3** relative to untreated control.**

time	control [%]	Cmpd. <b>2</b> , 3 μM [%]	uncertainty [%]
3 min	100	60.37	2.95
6 min	100	59.36	8.27
9 min	100	60.21	8.09
12 min	100	58.95	8.34
15 min	100	61.99	8.16
20 min	100	72.15	5.19
25 min	100	63.28	7.17
30 min	100	64.18	10.05

time	control [%]	Cmpd. <b>3</b> , 6 μM [%]	uncertainty [%]
3 min	100	71.17	4.33
6 min	100	46.38	2.91
9 min	100	41.85	4.49
12 min	100	36.40	4.36
15 min	100	31.98	4.58
20 min	100	25.39	2.41
25 min	100	27.01	3.60
30 min	100	26.07	4.82

### 6.2.6 Figure S1: Dose-response Curve of PqsD Inhibition by Compound 3

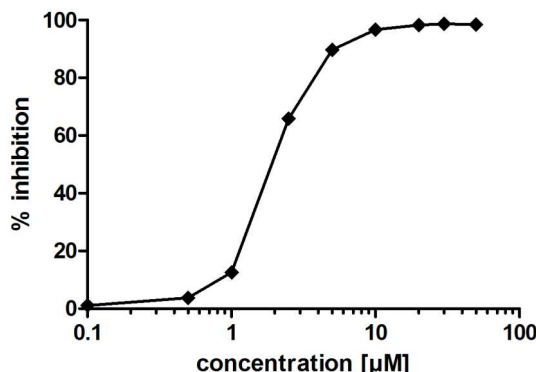


**Figure S1.** Inhibition of PqsD by compound **3** is plotted against the concentration (log scale). Data were generated using the screening assay procedure for *in vitro* PqsD inhibition as described above. Compounds **4** and **5** show similar curve shapes (data not shown).

### 6.2.7 Further HPLC-ESI MS Experiments

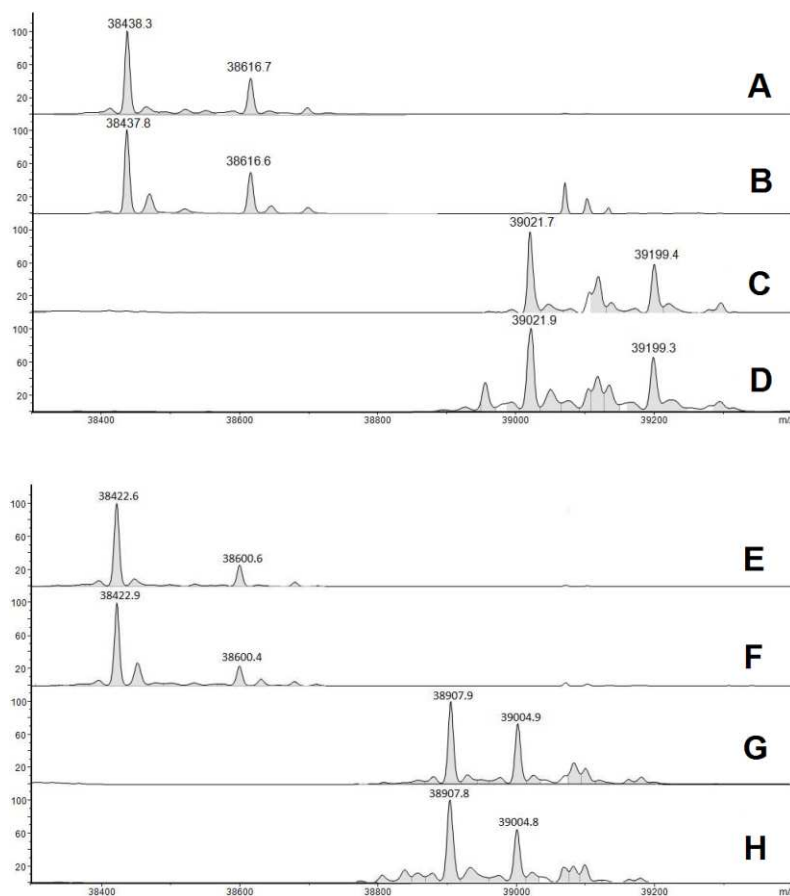


**Figure S2.** (A-D) PqsD containing a His<sub>6</sub>-tag was incubated in absence (A) or in presence (B) of compound **3**. Thereby, no anti-oxidative reagent was present. Samples were subjected to HPLC-ESI MS analysis, whereas no relevant amounts of oxidation products were observed. Subsequent addition of an excess of maleimid resulted in a shift of +582 (corresponding to a 6-fold addition of the labeling agent regardless of the presence of compound **3** (C: PqsD; D: PqsD pretreated with compound **3**). Maleimid labels all available cysteine residues present in PqsD, indicating that no cysteine was oxidized previously. (E-H) C112S mutant containing a His<sub>6</sub>-tag was treated in absence (E) or in presence (F) of compound **3** using the same procedure as described above. Subsequent addition of an excess of maleimid resulted in a shift of +485 (corresponding to a 5-fold addition of the labeling agent regardless of the presence of compound **3** (G: PqsD; H: PqsD pretreated with compound **3**). In all spectra, signals with a shift of +178 Da were observed. This is probably due to spontaneous  $\alpha$ -N-6-Phosphogluconoylation of the His<sub>6</sub>-tag in *E. coli* (S4).

### 6.2.8 Maldi-TOF Analysis

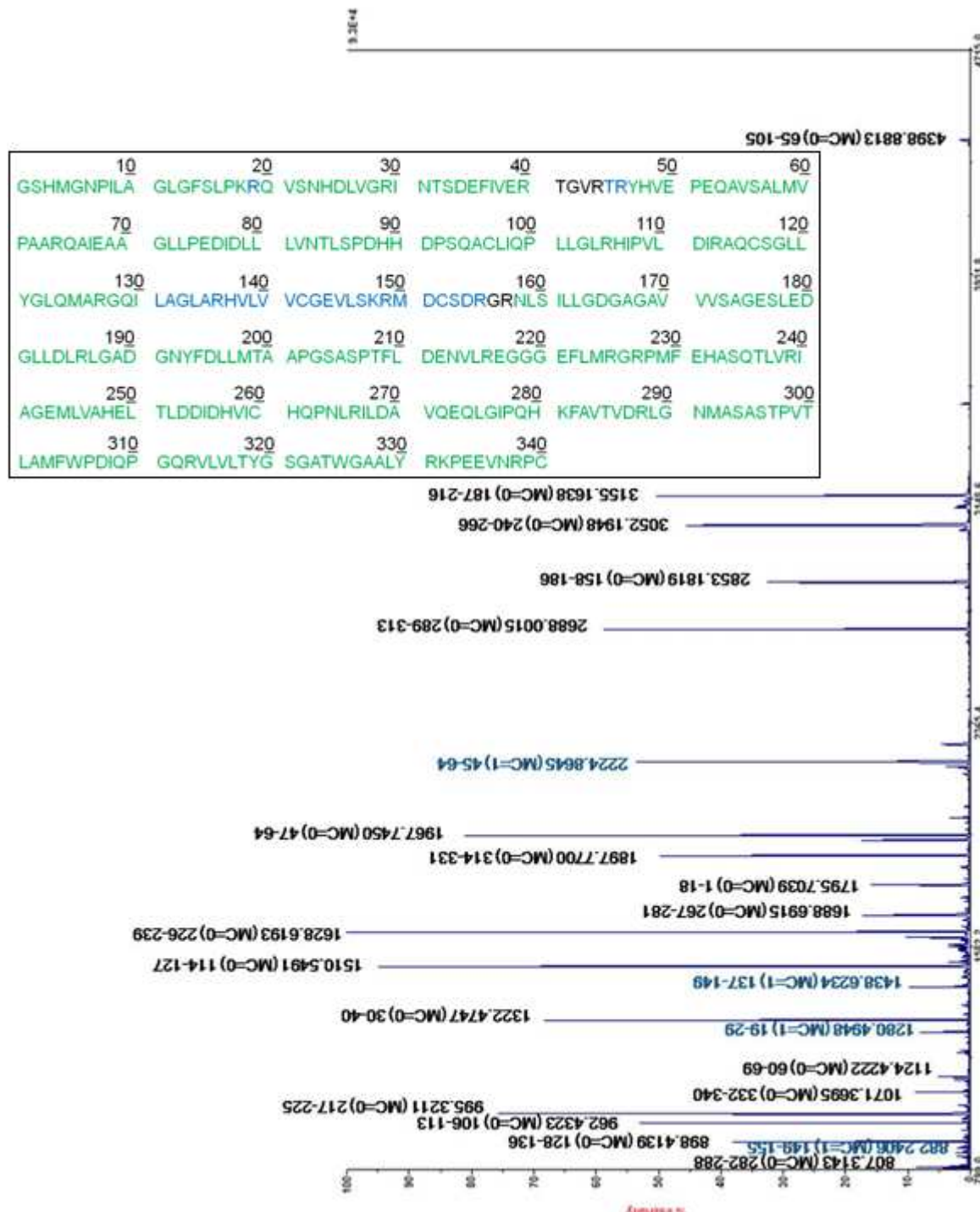


**Figure S3.** Maldi-TOF spectra of native PqsD after tryptic digestion. Blue labeled fragments bear one missed cleavage (MC). Fragments generated by complete digestion (MC=0) were labeled in black.

**Figure S4.** Sequence of the PqsD. 334 of 340 amino acids are visible in at least one peptide observed by Maldi-TOF, when native PqsD has been digested. Amino acids not observed in the experiment are Thr41, Gly42, Val43, Arg44, Gly156 and Arg157. (Numbering refers to the sequence of PqsD used in the experiment; in the X-ray structure denoted as Thr37, Gly38, Val39, Arg40, Gly152, Arg153 (A. K. Bera et al. *Biochemistry* 2009, 48, 8644).

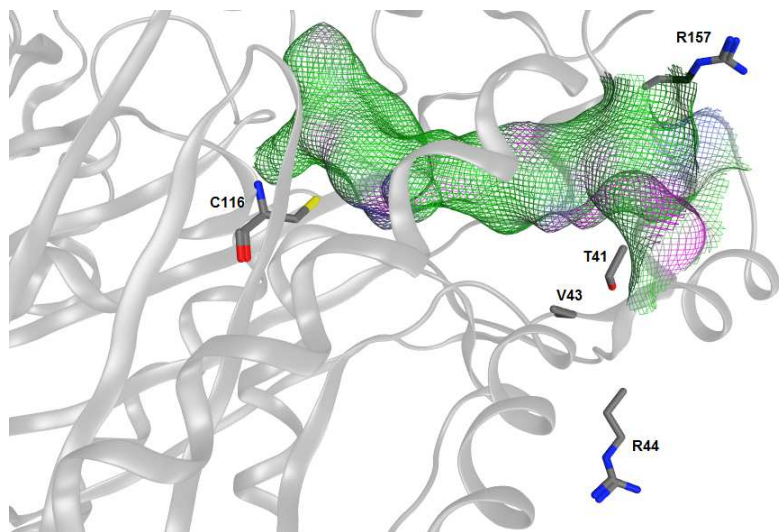


**Figure S5.** Molecular surface of the PqsD binding channel and side chains of the uncaptured amino acids Thr41, Gly42, Val43, Arg44, Gly156 and Arg157. The alkyl residues of Gly42, Val43 and Gly156 are unable to form covalent bonds. Thr41, Arg44 and Arg157 are located at the tunnel entrance, too far away from the binding site of compound 3, which is located deep in the active site near the catalytically active Cys116 (in the construct used for X-ray analysis denoted as Cys112).

**Table S4.** Comparison of peptide masses (calculated and observed by Maldi-TOF analysis) formed by tryptic digestion of untreated PqsD and PqsD treated with compound 3.

<i>m/z</i> (PqsD) calculated	<i>m/z</i> (PqsD) measured	<i>m/z</i> (PqsD+ cmpd. 3) measured	Position (Number of missed cleaves)	peptide sequence
4399.3329	4398.8813	4398.8477	65–105 (MC=0)	QAIEAAGLLPEDIDLLLVNTLSPDH HDPSQACLIQPLLGLR
3155.5353	3155.1638	3155.1670	187–216 (MC=0)	LGADGNYFDLLMTAAPGSASPTF LDENVLR
3052.5342	3052.1948	3052.1858	240–216 (MC=0)	IAGEMLVAHELTLDIDHVICHQP NLR
2853.5203	2853.1819	2853.1846	158–186 (MC=0)	NLSILLGDGAGAVVVSAGESLED GLLDR
2688.3272	2688.0015	2687.9995	289–313 (MC=0)	LGNMASASTPVTLAMFWPDIQPG QR
2225.1495	2224.8645	2224.8713	45–64 (MC=1)	TRYHVEPEQAVSALMVPAAR
1968.0007	1967.7450	1967.7517	47–64 (MC=0)	YHVEPEQAVSALMVPAAR
1898.0170	1897.7700	1897.7756	314–331 (MC=0)	VVLTYGSGATWGAALYR
1795.9523	1795.7039	1795.7120	1–18 (MC=0)	GSHMGNPILAGLGFSLPK
1688.9329	1688.6915	1688.6960	267–281 (MC=0)	ILDADVQEQLGIPQHK
1628.8325	1628.6193	1628.6277	226–239 (MC=0)	GRPMFEHASQTLVR
1510.7505	1510.5491	1510.5503	114–127 (MC=0)	AQCSGLLYGLQMAR

1438.8198	1438.6234	1438.6323	137–149 (MC=1)	HVLVVCGEVLSK
1322.6586	1322.4747	1322.4774	30–40 (MC=0)	INTSDEFIVER
1282.7187	-	-	137–148 (MC=0)	HVLVVCGEVLSK
1280.6818	1280.4948	1280.5020	19–29 (MC=1)	RQVSNHDLVGR
1124.5807	1124.4222	1124.4231	60–69 (MC=0)	QVSNHDLVGR
1071.5251	1071.3695	-	332–340 (MC=0)	KPEEVNRPC
995.4615	995.3211	995.3254	217–225 (MC=0)	EGGGEFLMR
962.5781	962.4323	962.4278	106–113 (MC=0)	HIPVLDIR
898.5468	898.4139	898.4203	128–136 (MC=0)	GQILAGLAR
882.3556	882.2406	882.2174	149–155 (MC=1)	RMDCSDR
807.4359	807.3143	807.3203	282–288 (MC=0)	FAVTVDR

All fragments without missed cleavages (MC=0) with  $m/z > 800$  are listed. Fragments with MC=1 contributing to coverage of the amino acid sequence were added.

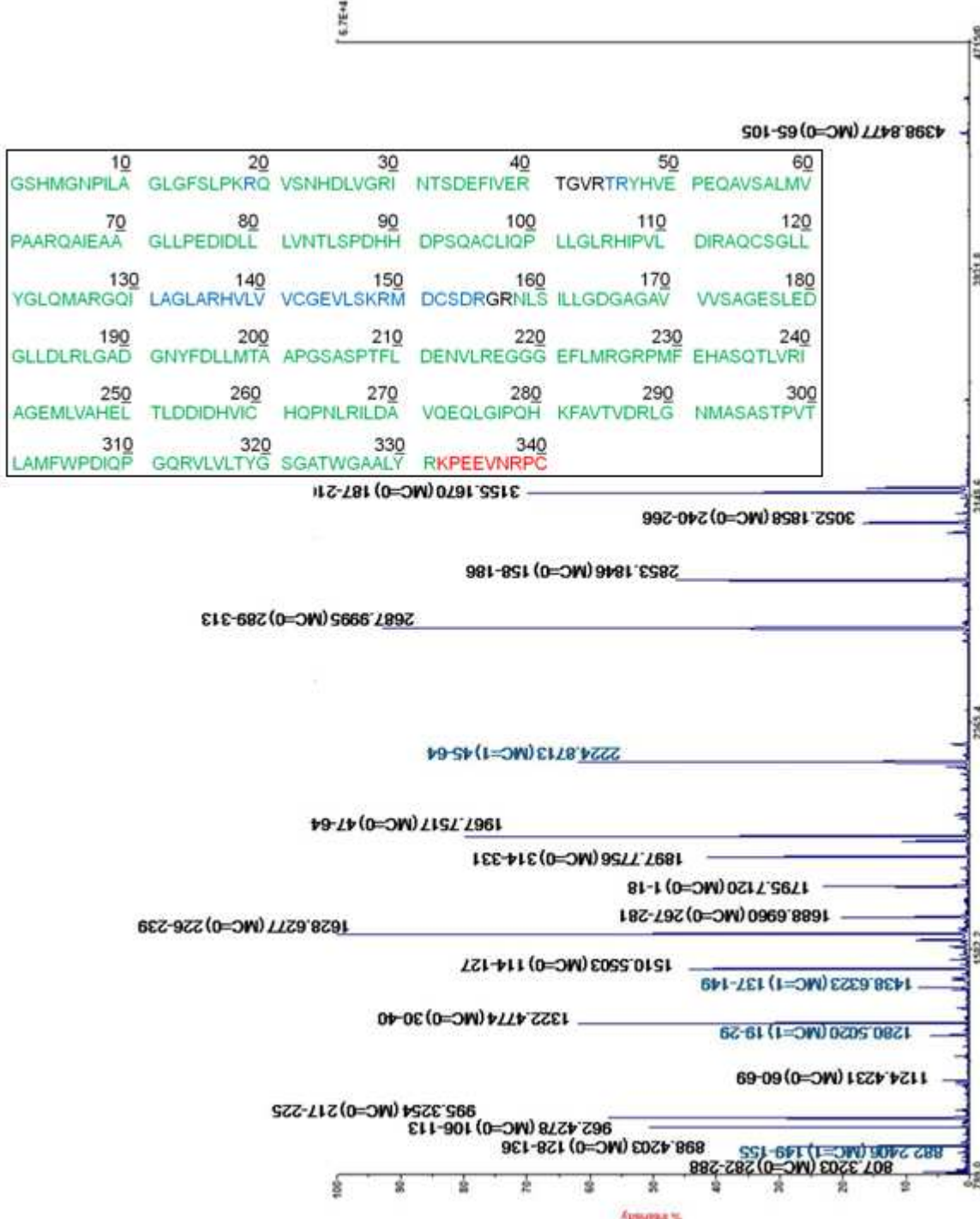


**Figure S6.** Mass spectra of PqsD/compound **3** after tryptic digestion. Blue labeled fragments bear one missed cleavage (MC). Fragments generated by complete digestion (MC=0) were labeled in black. Compared to untreated PqsD the only difference is the disappearance of the peptide  $m/z$  of 1071.

**Figure S7.** Amino acids observed after preincubation of PqsD with compound **3**. Compared to untreated PqsD the red labeled peptide at the C-terminus disappeared, maybe because of an oxidation of the terminal Cys340.

### 6.2.9 Separation of **3** into the Enantiomers (*R*)-**3** and (*S*)-**3** by Chiral-HPLC

The separation was performed using an Agilent 1200 HPLC system equipped with an MWD triggering an automated fraction collector (Agilent Technologies) in “time based” mode. ChemStation® software was used for control and report. The sample was manually injected. A Chiraldak IE® 5 $\mu$ m (250 / 10 mm) column (DAICEL Corporation) was used as stationary phase. The solvent system consisted of *n*-hexane (A) and *iso*-propanol (B). HPLC-Method: Flow rate 2.4 ml min<sup>-1</sup>. Isocratic run of 7% of B in A (v/v).

Determination of enantiomeric excess was performed using a Chiraldak IE® 5 $\mu$ m (250 / 4.6 mm) column (DAICEL Corporation) as stationary phase. The solvent system consisted of *n*-heptane (A) and *iso*-propanol (B). HPLC-Method: Flow rate 1 ml min<sup>-1</sup>. Isocratic run of 7% of B in A (v/v). The % ee of (*R*)-**9** and (*S*)-**9** was determined using the relative peak areas in the MWD trace.

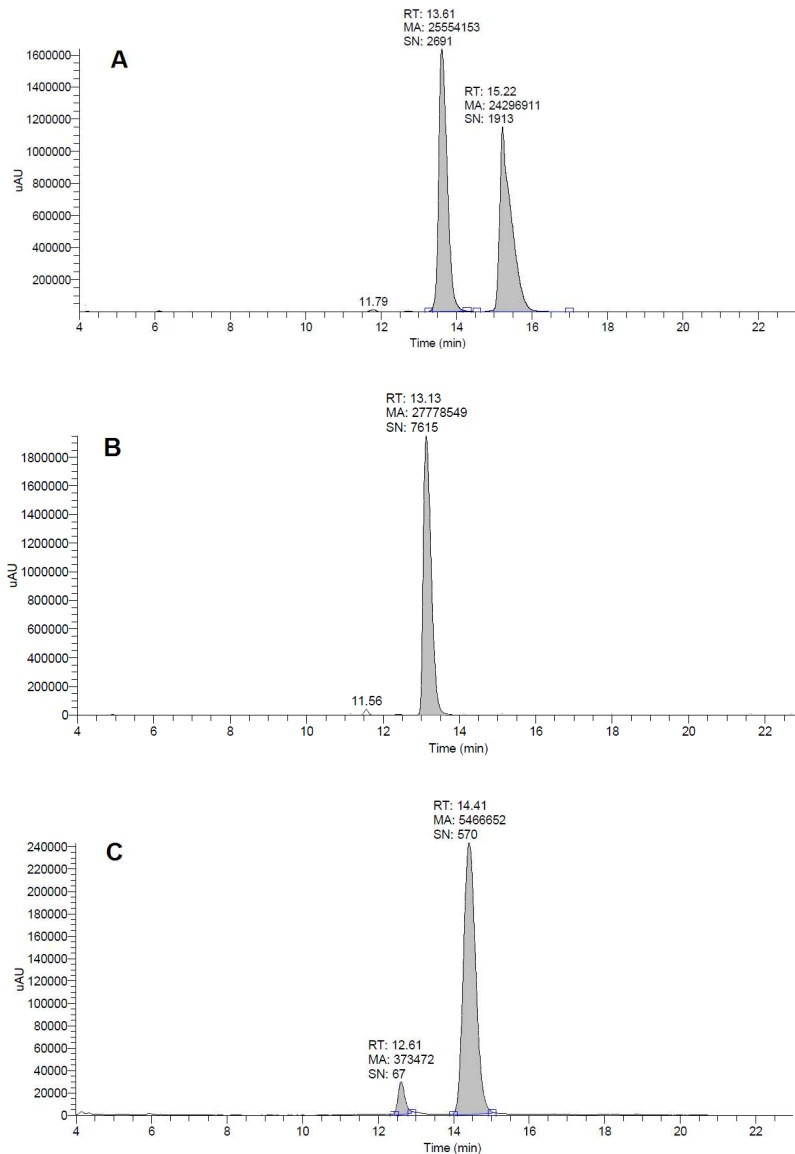


**Figure S8.** HPLC analysis of enantiomeric purity. (A) Racemic mixture **9**, (B) *S*-enantiomer (-) of **9** (>99.9% ee) and (C) *R*-enantiomer (+) of **9** (87.2% ee). Absolute configurations were derived from measurement of the optical rotation and comparison to literature.<sup>S6</sup>

### 6.2.10 Figure S9: Binding site analysis of (R)-3 and (S)-3 by SPR

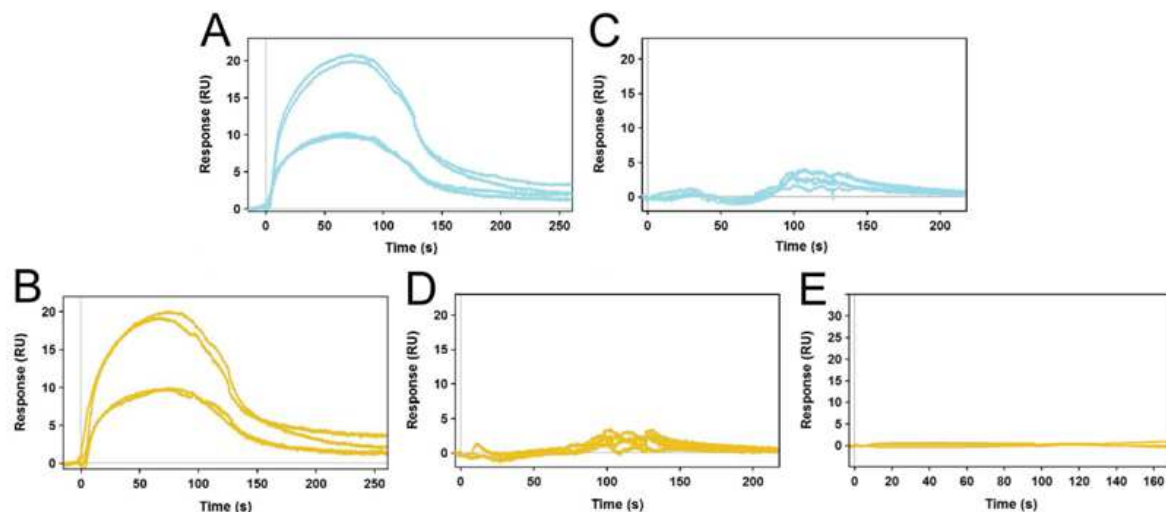


**Figure S9.** Binding site analysis of (R)-3 and (S)-3 by SPR. Addition of 250 and 125  $\mu$ M (R)-3 (blue) or (S)-3 (orange), respectively, to native PqsD resulted in response curves (A) and (B). When added to PqsD pretreated with ACoA, no response was observed in (C) and (D). When (R)-3 was added until saturation, subsequent addition of (S)-3 did not affect the observed response (E). The results indicate that the binding sites of both enantiomers are blocked by anthranilate.

### 6.2.11 Figure S10: Reversibility of PqsD Inhibition by the Enantiomers (R)-3 and (S)-3

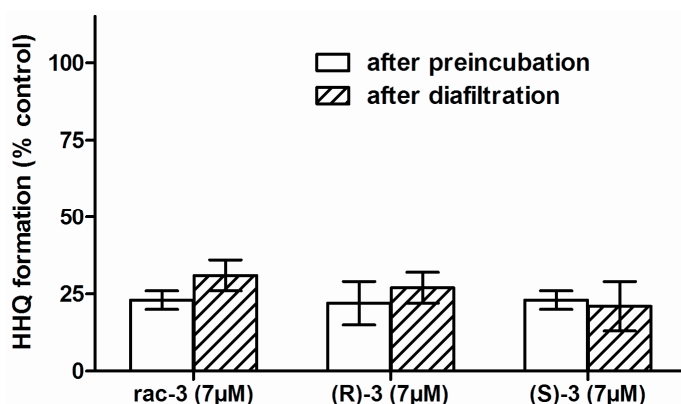


**Figure S10.** PqsD was preincubated with enantiomers (R)-3 and (S)-3 and the remaining HHQ formation was quantified with and without removal of unbound inhibitor by diafiltration. Centrifugal filter devices with a molecular weight limit of 10k were used to remove at least 95% inhibitor by three diafiltration steps as controlled by HPLC analysis, while PqsD was retained.

### 6.2.12 Representative ITC Curves

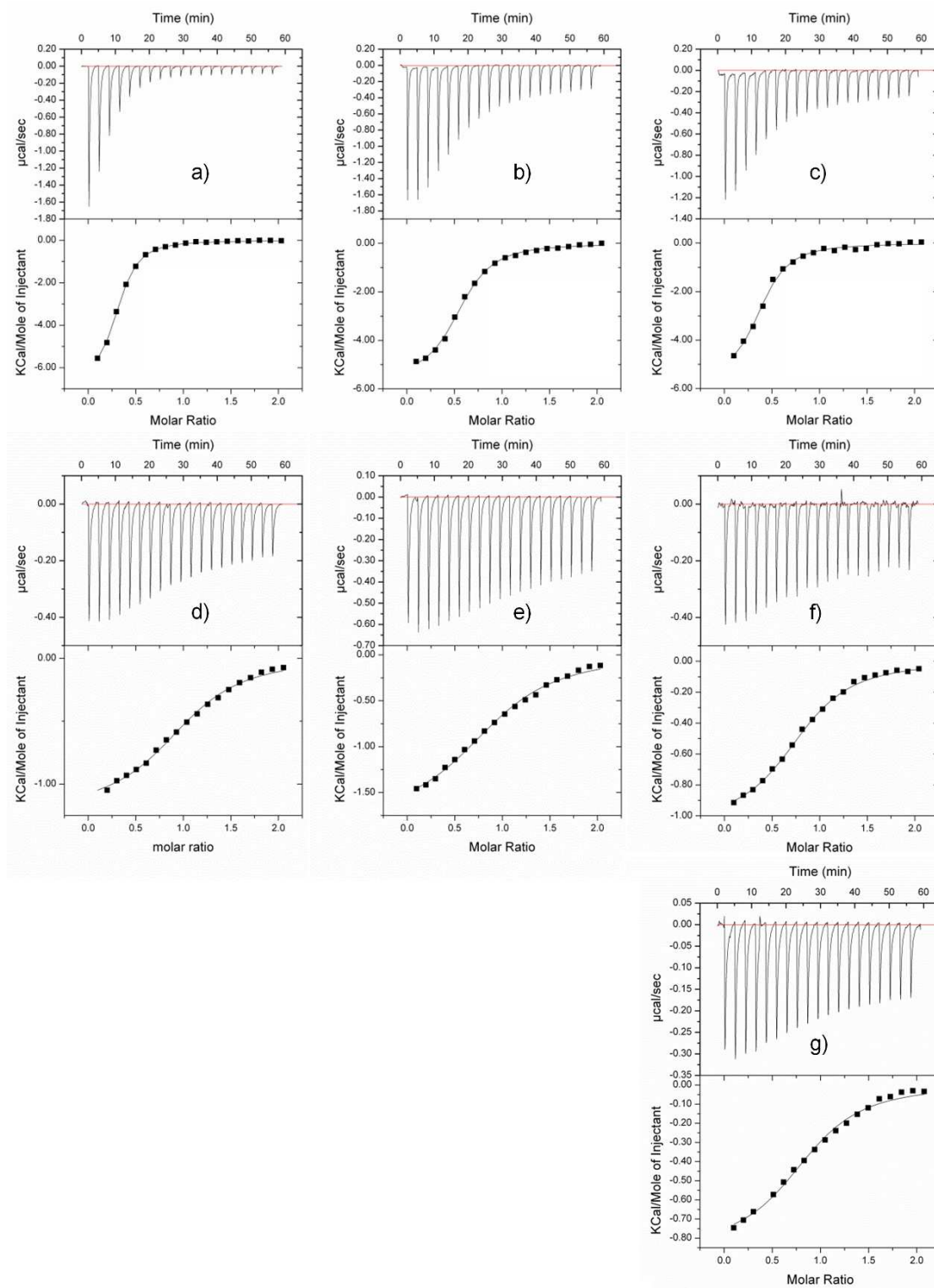


**Figure S11.** Representative ITC titrations of *R*-enantiomer against PqsD wild-type and mutants. 3500  $\mu\text{M}$  of compound against: a) PqsD wild-type (347  $\mu\text{M}$ ), b) S317A (351  $\mu\text{M}$ ), c) N287A (347  $\mu\text{M}$ ), d) C112A (350  $\mu\text{M}$ ), e) C112S (354  $\mu\text{M}$ ), f) H257F (352  $\mu\text{M}$ ), g) S317F (345  $\mu\text{M}$ ). The recorded change in heat is shown in units of  $\mu\text{cal sec}^{-1}$  as a function of time for successive injections of the ligand (upper panel). Integrated heats (black squares) plotted against the molar ratio of the binding reaction. The continuous line represents the results of the non-linear least squares fitting of the data to a binding model (lower panel).

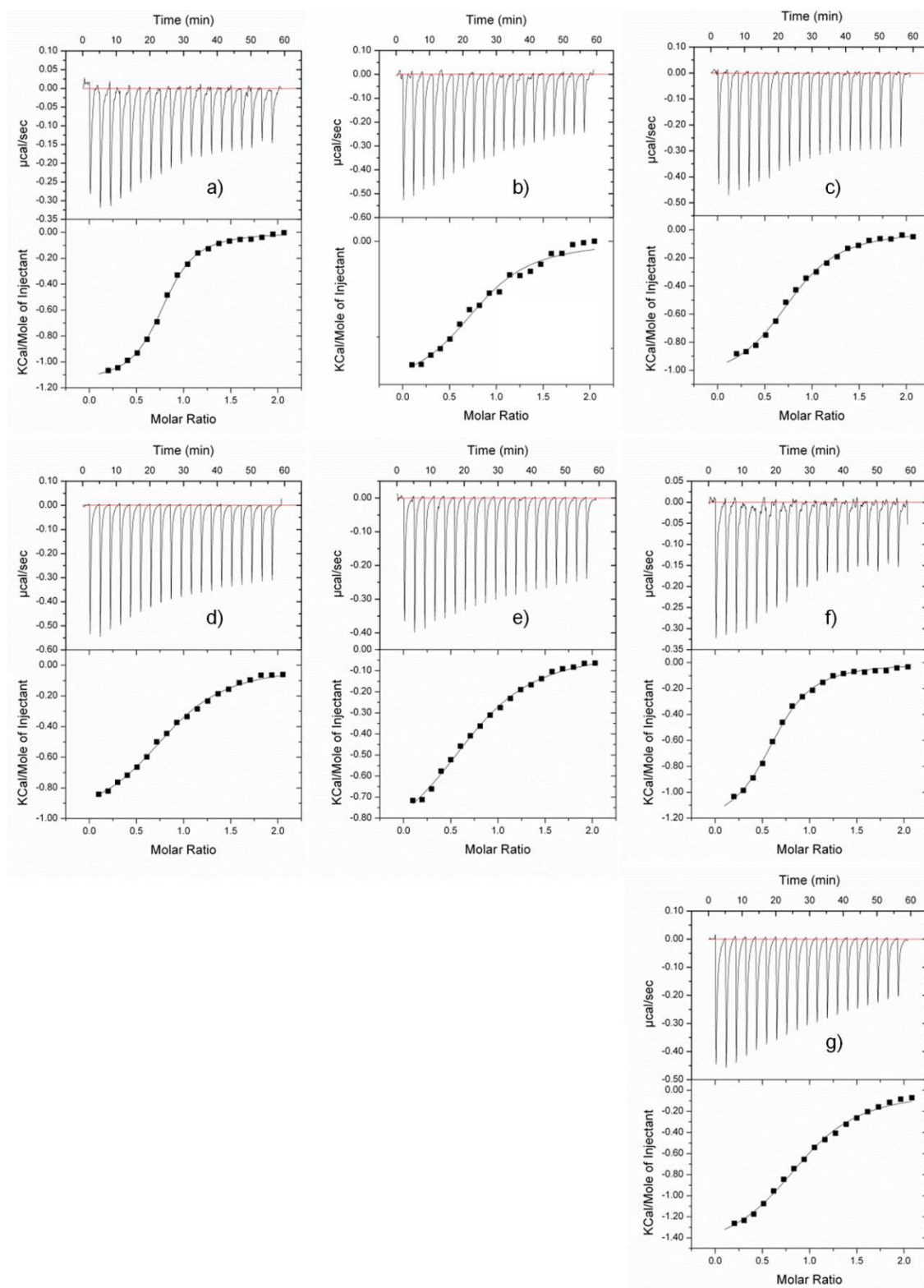


**Figure S12.** Representative ITC titrations of *S*-enantiomer against PqsD wild-type and mutants. 3500  $\mu\text{M}$  of compound against: a) PqsD wild-type (347 $\mu\text{M}$ ), b) S317A (351 $\mu\text{M}$ ), c) N287A (347 $\mu\text{M}$ ), d) C112A (350 $\mu\text{M}$ ), e) C112S (354 $\mu\text{M}$ ), f) H257F (352 $\mu\text{M}$ ), g) S317F (345 $\mu\text{M}$ ). The recorded change in heat is shown in units of  $\mu\text{cal sec}^{-1}$  as a function of time for successive injections of the ligand (upper panel). Integrated heats (black squares) plotted against the molar ratio of the binding reaction. The continuous line represents the results of the non-linear least squares fitting of the data to a binding model (lower panel).

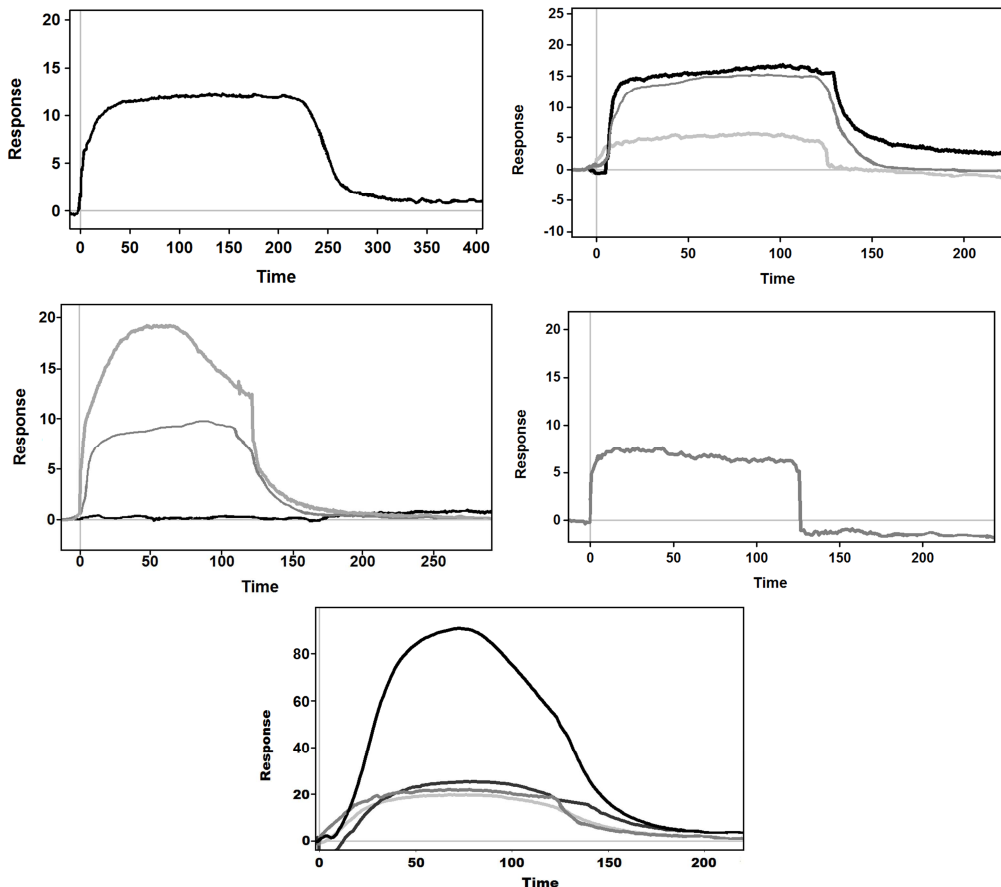
#### 6.2.13 References

- (S1) E. J. Simon, D. Shemin; The preparation of *S*-succinyl coenzyme A. *J. Am. Chem. Soc.* **1953**, *75*, 2520.
- (S2) L. Cook, B. Ternai, P. Ghosh; Inhibition of human sputum elastase by substituted 2-pyrone. *J. Med. Chem.* **1987**, *30*, 1017.
- (S3) V. T. H. Nguyen, E. Bellur, B. Appel, P. Langer; Synthesis of 4-alkyl- and 4-( $\omega$ -chloroalkyl)-3-hydroxy-5-alkylidenebutenolides based on cyclizations of 4-alkyl- and 4-( $\omega$ -chloroalkyl)-1,3-bis(trimethylsilyloxy)buta-1,3-dienes with oxalyl chloride. *Synthesis* **2006**, *17*, 2865.
- (S4) K. F. Geoghegan, H. B. F. Dixon, P. J. Rosner, L. R. Hoth, A. J. Lanzetti, K. A. Borzilleri, E. S. Marr, L. H. Pezzullo, L. B. Martin, P. K. LeMotte, A. S. McColl, A. V. Kamath, J. G. Stroh; Spontaneous  $\alpha$ -N-6-phosphogluconoylation of a “His tag in *Escherichia coli*: The cause of extra mass of 258 or 178 Da in fusion proteins. *Analytical Biochemistry* **1999**, *267*, 169.
- (S5) A. K. Bera, V. Atanasova, H. Robinson, E. Eisenstein, J. P. Coleman, E. C. Pesci; Structure of PqsD, a *Pseudomonas* quinolone signal biosynthetic enzyme, in complex with anthranilate. *Biochemistry* **2009**, *48*, 8644.
- (S6) H.-F. Duan, J.-H. Xie, W.-H. Shi, Q. Zhang, Q.-L. Zhou; Enantioselective rhodium-catalyzed addition of arylboronic acids to aldehydes using chiral spiro monophosphite ligands. *Organic Letters* **2006**, *8*, 1479.

### 6.3 Supporting Information der Publikation C

Die vollständige Supporting Information ist online verfügbar unter:  
<http://www.future-science.com/doi/suppl/10.4155/fmc.14.142>

#### S1: SPR Sensorgrams Compounds ‘Me-too’ Approach



**S1.** First row: left:Sensorgrams of **A1** and right: **A2-A4** (light greyA2, greyA3, and black lineA4). Second row: left:Sensorgrams of **A5-A7** (A5grey, A6light grey, and A7black line) and right:**A8**-(grey line). Last row: Sensorgrams of **A9 -A12** (light grey**A9**, dark grey**A10**, black**A11**, and grey line**A12**).

#### S2: Conversion to percentage of the response of the positive control and calculation of R<sub>max</sub>

Conversion of the analytes response into percentage of the response of the positive control

$$\%A = 100 \times \frac{R_{\text{Analyte}}}{R_{\text{positive control}}}$$

%A:	Percentage of the response of the analyte compared to the positive control’s response
R <sub>Analyte</sub> :	Response of the analyte
R <sub>positive control</sub> :	Response of the positive control

Calculation of R<sub>max</sub>:

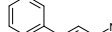
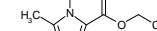
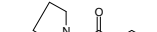
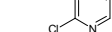
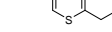
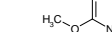
$$R_{\text{Max}} = R_{\text{Ligand}} \times \frac{M_{\text{Analyte}}}{M_{\text{Ligand}}}$$

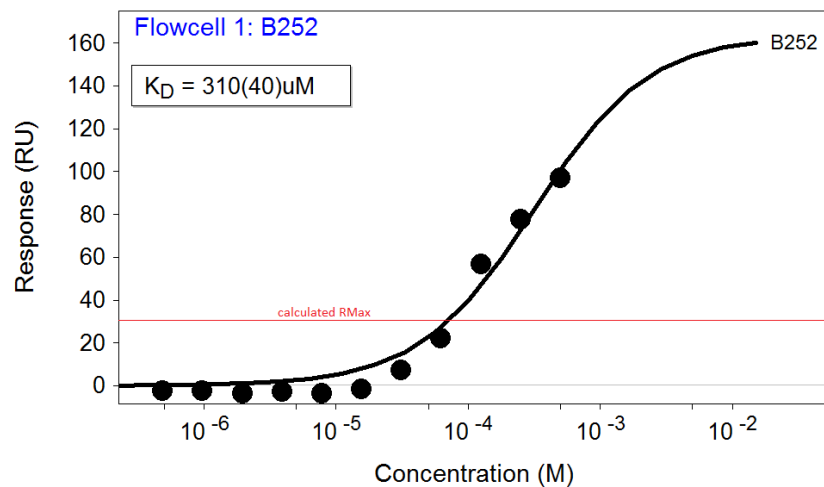
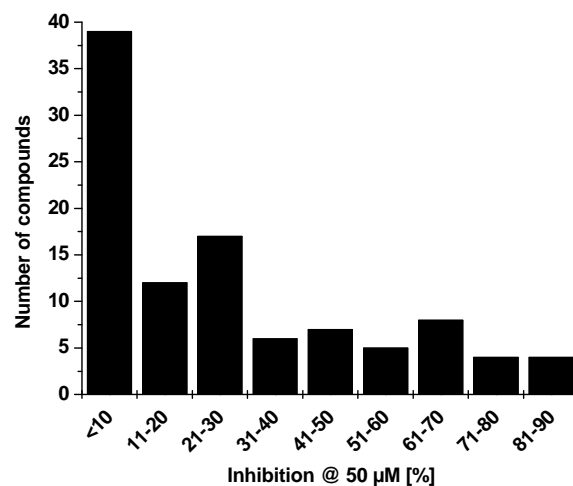
R <sub>max</sub> :	Maximal theoretically possible response
R <sub>Ligand</sub> :	immobilization level
M <sub>Analyte</sub> :	Molecular weight analyte
M <sub>Ligand</sub> :	Molecular weight ligand

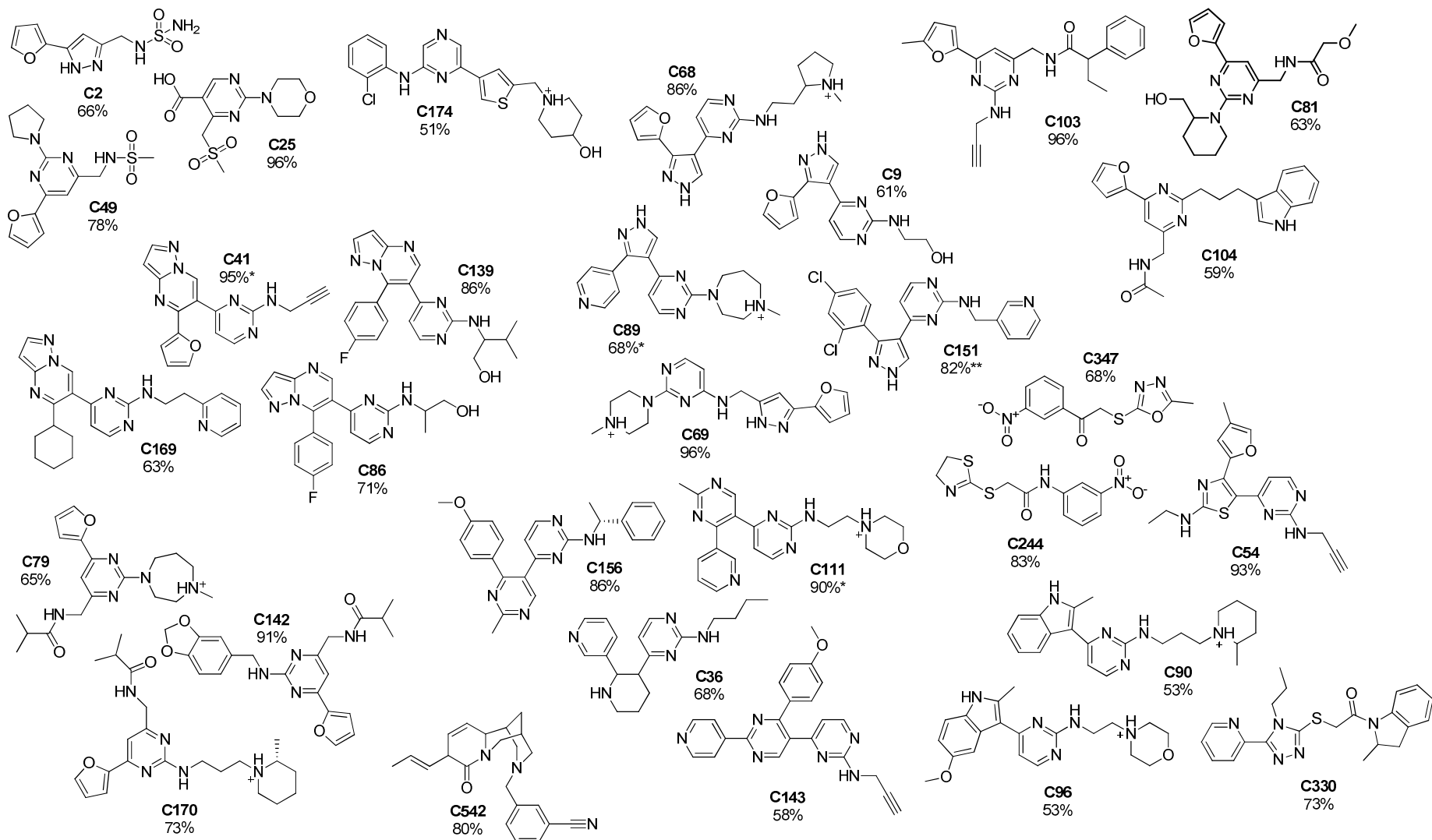
**S3: Inhibition values of the identified hit compounds**

Cmpd.	MW	Structure	Inhibition	Response	Cmpd.	MW	Structure	Inhibition	Response
<b>B11</b>	98.10		<10%	13.5	<b>B182</b>	143.21		<10%	16.7
<b>B48</b>	130.15		15%	13.9	<b>B185</b>	133.15		<10%	15.2
<b>B62</b>	144.18		<10%	13.4	<b>B186</b>	166.20		58%	14.8
<b>B91</b>	116.14		>99%	13.8	<b>B189</b>	108.10		20%	16.3
<b>B93</b>	128.19		<10%	12.8	<b>B190</b>	126.16		<10%	15.0
<b>B106</b>	112.13		<10%	17.7	<b>B199</b>	158.20		<10%	15.7
<b>B122</b>	147.54		<10%	14.7	<b>B276</b>	176.26		<10%	18.9
<b>B159</b>	152.19		29%	22.6	<b>B282</b>	159.19		85%	14.4
<b>B171</b>	97.12		<10%	15.1	<b>B284</b>	112.13		<10%	14.2
<b>B173</b>	112.13		<10%	16.3	<b>B300</b>	199.27		<10%	19.2
<b>B180</b>	129.18		31%	21.4	<b>B336</b>	110.16		<10%	15.4

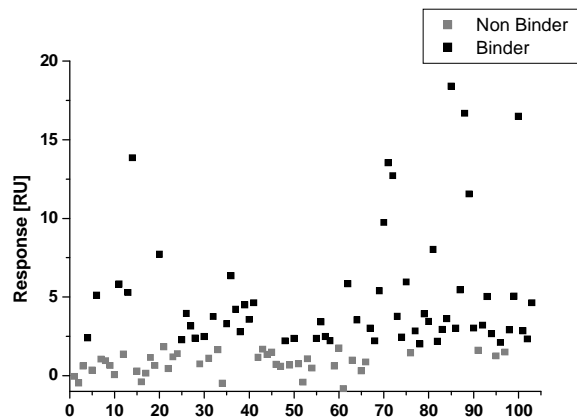
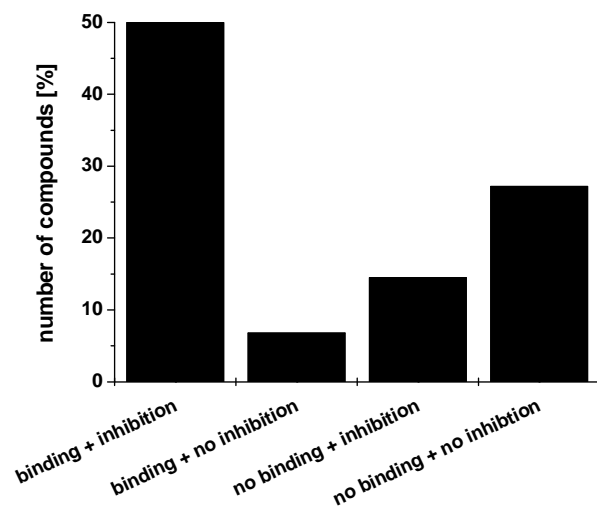
**S4: Inhibition values of the unspecific and non binders**

Cmpd.	MW	Structure	Inhibition	Response	Cmpd.	MW	Structure	Inhibition	Response
<b>B79</b>	82.11		<10%	17.5	<b>B59</b>	101.15		<10%	Non Binder
<b>B252</b>	170.21		99%	34.6	<b>B88</b>	147.61		<10%	Non Binder
<b>B379</b>	86.09		52%	16.2	<b>B100</b>	167.21		18%	Non Binder
					<b>B102</b>	157.21		<10%	Non Binder
					<b>B108</b>	128.56		<10%	Non Binder
					<b>B109</b>	128.19		<10%	Non Binder
					<b>B117</b>	112.11		<10%	Non Binder
					<b>B133</b>	144.56		<10%	Non Binder

**S5: Concentration dependent measurements of compound B252 by SPR****S6: Inhibition values of 2-aminopyrimidine derivatives excluded by virtual screening (n=103).**

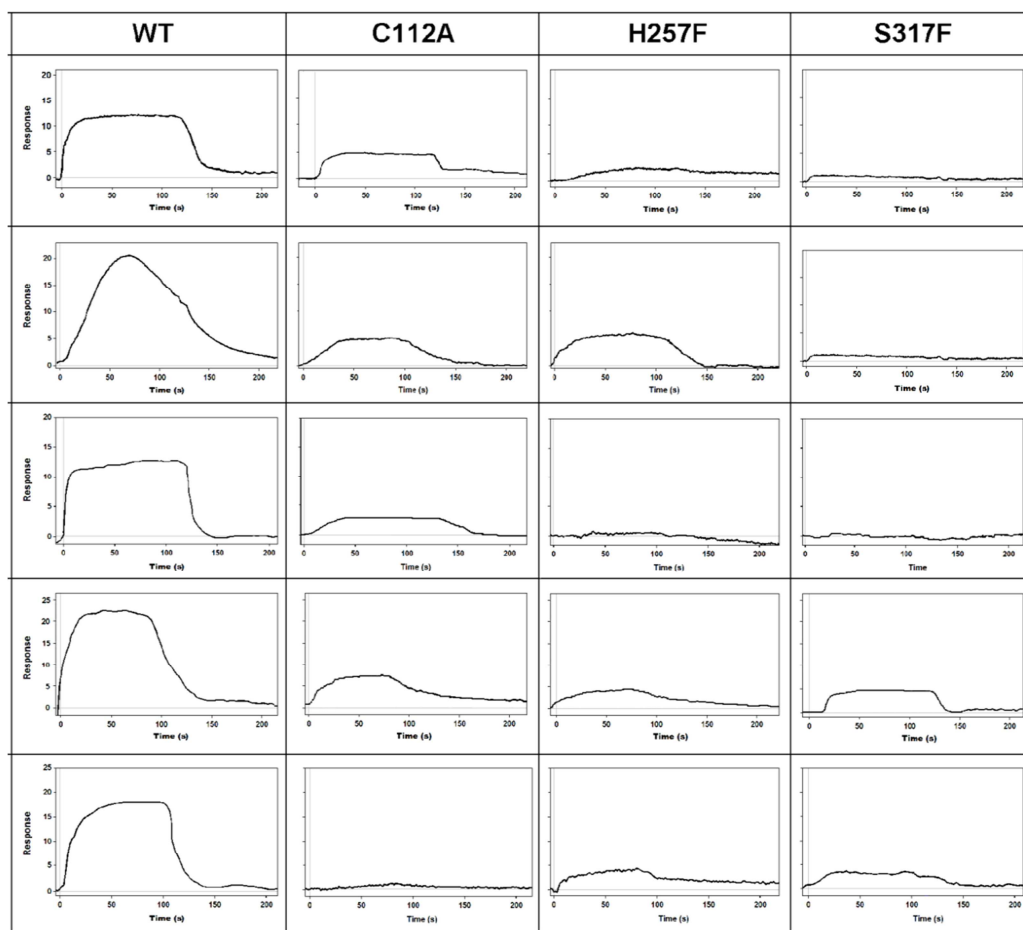
**S7: Structures of the identified PqsD inhibitors in the virtual screening approach and inhibition in % tested at 50 μM.**

Inhibition @\*25μM; \*\* 10μM

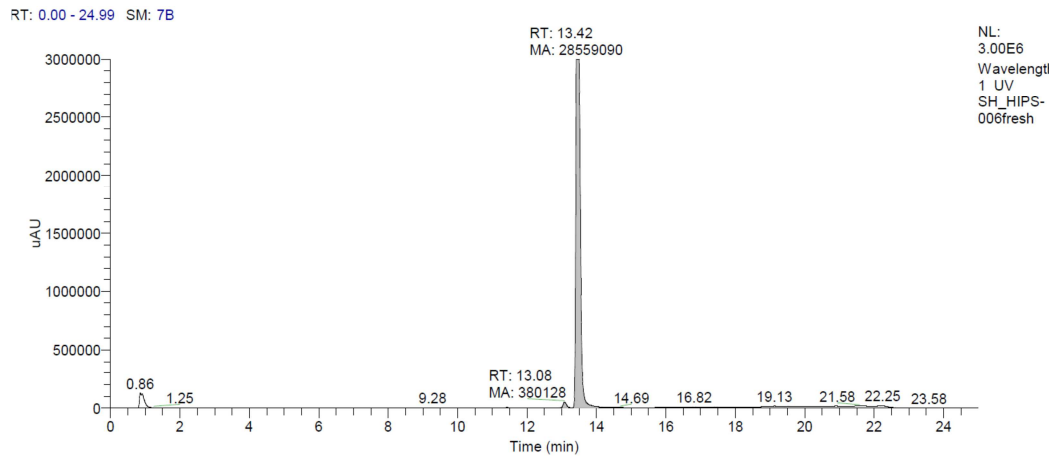
**S8: SPR plot: response of the 103 compounds excluded by virtual screening****S9 Correlation between binding and PqsD inhibition**

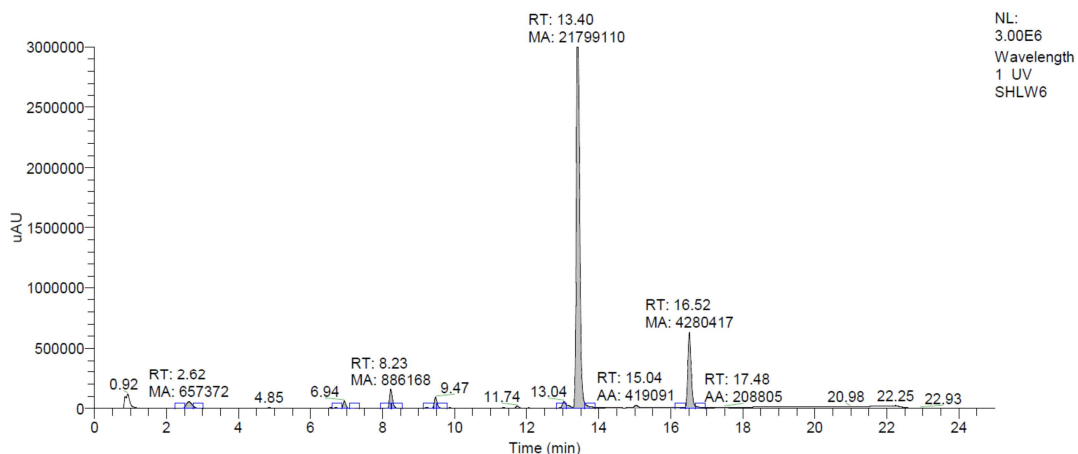
**S10: IC<sub>50</sub> values of all hitcompounds identified in strategy A, B, and C**

Compound	IC <sub>50</sub>
<b>A1</b>	0.15 ± 0.1 μM
<b>A4</b>	15.0 ± 3.3 μM
<b>A5</b>	15.7± 2.3 μM
<b>A8</b>	8.6± 0.8μM
<b>A11</b>	4.4 ± 0.6μM
<b>B91</b>	4.7 ± 1.3μM
<b>B186</b>	47.0 ± 14.1 μM
<b>B282</b>	31.8 ± 3.3 μM
<b>C2</b>	42.1± 8.7 μM
<b>C9</b>	33.2± 1.4 μM
<b>C25</b>	2.6± 0.3 μM
<b>C36</b>	31.8± 5.7 μM
<b>C41</b>	6.8± 0.1 μM
<b>C49</b>	15.5 ± 2.3 μM
<b>C54</b>	4.3± 0.1 μM
<b>C66</b>	11.6 ± 1.6 μM
<b>C67</b>	29.9 ± 5.3μM
<b>C69</b>	5.0 μM <sup>#</sup>
<b>C79</b>	40.9 ± 0.6 μM
<b>C81</b>	34.8 ± 3.9 μM
<b>C86</b>	44.6 ± 11.1 μM
<b>C90</b>	44.3 ± 5.1μM
<b>C96</b>	30%*
<b>C103</b>	5.0 ± 0.9μM
<b>C104</b>	28.3 ± 1.8 μM
<b>C111</b>	8.7± 3.4 μM
<b>C139</b>	17.9± 2.4 μM
<b>C142</b>	22.4± 2.0 μM
<b>C143</b>	41.1 ± 9.4 μM
<b>C151</b>	6.5 ± 0.3 μM
<b>C156</b>	25.3± 3.9 μM
<b>C169</b>	63%*
<b>C170</b>	21.2 ± 5.3 μM
<b>C174</b>	53.2 ± 4.6μM
<b>C244</b>	18.5 ± 8.2 μM
<b>C330</b>	30.0 μM <sup>#</sup>
<b>C347</b>	33.3 ± 9.1 μM
<b>C542</b>	18.4 ± 1.3μM

**S11: SPR sensorgrams: Binding to PqsD wildtype and PqsD mutants**

Compound order is as followed from up to down: **A1, A11, B91, C25, and C54.**

**S12: LC-MS spectra of a freshly prepared DMSO stock solution of A1 (1 $\mu$ M) after 60 min (top) and after 24 hour (bottom)**



### S13. Chemistry

#### a) General directions

Chemical names follow IUPAC nomenclature. Starting materials were purchased from Sigma-Aldrich, Acros, Maybridge, Combi Blocks, Fluka, ABCR, Alfa Aesar, Apollo and were used without purification.

Column chromatography (CC) was performed on silica gel (63–200 µm) and reaction progress was monitored by TLC on Alugram SIL G UV<sub>254</sub> (Macherey-Nagel).

<sup>1</sup>H NMR and <sup>13</sup>C NMR spectra were recorded on a Bruker AM500 spectrometer (500 MHz and 125 MHz) at 300 K in CD<sub>3</sub>OD, CDCl<sub>3</sub> or DMSO-d<sub>6</sub>. Chemicals shifts are reported in δ values (ppm), the hydrogenated residues of deuterated solvents were used as internal standard (CD<sub>3</sub>OD: δ = 3.31 ppm in <sup>1</sup>H NMR and δ = 49.2 ppm in <sup>13</sup>C NMR, CDCl<sub>3</sub>: δ = 7.27 ppm in <sup>1</sup>H NMR and δ = 77.0 ppm in <sup>13</sup>C NMR, DMSO-d<sub>6</sub>: δ = 2.50 ppm in <sup>1</sup>H NMR and δ = 39.5 ppm in <sup>13</sup>C NMR). Signals are described as s, br. s, d, t, dd, ddd, dt and m for singlet, broad singlet, doublet, triplet, doublet of doublet, doublet of doublet of doublet, doublet of triplet and multiplet, respectively. Coupling constants (*J*) are given in Hertz (Hz).

The reported yields are the isolated yields of purified material and are not optimized.

Purity of compounds **A1** to **A12** was determined using LC/MS as follows:

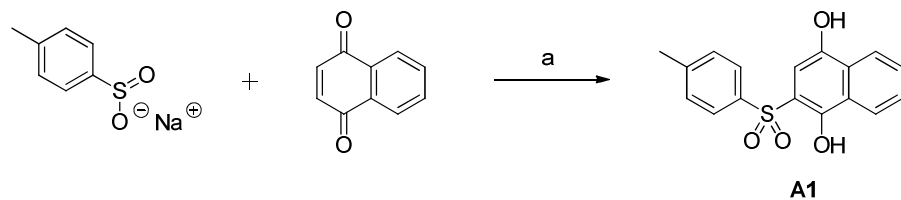
The SpectraSystems®-LC-system consisted of a pump, an autosampler, and a UV detector. Mass spectrometry was performed on a MSQ® electro spray mass spectrometer (Thermo Fisher, Dreieich, Germany). The system was operated by the standard software Xcalibur®.A RP C18 NUCLEODUR® 100-5 (125 x 3 mm) column (Macherey-Nagel GmbH, Duehren, Germany) was used as stationary phase. All solvents were HPLC grade.

Solvent system:

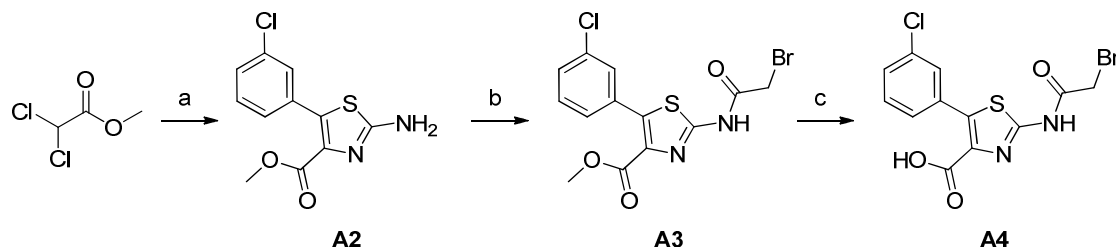
In a gradient run the percentage of acetonitrile (containing 0.1 % triflouro-acetic acid) in 0.1 % triflouro-acetic acid was increased from an initial concentration of 0 % at 0 min to 100 % at 15 min and kept at 100 % for 5 min.

The injection volume was 10 µL and flow rate was set to 800 µL/min. MS analysis was carried out at a spray voltage of 3800 V, a capillary temperature of 350 °C and a source CID of 10 V. Spectra were acquired in positive or negative mode from 100 to 1000 m/z and at 254 nm for the UV trace.

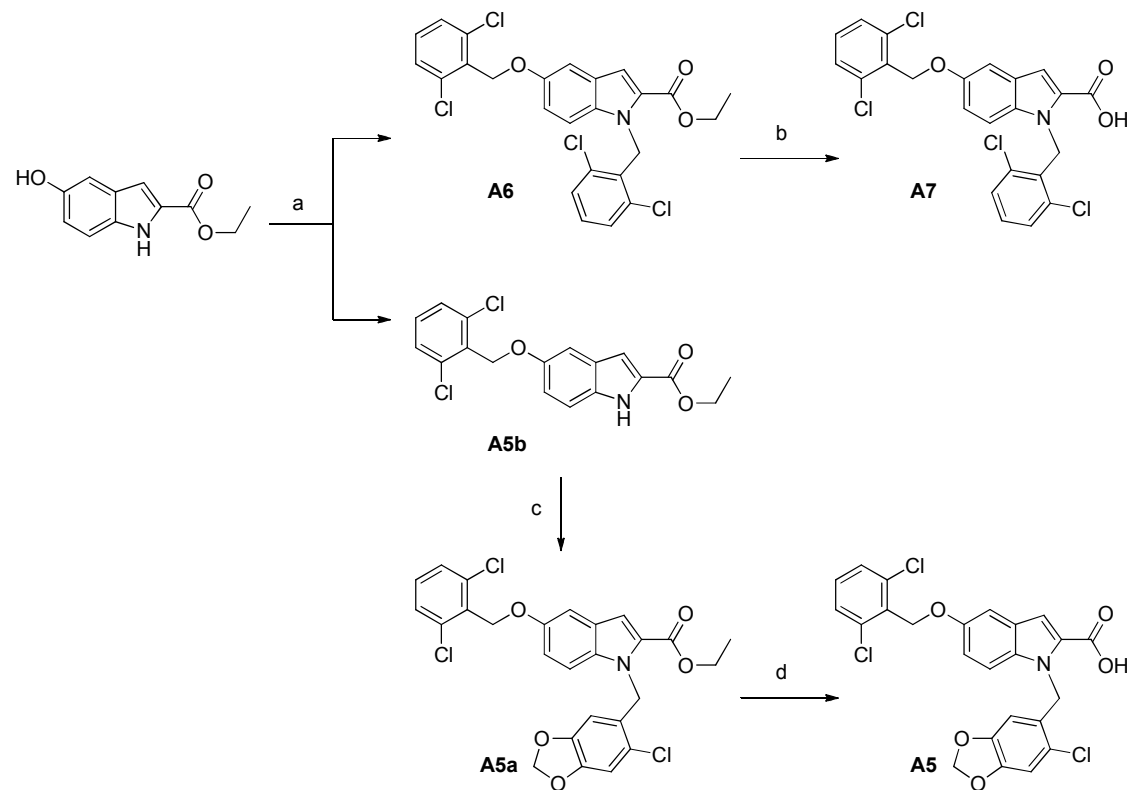
## b) Synthesis schemes

**Scheme S1.** Synthetic route to compound A1<sup>(S1)</sup>

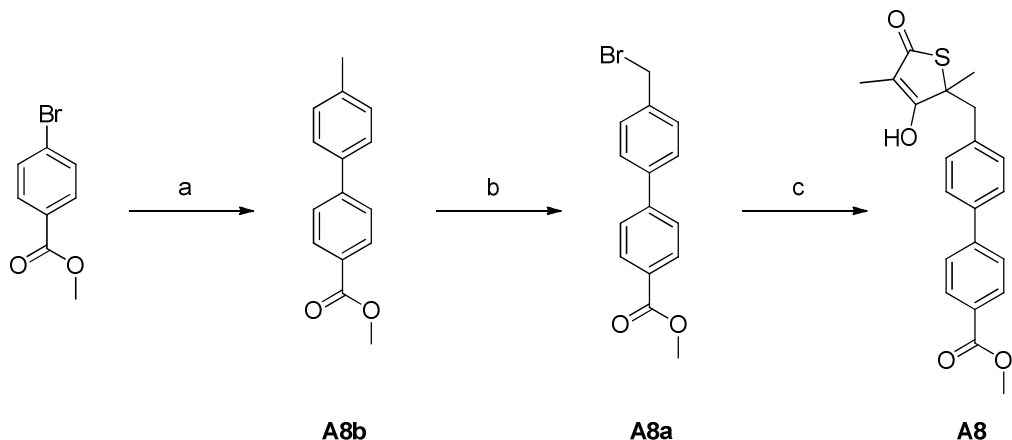
Reagents and conditions: (a) TFA, CH<sub>2</sub>Cl<sub>2</sub>, H<sub>2</sub>O, rt.

**Scheme S2.** Synthetic route to compounds A2–A4<sup>(S2)</sup>

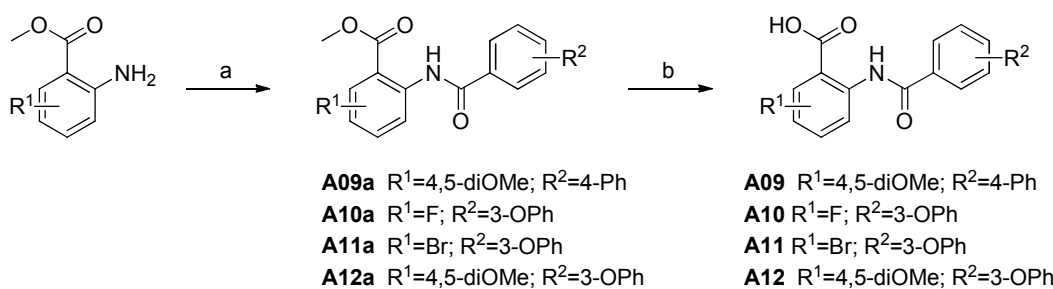
Reagents and conditions: (a) 1.) 3-chlorobenzaldehyde, KO*t*Bu, THF, -60 °C, 2.) thiourea, acetone, reflux; (b) 2-bromoacetyl chloride, TEA, CH<sub>2</sub>Cl<sub>2</sub>, 0 °C →rt; (c) 1 N NaOH, H<sub>2</sub>O, 60 °C.

**Scheme S3.** Synthetic route to compounds A5–A7<sup>(S3)</sup>

Reagents and conditions: (a) 2, 6-dichlorobenzyl chloride, Cs<sub>2</sub>CO<sub>3</sub>, DMF, rt; (b) 1 N NaOH, H<sub>2</sub>O, THF, MeOH, reflux; (c) chloropiperonyl chloride, NaH, DMF, rt; (d) 3 N KOH, H<sub>2</sub>O, THF, EtOH, reflux.

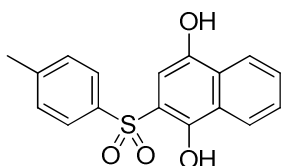
**Scheme S4.** Synthetic route to compound A8<sup>(S4, S5)</sup>

Reagents and conditions: (a)  $\text{Pd}(\text{PPh}_3)_4$ , tolylboronic acid,  $\text{Na}_2\text{CO}_3$ ,  $\text{MeOH}$ , toluene, reflux; (b)  $\text{NBS}$ , benzoyl peroxide,  $\text{CCl}_4$ , reflux; (c) 4-hydroxy-3,5-dimethyl-5H-thiophen-2-one, LHMDS,  $\text{THF}$ ,  $-78^\circ\text{C}$ .

**Scheme S5.** Synthetic route to compounds A9–A12<sup>(S6)</sup>

Reagents and conditions: (a) [1,1'-biphenyl]-4-carbonyl chloride or 3-phenoxybenzoyl chloride, TEA,  $\text{CH}_2\text{Cl}_2$ , rt; (b) 5 M NaOH, THF,  $\text{MeOH}$ ,  $\text{H}_2\text{O}$ , rt.

c) used methods of synthesis and spectroscopic data

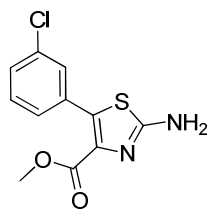


**2-tosylnaphthalene-1,4-diol (A1)** was prepared using the procedure described by Alhamadsheh *et al.*<sup>(S1)</sup>

$^1\text{H}$  NMR (500 MHz,  $\text{CD}_3\text{OD}$ )  $\delta = 8.26$  (ddd,  $J = 8.2, 6.9, 1.6$  Hz, 1H), 8.13 (ddd,  $J = 8.2, 1.3, 0.6$  Hz, 1H), 7.84 (d,  $J = 8.2$  Hz, 2H), 7.59 (ddd,  $J = 8.2, 6.9, 1.3$  Hz, 1H), 7.53 (ddd,  $J = 8.2, 6.9, 1.6$  Hz, 1H), 7.33 (d,  $J = 8.2$  Hz, 2H), 6.90 (s, 1H), 2.34 (s, 3H) ppm.

$^{13}\text{C}$  NMR (125 MHz,  $\text{CD}_3\text{OD}$ )  $\delta = 148.2, 146.3, 140.6, 131.1, 130.6, 129.9, 128.2, 128.1, 127.5, 124.5, 123.6, 117.8, 103.9, 21.6$  ppm.

LC/MS: m/z = 393 [ $\text{M} + \text{H}^+ + \text{CH}_3\text{SOCH}_3$ ];  $t_{\text{R}} = 12.19$  min; 99 % pure (UV).



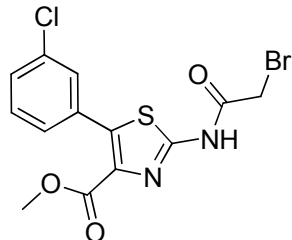
**methyl 2-amino-5-(3-chlorophenyl)thiazole-4-carboxylate (A2)** was prepared using the procedure described by *Al-Balas et al* with slight modifications <sup>(S2)</sup>.

3-Chlorobenzaldehyde (1 equiv) was added to a stirring solution of methyl 2,2-dichloroacetate (1 equiv) dissolved in anhydrous THF at 0 °C before dropwise addition of KOtBu (1 equiv; dissolved THF). The mixture was allowed to reach room temperature over a period of 16 h. H<sub>2</sub>O was added followed by an extraction with EtOAc. The combined organic layers were washed with H<sub>2</sub>O and dried over Na<sub>2</sub>SO<sub>4</sub>. The solvent was removed under reduced pressure and thiourea (1 equiv; dissolved in acetone) was added to the remaining solid. After stirring the mixture at 60 °C for 14 h the formed precipitate was filtered off and washed with acetone to provide the title compound; yield: 86 %.

<sup>1</sup>H NMR (500 MHz, DMSO-*d*<sub>6</sub>) δ = 9.17 (br. s., 1 H), 7.61–7.54 (m, 1 H), 7.49–7.41 (m, 3 H), 3.67 (s, 3 H) ppm.

<sup>13</sup>C NMR (125 MHz, DMSO-*d*<sub>6</sub>) δ = 166.7, 160.1, 132.8, 131.7, 130.7, 130.4, 130.1, 129.3, 128.8, 128.4, 52.1 ppm.

LC/MS: m/z = 269 [M + H<sup>+</sup>]; t<sub>R</sub> = 8.59 min; 95 % pure (UV).



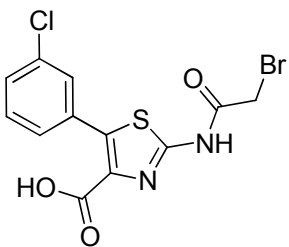
**methyl 2-(2-bromoacetamido)-5-(3-chlorophenyl)thiazole-4-carboxylate (A3)** was prepared using the procedure described by *Al-Balas et al* with slight modifications <sup>(S2)</sup>.

Methyl 2-amino-5-(3-chlorophenyl)thiazole-4-carboxylate (1 equiv) was added to a stirring solution of anhydrous CH<sub>2</sub>Cl<sub>2</sub> and TEA (2 equiv) at 0 °C before dropwise addition of 2-bromoacetyl chloride (1.2 equiv; dissolved in CH<sub>2</sub>Cl<sub>2</sub>). The mixture was allowed to reach room temperature over a period of 16 h. H<sub>2</sub>O was added followed by an extraction with EtOAc. The combined organic layers were washed with H<sub>2</sub>O and dried over Na<sub>2</sub>SO<sub>4</sub>. The solvent was removed under reduced pressure and the product was purified by CC (PE/EtOAc 7:3) and by washing with small portions of acetone; yield: 72 %.

<sup>1</sup>H NMR (500 MHz, DMSO-*d*<sub>6</sub>) δ = 13.04 (s, 1 H), 7.67–7.60 (m, 1 H), 7.54–7.43 (m, 3 H), 4.42 (s, 2 H), 3.70 (s, 3 H) ppm.

<sup>13</sup>C NMR (125 MHz, DMSO-*d*<sub>6</sub>) δ = 165.8, 161.8, 155.3, 137.2, 135.2, 132.8, 132.1, 130.1, 129.5, 128.7, 128.6, 51.8, 42.1 ppm.

LC/MS: m/z = 329 and 331 and 333 [M<sup>+</sup> – COOCH<sub>3</sub>]; t<sub>R</sub> = 11.40 min; >99 % pure (UV).

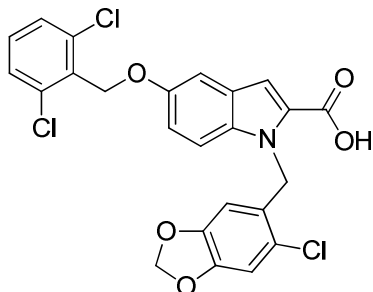


**2-(2-bromoacetamido)-5-(3-chlorophenyl)thiazole-4-carboxylic acid (A4)** was prepared using the procedure described by *Al-Balas et al.*<sup>(S2)</sup>.

<sup>1</sup>H NMR (500 MHz, DMSO-*d*<sub>6</sub>) δ = 12.96 (br. s., 2 H), 7.65–7.58 (m, 1 H), 7.51–7.43 (m, 3 H), 4.41 (s, 2 H) ppm.

<sup>13</sup>C NMR (125 MHz, DMSO-*d*<sub>6</sub>) δ = 165.7, 162.9, 155.1, 136.7, 136.0, 132.8, 132.5, 130.1, 129.5, 128.5, 128.5, 42.1 ppm.

LC/MS: m/z = 329 and 331 and 333 [M<sup>+</sup> – COOH]; t<sub>R</sub> = 10.02 min; 97 % pure (UV).



**1-((6-chlorobenzo[*d*][1,3]dioxol-5-yl)methyl)-5-((2,6-dichlorobenzyl)oxy)-1*H*-indole-2-carboxylic acid (A5)** was prepared using the procedure described by *Daines et al.*<sup>(S3)</sup> with several modifications<sup>(S3)</sup>.

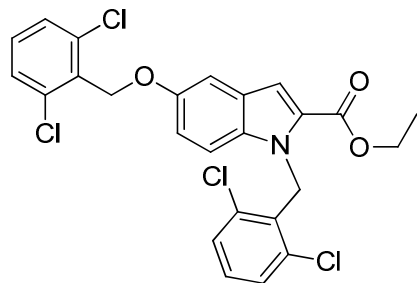
In a first step, ethyl 5-((2,6-dichlorobenzyl)oxy)-1*H*-indole-2-carboxylate (**A4b**; synthesized as described above in “A2”) (1 equiv) was added to a solution of NaH (1.5 equiv; rinsed with hexane) in DMF. After stirring the mixture for 1 h at room temperature, chloropiperonyl chloride (1 equiv, solved in a small amount of DMF) was added and the stirring was continued for further 5 h. The reaction mixture was poured into H<sub>2</sub>O and extracted with EtOAc. The combined organic layers were washed with H<sub>2</sub>O and dried over Na<sub>2</sub>SO<sub>4</sub>. The product **A4a** was purified by CC (PE/EtOAc 95:5).

In a second step, ethyl 1-((6-chlorobenzo[*d*][1,3]dioxol-5-yl)methyl)-5-((2,6-dichlorobenzyl)oxy)-1*H*-indole-2-carboxylate (**A4a**) (1 equiv) in THF/EtOH was treated with 3 M KOH (60 equiv) and refluxed for 1.5 h. Subsequently the reaction mixture was acidified with conc. HCl and extracted with EtOAc. For purification the compound was recrystallized from acetone; yield: 7 %.

<sup>1</sup>H NMR (500 MHz, DMSO-*d*<sub>6</sub>) δ = 12.98 (br. s, 1H), 7.56 (d, *J* = 8.2 Hz, 2H), 7.46 (t, *J* = 8.2 Hz, 1H), 7.42 (d, *J* = 2.1 Hz, 1H), 7.32 (d, *J* = 9.1 Hz, 1H), 7.13 (s, 1H), 7.30 (s, 1H), 7.01 (dd, *J* = 9.1, 2.1 Hz, 1H), 5.96 (s, 2H), 5.79 (s, 2H), 5.56 (s, 1H), 5.25 (s, 2H) ppm.

<sup>13</sup>C NMR (125 MHz, DMSO-*d*<sub>6</sub>) δ = 162.6, 153.6, 147.0, 146.9, 136.1, 134.54, 131.9, 131.5, 129.2, 128.73, 128.66, 125.9, 122.4, 116.8, 111.9, 110.2, 109.7, 105.7, 104.3, 102.0, 65.4, 45.1 ppm.

LC/MS: t<sub>R</sub> = 15.12 min; >99 % pure (UV).

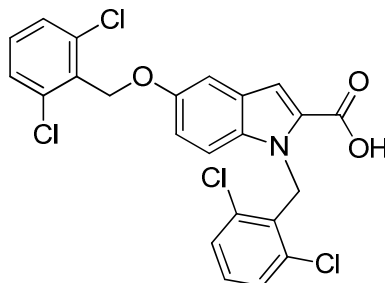


**ethyl 1-(2,6-dichlorobenzyl)-5-((2,6-dichlorobenzyl)oxy)-1H-indole-2-carboxylate (A6).** A solution of 5-hydroxy-1*H*-indole-2-carboxylic acid ethyl ester (1 equiv) in dry DMF was treated with  $\text{Cs}_2\text{CO}_3$  (1.5 equiv) followed by 2,6-dichlorobenzyl chloride (1.1 equiv). The reaction mixture was stirred at room temperature for 14 h. The reaction was diluted with EtOAc, washed with  $\text{H}_2\text{O}$  and the organic phase was dried over  $\text{Na}_2\text{SO}_4$ . The solvent was evaporated and the resulting solid (consisting of **A2** and **A4b**) was separated by CC (PE/EtOAc 98:2 → 95:5); yield (**A2**): 48 %.

$^1\text{H}$  NMR (500 MHz,  $\text{CDCl}_3$ )  $\delta$  = 7.36 (d,  $J$  = 8.2 Hz, 2H), 7.31–7.29 (m, 3H), 7.24 (d,  $J$  = 2.2 Hz, 1H), 7.23 (dd,  $J$  = 8.5, 7.6 Hz, 1H), 7.16 (dd,  $J$  = 8.5, 7.6 Hz, 1H), 7.02 (d,  $J$  = 9.1 Hz, 1H), 6.91 (dd,  $J$  = 9.1, 2.5 Hz, 1H), 6.30 (s, 2H), 5.26 (s, 2H), 4.41 (q,  $J$  = 7.3 Hz, 2H), 1.43 (t,  $J$  = 7.3 Hz, 3H) ppm.

$^{13}\text{C}$  NMR (125 MHz,  $\text{CDCl}_3$ )  $\delta$  = 162.5, 153.7, 137.1, 136.1, 134.9, 132.5, 132.4, 130.3, 129.8, 129.3, 129.0, 128.4, 126.5, 116.9, 112.1, 110.2, 104.8, 65.9, 60.6, 44.5, 14.4 ppm.

LC/MS: m/z = 522 and 524 and 526 [ $\text{M} + \text{H}^+$ ];  $t_{\text{R}}$  = 17.65 min; >99 % pure (UV).

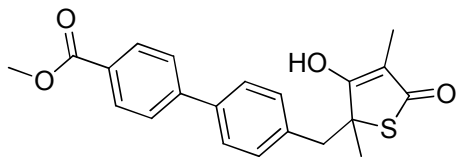


**1-(2,6-dichlorobenzyl)-5-((2,6-dichlorobenzyl)oxy)-1H-indole-2-carboxylic acid (A7).** A solution of ethyl 1-(2,6-dichlorobenzyl)-5-((2,6-dichlorobenzyl)oxy)-1*H*-indole-2-carboxylate (**A2**) (1 equiv) in THF/MeOH was treated with 1N NaOH (60 equiv) and refluxed for 1 h. Subsequent acidification of the reaction mixture with conc. HCl led to precipitation of the crude product, which was filtered off and washed with water. Purification by CC (EtOAc 100%) provided the pure compound; yield: 88 %.

$^1\text{H}$  NMR (500 MHz,  $\text{DMSO}-d_6$ )  $\delta$  = 13.00 (br. s., 1 H), 7.57–7.52 (m, 2 H), 7.49–7.43 (m, 3 H), 7.37–7.32 (m, 2 H), 7.21 (d,  $J$  = 0.6 Hz, 1 H), 7.00 (d,  $J$  = 9.1 Hz, 1 H), 6.89 (dd,  $J$  = 9.1, 2.5 Hz, 1 H), 6.21 (s, 2 H), 5.19 (s, 2 H) ppm.

$^{13}\text{C}$  NMR (125 MHz,  $\text{DMSO}-d_6$ )  $\delta$  = 163.2, 153.2, 136.1, 135.0, 134.2, 132.1, 131.9, 131.4, 130.3, 130.2, 129.3, 128.7, 126.1, 116.0, 111.6, 109.6, 104.3, 65.3, 44.0 ppm.

LC/MS: m/z = 494 and 496 and 498 [ $\text{M} + \text{H}^+$ ];  $t_{\text{R}}$  = 15.14 min; >99 % pure (UV).



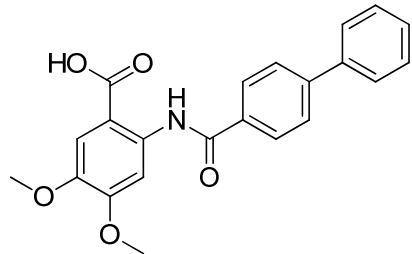
**methyl 4'-(3-hydroxy-2,4-dimethyl-5-oxo-2,5-dihydrothiophen-2-yl)methyl)-[1,1'-biphenyl]-4-carboxylate (A8).**

The precursor compounds **A8b** and **A8a** were prepared as described before<sup>(S4)</sup>. The conversion of **A8a** to **A8** was performed using the procedure described by Senior *et al.*<sup>(S5)</sup>.

<sup>1</sup>H NMR (500 MHz, CD<sub>3</sub>OD) δ = 8.05 (d, *J* = 8.5 Hz, 2H), 7.69 (d, *J* = 8.5 Hz, 2H), 7.55 (d, *J* = 8.2 Hz, 2H), 7.33 (d, *J* = 8.2 Hz, 2H), 3.91 (s, 3H), 3.24 (d, *J* = 13.6 Hz, 1H), 3.16 (d, *J* = 13.6 Hz, 1H), 1.70 (s, 3H), 1.58 (s, 3H) ppm.

<sup>13</sup>C NMR (125 MHz, CD<sub>3</sub>OD) δ = 197.2, 181.6, 168.5, 146.8, 139.7, 138.0, 132.3, 131.1, 130.0, 127.9, 127.5, 111.5, 59.2, 52.6, 45.0, 26.3, 7.4 ppm.

LC/MS: m/z = 410 [M + H<sup>+</sup> + CH<sub>3</sub>CN], 737 [2M + H<sup>+</sup>]; t<sub>R</sub> = 12.06 min; >99 % pure (UV).

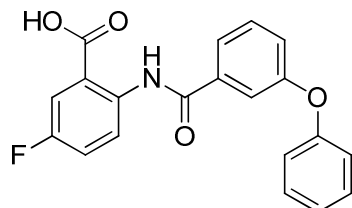


**2-([1,1'-biphenyl]-4-ylcarboxamido)-4,5-dimethoxybenzoic acid (A9)** was prepared using the procedure described by Hinsberger *et al.*<sup>(166)</sup>.

<sup>1</sup>H NMR (500 MHz, DMSO-*d*<sub>6</sub>) δ = 14.78 (br. s, 1 H), 8.54 (s, 1 H), 8.14–8.08 (m, 2 H), 7.78–7.73 (m, 2 H), 7.72–7.61 (m, 3 H), 7.56–7.33 (m, 3 H), 3.81 (s, 3 H), 3.74 (s, 3 H) ppm.

<sup>13</sup>C NMR (125 MHz, DMSO-*d*<sub>6</sub>) δ = 163.4, 150.5, 143.2, 142.9, 139.0, 135.7, 134.1, 129.0, 128.1, 127.8, 126.8, 126.8, 117.6, 117.4, 114.3, 102.6, 55.5, 55.4 ppm.

LC/MS: m/z = 378 [M + H<sup>+</sup>]; t<sub>R</sub> = 12.37 min; 96 % pure (UV).

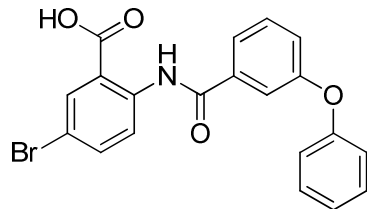


**5-fluoro-2-(3-phenoxybenzamido)benzoic acid (A10)** was prepared using the procedure described by Hinsberger *et al.*<sup>(S6)</sup>.

<sup>1</sup>H NMR (500 MHz, DMSO-*d*<sub>6</sub>) δ = 12.02 (br. s, 1 H), 8.62 (dd, *J* = 9.4, 5.2 Hz, 1 H), 7.74 (dd, *J* = 9.4, 3.2 Hz, 1 H), 7.72–7.68 (m, 1 H), 7.59 (dd, *J* = 7.9, 7.9 Hz, 1 H), 7.56–7.50 (m, 2 H), 7.49–7.39 (m, 2 H), 7.27 (ddd, *J* = 7.9, 2.6, 0.9 Hz, 1 H), 7.23–7.16 (m, 1 H), 7.14–7.04 (m, 2 H) ppm.

<sup>13</sup>C NMR (125 MHz, DMSO-*d*<sub>6</sub>) δ = 168.7 (d, *J*<sub>CF</sub> = 1.8 Hz), 163.8, 157.3, 157.0 (d, *J*<sub>CF</sub> = 242.0 Hz), 156.0, 137.2 (d, *J*<sub>CF</sub> = 1.8 Hz), 136.3, 130.8, 130.2, 124.1, 122.3 (d, *J*<sub>CF</sub> = 7.3 Hz), 122.0, 121.6, 120.9 (d, *J*<sub>CF</sub> = 22.0 Hz), 119.4 (d, *J*<sub>CF</sub> = 7.3 Hz), 119.1, 117.0 (d, *J*<sub>CF</sub> = 22.0 Hz), 116.9 ppm.

LC/MS: m/z = 351 [M + H<sup>+</sup>], 392 [M + H<sup>+</sup> CH<sub>3</sub>CN]; t<sub>R</sub> = 12.87 min; 96 % pure (UV).

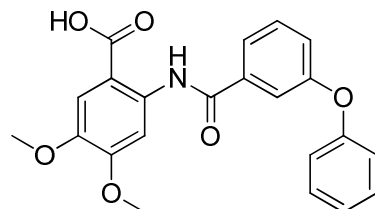


**5-bromo-2-(3-phenoxybenzamido)benzoic acid (A11)** was prepared using the procedure described by Hinsberger *et al.*<sup>(S6)</sup>.

<sup>1</sup>H NMR (500 MHz, DMSO-*d*<sub>6</sub>) δ = 12.05 (br. s, 1 H), 8.59 (d, *J* = 9.1 Hz, 1 H), 8.10 (d, *J* = 2.5 Hz, 1 H), 7.83 (dd, *J* = 9.1, 2.5 Hz, 1 H), 7.72–7.67 (m, 1 H), 7.63–7.57 (m, 1 H), 7.53–7.50 (m, 1 H), 7.47–7.40 (m, 2 H), 7.30–7.26 (m, 1 H), 7.24–7.17 (m, 1 H), 7.14–7.06 (m, 2 H) ppm.

<sup>13</sup>C NMR (125 MHz, DMSO-*d*<sub>6</sub>) δ = 168.6, 163.9, 157.3, 156.0, 140.0, 136.7, 136.2, 133.2, 130.8, 130.2, 130.1, 124.1, 122.2, 122.1, 121.6, 119.0, 116.9, 114.5 ppm.

LC/MS: m/z = 409 and 411 [M - H<sup>+</sup>]; t<sub>R</sub> = 13.90 min; 95 % pure (UV).



**4,5-dimethoxy-2-(3-phenoxybenzamido)benzoic acid (A12)** was prepared using the procedure described by Hinsberger *et al.*<sup>(S6)</sup>.

<sup>1</sup>H NMR (500 MHz, DMSO-*d*<sub>6</sub>) δ = 12.29 (br. s, 1 H), 8.45 (s, 1 H), 7.70–7.66 (m, 1 H), 7.59 (dd, *J* = 7.9, 7.9 Hz, 1 H), 7.52–7.49 (m, 1 H), 7.49–7.41 (m, 3 H), 7.27 (ddd, *J* = 8.2, 2.5, 0.9 Hz, 1 H), 7.21 (tt, *J* = 7.5, 1.0 Hz, 1 H), 7.14–7.06 (m, 2 H), 3.84 (s, 3 H), 3.78 (s, 3 H) ppm.

<sup>13</sup>C NMR (125 MHz, DMSO-*d*<sub>6</sub>) δ = 169.8, 163.6, 157.4, 155.9, 153.3, 143.8, 136.7, 136.5, 130.8, 130.3, 124.1, 121.9, 121.3, 119.2, 116.7, 112.8, 107.8, 103.1, 55.6, 55.6 ppm.

LC/MS: m/z = 394 [M + H<sup>+</sup>], 435 [M + H<sup>+</sup> CH<sub>3</sub>CN]; t<sub>R</sub> = 12.32 min; 97 % pure (UV).

**d) References**

- S1. Alhamadsheh MM, Waters NC, *et al.* Synthesis and biological evaluation of novel sulfonyl-naphthalene-1,4-diols as FabH inhibitors. *Bioorg. Med. Chem. Lett.* 18(24), 6402-6405, (2008).
- S2. Al-Balas Q, Anthony NG, *et al.* Identification of 2-aminothiazole-4-carboxylate derivatives active against *Mycobacterium tuberculosis* H37Rv and the beta-ketoacyl-ACP synthase mtFabH. *PlosOne*. 4(5), (2009).
- S3. Daines RA, Pendrak I, *et al.* First X-ray cocrystal structure of a bacterial FabH condensing enzyme and a small molecule inhibitor achieved using rational design and homology modeling. *J. Med. Chem.* 46(1), 5-8, (2003)
- S4. Mizuno CS, Chittiboyina AG, *et al.* Design, synthesis, and docking studies of telmisartan analogs for the treatment of metabolic syndrome. *Med. Chem. Res.* 18(8), 611-628, (2009).
- S5. Senior SJ, Illarionova PA, *et al.* Biphenyl-based analogues of thiolactomycin, active against *Mycobacterium tuberculosis* mtFabH fatty acid condensing enzyme. *Bioorg. Med. Chem. Lett.* 13(21), 3685-3688, (2003).
- S6. Hinsberger S, Hüsecken K, *et al.* Discovery of novel bacterial RNA polymerase inhibitors: pharmacophore-based virtual screening and hit optimization. *J. Med. Chem.* 56(21), 8332-8338, (2013).

**S14. Defined features used in the pharmacophore model**

Feature	Type
F1	Hyd Aro
F3	Don
F5	Acc&Don
F7	Aro Hyd
F13	Acc Acc2&CN2
F14	Don
F15	Hyd pi
F19	Acc Ani&Acc
F20	Acc Ani&Acc
F21	Don&Acc
F23	Acc Don pi Aro
<b>Projections (potential interaction partners on protein side)</b>	
F2, F4	PiN
F8	Don2 /Acc2/PiN
F9	Acc2&Don2
F10	Acc2
F11	Acc2
F12	Acc2&Don2
F16	Don2
F17	PiN&(Don2 Acc2)
F18	PiN
F22	PiN
F24	Acc2
F25	PiN

Primary features (from ligands): Acc – H-bond acceptor, Don – H-bond donor, Hyd – hydrophobic centroid, Aro – aromatic center, Ani – anionic atom, pi – planar atom, CN2 – NCN+ center;

Projections: Acc2 –H-bond acceptor projection, Don2 –H-bond donor projection, PiN – aromatic or pi ring center;

## 7 Appendix

### 7.1 Curriculum Vitae

#### PERSÖNLICHE DATEN

Name	Elisabeth Weidel
Geburtsdaten	18. April 1987 in Jena
Familienstand	ledig
Nationalität	deutsch

#### WISSENSCHAFTLICHER WERDEGANG

ab 09/2011	<b>Promotion</b> unter Anleitung von Prof. Dr. Rolf Hartmann am Helmholtz-Institut für Pharmazeutische Forschung Saarland (HIPS), Abteilung Drug Discovery and Optimization (DDOP), Saarbrücken Titel der Dissertation: „ <i>Identifizierung und Charakterisierung von Quorum-Sensing-Inhibitoren mittels biophysikalischer Methoden</i> “
10/2006 – 03/2011	<b>Studium der Lebensmittelchemie</b> , Technische Universität Kaiserslautern Abschluss: Diplom (Note 1,2)
10/2010 – 03/2011	<b>Diplomarbeit</b> , Technische Universität Kaiserslautern unter der Betreuung von Prof. Dr. Elke Richling, Titel der Diplomarbeit „Vorkommen von Chlorogensäuren in Kartoffeln und Kartoffelprodukten“ (Note 1,0).
09/2010 – 10/2010	<b>1. Staatsexamen</b> , Technische Universität Kaiserslautern (Note 1,3)
03/2010 – 05/2010	<b>Forschungspraktikum</b> an der Technischen Universität Kaiserslautern unter der Betreuung von Dr. Markus Schantz, Arbeitsgruppe Prof. Dr. Elke Richling, Titel der Arbeit: „Anthocyane in schwarze Johannisbeersäften und Konfitüren“ (Note 1,0)

#### SCHULBILDUNG

09/2000 – 06/2006	Allgemeine Hochschulreife, Gymnasium Wendalinum, St. Wendel Abschluss: Abitur (Note 2,4)
09/1997 – 09/2000	Unterstufe Gesamtschule Marpingen, Marpingen
09/1993 – 06/1997	Nikolaus- Obertreis -Grundschule, St. Wendel

## 7.2 Publikationen

1. Weidel, E., Schantz, M., and Richling, E. (2011) Anthocyanin contents in black currant (*ribes nigrum* L.) juices and fruit drinks. *Fruit processing*, 21, (3), 102-107
2. Steinbach, A., Maurer C.K., Weidel, E., Henn, C., Brengel, C., Hartmann, R.W., and Negri, M. (2013) Molecular basis of HHQ biosynthesis: molecular dynamics simulations, enzyme kinetic and surface plasmon resonance studies. *BMC Biophys.* 2013, 6:10, Published online Aug 1, 2013. doi: 10.1186/2046-1682-6-10
3. Weidel, E., De Jong, J.C., Brengel, C., Storz, M.P., Braunshausen, A., Negri, M., Plaza, A., Müller, R., and Hartmann, R.W. (2013) Structure optimization of 2-Benzamidobenzoic Acids as PqsD Inhibitors for *Pseudomonas Aeruginosa* Infections and Elucidation of Binding Mode by SPR, STD NMR, and Molecular Docking. *J. Med. Chem.*, **56**, (15), 6146–6155.
4. Storz, M.P., Brengel, C., Weidel, E., Hoffmann, M., Hollemeyer, K., Steinbach, A., Müller, R., Empting, M., and Hartmann, R.W. (2013) Biochemical and Biophysical Analysis of a Chiral PqsD Inhibitor Revealing Tight-binding Behavior and Enantiomers with Contrary Thermodynamic Signatures. *ACS Chem. Biol.*, **8**, (12), 2794–2801.
5. Weidel, E., Schantz, M., and Richling, E. (2014) A Rapid Method for Quantifying Chlorogenic Acid Levels in Potato Samples. *Journal of AOAC.*, **97** (3), 902-907
6. Weidel, E., Negri, M., Empting, M., Hinsberger, S., and Hartmann, R.W. (2014) Composing Compound Libraries for Hit Discovery – Rationality-Driven Preselection or Random Choice by Structural Diversity? *Future Med. Chem.* **6**(18) 2057-2072
7. Allegretta, G., Weidel, E., Empting, M., Hartmann, R.W. (2015) Catechol-based substrates of chalcone synthase as a scaffold for novel inhibitors of PqsD. *Eur. J. Med. Chem.* **90**, 351-359
8. Sahner, J.H., Empting, M., Kamal, A., Weidel, E., Börger, C., Hartmann, R.W. Exploring the chemical space of ureidothiophene-2-carboxylic acids as inhibitors of the quorum sensing enzyme PqsD from *Pseudomonas aeruginosa*. *Eur. J. Med. Chem.* 2015, **90**, 351–359.

### 7.3 Poster Präsentationen

1. Weidel, E., Negri, M., Braunshausen, A., and Hartmann, R.W. SPR based library screening for identification of new PqsD inhibitors. *6<sup>th</sup> Summer School “Medicinal Chemistry”*. Sept. 2012. Regensburg, Germany.
2. Weidel, E., De Jong, J.C., Brengel, C., Storz, M.P., Negri, M., Plaza, A., Steinbach, A., Braunshausen, A., Müller, R., and Hartmann, R.W., and Haupenthal, J. Structure Optimization of 2-Benzamidobenzoic Acids as PqsD Inhibitors for *P. aeruginosa* Infections and Elucidation of Binding Mode by SPR, STD NMR and Molecular Docking. *DPhG Annual Meeting 2013 “Drug Discovery inspired by Nature”*. October 2013. Freiburg, Germany.

## 8 Danksagung

Ich möchte mich hier an dieser Stelle herzlich bei allen beteiligten Personen bedanken, die diese Arbeit ermöglicht haben.

Besonderen Dank gilt Prof. Dr. Rolf W. Hartmann für die Möglichkeit eine Promotion in seiner Arbeitsgruppe durchzuführen, sowie das Überlassen des interessanten Themas, der guten Betreuung und das entgegengebrachte Vertrauen.

Prof. Dr. Claus-Michael Lehr danke ich für die Begleitung der Promotion sowie die Übernahme des Zweitgutachtens.

Martin Empting, Matthias Negri und Claudia Henn möchte ich für die gute Betreuung danken; Claudia für die Einarbeitung in den Umgang mit der SPR, Matthias und Martin für die stets vorhandene Bereitschaft über Probleme zu diskutieren und Lösungen zu finden.

Allen ehemaligen und aktuellen Mitgliedern der PQS Gruppe danke ich für die gute Zusammenarbeit und die gute Atmosphäre während den Projektmeetings.

Katrin Schmitt und Martina Schwarz danke ich für ihr Organisationstalent und ihre Hilfsbereitschaft. Auch den anderen an der Organisation beteiligten Personen wie Lothar Jager und Dr. Stefan Boettcher möchte ich für den reibungslosen Ablauf am Institut danken.

Den fleißigen und immer gut gelaunten Mädels Simone Amman, Aline Kirchhoff und Carina Scheid danke ich für die Übernahme der Testung sowie für die angenehme Stimmung im Labor zu welcher auch Tamara Paul und Isabella Reichert beigetragen haben.

Darüber hinaus möchte ich mich bei Dr. Stefan Boettcher und Martina Fruth für praktische Hinweise und die gemeinsame Betreuung des „instrumentelle Analytik“ Praktikums bedanken, sowie bei Sebastian Krug für das Einarbeiten in die einzelnen Verusche und das Überlassen seiner Unterlagen.

Fernerhin gilt mein Dank Nico Dankbar von Xantec Bioanalytics für die freundliche, zeitnahe und kompetente Unterstützung und der gute Erreichbarkeit bei SPR Problemen.

Ruben Postel, Laurens van der Flier, Emmanuel Bey, Jens Burkhardt, Chris van Koppen, Axel Koch sowie Carsten Börger und Victor Olmos danke ich für die gute Organisation und die freundliche Stimmung im SMA Projekt und der netten Atmosphäre bei den F2F-Meetings.

Ein besonderer Dank gilt meinen Bürokollegen insbesondere Michael, Martina, Kristina, Christine, Benny, Ines, Martin, Ändy, Mize, Steffi, Roman, Marica und Walid die zu einer guten

Büroatmosphäre beigetragen haben. Trotz des stets vorhandenen Lärmpegels, waren die Zeiten mit euch immer unterhaltsam und humorvoll.

Benjamin Kirsch danke ich für das Zusenden täglicher Erheiterungen und das Näherbringen von Lachsclown und anderen Webseiten, sowie für das besitzanzeigende Labeling meiner Bürountensilien mit „em Lilli sei“.

Kristina Hüsecken danke ich für die gemeinsame Leidenszeit bei der Bewältigung diverser durch Schrotti, der Prinzessin oder von Black Beauty verursachten SPR-Problemen, ihrer direkten Art Unordnung im Labor anzusprechen und für ihre gnadenlose Ehrlichkeit, die die Büroatmosphäre sowie so manchen Topmodels-Abend erheitert hat.

Stefan Hinsberger für seinen Humor, die gemeinsame „Marpingen-Abneigung“, seiner Klatschweibfähigkeit sowie seiner Freundschaft und besonders für seinen grünen Daumen, nur so wird der Anbau von Schimmel zu einem echten Meisterwerk.

Juliette Emmerich danke ich für ihre Freundschaft und das große Engagement, diese stets aufrecht zu erhalten und auch wenn du es nicht hören willst für deine Art Lyoner auszusprechen ;-)

Ines Joachim für die gemeinsame Mittagessenszeit und insbesondere ihrem Bedürfnis andere durchzufüttern, von welchem ich oftmals profitiert habe. Darüber hinaus für die selbstgemachten Maultaschen, ihrem großen Engagement anderen zu helfen sowie ihrer Bereitschaft mich ins Lädchen zu begleiten.

Martina Fruth möchte ich für die schöne Zeit in Saarbrücken und insbesondere in New York danken und dafür, dass sie meinen kulinarischen Horizont um glutenfreie Nahrungsmittel erweitert hat. Du bist die beste Gluten-freie Pancakes- und Waffelbäckerin der Welt! Darüber hinaus danke ich dir dafür, dass du stets ein offenes Ohr hattest und für die vielen anstrengenden Laufeinheiten.

Ein besonderer Dank gilt Michael Storz, der mir nicht nur ein fundiertes Fußballwissen vermittelt hat, ohne ihn wüsste ich immer noch nicht was „eine falsche 9“ ist ☺, sondern der mir auch die Vorzüge der Schwäbischen Küche näher gebracht hat (sein Maultaschenkreuzzug hat auch vor mir nicht Halt gemacht). Ich danke dir dafür, dass langweilige Bürozeiten quasi nie vorhanden waren und „uns“ (bzw. dir ;-)) auch nach drei Jahren kein Thema zu doof war, um nicht darüber zu diskutieren. Darüber hinaus danke ich dir für dein engagiertes Korrektur lesen, die Beantwortung meiner Fragen, deine Hilfsbereitschaft sowie insbesondere deiner Freundschaft.

Zu guter Letzt möchte ich noch bei meiner Familie und bei meinen Freunden für ihre unermüdliche Unterstützung und ihren Stolz auf das was ich tue, bedanken. Ihr wart mir ein großer Rückhalt auf den stets Verlass war.